CRANFIELD UNIVERSITY

Catherine M. Wiltshire

Organic carbon across the terrestrial-to-aquatic continuum: Assessing source and delivery processes using a combined fingerprinting and carbon loss modelling approach

School of Water, Energy and Environment

PhD
Academic Year: 2018 - 2022

Supervisors: Dr. Toby W. Waine,
Prof. Jeroen Meersmans (University of Liège)
Associate Supervisors: Dr. Robert Grabowski,
Dr. Miriam Glendell (James Hutton Institute)

March 2022

CRANFIELD UNIVERSITY

School of Water, Energy and Environment

PhD

Academic Year 2018 - 2022

Catherine M. Wiltshire

Organic carbon across the terrestrial-to-aquatic continuum: Assessing source and delivery processes using a combined fingerprinting and carbon loss modelling approach

Supervisors: Dr. Toby W. Waine,
Prof. Jeroen Meersmans (University of Liège)
Associate Supervisors: Dr. Robert Grabowski,
Dr. Miriam Glendell (James Hutton Institute)

March 2022

ABSTRACT

Quantifying land use sources and understanding the dynamics of organic carbon (OC) in river catchments are essential to reduce both on-site and off-site impacts of soil OC (SOC) erosion. The aim of this research is to improve determination of the dominant terrestrial land-use sources of OC in freshwater sediment at a catchment scale and to assess the likely processes driving spatial and temporal changes in these sources. Four interlinked studies were conducted on two catchments to investigate specific objectives.

First, OC fingerprinting and carbon loss modelling (a combination of “net” soil erosion and OC spatial distribution modelling) were carried out using existing OC and *n*-alkane biomarker data from Carminowe Creek, a mixed land use catchment in Cornwall, UK. This unique combination of two sediment origin techniques crucially identified that riparian woodland disconnected upslope eroded SOC and, concomitantly, provided an input of woodland-derived OC to the streams, giving an increased understanding of sediment and OC transport processes.

Secondly, extensive new data from Loch Davan catchment, Aberdeenshire, was used to find the effect of novel combinations of *n*-alkane concentration ratios, *n*-alkane compound-specific stable isotopes (CSSI) and short-chain neutral lipid fatty acid (SC-NLFA) biomarkers on land use source discrimination using a Bayesian un-mixing model. In comparison to using only *n*-alkane ratios, a combination of *n*-alkane ratios and CSSI improved discrimination between arable and pasture land uses and using a combination of *n*-alkane ratios and SC-NLFA reduced error when discriminating four land uses (arable, pasture, forest and moorland).

Thirdly, in an innovative approach, OC source proportions were identified, in both streambed and suspended sediment (SS), at a headwater sub-catchment and catchment scale. Different drivers of OC dynamics were detectable at the two different scales (sub-catchment and catchment scale), and different dominant

land use sources were found in streambed and SS OC leading to improved identification of processes driving spatial and temporal OC dynamics.

And finally, soil erosion “hotspots” (i.e. where there is high risk of soil degradation) can be identified by modelling catchment erosion using a variety of different erosion models. The utility of these soil erosion models in identifying hotspots, and guiding Best Management Practices (BMP), depends upon their accuracy and there is a need to assess model usefulness. Thus, a new method was developed and tested using streambed sediment land use -specific yields estimated using OC fingerprinting as a benchmark to determine which erosion model best identified the relative land use OC yields in streambed sediment.

The new methods and findings from their application will improve determination of dominant terrestrial land-use sources of OC in freshwater sediment at a catchment scale, and support development of BMP to reduce impacts on land productivity and water quality due to changes in climate and human activity.

Keywords:

Organic carbon fingerprinting, carbon loss modelling, soil erosion, connectivity, *n*-alkanes, short-chain neutral lipid fatty acids

This work was supported by the Natural Environment Research Council and the Biotechnology and Biological Sciences Research Council (Grant number NE/R010218/1) through a studentship award to the author of this thesis by STARS (Soils Training and Research Studentships) Centre for Doctoral Training and Research Programme.

ACKNOWLEDGEMENTS

Firstly, I wish to express my sincere appreciation to all my supervisors. Without their unwavering help, encouragement, and inspiration, the achievement of this PhD would not have been realized. To Dr Toby Waine who has been there from the beginning and has provided help, guidance, and example of what it takes to successfully complete a PhD and become a well-rounded member of the academic community. To Prof. Jeroen Meersmans who's constant and infectious enthusiasm for his subject, boundless energy and continuing support for this project have been one of my main motivations to begin, continue, and successfully end this PhD process. To Dr Bob Grabowski who convincingly guided me through the wonderful world of soils and sediments and constantly encouraged me to venture into the equally wonderful world of collaboration and publication. Your encouragement and guidance always arrived just when I needed them. To Dr Miriam Glendell whose support, hospitality and role as co-ordinator significantly contributed to all aspects of this project and especially to the fieldwork and laboratory analysis without which this thesis would not exist. In addition, your outstanding editing skills have helped immeasurably to make this thesis what it is today.

Secondly, thank you to everyone at the James Hutton Institute, Aberdeen, who have helped me along this PhD journey. To Dr Barry Thornton, Dr Steve Addy and Dr Nikki Baggaley for giving me the benefit of their time, energy and expertise. To Helen Watson and Carol Taylor for sample collection, processing, and helping fieldwork go as smoothly as possible. My thanks also go to Dave Parish at the Game and Wildlife Conservancy Trust, Scottish Demonstration Farm, for invaluable advice and data which enriched my knowledge of my study catchment.

Thirdly, the contribution of the STARS CDT to this PhD cannot be understated. Without the support and camaraderie of all the STARS students, supervisors, and management team this PhD experience would have been significantly the poorer.

And last, but by no means least, thank you to my family and friends. You are all amazing people. Seeing all that you have achieved and are continuing to achieve in life will always keep me reaching for y own goals.

TABLE OF CONTENTS

LIST OF FIGURES

LIST OF TABLES

LIST OF EQUATIONS

LIST OF ABBREVIATIONS

BMP	Best Management Practices
C	Carbon
CI	Connectivity Index
CLM	Carbon Loss Model
CSSI	Compound-specific stable isotopes
DEM	Digital Elevation Model
ERM	Erosion Risk Model
FGS	Fine grained sediment
NLFA	Neutral Lipid Fatty Acid
OC	Organic Carbon
OCF	Organic Carbon Fingerprinting
RUSLE	Revised Universal Soil Loss Equation
SC-NLFA	Short Chain Neutral Lipid Fatty Acid
SOC	Soil Organic Carbon
SS	Suspended Sediment

1 Introduction

"…soils are recognised as a vital part of our economy, environment and heritage, to be safeguarded for existing and future generations"

The Scottish Soil Framework (Scottish Government, 2009)

Soils are the largest carbon pool on Earth and provide vital ecosystem services, including biomass production, grazing land, forestry and water filtering capacity (European Commission, 2021; Vogel et al., 2018; Wiesmeier et al., 2019). The ability to store carbon and absorb water (reducing the risk of flooding and drought), makes soil an indispensable part of climate change mitigation and adaptation (European Commission, 2021). This has led to "healthy soil" being a key part of many policies and strategies to further climate, biodiversity and economic objectives within the EU; such as the Green Deal for Europe (European Commission, 2022a), EU Soil Observatory (European Commission, 2022b) and the Scottish Soil Framework (Scottish Government, 2009). The recent EU Soil Strategy is an important deliverable of the European Green Deal (European Commission, 2022a) and aims to increase the carbon in agricultural soils, and ensure that, "by 2050, all soil ecosystems are in a healthy condition" (European Commission, 2021). One of the main obstacles to achieving these aims is soil erosion. Soil erosion leads to loss of fertile productive soil (Verstraeten et al., 2002), and leads to damaging off-site problems including water pollution and detrimental effects on infrastructure and aquatic environments due to sedimentation (Bilotta and Brazier, 2008; Owens et al., 2016; Rickson, 2014). Soil erosion is affect by the frequency and intensity of rainfall events, both of which are expected to increase under climate change (Nearing, Pruski and O'Neal, 2004). Identification of soil erosion "hotspots", where there is high risk of soil degradation, is a key step in ensuring land can be cultivated to maintain healthy soils and minimize the risk to watercourses (Baggaley et al., 2020).

Hotspots occur due to the combined effect of land management intensity and soil properties (Cloy et al., 2021) and there is no simple link between soil erosion hotspots and the soil organic carbon (OC) load in the waterways. The amount of

soil OC (SOC) and sediment eroded within a catchment is affected by catchment properties such as topography (slope), soil properties such as structure, texture, chemistry and OC content (soil erodibility), and also changes in land use and management - activities such as agriculture, deforestation and construction. The likelihood that the eroded sediment and OC will reach the waterways depends on the relationship between the catchment and the waterways - the connectivity (Fryirs, 2013).

In recent years, organic sediment fingerprinting (SF) techniques have been successfully employed to estimate the relative contribution of different terrestrial sources to organic matter load in waterways using vegetation and land use specific biomarkers, including a combination of bulk stable carbon and nitrogen isotopes and *n*-alkanes (Glendell et al., 2018; Zhang et al., 2017) and compound-specific stable isotopes (CSSI) of fatty acids and *n*-alkanes (Alewell et al., 2016; Cooper et al., 2015; Hirave et al., 2020a). The SF approach involves the collection of terrestrial catchment source samples and comparison of their physical and biogeochemical features or "fingerprints" to estimate the relative contribution of different upstream sources to a "sink" sediment (e.g., stream or lake). With a suitable set of OC biomarkers (or tracers), statistical unmixing models can be used to identify both the sediment sources and the amount of sediment contributed by each source. Bayesian modelling techniques are commonly employed (Cooper et al., 2015; Kelsey et al., 2020; Mabit et al., 2018) due to their ability to account for variability in both source and mixture (Stock and Semmens, 2016).

Tracers used in organic carbon fingerprinting (OCF) must be characteristic of the sources and be able to both identify and differentiate between them (Collins et al., 2020). In addition, tracers must be conservative (stable) between their upslope origins and the point at which they are sampled in the "sink" sediments (Collins et al., 2020). The primary source of SOC is from plant tissue, and a variety of organic compounds are transferred from plant to soil via plant residue deposition (e.g. leaf litter, root turnover). Bulk stable isotope signature for carbon (^{13}C) has been used previously as a tracer within OCF approaches (Glendell et

al., 2018; Zhang et al., 2017). However, more recent studies have suggested that it is not conservative (Hirave et al., 2020b). In contrast, *n*-alkanes, which are vegetation-specific neutral lipids derived from plant waxes (Lichtfouse et al., 1998), are considered to be comparatively stable against degradation in soil and sediment environments because of their relatively low solubility in water and resistance to microbial degradation (Collins et al., 2020; Eglinton and Eglinton, 2008; Lichtfouse et al., 1998). The different numbers of C atoms in the *n*-alkane molecule are characteristic of different origins. Short-chain *n*-alkanes (<C20) are dominant for bacteria or algae/plankton sources (Meyers, 2003). Submerged and floating aquatic macrophytes and lower plants (e.g. mosses) are dominated by mid-length chain *n*-alkanes (i.e., C20-C25) (Ficken et al., 2000; Meyers, 2003). Higher terrestrial plants are dominated by long-chain *n*-alkanes (>C25) with a strong odd-to-even carbon preference (odd-carbon-numbered chains predominate) (Eglinton and Hamilton, 1967; Ficken et al., 2000): Trees and shrub are dominated by C27 or C29 and grass is dominated by C31 or C33 (Bush and McInerney, 2013; Meyers, 2003; Zech et al., 2013). Therefore, long-chain (> C23) *n*-alkanes are suitable for tracing the origin of SOC from different land uses since as they are predominantly produced by higher plants. Ratios are commonly calculated for use as tracers: the relative percentage of *n*-alkanes C27, C29 and C31 (Torres et al., 2014); the C27 to C31 ratio (Puttock et al., 2014); PAQ, to understand aquatic versus terrestrial plant input (Ficken et al., 2000); the Odd-to-Even Predominance (OEP) for which higher values indicate less degraded organic matter (Zech et al., 2013); and the Average Chain length (ACL) (Fang et al., 2014) a summary of which can be found in Chapter 2 (Table 2).

The “fingerprint” for a specific soil can be considered the combination of past and present tracers (i.e. past and current vegetation) at a particular site. Consequently, due to rotation between land uses in agricultural catchments, arable, pasture and grasslands could end up with a very similar fingerprint (Upadhayay et al., 2017) and using a single technique can lead to limited land-use based source differentiation (Alewell et al., 2016; Glendell et al., 2018). In addition to *n*-alkane ratios, there are other land use specific tracers. Variability in the carbon isotopic signatures ($\delta^{13}C$) of organic compounds is driven both by

plant physiology/biochemistry and environmental factors (e.g. temperature, humidity, isotopic composition of water/CO_2) and is, therefore, (theoretically) unique for each individual plant and able to differentiate between different land cover types (Cooper et al., 2015 and references therein). Measuring $\delta^{13}C$ of individual *n*-alkanes or fatty acids provides a compound-specific stable isotope (CSSI) signature (Chikaraishi and Naraoka, 2003). Once fresh plant material has degraded to humic substances within the soil the CSSI signature is not expected to degrade over time (Blessing, Jochmann and Schmidt, 2008; Hirave et al., 2020b). CSSI analysis using long-chain fatty acids (LCFAs, >C22) or *n*-alkanes have been successfully employed in land-use-specific sediment source apportionment (Alewell et al., 2016; Blake et al., 2012; Gibbs, 2008; Hancock and Revill, 2013; Hirave et al., 2020a; Lavrieux et al., 2019; Mabit et al., 2018; Upadhayay et al., 2017). However, more research is needed to assess if the addition of CSSI to n-alkane ratios improves land use discrimination in river catchments. In addition, tracing terrestrial-to-aquatic fluxes of SOC can be further complicated by the direct deposition of organic material (leaf fall/litter) into the waterways from which the sediment samples are taken, masking the signature from any eroded terrestrial soil. Combining soil tracers of plant, fungal and bacterial origin may provide a fingerprint more characteristic of the soil rather than just the current land cover vegetation and allow greater discrimination between land uses. Similar to *n*-alkanes, fatty acids are transferred from plant leaves and roots and bind strongly to mineral particles in the soil (Blake et al., 2012). Short chain (shorter than C22) neutral lipid fatty acids (NLFA) can be of microbial or fungal rather than plant origin and have conventionally not been used as tracers in biogeochemical fingerprinting. Fatty acids (FA) are commonly used to measure abundance in soil microbial and fungal communities and the spatial distributions of soil microbial communities have been shown to depend mainly on soil properties (soil types and land cover) (Xue et al., 2018). Neutral lipids can persist in soils for decades and have proved to be effective tracers in distinguishing past land use (Lavrieux et al., 2012). Evidence that shorter chain FA may be preferentially degraded by soil microorganisms (Matsumoto et al., 2007) could suggest legacy effects of past crop cover or agricultural rotation may not be as

pronounced in the signature of SC-NLFA (Blake et al., 2012). Previous studies have found that fatty acids (FA), considered common to prokaryotic and eukaryotic organisms, were particularly relevant for land-use discrimination and distinguishing crop-specific signatures (Blake et al., 2012; Ferrari et al., 2015). Currently, research is needed to explore the potential of combined *n*-alkane ratios, CSSI and SC-NLFA to improve land use discrimination in OCF - improving the accuracy with which land use specific origins of stream OC can be identified.

Although OCF using suitable tracers can be used to identify the land use specific origin of stream OC, e.g., arable land, it is unlikely to pinpoint the exact origin of that OC as the same land use can exist in multiple locations in a catchment. Therefore, research is also needed to investigate if combining OCF source apportionment with other estimates of soil OC origins can further improve accuracy in apportioning OC sources.

The high degree of spatial heterogeneity in many river catchments - due to different combinations of catchment characteristics such as topography, soil properties, land use and management results in different likelihoods of soil erosion and connectivity to the streams (Vercruysse, Grabowski and Rickson, 2017). Discrepancy between upslope erosion sources and SOC transferred to waterbodies can be due to catchment connectivity factors, such as preferential runoff pathways (e.g. tramlines) and buffer zones (e.g. permanent riparian vegetation) (Gomes et al., 2019; Grabowski and Gurnell, 2016; Wohl et al., 2019). Catchment erosion sources can be predicted using erosion models that make quantitative predictions about how soil is redistributed within catchments. The Revised Universal Soil Loss Equation (RUSLE) (Desmet and Govers, 1996; Renard et al., 1997; Wischmeier and Smith, 1978) is a popular model for soil erosion prediction due to its simplicity in terms of required input data and relative reliability of soil loss estimates (Risse et al., 1993) and has been used extensively worldwide to predict potential soil loss by water erosion (Alewell et al., 2019; Borrelli et al., 2014; Borselli, Cassi and Torri, 2008; Ganasri and Ramesh, 2016; Mahoney, Blandford and Fox, 2021; Michalek, Zarnaghsh and Husic, 2021; Rajbanshi and Bhattacharya, 2020; Tan et al., 2018; Wu, He and Ma, 2020). It

estimates long-term average annual soil loss based on rainfall intensity, soil properties (erodibility), topography and land use and management. The extensive scientific literature and data accessibility for RUSLE (Alewell et al., 2019; ESDAC, 2014, 2015a; Panagos et al., 2014, 2015a) mean it is readily applied to a wide variety of catchments using existing data. RUSLE was originally designed for use in agricultural environments with primarily mineral soils and moderate slopes. Alternatively, in Scotland, tools have been developed to represent the specific soil conditions in that region and to predict how soils respond to land use and management pressures. These soil risk maps help stakeholders plan agricultural activities to minimize the risk of erosion and manage their soils sustainably (Baggaley et al., 2020; Lilly and Baggaley, 2018). The erosion risk map (ERM) of Lilly and Baggaley (2018) covers a large proportion of the Scottish mainland and shows the erosion risk of bare soil under intense or extended rainfall; risk for mineral soils is classified separately from those with organic (peaty) surface layers.

Irrespective of the erosion model chosen, there is unlikely to be a simple link between areas of soil erosion and the OC load in waterways due to the diverse processes influencing the fluxes of SOC in catchments. The probability that eroded soil propagates downslope to a waterway potentially causing off-site effects depends on the degree of connectivity between the source and the waterway (Borselli, Cassi and Torri, 2008; Fryirs, 2013). The index of connectivity (CI) approach of Borselli et al. (2008) was designed to assess catchment connectivity using the available topographic information only. This sediment connectivity index was successfully applied in other European catchments (López-Vicente et al., 2013) and was further developed by Cavalli et al. (2013) to allow calculation of the index using only a high resolution digital terrain model, such as those derived from LiDAR. Using the CI approach, sources identified using soil erosion methods (e.g. RUSLE) can be connected, through catchment slopes, to terrain “sinks”, providing an estimate of connection between upslope erosion hotspots and streams. Measuring and mapping the soil OC content of catchment soils and combining this with RUSLE and CI in a “carbon loss model” (CLM), can give an alternative (to OCF) estimation of the relative importance of

land use sources of SOC to catchment streams. Currently, research is needed to assess whether combining a CLM with OCF source apportionment can help to, i) reduce ambiguity in apportioning OC fluxes when the same land use exists in multiple locations within a catchment, and ii) identify factors affecting OC delivery to streams e.g., buffer zones.

Additionally, in combining a CLM with OCF, the OCF source apportionment can be considered as a “land use -specific” relative OC yield (Blake et al., 2012) which is compared to the relative importance of land use sources estimated by the CLM. The utility of any soil erosion risk model in identifying hotspots and guiding BMP depends upon their accuracy. Batista et al. (2019) refuted the notion that soil erosion models can be validated and instead emphasized the necessity of defining “fit-for-purpose tests” that allow for a broad investigation of model usefulness. The spatial and temporal variability of soil erosion require multiple observations in time and space, making quantitative erosion measurements expensive, time consuming and uncertain (Batista et al., 2019). This results in a limited amount of detailed data quantifying sediment yields, especially at a catchment scale (Rompaey et al., 2001). Research is currently needed to assess if OCF estimates of “land use -specific” relative OC yield (when used as a benchmark) could be an invaluable tool to evaluate if erosion models are “fit-for-purpose” or assess the suitability of one erosion model over another.

There remain challenges in the application OCF including i) effects on tracer signatures due to sorting effect of particles by size during mobilization, transport and deposition and ii) ensuring all sources of SOC are included. More research is needed to identify methods to address these challenges as better understanding of the tracers used in OCF - how their fingerprints are affected in the field by erosion, transport and deposition environments, and in sample collection, processing and analysis - leads to reduced uncertainty in OCF source apportionment. Improved confidence in OCF could lead to an improved understanding of catchment OC dynamics and an improved benchmark to assess if erosion models are “fit-for-purpose”.

1.1 Research aim and objectives

Improved identification of “hotspots”, where there is high risk of OC erosion and soil degradation, is a key step to help maintain the “healthy soils” that are a key part of policies and strategies to further climate, biodiversity and economic objectives within the EU. The aim of this research is to improve determination of the dominant terrestrial land-use sources of OC in freshwater sediment at a catchment scale and to assess the likely catchment processes driving spatial and temporal changes in these sources. This research would support the development of targeted sediment management strategies to reduce impacts on land productivity and water quality due to changes in climate and human activity.

Figure 1 Research aim and objectives

Objective 1: To assess if combining OCF and a carbon loss model (CLM) can enhance knowledge of the fate of eroded soil OC and terrestrial-to-aquatic OC fluxes

Objective 2: To assess if the use of sediment-associated shorter-chain neutral lipids fatty acid (SC-NLFA) concentrations and carbon isotope signatures in addition to those for longer-chain *n*-alkane tracers, improves the ability of sediment fingerprinting to distinguish between land-use specific sources of freshwater OC load

Objective 3: To consider land-use specific origins of freshwater OC in streambed and suspended sediment and estimate intra-annual catchment soil OC dynamics using OCF.

Objective 4: To compare CLM constructed using i) RUSLE and ii) the Scottish erosion risk map (ERM) of Lilly and Baggaley, (2018), to determine which erosion model best identifies the relative land use OC yields in streambed sediment using OCF as a benchmark

1.2 Study Sites

1.2.1 Objective 1 - Carminowe Creek, Cornwall, UK

In the mixed land use Carminowe Creek catchment, there has been an increasing input of woodland-derived organic matter to sediments at the catchment outlet (Loe Pool) over a period of 60 years. The increased input is likely related to enhanced soil erosion, or an increase in riparian woodland disconnecting inputs from upslope arable sources (Glendell et al., 2018). Existing data of Glendell et al. (2018) was used to assess if combining OCF and a CLM could enhance knowledge of the fate of eroded soil OC and terrestrial-to-aquatic OC fluxes in the catchment.

1.2.2 Objectives 2, 3 and 4 - Loch Davan and Logie Burn, Aberdeenshire, Scotland, UK

Between 2007 and 2018, Loch Davan and its main feeder stream, Logie Burn, were classified as having poor to moderate ecological status (SEPA, 2021). It

was likely that inputs of nutrient rich sediment resulting from land use intensification had contributed to a significant reduction in the loch area over the last century (Addy, Ghimire and Cooksley, 2012). Thus, the catchment is well suited to the study and research findings would have direct management applications in identifying erosion risk “hotspots” and the sources and drivers of OC input to the Logie Burn and its tributaries.

1.3 Thesis outline

The thesis has been written in a paper format and is made up of four journal articles arranged as individual chapters (Chapters 2 to 5) followed by a discussion and conclusions. Chapter 2 will be published in the Journal of Soils and Sediments (accepted on Tuesday 15th March 2022). Chapters 3, 4 and 5 will be submitted for review after completion of this thesis. All original work was carried out by the author of this thesis, with contributions of the co-authors as stated in Table 1.1.

Chapter 2: Showed how uniquely combining multiple modelling approaches to investigate catchment carbon dynamics allowed for an increased understanding of sediment and organic carbon transport processes in the study catchment, in Cornwall.

In *Chapter 3:* Showed that using a combination of soil biomarkers of plant, fungal and bacterial origin would allow greater discrimination between land uses in OCF and explored the potential of short chain (shorter than C22) neutral lipid fatty acids to improve land use discrimination in the Loch Davan catchment in Scotland as a case study.

In *Chapter 4:* Streambed and suspended sediments were compared to, i) define temporal changes in land use sources using OCF and ii) investigate factors affecting *n*-alkane biomarker signature

In *Chapter 5:* OCF was used as a benchmark to compare the ability of different erosion models to predict relative land use OC yields in streambed sediment and, by extension, the soil OC degradation hotspots to be targeted for Best Management Practices (BMP)

An appendix is included at the end of the document providing additional information on the data used in this thesis.

Table 1: Author contributions to chapters already submitted or intended for publication in peer-reviewed academic journals.

Author	Contribution
Katy Wiltshire	Data analysis, methodology development, discussion, layout, writing (All Chapters)
Toby Waine (supervisor) Robert Grabowski (co-supervisor)	Guidance on method and structure, advice, editing (All Chapters)
Jeroen Meersmans (supervisor) Miriam Glendell (co-supervisor)	Conceptualisation and funding acquisition. Guidance on method and structure, advice, editing (All Chapters)
Barry Thornton (Laboratory advisor)	Guidance on laboratory analysis and methods (Chapter 3 and 4).
Steve Addy (Fieldwork and catchment advisor)	Guidance on catchment definition and fieldwork organisation (Chapter 3 and 4)
Nikki Baggaley (Soils and soil erosion advisor)	Guidance on soil erosion data availability and interpretation (Chapter 5)
Fiona Napier (Case partner)	Guidance on catchment definition and analysis (Chapters 3, 4 and 5)

1.4 References

Addy, S., Ghimire, S. and Cooksley, S. (2012) 'Assessment of the multiple benefits of river restoration: the Logie Burn meander reconnection project', *BHS Eleventh National Symposium, Hydrology for a changing world, Dundee 2012*, , pp. 01–05.

Alewell, C., Birkholz, A., Meusburger, K., Schindler Wildhaber, Y. and Mabit, L. (2016) ‘Quantitative sediment source attribution with compound-specific isotope analysis in a C3 plant-dominated catchment (central Switzerland)’, *Biogeosciences*, 13(5), pp. 1587–1596.

Alewell, C., Borrelli, P., Meusburger, K. and Panagos, P. (2019) ‘Using the USLE: Chances, challenges and limitations of soil erosion modelling’, *International Soil and Water Conservation Research*, 7(3) Elsevier Ltd, pp. 203–225.

Baggaley, N., Lilly, A., Blackstock, K., Dobbie, K., Carson, A. and Leith, F. (2020) ‘Soil risk maps – Interpreting soils data for policy makers, agencies and industry’, *Soil Use and Management*, 36(1), pp. 19–26.

Batista, P.V.G., Davies, J., Silva, M.L.N. and Quinton, J.N. (2019) ‘On the evaluation of soil erosion models: Are we doing enough?’, *Earth-Science Reviews*, 197(July) Elsevier, p. 102898.

Blake, W.H., Ficken, K.J., Taylor, P., Russell, M.A. and Walling, D.E. (2012) ‘Tracing crop-specific sediment sources in agricultural catchments’, *Geomorphology*, 139–140 Elsevier B.V., pp. 322–329.

Blessing, M., Jochmann, M.A. and Schmidt, T.C. (2008) ‘Pitfalls in compound-specific isotope analysis of environmental samples’, *Analytical and Bioanalytical Chemistry*, 390(2), pp. 591–603.

Borrelli, P., Märker, M., Panagos, P. and Schütt, B. (2014) ‘Modeling soil erosion and river sediment yield for an intermountain drainage basin of the Central Apennines, Italy’, *Catena*, 114 Elsevier B.V., pp. 45–58.

Borselli, L., Cassi, P. and Torri, D. (2008) ‘Prolegomena to sediment and flow connectivity in the landscape: A GIS and field numerical assessment’, *Catena*, 75(3), pp. 268–277.

Bush, R.T. and McInerney, F.A. (2013) ‘Leaf wax n-alkane distributions in and across modern plants: Implications for paleoecology and chemotaxonomy’, *Geochimica et Cosmochimica Acta*, 117 Elsevier Ltd, pp. 161–179.

Cavalli, M., Trevisani, S., Comiti, F. and Marchi, L. (2013) ‘Geomorphometric assessment of spatial sediment connectivity in small Alpine catchments’, *Geomorphology*, 188 Elsevier B.V., pp. 31–41.

Chikaraishi, Y. and Naraoka, H. (2003) Compound-specific δD-δ13C analyses of n-alkanes extracted from terrestrial and aquatic plants *Phytochemistry*.

Cloy, J.M., Lilly, A., Hargreaves, P.R., Gagkas, Z., Dolan, S., Baggaley, N.J., Stutter, M., Crooks, B., Elrick, G. and McKenzie, B.. (2021) *A state of knowledge overview of identified pathways of diffuse pollutants to the water environment. CRW2018_18.*

Collins, A.L., Blackwell, M., Boeckx, P., Chivers, C.A., Emelko, M., Evrard, O., Foster, I., Gellis, A., Gholami, H., Granger, S., Harris, P., Horowitz, A.J., Laceby, J.P., Martinez-Carreras, N., Minella, J., Mol, L., Nosrati, K., Pulley, S., Silins, U., da Silva, Y.J., Stone, M., Tiecher, T., Upadhayay, H.R. and Zhang, Y. (2020) *Sediment source fingerprinting: benchmarking recent outputs, remaining challenges and emerging themes*. Journal of Soils and Sediments.

Cooper, R.J., Pedentchouk, N., Hiscock, K.M., Disdle, P., Krueger, T. and Rawlins, B.G. (2015) ‘Apportioning sources of organic matter in streambed sediments: An integrated molecular and compound-specific stable isotope approach’, *Science of the Total Environment*, 520 Elsevier B.V., pp. 187–197.

Desmet, P.J.J. and Govers, G. (1996) ‘A GIS procedure for automatically calculating the USLE LS factor on topographically complex landscape units’, *Journal of Soil and Water Conservation*, 51(5), pp. 427–433.

Eglinton, G. and Hamilton, R.J. (1967) ‘Leaf epicuticular waxes’, *Science*, 156(3780), pp. 1322–1335.

Eglinton, T.I. and Eglinton, G. (2008) ‘Molecular proxies for paleoclimatology’, *Earth and Planetary Science Letters*, 275(1–2), pp. 1–16.

ESDAC (2014) *Soil Erodibility (K- Factor) High Resolution dataset for Europe*., *Joint Research Centre of the European Commission* Available at: https://esdac.jrc.ec.europa.eu/content/soil-erodibility-k-factor-high-resolution-

dataset-europe (Accessed: 7 June 2019).

ESDAC (2015) *Estimating the soil erosion cover-management factor at European scale*., *Joint Research Centre of the European Commission* Available at: https://esdac.jrc.ec.europa.eu/content/cover-management-factor-c-factor-eu (Accessed: 19 March 2012).

European Commission (2021) *EU Soil Strategy for 2030: Reaping the benefits of healthy soils for people, food, nature and climate*.

European Commission (2022a) *A European Green Deal: Striving to be the first climate-neutral continent*. Available at: https://ec.europa.eu/info/strategy/priorities-2019-2024/european-green-deal_en (Accessed: 13 March 2022).

European Commission (2022b) *EU Soil Observatory (EUSO)*. Available at: https://joint-research-centre.ec.europa.eu/eu-soil-observatory-euso_en (Accessed: 13 March 2022).

Fang, J., Wu, F., Xiong, Y., Li, F., Du, X., An, D. and Wang, L. (2014) 'Source characterization of sedimentary organic matter using molecular and stable carbon isotopic composition of n-alkanes and fatty acids in sediment core from Lake Dianchi, China', *Science of the Total Environment*, 473–474, pp. 410–421.

Ferrari, A.E., Ravnskov, S., Larsen, J., Tønnersen, T., Maronna, R.A. and Wall, L.G. (2015) 'Crop rotation and seasonal effects on fatty acid profiles of neutral and phospholipids extracted from no-till agricultural soils', *Soil Use and Management*, 31(1), pp. 165–175.

Ficken, K.J., Li, B., Swain, D.L. and Eglinton, G. (2000) 'An n-alkane proxy for the sedimentary input of submerged/floating freshwater aquatic macrophytes', *Organic Geochemistry*, 31(7–8), pp. 745–749.

Fryirs, K. (2013) '(Dis)Connectivity in catchment sediment cascades: A fresh look at the sediment delivery problem', *Earth Surface Processes and Landforms*, 38(1), pp. 30–46.

Ganasri, B.P. and Ramesh, H. (2016) ‘Assessment of soil erosion by RUSLE model using remote sensing and GIS - A case study of Nethravathi Basin’, *Geoscience Frontiers*, 7(6) Elsevier Ltd, pp. 953–961.

Gibbs, M.M. (2008) ‘Identifying source soils in contemporary estuarine sediments: A new compound-specific isotope method’, *Estuaries and Coasts*, 31(2), pp. 344–359.

Glendell, M., Jones, R., Dungait, J.A.J., Meusburger, K., Schwendel, A.C., Barclay, R., Barker, S., Haley, S., Quine, T.A. and Meersmans, J. (2018) ‘Tracing of particulate organic C sources across the terrestrial-aquatic continuum, a case study at the catchment scale (Carminowe Creek, southwest England)’, *Science of the Total Environment*, 616, pp. 1077–1088. Available at: 10.1016/j.scitotenv.2017.10.211 (Accessed: 5 September 2018).

Gomes, T.F., Van de Broek, M., Govers, G., Silva, R.W.C., Moraes, J.M., Camargo, P.B., Mazzi, E.A. and Martinelli, L.A. (2019) ‘Runoff, soil loss, and sources of particulate organic carbon delivered to streams by sugarcane and riparian areas: An isotopic approach’, *Catena*, 181(June) Elsevier, p. 104083.

Grabowski, R.C. and Gurnell, A.M. (2016) ‘Diagnosing problems of fine sediment delivery and transfer in a lowland catchment’, *Aquatic Sciences*, 78(1) Springer Basel, pp. 95–106.

Hancock, G.J. and Revill, A.T. (2013) ‘Erosion source discrimination in a rural Australian catchment using compound-specific isotope analysis (CSIA)’, *Hydrological Processes*, 27(6), pp. 923–932.

Hirave, P., Glendell, M., Birkholz, A. and Alewell, C. (2020a) ‘Compound-specific isotope analysis with nested sampling approach detects spatial and temporal variability in the sources of suspended sediments in a Scottish mesoscale catchment’, *Science of The Total Environment*, (xxxx) The Authors, p. 142916.

Hirave, P., Wiesenberg, G.L.B., Birkholz, A. and Alewell, C. (2020b) ‘Understanding the effects of early degradation on isotopic tracers: implications for sediment source attribution using compound-specific isotope analysis (CSIA)’,

Biogeosciences Discussions, (June), pp. 1–18.

Kelsey, S.A., Grottoli, A.G., Bauer, J.E., Lorenz, K., Lal, R., Matsui, Y. and Huey-Sanders, T.M. (2020) 'Effects of agricultural and tillage practices on isotopic signatures and fluxes of organic and inorganic carbon in headwater streams', *Aquatic Sciences*, 82(2) Springer International Publishing, pp. 1–13.

Lavrieux, M., Birkholz, A., Meusburger, K., Wiesenberg, G.L.B., Gilli, A., Stamm, C. and Alewell, C. (2019) 'Plants or bacteria? 130 years of mixed imprints in Lake Baldegg sediments (Switzerland), as revealed by compound-specific isotope analysis (CSIA) and biomarker analysis', *Biogeosciences*, 16(10), pp. 2131–2146.

Lavrieux, M., Bréheret, J.G., Disnar, J.R., Jacob, J., Le Milbeau, C. and Zocatelli, R. (2012) 'Preservation of an ancient grassland biomarker signature in a forest soil from the French Massif Central', *Organic Geochemistry*, 51, pp. 1–10.

Lichtfouse, É., Chenu, C., Baudin, F., Leblond, C., Da Silva, M., Behar, F., Derenne, S., Largeau, C., Wehrung, P. and Albrecht, P. (1998) 'A novel pathway of soil organic matter formation by selective preservation of resistant straight-chain biopolymers: Chemical and isotope evidence', *Organic Geochemistry*, 28(6), pp. 411–415.

Lilly, A. and Baggaley, N.J. (2018) *Soil erosion risk map of Scotland* James Hutton Institute, Aberdeen

López-Vicente, M., Poesen, J., Navas, A. and Gaspar, L. (2013) 'Predicting runoff and sediment connectivity and soil erosion by water for different land use scenarios in the Spanish Pre-Pyrenees', *Catena*, 102 Elsevier B.V., pp. 62–73.

Mabit, L., Gibbs, M., Mbaye, M., Meusburger, K., Toloza, A., Resch, C., Klik, A., Swales, A. and Alewell, C. (2018) 'Novel application of Compound Specific Stable Isotope (CSSI) techniques to investigate on-site sediment origins across arable fields', *Geoderma*, 316(August 2017) Elsevier, pp. 19–26.

Mahoney, D., Blandford, B. and Fox, J. (2021) 'Coupling the probability of connectivity and RUSLE reveals pathways of sediment transport and soil loss

rates for forest and reclaimed mine landscapes', *Journal of Hydrology*, 594(January) Elsevier B.V., p. 125963.

Meyers, P.A. (2003) 'Application of organic geochemistry to paleolimnological reconstruction: a summary of examples from the Laurention Great Lakes', *Organic Geochemistry*, 34, pp. 261–289.

Michalek, A., Zarnaghsh, A. and Husic, A. (2021) 'Modeling linkages between erosion and connectivity in an urbanizing landscape', *Science of the Total Environment*, 764 Elsevier B.V., p. 144255.

Nearing, M.A., Pruski, F.F. and O'Neal, M.R. (2004) 'Expected climate change impacts on soil erosion rates: A review', *Journal of Soil and Water Conservation*, 59(1), pp. 43–50.

Panagos, P., Ballabio, C., Borrelli, P., Meusburger, K., Klik, A., Rousseva, S., Tadić, M.P., Michaelides, S., Hrabalíková, M., Olsen, P., Aalto, J., Lakatos, M., Rymszewicz, A., Dumitrescu, A., Beguería, S. and Alewell, C. (2015) 'Rainfall erosivity in Europe', *Science of the Total Environment*, 511, pp. 801–814.

Panagos, P., Meusburger, K., Ballabio, C., Borrelli, P. and Alewell, C. (2014) 'Soil erodibility in Europe: A high-resolution dataset based on LUCAS', *Science of the Total Environment*, 479–480(1) Elsevier B.V., pp. 189–200.

Puttock, A., Dungait, J.A.J., Macleod, C.J.A., Bol, R. and Brazier, R.E. (2014) 'Organic Carbon From Dryland Soils', *Journal of Geophysical Research: Biogeosciences*, 119, pp. 2345–2357.

Rajbanshi, J. and Bhattacharya, S. (2020) 'Assessment of soil erosion, sediment yield and basin specific controlling factors using RUSLE-SDR and PLSR approach in Konar river basin, India', *Journal of Hydrology*, 587(January) Elsevier, p. 124935.

Renard, K.G., Foster, G.R., Weesies, G.A., Mc Cool, D.K. and Yoder, D.C. (1997) *Predicting soil erosion by water: A guide to conservation planning with the revised universal soil loss equation (RUSLE).*Agricultur. Washington, D.C.: U.S. Dept. of Agriculture, Agricultural Research Service.

Risse, L.M., Nearing, M.A., Nicks, A.D. and Laflen, J.M. (1993) 'Error Assessment in the Universal Soil Loss Equation', *Soil Science Society of America Journal*, 57(3)

Van Rompaey, A.J.J., Verstraeten, G., van Oost, K., Govers, G. and Poesen, J. (2001) 'Modelling mean annual sediment yield using a distributed approach', *Earth Surface Processes and Landforms*, 1236, pp. 1221–1236.

Scottish Government (2009) *The Scottish Soil Framework*.

SEPA (2021) *Water Classification Hub*., *Scottish Environment Protection Agency*

Stock, B.C. and Semmens, B.X. (2016) *MixSIAR GUI User Manual. Version 3.1*

Tan, Z., Leung, L.R., Li, H.Y. and Tesfa, T. (2018) 'Modeling Sediment Yield in Land Surface and Earth System Models: Model Comparison, Development, and Evaluation', *Journal of Advances in Modeling Earth Systems*, 10(9), pp. 2192–2213.

Torres, T., Ortiz, J.E., Martín-Sánchez, D., Arribas, I., Moreno, L., Ballesteros, B., Blázquez, A.N.A., Domínguez, J.A. and Estrella, T.R. (2014) 'The long pleistocene record from the pego-oliva marshland (Alicante-Valencia, Spain)', *Geological Society Special Publication*, 388(1), pp. 429–452.

Upadhayay, H.R., Bodé, S., Griepentrog, M., Huygens, D., Bajracharya, R.M., Blake, W.H., Dercon, G., Mabit, L., Gibbs, M., Semmens, B.X., Stock, B.C., Cornelis, W. and Boeckx, P. (2017) 'Methodological perspectives on the application of compound-specific stable isotope fingerprinting for sediment source apportionment', *Journal of Soils and Sediments*, 17(6) Journal of Soils and Sediments, pp. 1537–1553.

Vercruysse, K., Grabowski, R.C. and Rickson, R.J. (2017) 'Suspended sediment transport dynamics in rivers: Multi-scale drivers of temporal variation', *Earth-Science Reviews*, 166 Elsevier B.V., pp. 38–52.

Vogel, H.J., Bartke, S., Daedlow, K., Helming, K., Kögel-Knabner, I., Lang, B., Rabot, E., Russell, D., Stößel, B., Weller, U., Wiesmeier, M. and Wollschläger,

U. (2018) ‘A systemic approach for modeling soil functions’, *Soil*, 4(1), pp. 83–92.

Wiesmeier, M., Urbanski, L., Hobley, E., Lang, B., von Lützow, M., Marin-Spiotta, E., van Wesemael, B., Rabot, E., Ließ, M., Garcia-Franco, N., Wollschläger, U., Vogel, H.J. and Kögel-Knabner, I. (2019) ‘Soil organic carbon storage as a key function of soils - A review of drivers and indicators at various scales’, *Geoderma*, 333(July 2018) Elsevier, pp. 149–162.

Wischmeier, W. and Smith, D. (1978) *Predicting rainfall erosion losses: a guide to conservation planning. Agricultural Handbook No. 537.* U. S. Department of Agriculture., Washington (DC)

Wohl, E., Brierley, G., Cadol, D., Coulthard, T.J., Covino, T., Fryirs, K.A., Grant, G., Hilton, R.G., Lane, S.N., Magilligan, F.J., Meitzen, K.M., Passalacqua, P., Poeppl, R.E., Rathburn, S.L. and Sklar, L.S. (2019) ‘Connectivity as an emergent property of geomorphic systems’, *Earth Surface Processes and Landforms*, 44(1), pp. 4–26.

Wu, L., He, Y. and Ma, X. (2020) ‘Can soil conservation practices reshape the relationship between sediment yield and slope gradient?’, *Ecological Engineering*, 142(October 2019) Elsevier, p. 105630.

Xue, P.P., Carrillo, Y., Pino, V., Minasny, B. and McBratney, A.B. (2018) ‘Soil Properties Drive Microbial Community Structure in a Large Scale Transect in South Eastern Australia’, *Scientific Reports*, 8(1) Springer US, pp. 1–11.

Zech, M., Krause, T., Meszner, S. and Faust, D. (2013) ‘Incorrect when uncorrected: Reconstructing vegetation history using n-alkane biomarkers in loess-paleosol sequences - A case study from the Saxonian loess region, Germany’, *Quaternary International*, 296 Elsevier Ltd and INQUA, pp. 108–116.

Zhang, Y., Collins, A.L., McMillan, S., Dixon, E.R., Cancer-Berroya, E., Poiret, C. and Stringfellow, A. (2017) ‘Fingerprinting source contributions to bed sediment-associated organic matter in the headwater subcatchments of the River Itchen SAC, Hampshire, UK’, *River Research and Applications*, 33(10), pp. 1515–1526.

2 Assessing the source and delivery processes of organic carbon within a mixed land use catchment using a combined *n*-alkane and carbon loss modelling approach

Abstract

Purpose: Understanding fluxes of soil organic carbon (OC) from the terrestrial-to-aquatic environments is crucial to evaluate their importance within the global carbon cycle. Sediment fingerprinting (SF) is increasingly used to identify land use specific sources of OC, and, while this approach estimates the relative contribution of different sources to OC load in waterways, the high degree of spatial heterogeneity in many river catchments makes it challenging to precisely align the source apportionment results to the landscape. In this study, we integrate OC SF source apportionment with a carbon loss model (CLM) with the aim of: i) reducing ambiguity in apportioning OC fluxes when the same land use exists in multiple locations within a catchment, and ii) identifying factors affecting OC delivery to streams e.g., buffer zones.

Methods: Two main approaches were used in this study: (i) identification of the sources of freshwater bed sediment OC using *n*-alkane biomarkers and a Bayesian based unmixing model, and (ii) modelling and analysis of spatial data to construct a CLM using a combination of soil OC content modelling, RUSLE soil erosion modelling and a connectivity index. The study was carried out using existing OC and *n*-alkane biomarker data from a mixed land use UK catchment.

Results: SF revealed that woodland was the dominant source of the OC found in the streambed fine sediment, contributing between 81% and 85% at each streambed site. In contrast, CLM predicted that arable land was likely the dominant source of OC, with negligible inputs from woodland. The areas of greatest OC loss in the CLM were predicted to be from arable land on steeper slopes surrounding the stream channels. Results suggest extensive riparian woodland disconnected upslope eroded soil OC and, concomitantly, provided an input of woodland-derived OC to the streams. It is likely the woodland

contribution to streambed OC is derived from litter and leaves rather than soil erosion.

Conclusion: This study demonstrates how location-specific OC sources and delivery processes can be better determined using sediment fingerprinting in combination with CLM, rather than using sediment fingerprinting alone. It highlights that, although wooded riparian buffer strips may reduce the impact of upslope, eroded soil OC on waterways, they could themselves be a source of OC to stream sediments through more direct input (e.g., organic litter or leaf debris). Characterising this direct woodland OC as a separate source within future fingerprinting studies would allow the contributions from any eroded woodland soil OC to be better estimated.

Introduction

Soils provide essential ecosystem services, including biomass production, grazing land, forestry, water filtering capacity and, most critically for climate regulation, storage of carbon (Vogel et al., 2018; Wiesmeier et al., 2019). The importance of soil organic carbon (SOC) is widely recognized for soil structure, productivity, and the global C cycle. Soil erosion linked to climate change and human activity threatens the ability of this largely non-renewable resource (Gobin et al., 2004) to continue its vital roles and has detrimental effects on infrastructure and aquatic environments due to excess land to water sediment fluxes (Bilotta and Brazier, 2008; Owens et al., 2016; Rickson, 2014).

The assessment of the relative contribution of different terrestrial sources to organic matter load in waterways can be achieved using sediment fingerprinting (SF) with plant-specific biomarkers (Alewell et al., 2016; Cooper et al., 2015; Glendell et al., 2018; Hirave et al., 2020a; Zhang et al., 2017). Although SF can identify the land use specific origin of stream OC, it cannot pinpoint the exact origin of that OC if the same land use exists in multiple locations within a catchment - each with different susceptibility to erosion and connectivity to the streams. Source classifications within SF are often too broad (e.g., arable land or forest) to enable precise sources (e.g., specific fields or landscape features) to be determined and management strategies to be targeted (Owens et al., 2016).

The ambiguity in OC origin can be reduced if the spatial distribution of erosion prone areas and their likely connection to the streams can be identified. Net catchment erosion can be modelled using sediment delivery models (e.g., WaTEM/SEDEM (Van Oost, Govers and Desmet, 2000; Van Rompaey et al., 2001; Verstraeten et al., 2002)), however, accurate predictions for these models require calibration, commonly carried out using outlet sediment yield data (Krasa et al., 2019; Luo et al., 2020). However, sediment yield data are not available for many catchments, and is usually only available at the catchment outlet. For catchments where a lack of sediment yield data may negate the advantage that could be obtained from the application of more sophisticated erosion and routing models, a simple carbon loss model (CLM) can be constructed using spatially distributed carbon sampling (commonly collected for land use specific SF), together with an empirical erosion model, such as the Revised Universal Soil Loss Equation (RUSLE) (Desmet and Govers, 1996; Renard et al., 1997; Wischmeier and Smith, 1978), and a connectivity index (CI) which provides an estimate of potential connection between areas of upslope erosion and streams. The extensive literature and data accessibility for RUSLE and CI mean these methods can be easily applied in a wide variety of catchments using available data (Alewell et al., 2019; Cavalli et al., 2013; ESDAC, 2014, 2015a; Panagos et al., 2014, 2015a).

In Carminowe Creek catchment, Cornwall, UK, there has been an increasing input of woodland-derived organic matter to sediments in Loe Pool (the lake at the catchment outlet) over a period of 60 years (Glendell et al., 2018). Glendell et al. (2018) concluded this increase could be related to enhanced soil erosion, or alternatively, an increase in riparian woodland disconnecting OM inputs from upslope arable land uses. They suggested that coupling fingerprinting with soil erosion modelling could be a useful tool for quantifying these terrestrial-to-aquatic OC fluxes. To this end, this study quantifies the relative contributions of woodland and arable soil OC to the sediments of multiple sites in streams leading to Loe Pool using the existing *n*-alkane biomarker data of Glendell et al. (2018) with a Bayesian unmixing model SF approach. SF estimates were compared with the sources of eroded soil OC reaching the streams estimated using a CLM to assess

the origins and delivery processes of streambed OC. The aim of this paper is to evaluate whether location-specific OC sources and delivery processes can be better determined using SF in combination with CLM, rather than SF alone.

2.1 Material and methods

Two main approaches were used in the study: (i) identification of the sources of freshwater bed sediment OC using *n*-alkane biomarkers and a Bayesian based unmixing model, and (ii) modelling and analysis of spatial data to construct a CLM using a combination of % SOC content modelling, RUSLE soil erosion modelling and a connectivity index (CI) (Borselli, Cassi and Torri, 2008; Cavalli et al., 2013) (SOC% x RUSLE x CI).

2.1.1 Study catchment

Carminowe Creek catchment (4.8 km^2) in south-west England, UK (Figure 2) drains into a large freshwater lake, Loe Pool (0.54 km^2). Carminowe Creek comprises two main streams (referred to below as “North” and “South” streams), with a joint outlet to Loe Pool on its eastern side. The mean annual precipitation is ca. 1,000 mm and mean annual temperature is ca. 11°C (Met Office, 2021a). The catchment bedrock of Devonian mudstone, siltstone and sandstone is overlaid by freely draining loamy soils. The principal land use within the catchment is arable with areas of permanent grassland found on steeper slopes and woodland predominantly found along the riparian corridor (Glendell et al., 2018).

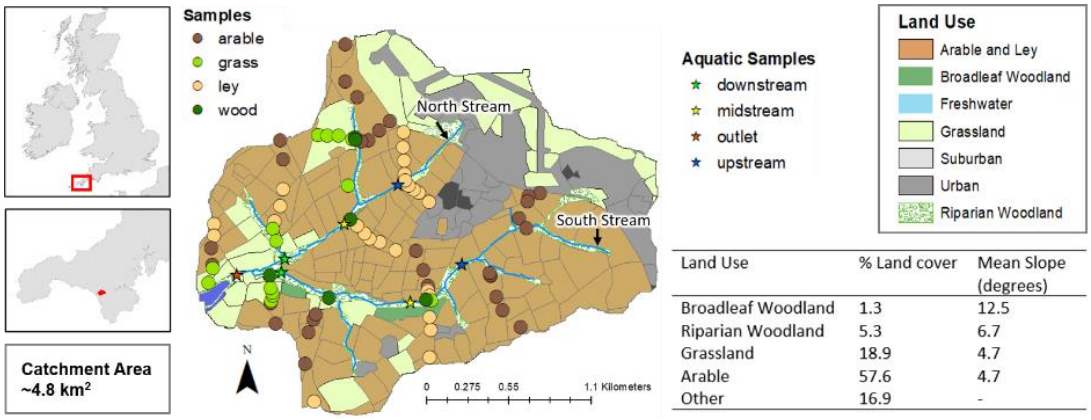

Land Use	% Land cover	Mean Slope (degrees)
Broadleaf Woodland	1.3	12.5
Riparian Woodland	5.3	6.7
Grassland	18.9	4.7
Arable	57.6	4.7
Other	16.9	-

Figure 2: Carminowe Creek catchment, UK, showing the different land uses and terrestrial and aquatic sample locations (adapted from Glendell et al. (2018)) and a summary of percentage cover and mean slope (in degrees – derived from LiDAR based digital terrain and surface model for SW England [TELLUS SW-Project] ©NERC (Centre for Ecology & Hydrology; British Antarctic Survey; British Geological Survey) (Ferraccioli et al., 2014)) for catchment land uses

2.1.2 Samples and analysis

Existing soil and sediment data were used for this research. Full details of sample collection, processing and analysis can be found in Glendell et al. (2018) and are briefly summarised here. Four land uses were considered in their study: Arable, temporary grassland referred to as “ley”, permanent grassland referred to as “grassland” and woodland (including riparian woodland areas). Seventy-five soil cores (8 cm diameter, depth 0–15 cm) were taken (30 from arable, 26 from ley, 14 from grassland and five from woodland were collected from 0–15 cm soil depth in summer 2015 (Figure 2). Where required (e.g., in woodland) leaf litter was removed from the surface before sample collection. In addition, streambed sediment samples were collected at six locations along the North and South tributaries (upstream, midstream and downstream) and at the joint catchment outlet. These locations will be referred to as Outlet (OL), North Lower (NL), North Mid (NM), North Upper (NU), South Lower (SL), South Mid (SM) and South Upper (SU). Soil samples were oven dried at 40 °C before sieving. Streambed samples were wet sieved to remove coarse vegetation debris. The criteria for sieving the source and sediment samples were to retain as much soil/sediment as possible

while removing anomalously large residual vegetation or sandy/stoney debris. For the streambed sediments a 250 µm sieve removed coarser vegetation/sand debris from the finer sediments but as this sieve size would have removed too much soil from the courser soil samples these were sieved to 2mm. In each case the soil/sediment passing through the sieve was retained for analysis.

All the soil and streambed samples were processed and analysed for total C (n = 75), however, *n*-alkane concentrations (µg g^{-1} C) were only obtained for a sub-set of soil source samples (eleven from arable, nine from ley, seven from permanent grassland and four from woodland land use) selected on the basis of likely high hydrological connectivity with the streams to characterise for SF (Glendell et al., 2018).

2.1.3 Software and Data Maps

The 1 m x 1 m resolution Digital Elevation Model (DEM) was obtained from LiDAR based Digital Terrain Model data for South West England (Ferraccioli et al., 2014). Pit-filling was undertaken in ESRI ArcMap (V10.6) (ESRI, 2017) prior to topographic data generation to remove potential processing errors within the DEM. For the estimation of soil loss in RUSLE, the DEM was resampled to a resolution of 20 m x 20 m. Twenty metres is a typical resolution for DEM in erosion modelling as the processes to be captured by the RUSLE erosion modelling are at a hill-slope scale (Van Oost et al., 2006). The land cover dataset was based on the Centre for Ecology & Hydrology (CEH) Land Cover map of 2015 (LCM2015), as adapted by Glendell et al. (2018) (Figure 2). Sub-catchments contributing to the seven streambed sediment sample sites were delineated in ESRI ArcMap (*V10.6*) (ESRI, 2017). In addition, a stream buffer representing the land within 20 m of the stream was delineated for each of the sub-catchments (20 m was selected to match the resolution of the CLM maps).

Unless otherwise stated, all statistical analyses were carried out in R (version 3.6.3) (R Core Team, 2020) and RStudio (version 1.1.463) (RStudio Team, 2018).

2.1.4 *N*-alkane tracers

Due to their nature (straight-chain hydrocarbons lacking functional groups), *n*-alkanes are stable, long-lived molecules that can survive in the fossil record for millennia (Bush and McInerney, 2013) leading to their use as biomarkers in tracing vegetation changes, not only over decades and centuries (Chen et al., 2017, 2022; Glendell et al., 2018; Wang et al., 2015), but in studies of paleoecology and paleoclimatology (Glaser and Zech, 2005; Meyers, 2003; Zech et al., 2009). *N*-alkanes within sediments are more resistant to degradation than other organic biomarkers (e.g. sterols, *n*-alkanoic acids, *n*-alkanols). The longer the chain length, the less soluble the *n*-alkane becomes in water, reducing their metabolism by microorganisms (Cranwell, 1981; Ranjan et al., 2015). As a result, alkanes of chain-length >C24 are generally resistant to biodegradation (Singh, Kumari and Mishra, 2012) and are suitable as conservative sediment tracers.

Selection of the sub-set of source soil samples for *n*-alkane analysis in this catchment (Glendell et al., 2018) was originally carried out with the aim of sediment source fingerprinting at the catchment outlet. Therefore, source soil samples within the sub-catchments at the seven streambed sediment sample locations were unevenly distributed. For this reason, all soil samples from the entire catchment were included in the *n*-alkane source apportionment model to characterise the land use sources. To characterize the *n*-alkane distribution within soils under different land use sources this study used *n*-alkane concentrations (μg g^{-1} C) for chain lengths C15 to C33. *N*-alkanes proxies obtained from the relative abundances of *n*-alkanes were used as “fingerprints”: the relative percentage of *n*-alkanes C27, C29 and C31 (Torres et al., 2014); the C27 to C31 ratio (Puttock et al., 2014); P_{aq}, to understand aquatic versus terrestrial plant input (Ficken et al., 2000); the Odd-to-Even Predominance (OEP) (Zech et al., 2013; and the Average Chain length (ACL) (Fang et al., 2014) were used (Table 2).

Table 2 Description of *n*-alkane derived ratios considered as tracers within the MixSIAR sediment fingerprinting source apportionment model for Carminowe Creek catchment, UK

***n*-alkane ratios**	**Description**
$\%C_{27}$, $\%C_{29}$, $\%C_{31}$	Percentage of alkane "i" where: $\%C_i = \frac{C_i}{(C27+C29+C31)}$ (Torres et al., 2014)
C_{27} / C_{31}	C27 to C31 ratio estimating the proportion of wood to grass derived organic matter (Puttock et al., 2014)
$\boldsymbol{PAQ} = \frac{\mathbf{C23 + C25}}{\mathbf{C23 + C25 + C29 + C31}}$	P_{aq}, to understand aquatic versus terrestrial plant input (Ficken et al., 2000)
$\boldsymbol{OEP} = \frac{\mathbf{C27 + C29 + C31 + C33}}{\mathbf{C26 + C28 + C30 + C32}}$	Odd-over-even predominance (OEP). (Zech et al., 2013)
$\boldsymbol{ACL} = \frac{\mathbf{27 \times C27 + 29 \times C29 + 31 \times C31 + 33 \times C33}}{\mathbf{C27 + C29 + C31 + C33}}$	Average Chain length (Fang et al., 2014)

2.1.4.1 Tracer selection

The Bayesian source apportionment model applied in this study, MixSIAR, accounts for the variability in both sources and mixture through uncertain source characterisation and thus offers an advancement on conventional linear models (Stock and Semmens, 2016). The geology and soils in this small catchment are uniform, which should minimise within-source group tracer variability due to these factors. The study of Glendell et al. (2018) found that the *n*-alkane tracers could not distinguish well between the arable and ley land uses in this catchment and therefore in the tracer selection procedure these land uses were combined giving three land use sources arable (n=20), grassland (n=7) and woodland (n=4). *N*-alkane tracers were selected using the following procedure. Firstly each tracer was assessed for normality using the Kolmogorov-Smirnov test. A "range test" was then carried out by comparing boxplots of each potential tracer in source samples against the mixtures (streambed sediment) to assess if the range of values for the streambed sediments was within the full range of values for the

terrestrial land use sources. The boxplots were created in Excel with the “full range” defined by the whiskers (extending up from the top of the box to the largest data element that is ≤1.5 times the interquartile range (IQR) and down from the bottom of the box to the smallest data element that is >1.5 times IQR); values outside this range were considered outliers. The full range (excluding outliers) was used to account for the small sample sizes available to characterise each land use and the variability in the source fingerprints. The streambed sediment mixtures are represented by a single measurement in each case without any knowledge of the potential mean and distribution. It is therefore possible that the single measurement represents either a value close to the maximum or minimum of the possible tracer values rather than the mean and therefore selecting tracers based on the means and inter-quartile range of the sources was considered too restrictive. Finally, a Kruskal-Wallis non-parametric test followed by a post-hoc Dunn test was employed to determine if the tracers could distinguish between the three land use sources.

2.1.4.2 Virtual mixtures

Once a suitable set of *n*-alkane tracers had been selected land use discrimination was assessed using a “virtual” mixture with 50/50 contributions from each source by taking the mean of the two sources to represent a 50% contribution from each. Errors were calculated as mean absolute differences between the modelled (MixSIAR) and virtual mixture composition.

2.1.4.3 Bayesian unmixing model (MixSIAR) implementation

MixSIAR uses the mean and standard deviation to characterise tracer properties. MixSIAR is “fully Bayesian” (source data fit hierarchically) and estimates the ‘true’ source means and variances used in the mixture likelihood. Source means and standard deviations used in the mixture likelihood are allowed to deviate from the user specified values with the amount of deviation dependent on source sample sizes. Estimates of sediment proportions are made using Markov chain Monte Carlo (MCMC) simulations. A full description of this model can be found in Stock and Semmens (2016) and Stock et al. (2018). MixSIAR was formulated using a residual error term and an uninformative prior in all model runs. The MCMC

parameters were set as follows: chain length = 100,000, burn = 50,000, thin = 50, chains = 3 (convergence of all models was evaluated using the Gelman-Rubin diagnostic).

2.1.5 Carbon Loss model

A carbon loss model (CLM) was constructed as follows:

$$CLM = \text{SOC\%} \times \text{SL} \times \text{CI} \quad \textbf{(2-1)}$$

where SOC% is a map of the soil organic carbon content (%), SL is a soil loss map constructed using RUSLE and CI is a map of connectivity index as defined by Borselli et al., (2008) and Cavalli et al., (2013).

2.1.5.1 SOC content mapping

To map soil OC (%) across the catchment, soil samples were interpolated using a linear regression model implemented in R (version 3.6.3) (R Core Team, 2020) packages “raster” (Hijmans, 2020), “sp” (Pebesma and Bivand, 2005) and “gstat” (Pebesma, 2004). Seven land-use and topographic environmental predictor maps were generated using ESRI ArcMap (V10.6) (ESRI, 2017): land use, slope, curvature, flow length (longest upslope distance along the flow path, from each cell to the top of the drainage divide), accumulated flow (accumulated weight of all cells flowing into each downslope cell), topographic wetness index (Mayer et al., 2019) and aspect (i.e. compass direction that the steepest slope is facing at a given location). The land uses considered within the model were grassland, arable (a combination of arable and temporary grassland or ley), broadleaf woodland and riparian woodland as these were the land uses available on the land use map adapted from Glendell et al. (2018). Climate and soil parameters were not considered as predictors, as, except for one sample, all samples were taken on the same soil type and climate data were not expected to vary significantly across this small catchment (<5km^2). The model was selected by highest adjusted R^2 and lowest Akaike Information Criterion (AIC) (Meersmans et al., 2012). A leave-one-out cross-validation was implemented, and the root

mean square error (RMSE) and R^2 of the model simulations were calculated to check model accuracy against observations.

2.1.5.2 Connectivity Index

To define the degree of connectivity between upslope sediment sources and catchment streams, CI was calculated using the method of Cavalli et al. (2013) and the catchment DEM using ESRI ArcMap (V10.6) (ESRI, 2017). For use as a weighting with the soil organic carbon content and RUSLE, CI was re-scaled from 0 to 1.

2.1.5.3 Soil loss modelling

Long-term average annual soil loss in RUSLE is calculated as:

$$SL = R.K.L.S.C.P \quad \textbf{(2-2)}$$

where SL is the mean soil loss (t ha^{-1} yr^{-1}), R is the rainfall intensity factor (MJ mm ha^{-1} h^{-1} yr^{-1}), K is the soil erodibility factor (t ha h ha^{-1} MJ^{-1} mm^{-1}), S and L are the slope and slope-length factors, C and P are the dimensionless cover-management factor and conservation support practice factor that are heavily dependent on the land use and management. In this small catchment (<5 km^2), single values were used for the RUSLE R and K factors, based on existing derived spatial datasets (R - ESDAC, 2015; Panagos et al., 2015) (K - ESDAC, 2014; Panagos et al., 2014) (Table 2). A C factor map was created by assigning literature values for arable land, grassland, forest and urban areas to the land cover map (Section 2.1.3) (Bakker et al., 2008; Borrelli et al., 2018b; Gadiga and Martins, 2015; Oliveira, Nearing and Wendland, 2015; Van Rompaey and Govers, 2002) (Table 3). The conservation support practice factor (P) was not considered in this study and was set to 1. RUSLE LS factor was generated from the DEM in R (version 3.6.3) (R Core Team, 2020) using packages “raster” (Hijmans, 2020) and “RSAGA” (Brenning et al., 2018: version 7.6.3, method “Desmet and Govers”). The RUSLE factor maps and %SOC map were used to calculate SOC loss using packages “raster”, “RSAGA” and “rgdal” (Bivand, Keitt and Rowlingson, 2019).

Table 3 RUSLE factors used to estimate long-term average annual soil loss for Carminowe Creek catchment, UK. R is the rainfall intensity factor (MJ mm ha^{-1} h^{-1} yr^{-1}), K is the soil erodibility factor (t ha h ha^{-1} MJ^{-1} mm^{-1}), S and L are the slope and slope-length factors, C and P are the dimensionless cover-management factor and conservation support practice factor.

RUSLE Factor	Value	
R	586.85 (MJ mm ha^{-1} h^{-1} yr^{-1})	
C $_{arable}$	0.21	(Range 0.12 - 0.34)
C $_{forest}$	0.005	(Range 0.01 - 0.001)
C $_{grassland}$	0.0625	(Range 0.2 - 0.005)
C $_{urban}$	0.005	(Range 0.01 - 0.001)
K	0.041 (t ha h ha^{-1} MJ^{-1} mm^{-1})	
P	1	

2.1.5.4 Land use specific distribution of carbon loss

The value of C-factor within RUSLE model can be used to account for the differences in erosion potential between land uses. However, the range of values found for the C factor in the literature (Table 3) can lead to a one or two orders of magnitude difference in RUSLE output. Therefore, it was important to evaluate the magnitude of the errors associated with the RUSLE C-factor as well as that introduced by the modelling of SOC content (%SOC) using a Monte Carlo analysis with 3,000 iterations. The RUSLE C factor was sampled from a uniform distribution defined by the maximum and minimum values found in the literature (Table 3) and %SOC content was sampled from a uniform distribution defined by +/-1 RMSE from the leave-one-out cross-validation of the %SOC content map (see 2.1.5.1). At each iteration the SOC loss from arable and woodland land uses were calculated, generating a probability distribution for comparison with sediment source proportions estimated using SF.

2.2 Results

2.2.1 *N*-alkane distribution

The *n*-alkane distribution of the samples in this catchment are discussed in Glendell et al., (2018) and are summarised here. As expected, C27 and C29 dominated the woodland *n*-alkane distribution (63%) with a smaller contribution from those homologues dominant in grasslands (C31, C33 - combined proportion of 28%) (Figure 3a). Conversely, the arable land use *n*-alkane distribution was dominated by contributions from C31, C33 homologues dominant in grasslands (combined proportion of 56%) with smaller contributions from those homologues dominant in woodlands (C27, C29 - combined proportion of 36%). Both land uses had a much smaller contribution from homologues' dominant in lower plants and mosses (C23, C25 - combined proportion of 8-9%). The relative proportions of the *n*-alkane homologues in the streambed sediments were dominated by C27 and C29 (combined proportion of 67-71% for all streambed sites except OL which had a slightly lower proportion of 62%) (Figure 3a).

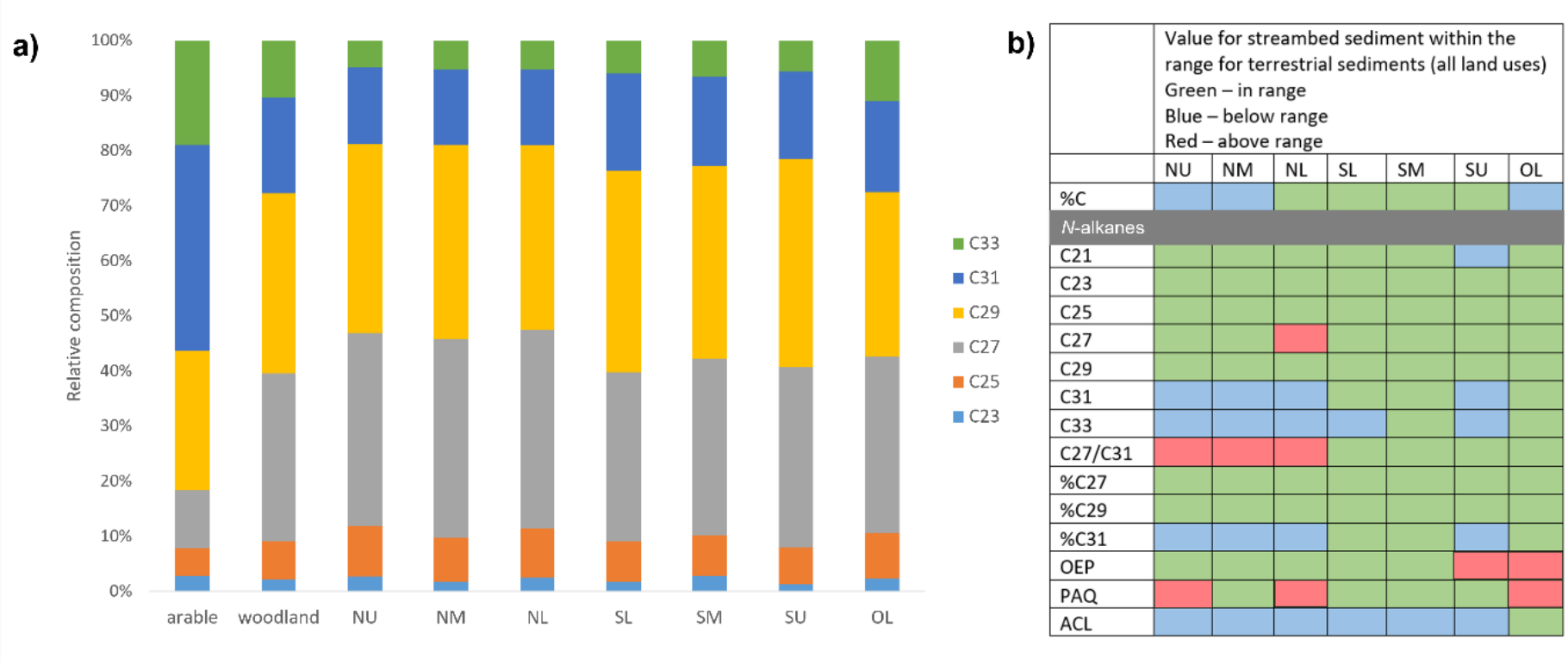

Figure 3 a) Relative mean concentration (%) for mid and long-chain *n*-alkane homologues for the soils of land uses, arable and woodland and streambed sediments OL, NU, NM, NL, SU, SM and SL, and b) Range comparison for %C, mid and long-chain *n*-alkane homologues, and *n*-alkane ratios between terrestrial land uses and streambed sediments OL, NU, NM, NL, SU, SM and SL for the Carminowe Creek catchment, UK

2.2.2 Source apportionment

To evaluate whether location-specific OC sources and delivery processes can be better determined using SF in combination with a CLM, rather than SF alone the relative contributions of woodland and other land uses were first quantified using the *n*-alkane biomarker data and MixSIAR.

The Kolmogorov-Smirnov test revealed that all *n*-alkane tracers (C27/C31 ratio, %C27, %C29, %C31, OEP, PAQ and ACL) were not significantly different from a normal distribution ($p > 0.05$). The Kruskal-Wallis non-parametric test for the three land use sources (arable, grassland and woodland) revealed that the distribution of *n*-alkane tracers was not the same for every land use ($p < 0.05$) for all tracers except OEP. However, the post-hoc Dunn test which compares the land uses pairwise revealed the *n*-alkane tracers could not distinguish grassland from arable. Consequently, as this study is essentially concerned with the relative contribution of woodland and "non-woodland" sources the grassland and arable data were combined into one source which will henceforth be referred to as "arable". Analysing this combined arable source, the Kolmogorov-Smirnov test revealed that all *n*-alkane tracers were not significantly different from a normal distribution ($p > 0.05$), except for C27/C31 ratio ($p=0.022$). The Kruskal-Wallis non-parametric test for the two land use sources (arable and woodland) revealed that the distribution of *n*-alkane tracers was not the same for every land use ($p < 0.05$) for all tracers except OEP. OEP was therefore excluded as a tracer. The range test revealed that for %C27 and %C29 the range of values for the streambed sediments was within the full range of values for the terrestrial land use sources and these two tracers were therefore selected for use in source apportionment (Figure 4). The difference in range between the streambed sediment *n*-alkanes and those of the terrestrial land uses was primarily due to the relative depletion of %C31 in the streambed sediments (Figure 3b) which commensurately reduced the average chain length (ACL) and increased the C27/C31 ratio. The values of the *n*-alkane proxy for aquatic versus terrestrial plant input (PAQ) were generally within the range of the woodland (PAQ 0.12-0.17) however, a few sample sites had larger PAQ values (0.19-0.2). Ankit et al.,

(2022) ascribe PAQ values <0.1 to terrestrial vegetation and 0.1–0.4 to emergent macrophytes which could suggest some input of *n*-alkanes from the latter in streambed sediments. However, the woodland PAQ values are also all above 0.1 and it unlikely that emergent macrophytes would make a significant contribution to terrestrial soils. Using MixSIAR and the selected *n*-alkane tracers (%C27 and %C29) land use discrimination was assessed using a “virtual” mixture. The mean absolute difference between the modelled (MixSIAR) and virtual mixture composition was only 0.2% suggesting *n*-alkane tracers %C27 and %C29 could discriminate well between the two land use sources.

Source apportionment using MixSIAR with n-alkane tracers %C27 and %C29 found the dominant OC source at every streambed site was woodland. There was little difference between the seven streambed sites with woodland contributing between 81% and 85% at each site (Table 4).

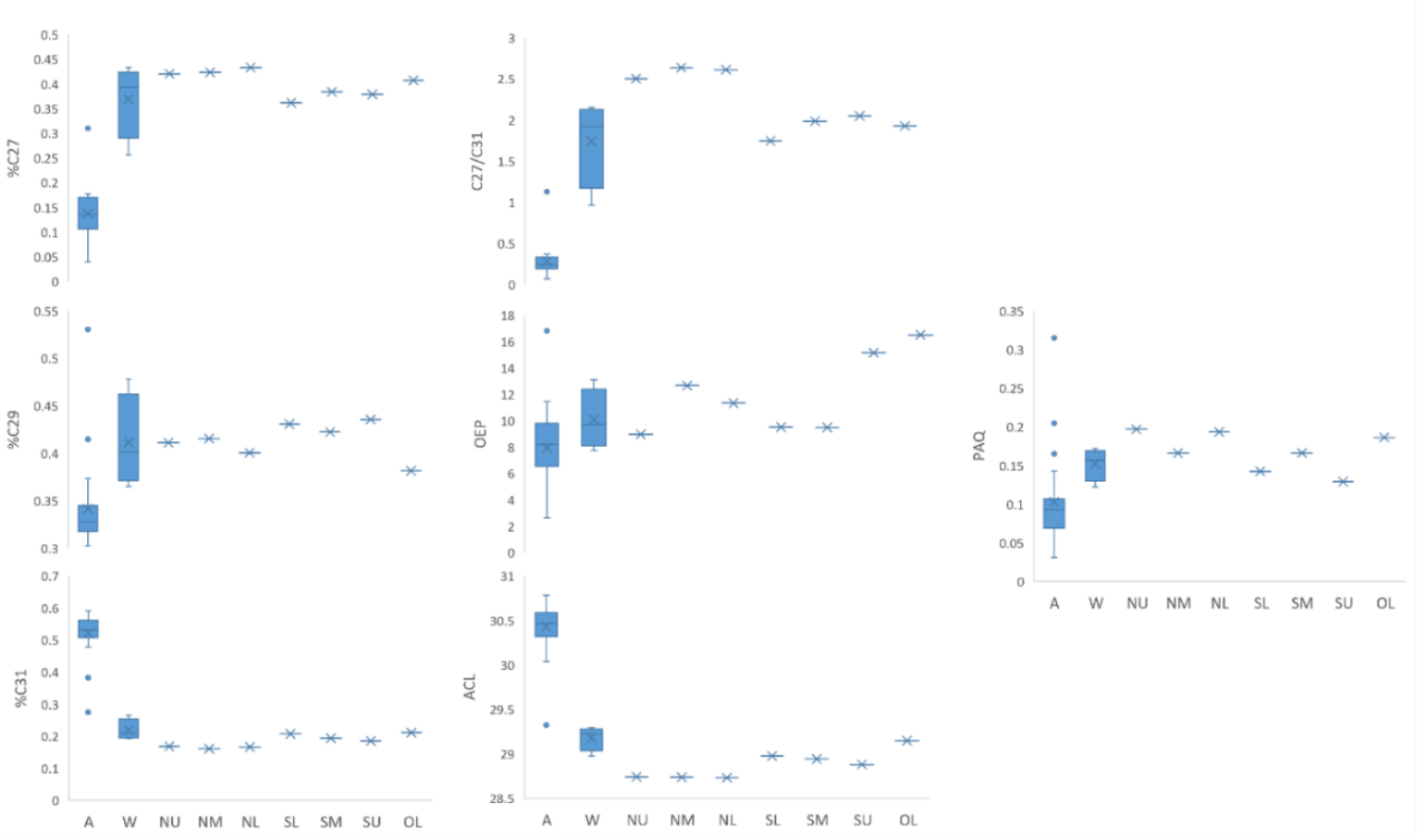

Figure 4 Box plots of *n*-alkane ratios for the soils of land use types, arable (A), and woodland (W) and streambed sediments OL, NU, NM, NL, SU, SM and SL for the Carminowe Creek catchment. The middle line of the box represents the median and the "x" the mean. The box represents the first to third quartile and the whiskers extend from minimum to maximum values excluding outliers (blue dots)

Table 4 Proportion of woodland soil OC input to the streambed sediments OL, NU, NM, NL, SU, SM and SL for the Carminowe Creek catchment estimated using Sediment fingerprinting (SF) and a Carbon loss model (CLM) at a sub-catchment and 20 m stream buffer scale

	Estimated proportion of woodland soil OC (% ± 1SD)						
	OL	NL	NM	NU	SL	SM	SU
SF	81.64± 13.14	85.07± 11.58	85.47± 11.03	84.61± 11.70	81.39± 12.68	82.23± 12.43	83.29± 11.79
CLM (sub-catchment)	0.81± 0.52	0.40± 0.26	0.34± 0.22	0.65± 0.42	1.37± 0.88	1.17± 0.77	0.38± 0.26
CLM (20m buffer)	3.64± 2.24	1.39± 0.89	0.98± 0.65	1.21± 0.76	7.68± 4.43	3.18± 2.04	1.11± 0.74

2.2.3 Carbon Loss model

The %OC of the samples in this catchment are discussed in Glendell et al., (2018) and are summarised here. The mean %OC was greatest within woodland (7.80±1.98%) land use followed by grassland (5.40±1%), ley (3.77±1.01%) and arable land use (3.05±0.61%). In general, the %OC content of streambed sediments was lower than that of terrestrial land uses, with the highest %OC in streambed sediments (Site SM 3.7%) comparable to that of ley and arable soils. The lowest %OC were found at sites NU (1.16%) and OL (1.55%), which had relatively little woodland nearby, with NU being surrounded by arable and grassland and OL located near steeply sloping grasslands. The largest %OC was seen at site SM (3.68%), which is located next to an extended area of woodland.

The CLM required the spatial distribution of soil OC and to this end the %OC across the catchment was predicted by interpolating %OC of each soil sample using linear regression (Table 5). Land use showed the strongest significant relationship ($p<0.05$) with %OC (adjusted $R^2=0.54$). OC content showed weak significant relationships ($p<0.05$) with curvature (adjusted $R^2=0.07$), TWI (adjusted $R^2=0.12$), flow length (adjusted $R^2=0.18$) and accumulated flow (adjusted $R^2=0.13$), however, when considered together with land use none of

these other covariates were significant. No significant relationships with %OC were found for the other covariates (slope and aspect). The highest adjusted R^2 (0.54) and lowest AIC were obtained when land use alone was used as a predictor (Table 5). The leave-one-out cross-validation checking model accuracy against observations had a root mean square error (RMSE) of 1.35 and R^2 of 0.43. The land uses considered within the model were grassland, arable (a combination of arable and ley), broadleaf woodland and riparian woodland (Section 2.1.3). The highest SOC content was predicted in broadleaved woodland (7.29%), followed by grassland (5.76%), riparian woodland (5.26%) and arable land (3.17%).

The combined CLM (SOC% x RUSLE x CI) reveals areas of greatest OC loss are predicted in arable land on the relatively steeper slopes surrounding the stream channels (Figure 5). In each of the seven sub-catchments of Carminowe Creek (OL, NU, NM, NL, SU, SM and SL), the proportion of woodland soil OC input to the streambed sediments was estimated using the CLM at a sub-catchment and 20 m stream buffer scale (Table 4). The two scales (sub-catchment and 20 m stream buffer) were used to assess if streambed OC proportions were more aligned with local riparian conditions, rather than those in the wider sub-catchment. At the sub-catchment scale woodland represents only 6% to 9% of the total land use for each streambed sediment site. This percentage rises at the 20m buffer scale (37-58%) as most of the woodland is located in close proximity to the streams. The CLM estimated that woodland soil OC represented a relatively small proportion of eroded soil OC likely to reach the streams (<1.4 at a sub-catchment scale and up to up to 7.7±4.4% at a 20 m stream buffer scale) with the overwhelming majority originating in arable land.

Table 5 SOC content regression relationship and Root Mean Square Error (RMSE) and R^2 value resulting from leave-one-out cross-validation. In the context of the linear regression relationship, the variables "grassland", "riparian" and "woodland" are dummy variables which are equal to one when that land use is present and zero otherwise.

SOC content regression relationship	RMSE	R^2

SOC% =3.1694 + 2.5950(grassland) + 2.0931(riparian) + 4.1166(woodland)	1.35	0.43

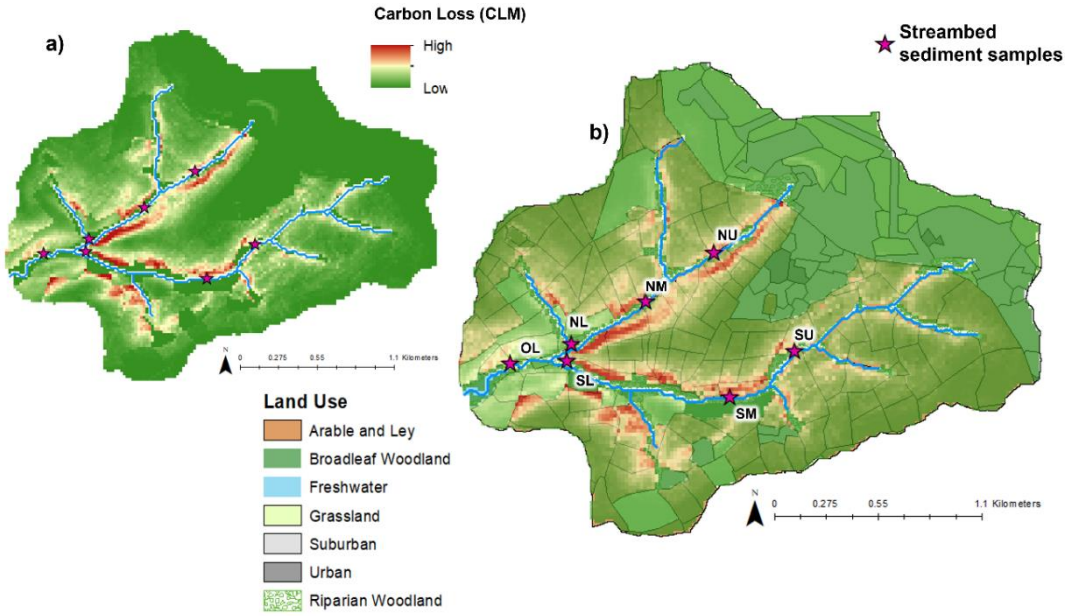

Figure 5 a) Carbon Loss Model (CLM) and b) Combined CLM and land use map for Carminowe Creek catchment, UK

2.3 Discussion

We combined a CLM with SF to characterize OC distribution in soils under different land uses and to quantify the sources of OC in Carminowe Creek, a small, mixed land use, UK catchment.

The CLM predicted areas of greatest OC loss in arable land on the relatively steeper slopes surrounding the stream channels. The proportion of woodland soil OC input to the streambed OC estimated by CLM at a sub-catchment scale, <1.4% is smaller than would be expected given its area coverage (6-9%), close proximity to the streams (high connectivity), and relatively high %OC (5.26-7.29 cf. 3.17-5.76% for arable). This is due mainly to a greater protection from erosion afforded by the permanent vegetation found in woodland compared to arable land which has more variable vegetation cover due to human-induced processes (Poesen, 2018). This is reflected in the RUSLE C-factor which is much higher

(resulting in a significantly higher level of estimated erosion) for arable land than woodland (arable 0.12 - 0.34, woodland 0.01-0.001). In addition, some of the arable land in this catchment is located on the steep slopes leading down to the stream network which is likely to increase both the speed, and the erosive potential of water runoff and increase the probability of eroded sediment reaching the streams (Renard et al., 1997). The proportion of woodland soil OC input to the streambed OC estimated by CLM at a 20 m stream buffer scale is larger (up to 7.7%) due to the larger proportion of woodland at this scale (37-58%) but is still significantly smaller than the contribution from arable land due to the higher levels of erosion predicted for that land use. There is a large discrepancy between the CLM estimates of woodland soil OC contributions to streambed OC and those estimated by SF. Neither the carbon loss estimated in close proximity to the streams (CLM 20 m stream buffer scale), nor that in the wider catchment, came close to the 81% - 85% woodland contribution estimated by SF. The discrepancy between the CLM estimates of woodland soil OC contributions to streambed OC and those estimated by SF suggests that woodland soil is being input to streams by processes not modelled by the CLM and/or, there is a source of woodland vegetation biomarkers not originating from soil.

Carminowe Creek has extensive riparian woodland. This, riparian woodland vegetation can reduce delivery of upslope fine-grained sediment to streams (Grabowski and Gurnell, 2016; Wu et al., 2021) and, therefore, Carminowe Creek's extensive riparian woodland is likely to have reduced the presence of eroded arable soil OC in the creek bed sediments. As SF estimates OC source contributions directly from streambed sediments, it represents a combination of both potential contribution from upslope terrestrial sources and processes within the stream channel and riparian zone. Terrestrial-to-aquatic fluxes of OC can originate in this active and dynamic river "corridor", which encompasses both the active stream channel and the riparian zone (Wohl et al, 2017) through direct input (e.g. organic litter or leaf debris) and overflow of river banks and the riparian zone (Borrelli et al., 2018b; Bright et al., 2020). Bank erosion could, therefore, have contributed woodland soil to the streams. However, a recent assessment of branched tetraether lipids (membrane lipids of soil bacteria) in Carminowe Creek

suggested the absence of a clearly recognizable soil brGDGT (branched glycerol dialkyl glycerol tetraethers) signal in creek bed sediments could be explained if there was a relatively limited input of soil material into the creek (Guo et al., 2020). Lewis et al., (2021) found the amount of wood in streams was best explained by riparian tree canopy cover and the length of tree-lined channel upstream. There could be leaves/needles directly associated with this deposited woody debris and its presence in the stream channel can capture additional leaf litter and/or twigs (Lewis et al., 2021).

Hirave et al. (2020b) found little or no difference between *n*-alkane concentrations between fresh plant biomass and the soil organic horizon (O horizon) suggesting that it may be difficult to distinguish between *n*-alkane signatures from those two sources. Stout, (2020) found the average chain length and OEP (odd-even predominance) of fresh mature leaves increased and decreased respectively in the corresponding leaf litter and further in the corresponding soil, which they attributed to preferential and progressive degradation of the more abundant C27/C29 homologues relative to the less abundant C31/C33. As a result, OEP is relatively higher and %C31 relatively lower for leaves/litter compared to the more degraded OM in the associated soil. In this study, when comparing the streambed sediment to the terrestrial soils, the OEP values of streambed sediments were similar to or greater, and the %C31 values similar or lower. Direct input of leaf/wood organic matter to the stream sediments could explain the respectively higher and lower OEP and %C31 values of these sediments. Characterising this direct woodland OC as a separate source within future fingerprinting studies would allow the relative contributions from this more direct source and any eroded woodland soil OC to be estimated. This may require the inclusion of biomarkers of plant, fungal and bacterial origin to provide a fingerprint more characteristic of the soil rather than just the vegetation. Although, the bacterial brGDGT biomarkers of Guo et al. (2020) were not found to be land-use-specific, other biomarkers, such as fatty acids considered common to prokaryotic and eukaryotic organisms, have been found relevant for land use discrimination (Ferrari et al., 2015).

Monte Carlo techniques were used to propagate uncertainties in both the SF and CLM estimates of land use contributions to streambed OC. As the study is concerned with relative contributions from land use sources the CLM uncertainty analysis was concentrated on factors that were strongly land use dependent (RUSLE C-factor and OC spatial modelling). The uncertainties associated with the other RUSLE factors and CI were considered independent of land use. Uncertainties in SF results can arise due to factors affecting source and sediment characterisation such as sample size and particle size fractions. The sample size for characterising streambed sediment and woodland in this study was small (only one sample for each streambed site and four samples for the woodland soil). The authors recommend as large a sample size as possible (within practicality and budget constraints) to facilitate a more robust characterisation of the distributions of both soil sources and streambed mixtures resulting in a more robust range test of tracer conservativeness. Finer, lighter particles are more likely to be mobilised by water in the terrestrial environment and therefore, as in this study, aqueous sediments may end up with a finer particle size distribution than terrestrial sediments. The particle size fractions of the soil and sediment samples used in this study were determined by using sieve sizes that retained as much soil/sediment as possible, while removing anomalously large debris. This resulted in different size fractions, <2 mm and <250 µm respectively, for the soil and (relatively finer) streambed sediments. In the study of Geng et al. (2019), the distribution and preservation of *n*-alkanes was found to differ between coarse (>250 µm) particulate organic matter (POM) and fine POM (<250 µm). The coarse POM had a greater abundance of plant-derived *n*-alkanes (n > 20) with chain-length shortening in the fine POM fraction suggesting a stronger decomposition of *n*-alkanes in that fraction. The respectively higher and lower OEP and %C31 values found for the Carminowe Creek streambed sediments (<250 µm) indicate less degradation than the coarser (<2 mm) soil sediments and, therefore, there is unlikely to be an effect due to particle size similar to that found by Geng et al. (2019). It is generally accepted that OM (including *n*-alkanes) are preferentially associated with the finer particle size fractions (<63 µm) (Quenea et al., 2004; Quénéa et al., 2006). In addition, studies have found the majority of OC resides

in the finer soil fractions (De Mastro et al., 2020; Yu et al., 2019). This finer fraction was present in both soil and sediment samples, however, runoff from eroding landscapes can be enriched in these finer, clay sized particles (Nitzsche et al., 2022; Starr et al., 2000) and could have affected the *n*-alkane distribution of streambed sediments relative to the source samples in this study (Laceby et al., 2017). In future studies, analysing terrestrial source soils at different particle size fractions could help quantify any effects on *n*-alkane distributions due to this factor. Uncertainty could be further reduced by using different methods to isolate the finer fraction within the soil samples. Under field conditions, various mechanisms cause soil aggregates to break apart creating finer particle fractions; disintegration of aggregates is a complicated mixture of mechanical (raindrop impact, field traffic/tillage, roots, earthworms) and hydraulic stresses (Felde et al., 2021). Therefore, using different methods to isolate the finer fraction within the soil samples could highlight any differences in biomarker distribution due to breaking down aggregates using methods such as dry crushing (along more "natural planes of mechanical weakness" i.e., those likely to fail in the field (Felde et al., 2021)) compared to wet/dry sieving and/or sample grinding.

2.4 Conclusions

This study revealed that combing a CLM with SF enhanced the understanding of the fate of eroded OC and terrestrial-to-aquatic fluxes for a mixed land use catchment. The results of this study support others that found riparian buffers reduced soil OC loss from terrestrial-to-aquatic ecosystems (Liu et al., 2020; Valera et al., 2019; Zhang et al., 2010). The approach has highlighted that the amount of upslope OC erosion cannot be reliably equated with delivery to streams unless i) sites of intermediate storage or "buffers" are also considered (Owens, 2020; Trimble, 1983) and, ii) estimates of other plant-derived OC sources e.g., direct input of leaf/wood organic matter can be made. It is likely that, although wooded riparian buffer strips may reduce the impact of upslope, eroded soil OC on waterways, they could themselves be a source of OC to stream sediments through more direct input (e.g., organic litter or leaf debris). Characterising this direct woodland OC as a separate source within future

fingerprinting studies would allow the contributions from any eroded woodland soil OC to be better estimated. This study was focussed on streambed sediments and therefore, average, longer-term OC fluxes. In future studies it will be important to assess suspended sediment as well as bed sediments to assess any seasonal changes in terrestrial OC origins and delivery processes.

2.5 References

Alewell, C., Birkholz, A., Meusburger, K., Schindler Wildhaber, Y. and Mabit, L. (2016) 'Quantitative sediment source attribution with compound-specific isotope analysis in a C3 plant-dominated catchment (central Switzerland)', Biogeosciences, 13(5), pp. 1587–1596.

Alewell, C., Borrelli, P., Meusburger, K. and Panagos, P. (2019) 'Using the USLE: Chances, challenges and limitations of soil erosion modelling', International Soil and Water Conservation Research, 7(3) Elsevier Ltd, pp. 203–225.

Ankit, Y., Muneer, W., Gaye, B., Lahajnar, N., Bhattacharya, S., Bulbul, M., Jehangir, A., Anoop, A. and Mishra, P.K. (2022) 'Apportioning sedimentary organic matter sources and its degradation state- Inferences based on aliphatic hydrocarbons amino acids and δ15N', Environmental Research, 205

Bakker, M.M., Govers, G., van Doorn, A., Quetier, F., Chouvardas, D. and Rounsevell, M. (2008) 'The response of soil erosion and sediment export to land-use change in four areas of Europe: The importance of landscape pattern', Geomorphology, 98(3–4), pp. 213–226.

Bivand, R., Keitt, T. and Rowlingson, B. (2019) rgdal: Bindings for the 'Geospatial' Data Abstraction Library. R package. 1.4-8.

Borrelli, P., Panagos, P., Lugato, E., Alewell, C., Ballabio, C., Montanarella, L. and Robinson, D.A. (2018) 'Lateral carbon transfer from erosion in noncroplands matters', Global Change Biology, 24(8), pp. 3283–3284.

Borselli, L., Cassi, P. and Torri, D. (2008) 'Prolegomena to sediment and flow connectivity in the landscape: A GIS and field numerical assessment', Catena, 75(3), pp. 268–277.

Brenning, A., Becker, M. and Bangs, D. (2018) RSAGA: SAGA Geoprocessing and Terrain Analysis. R package 1.3.0.

Bright, C.E., Mager, S.M. and Horton, S.L. (2020) ‘Catchment-scale influences on riverine organic matter in southern New Zealand’, Geomorphology, 353 Elsevier B.V., p. 107010.

Bush, R.T. and McInerney, F.A. (2013) ‘Leaf wax n-alkane distributions in and across modern plants: Implications for paleoecology and chemotaxonomy’, Geochimica et Cosmochimica Acta, 117 Elsevier Ltd, pp. 161–179.

Cavalli, M., Trevisani, S., Comiti, F. and Marchi, L. (2013) ‘Geomorphometric assessment of spatial sediment connectivity in small Alpine catchments’, Geomorphology, 188 Elsevier B.V., pp. 31–41.

Chen, F.X., Fang, N.F., Wang, Y.X., Tong, L.S. and Shi, Z.H. (2017) ‘Biomarkers in sedimentary sequences: Indicators to track sediment sources over decadal timescales’, Geomorphology, 278 Elsevier B.V., pp. 1–11.

Chen, Y., Wang, Y., Yu, K., Zhao, Z. and Lang, X. (2022) ‘Occurrence characteristics and source appointment of polycyclic aromatic hydrocarbons and n-alkanes over the past 100 years in southwest China’, Science of The Total Environment, 808 Elsevier B.V., p. 151905.

Cooper, R.J., Pedentchouk, N., Hiscock, K.M., Disdle, P., Krueger, T. and Rawlins, B.G. (2015) ‘Apportioning sources of organic matter in streambed sediments: An integrated molecular and compound-specific stable isotope approach’, Science of the Total Environment, 520 Elsevier B.V., pp. 187–197.

Cranwell, P.A. (1981) ‘Diagenesis of free and bound lipids in terrestrial detritus deposited in a lacustrine sediment’, Organic Geochemistry, 3(3), pp. 79–89.

Desmet, P.J.J. and Govers, G. (1996) ‘A GIS procedure for automatically calculating the USLE LS factor on topographically complex landscape units’, Journal of Soil and Water Conservation, 51(5), pp. 427–433.

ESDAC (2014) Soil Erodibility (K- Factor) High Resolution dataset for Europe., Joint Research Centre of the European Commission Available at: https://esdac.jrc.ec.europa.eu/content/soil-erodibility-k-factor-high-resolution-dataset-europe (Accessed: 7 June 2019).

ESDAC (2015a) Estimating the soil erosion cover-management factor at European scale., Joint Research Centre of the European Commission Available at: https://esdac.jrc.ec.europa.eu/content/cover-management-factor-c-factor-eu (Accessed: 19 March 2012).

ESDAC (2015b) Rainfall Erosivity in the EU and Switzerland (R-factor)., European Commission, Joint Research Centre Available at: https://esdac.jrc.ec.europa.eu/content/rainfall-erosivity-european-union-and-switzerland (Accessed: 7 June 2019).

ESRI (2017) ArcGIS Desktop 10.6. Environmental Systems Research Institute, Redlands, CA

Fang, J., Wu, F., Xiong, Y., Li, F., Du, X., An, D. and Wang, L. (2014) 'Source characterization of sedimentary organic matter using molecular and stable carbon isotopic composition of n-alkanes and fatty acids in sediment core from Lake Dianchi, China', Science of the Total Environment, 473–474, pp. 410–421.

Felde, V.J.M.N.L., Schweizer, S.A., Biesgen, D., Ulbrich, A., Uteau, D., Knief, C., Graf-Rosenfellner, M., Kögel-Knabner, I. and Peth, S. (2021) 'Wet sieving versus dry crushing: Soil microaggregates reveal different physical structure, bacterial diversity and organic matter composition in a clay gradient', European Journal of Soil Science, 72(2), pp. 810–828.

Ferraccioli, F., Gerard, F., Robinson, C., Jordan, T., Biszczuk, M., Ireland, L., Beasley, M., Vidamour, A., Barker, A., Arnold, R., Dinn, M., Fox, A. and Howard, A. (2014) LiDAR based Digital Terrain Model (DTM) data for South West England. NERC Environmental Information Data,

Ferrari, A.E., Ravnskov, S., Larsen, J., Tønnersen, T., Maronna, R.A. and Wall, L.G. (2015) 'Crop rotation and seasonal effects on fatty acid profiles of neutral

and phospholipids extracted from no-till agricultural soils', Soil Use and Management, 31(1), pp. 165–175.

Ficken, K.J., Li, B., Swain, D.L. and Eglinton, G. (2000) 'An n-alkane proxy for the sedimentary input of submerged/floating freshwater aquatic macrophytes', Organic Geochemistry, 31(7–8), pp. 745–749.

Gadiga, B.L. and Martins, A.K. (2015) 'The use of Revised Universal Soil Loss Equation (RUSLE) as a Potential Technique in Mapping Areas Vulnerable to Soil Erosion in the Upper Yedzaram Catchment of Mubi', International Journal of Engineering Research and, V4(03), pp. 432–437.

Geng, J., Cheng, S., Fang, H., Pei, J., Xu, M., Lu, M., Yang, Y., Cao, Z. and Li, Y. (2019) 'Different molecular characterization of soil particulate fractions under N deposition in a subtropical forest', Forests, 10(10), pp. 1–18.

Glaser, B. and Zech, W. (2005) 'Reconstruction of climate and landscape changes in a high mountain lake catchment in the Gorkha Himal, Nepal during the Late Glacial and Holocene as deduced from radiocarbon and compound-specific stable isotope analysis of terrestrial, aquatic and microbi', Organic Geochemistry, 36(7), pp. 1086–1098.

Glendell, M., Jones, R., Dungait, J.A.J., Meusburger, K., Schwendel, A.C., Barclay, R., Barker, S., Haley, S., Quine, T.A. and Meersmans, J. (2018) 'Tracing of particulate organic C sources across the terrestrial-aquatic continuum, a case study at the catchment scale (Carminowe Creek, southwest England)', Science of the Total Environment, 616, pp. 1077–1088. Available at: 10.1016/j.scitotenv.2017.10.211 (Accessed: 5 September 2018).

Gobin, A., Jones, R., Kirkby, M., Campling, P., Govers, G., Kosmas, C. and Gentile, A.R. (2004) 'Indicators for pan-European assessment and monitoring of soil erosion by water', Environmental Science and Policy, 7(1), pp. 25–38.

Grabowski, R.C. and Gurnell, A.M. (2016) 'Diagnosing problems of fine sediment delivery and transfer in a lowland catchment', Aquatic Sciences, 78(1) Springer Basel, pp. 95–106.

Guo, J., Glendell, M., Meersmans, J., Kirkels, F., Middelburg, J.J. and Peterse, F. (2020) 'Assessing branched tetraether lipids as tracers of soil organic carbon transport through the Carminowe Creek catchment (southwest England)', Biogeosciences, 17(12), pp. 3183–3201.

Hijmans, R.J. (2020) Raster: Geographic Data Analysis and Modeling. R package 3.0-12.

Hirave, P., Glendell, M., Birkholz, A. and Alewell, C. (2020a) 'Compound-specific isotope analysis with nested sampling approach detects spatial and temporal variability in the sources of suspended sediments in a Scottish mesoscale catchment', Science of The Total Environment, (xxxx) The Authors, p. 142916.

Hirave, P., Wiesenberg, G.L.B., Birkholz, A. and Alewell, C. (2020b) 'Understanding the effects of early degradation on isotopic tracers: implications for sediment source attribution using compound-specific isotope analysis (CSIA)', Biogeosciences Discussions, (June), pp. 1–18.

Krasa, J., Dostal, T., Jachymova, B., Bauer, M. and Devaty, J. (2019) 'Soil erosion as a source of sediment and phosphorus in rivers and reservoirs – Watershed analyses using WaTEM/SEDEM', Environmental Research, 171(January) Elsevier Inc., pp. 470–483.

Laceby, J.P., Evrard, O., Smith, H.G., Blake, W.H., Olley, J.M., Minella, J.P.G. and Owens, P.N. (2017) 'The challenges and opportunities of addressing particle size effects in sediment source fingerprinting: A review', Earth-Science Reviews, 169(December 2016), pp. 85–103.

Lewis, G.P., Weigel, A.M., Duskin, K.M. and Haney, D.C. (2021) 'Wood abundance in urban and rural streams in northwestern South Carolina', Hydrobiologia, 2 Springer International Publishing

Liu, X., Zou, X., Cao, M. and Luo, T. (2020) 'Organic carbon storage and 14C apparent age of upland and riparian soils in a montane subtropical moist forest of southwestern China', Forests, 11(6), pp. 1–19.

Luo, Y., Wang, H., Meersmans, J., Green, S.M., Quine, T.A. and Feng, S. (2020) 'Modeling soil erosion between 1985 and 2014 in three watersheds on the carbonate-rock dominated Guizhou Plateau, SW China, using WaTEM/SEDEM', Progress in Physical Geography, , pp. 1–29.

De Mastro, F., Cocozza, C., Brunetti, G. and Traversa, A. (2020) 'Chemical and spectroscopic investigation of different soil fractions as affected by soil management', Applied Sciences (Switzerland), 10(7)

Mayer, S., Kühnel, A., Burmeister, J., Kögel-Knabner, I. and Wiesmeier, M. (2019) 'Controlling factors of organic carbon stocks in agricultural topsoils and subsoils of Bavaria', Soil and Tillage Research, 192(January) Elsevier, pp. 22–32.

Meersmans, J., Martin, M.P., De Ridder, F., Lacarce, E., Wetterlind, J., De Baets, S., Bas, C. Le, Louis, B.P., Orton, T.G., Bispo, A. and Arrouays, D. (2012) 'A novel soil organic C model using climate, soil type and management data at the national scale in France', Agronomy for Sustainable Development, 32(4), pp. 873–888.

Met Office (2021) UK climate averages. Available at: https://www.metoffice.gov.uk/research/climate/maps-and-data/uk-climate-averages/gbukbmeyr (Accessed: 14 January 2021).

Meyers, P.A. (2003) 'Application of organic geochemistry to paleolimnological reconstruction: a summary of examples from the Laurention Great Lakes', Organic Geochemistry, 34, pp. 261–289.

Nitzsche, K.N., Kleeberg, A., Hoffmann, C., Merz, C., Premke, K., Gessler, A., Sommer, M. and Kayler, Z.E. (2022) 'Kettle holes reflect the biogeochemical characteristics of their catchment area and the intensity of the element-specific input', Journal of Soils and Sediments, Springer Berlin Heidelberg, pp. 994–1009.

Oliveira, P.T.S., Nearing, M.A. and Wendland, E. (2015) 'Orders of magnitude increase in soil erosion associated with land use change from native to cultivated

vegetation in a Brazilian savannah environment', Earth Surface Processes and Landforms, 40(11), pp. 1524–1532.

Van Oost, K., Govers, G. and Desmet, P. (2000) 'Evaluating the effects of changes in landscape structure on soil erosion by water and tillage', Landscape Ecology, 15(6), pp. 577–589.

Van Oost, K., Van Rompaey, A.J.J., Notebaert, B., Vaes, B., Verstraeten, G. and Govers, G. (2006) WaTEM/SEDEM version 2006 Manual 2004.

Owens, P.N. (2020) 'Soil erosion and sediment dynamics in the Anthropocene: a review of human impacts during a period of rapid global environmental change', Journal of Soils and Sediments, 20 Journal of Soils and Sediments, pp. 4115–4143.

Owens, P.N., Blake, W.H., Gaspar, L., Gateuille, D., Koiter, A.J., Lobb, D.A., Petticrew, E.L., Reiffarth, D.G., Smith, H.G. and Woodward, J.C. (2016) 'Fingerprinting and tracing the sources of soils and sediments: Earth and ocean science, geoarchaeological, forensic, and human health applications', Earth-Science Reviews, 162 Elsevier B.V., pp. 1–23.

Panagos, P., Ballabio, C., Borrelli, P., Meusburger, K., Klik, A., Rousseva, S., Tadić, M.P., Michaelides, S., Hrabalíková, M., Olsen, P., Aalto, J., Lakatos, M., Rymszewicz, A., Dumitrescu, A., Beguería, S. and Alewell, C. (2015) 'Rainfall erosivity in Europe', Science of the Total Environment, 511, pp. 801–814.

Panagos, P., Meusburger, K., Ballabio, C., Borrelli, P. and Alewell, C. (2014) 'Soil erodibility in Europe: A high-resolution dataset based on LUCAS', Science of the Total Environment, 479–480(1) Elsevier B.V., pp. 189–200.

Pebesma, E.J. (2004) 'Multivariable geostatistics in S: the gstat package', Computers and Geosciences, 30, pp. 683–691.

Pebesma, E.J. and Bivand, R.S. (2005) Classes and methods for spatial data in R: The sp package. R News 5 (2)

Poesen, J. (2018) ‘Soil erosion in the Anthropocene: Research needs’, Earth Surface Processes and Landforms, 43(1), pp. 64–84.

Puttock, A., Dungait, J.A.J., Macleod, C.J.A., Bol, R. and Brazier, R.E. (2014) ‘Organic Carbon From Dryland Soils’, Journal of Geophysical Research: Biogeosciences, 119, pp. 2345–2357.

Quenea, K., Derenne, S., Largeau, C., Rumpel, C. and Mariotti, A. (2004) ‘Variation in lipid relative abundance and composition among different particle size fractions of a forest soil’, Organic Geochemistry, 35(11-12 SPEC. ISS.), pp. 1355–1370.

Quénéa, K., Largeau, C., Derenne, S., Spaccini, R., Bardoux, G. and Mariotti, A. (2006) ‘Molecular and isotopic study of lipids in particle size fractions of a sandy cultivated soil (Cestas cultivation sequence, southwest France): Sources, degradation, and comparison with Cestas forest soil’, Organic Geochemistry, 37(1), pp. 20–44.

R Core Team (2020) R: A language and environment for statistical computing 3.6.3. R Foundation for Statistical Computing, Vienna, Austria

Ranjan, R.K., Routh, J., Val Klump, J. and Ramanathan, A.L. (2015) ‘Sediment biomarker profiles trace organic matter input in the Pichavaram mangrove complex, southeastern India’, Marine Chemistry, 171 Elsevier B.V., pp. 44–57.

Renard, K.G., Foster, G.R., Weesies, G.A., Mc Cool, D.K. and Yoder, D.C. (1997) Predicting soil erosion by water: A guide to conservation planning with the revised universal soil loss equation (RUSLE).Agricultur. Washington, D.C.: U.S. Dept. of Agriculture, Agricultural Research Service.

Van Rompaey, A.J.J. and Govers, G. (2002) ‘Data quality and model complexity for regional scale soil erosion prediction’, International Journal of Geographical Information Science, 16(7), pp. 663–680.

Van Rompaey, A.J.J., Verstraeten, G., van Oost, K., Govers, G. and Poesen, J. (2001) ‘Modelling mean annual sediment yield using a distributed approach’, Earth Surface Processes and Landforms, 1236, pp. 1221–1236.

RStudio Team (2018) RStudio: Integrated Development for R 1.1.463. PBC, Boston, MA

Singh, S.N., Kumari, B. and Mishra, S. (2012) 'Microbial Degradation of Alkanes', in Microbial Degradation of Xenobiotics. , pp. 439–469.

Starr, G.C., Lal, R., Malone, R., Hothem, D., Owens, L. and Kimble, J. (2000) 'Modeling soil carbon transported by water erosion processes', Land Degradation and Development, 11(1), pp. 83–91.

Stock, B.C., Jackson, A.L., Ward, E.J., Parnell, A.C., Phillips, D.L. and Semmens, B.X. (2018) MixSIAR model description

Stock, B.C. and Semmens, B.X. (2016) MixSIAR GUI User Manual. Version 3.1

Stout, S.A. (2020) 'Leaf wax n-alkanes in leaves, litter, and surface soil in a low diversity, temperate deciduous angiosperm forest, Central Missouri, USA', Chemistry and Ecology, Taylor & Francis, pp. 810–826.

Torres, T., Ortiz, J.E., Martín-Sánchez, D., Arribas, I., Moreno, L., Ballesteros, B., Blázquez, A.N.A., Domínguez, J.A. and Estrella, T.R. (2014) 'The long pleistocene record from the pego-oliva marshland (Alicante-Valencia, Spain)', Geological Society Special Publication, 388(1), pp. 429–452.

Trimble, S.W. (1983) 'A sediment budget for Coon Creek basin in the Driftless Area, Wisconsin, 1853-1977', American Journal of Science, 283, pp. 454–474.

Valera, C.A., Pissarra, T.C.T., Filho, M.V.M., do Valle Júnior, R.F., Oliveira, C.F., Moura, J.P., Fernandes, L.F.S. and Pacheco, F.A.L. (2019) 'The buffer capacity of riparian vegetation to control water quality in anthropogenic catchments from a legally protected area: A critical view over the Brazilian new forest code', Water (Switzerland), 11(3)

Verstraeten, G., Van Oost, K., Van Rompaey, A., Poesen, J. and Govers, G. (2002) 'Evaluating an integrated approach to catchment management to reduce soil loss and sediment pollution through modelling', Soil Use and Management, 18(4), pp. 386–394.

Vogel, H.J., Bartke, S., Daedlow, K., Helming, K., Kögel-Knabner, I., Lang, B., Rabot, E., Russell, D., Stößel, B., Weller, U., Wiesmeier, M. and Wollschläger, U. (2018) 'A systemic approach for modeling soil functions', Soil, 4(1), pp. 83–92.

Wang, Y., Yang, H., Zhang, J., Xu, M. and Wu, C. (2015) 'Biomarker and stable carbon isotopic signatures for 100-200year sediment record in the Chaihe catchment in southwest China', Science of the Total Environment, 502 Elsevier B.V., pp. 266–275.

Wiesmeier, M., Urbanski, L., Hobley, E., Lang, B., von Lützow, M., Marin-Spiotta, E., van Wesemael, B., Rabot, E., Ließ, M., Garcia-Franco, N., Wollschläger, U., Vogel, H.J. and Kögel-Knabner, I. (2019) 'Soil organic carbon storage as a key function of soils - A review of drivers and indicators at various scales', Geoderma, 333(July 2018) Elsevier, pp. 149–162.

Wischmeier, W. and Smith, D. (1978) Predicting rainfall erosion losses: a guide to conservation planning. Agricultural Handbook No. 537. U. S. Department of Agriculture., Washington (DC)

Wu, C.L., Herrington, S.J., Charry, B., Chu, M.L. and Knouft, J.H. (2021) 'Assessing the potential of riparian reforestation to facilitate watershed climate adaptation', Journal of Environmental Management, 277(May 2020) Elsevier Ltd, p. 111431.

Yu, M., Eglinton, T.I., Haghipour, N., Montluçon, D.B., Wacker, L., Wang, Z., Jin, G. and Zhao, M. (2019) 'Molecular isotopic insights into hydrodynamic controls on fluvial suspended particulate organic matter transport', Geochimica et Cosmochimica Acta, 262(238), pp. 78–91.

Zech, M., Buggle, B., Leiber, K., Marković, S., Glaser, B., Hambach, U., Huwe, B., Stevens, T., Sümegi, P., Wiesenberg, G. and Zöller, L. (2009) 'Reconstructing Quaternary vegetation history in the Carpathian Basin, SE-Europe, using n-alkane biomarkers as molecular fossils: Problems and possible solutions, potential and limitations', Quaternary Science Journal, 58(2), pp. 148–155.

Zech, M., Krause, T., Meszner, S. and Faust, D. (2013) ‘Incorrect when uncorrected: Reconstructing vegetation history using n-alkane biomarkers in loess-paleosol sequences - A case study from the Saxonian loess region, Germany’, Quaternary International, 296 Elsevier Ltd and INQUA, pp. 108–116.

Zhang, X., Liu, X., Zhang, M. and Dahlgren, R.A. (2010) ‘A Review of Vegetated Buffers and a Meta-analysis of Their Mitigation Efficacy in Reducing Nonpoint Source Pollution’, Journal of Environmental Quality, 39, pp. 76–84.

Zhang, Y., Collins, A.L., McMillan, S., Dixon, E.R., Cancer-Berroya, E., Poiret, C. and Stringfellow, A. (2017) ‘Fingerprinting source contributions to bed sediment-associated organic matter in the headwater subcatchments of the River Itchen SAC, Hampshire, UK’, River Research and Applications, 33(10), pp. 1515–1526.

3 Assessing *n*-alkane and neutral lipid biomarkers as tracers for land-use specific sediment sources

Abstract

Organic carbon (OC) fingerprinting (OCF) methods using taxonomical/plant-specific biomarkers such as *n*-alkanes have been successfully used to distinguish sediment sources originating from different land uses at a catchment scale. In this study, we hypothesise that using a combination of soil biomarkers of plant, fungal and bacterial origin may allow greater discrimination between land uses in OCF studies, and we explore the potential of short chain (shorter than C22) neutral lipid fatty acids (SC-NLFA) to improve land use discrimination, considering the Loch Davan catchment (34 km^2) in Scotland as a case study. Fatty acids are commonly used to measure abundance and diversity of soil microbial and fungal communities. The spatial distribution of these soil communities has been shown to depend mainly on soil properties and therefore soil types and land management practices. *N*-alkane and SC-NLFA concentrations and their compound specific isotope signatures (CSSI) in four land cover classes (crop land, pasture, forest, and moorland) were characterised and their contribution to six virtual sediment mixture samples was modelled. Using a Bayesian un-mixing model, the performance of the combined *n*-alkane and SC-NLFA biomarkers in distinguishing OC sources was then compared to OCF using *n*-alkane biomarkers alone. The addition of SC-NLFA biomarkers led to a significant decrease in error when distinguishing between all land use specific sediment sources (error reduction 1.8-9%). Distinguishing between arable and pasture land is known to be difficult due to agricultural rotation and, although the addition of SC-NLFA biomarkers did improve the discrimination between arable and pasture land use, it was the addition of *n*-alkane CSSI $\delta^{13}C$ that provided the greatest reduction in error when discriminating between these land uses. These results suggest that if a catchment OCF study was required to distinguish only arable and pasture land use, the combined use of *n*-alkane ratios and CSSI should improve the discrimination. However, for this catchment, where discrimination between four different land uses was required, the combination of

n-alkane ratios and SC-NLFA tracers provided the best capability for land use sediment source discrimination based on their reproduction of known source apportionments. The use of virtual mixtures as presented in this study provides a simple method that could be carried out before any OCF study to determine if addition or removal of tracers can improve relative error in source discrimination.

3.1 Introduction

Fine grained sediment is a natural and important component of fluvial systems, however, increased fluxes can impact stream ecological health and river functioning (Owens et al., 2005; Scheurer et al., 2009; Stenfert Kroese et al., 2020). Catchment soils provide a broad range of ecosystem services and fulfil many roles including structural and resources, filter and reservoir, fertility and biodiversity and climate regulation (Dominati, Patterson and Mackay, 2010; McBratney, Field and Koch, 2014). Natural processes such as erosion, fertility loss and the loss of soil carbon can be greatly accelerated by changes in climate and human activity (Battin et al., 2009; Gobin et al., 2004; Koch et al., 2013), resulting in increased lateral fluxes of soil OC (SOC) to waterways. Therefore, it is of vital importance to identify sources of sediment within catchments to inform effective management strategies.

Sediment fingerprinting has emerged in the last 20 years as an essential approach to quantify the relative contribution of different land use sources to organic matter load in waterways (Alewell et al., 2016; Chen et al., 2017; Glendell et al., 2018; Hancock and Revill, 2013; Liu et al., 2021b; Walling, Owens and Leeks, 1999). However, broad land use classifications (e.g., agricultural land cover, natural land cover) do not enable precise SOC origins to be determined or, consequently, management strategies to be targeted (Owens et al., 2016). The narrower the source group classifications (e.g., cropland, pasture, forest, moorland) the greater the spatial resolution of sediment origin, however, each source needs to be clearly discriminated by at least one tracer. In consequence, the more numerous the source groups, the more unlikely it is that clear discriminators will be available for every source (Collins et al., 2020; Pulley and Collins, 2018). Virtual sample mixtures (e.g. the mean of two sources

representing a 50% contribution from each) may be used to evaluate OC fingerprinting (OCF) un-mixing model predictions (Pulley and Collins, 2018) and were used by Palazón et al., (2015) to support the selection of a OCF procedure with the greatest capacity for source discrimination. Virtual mixtures could, therefore, be used to assess if using a particular set of tracers can successfully distinguish between all chosen land use sources and, in addition, provide a method of testing whether the addition or removal of tracers improves land use discrimination when using an un-mixing model for OCF.

Fingerprinting methods using taxonomic /plant-specific tracers (e.g. *n*-alkane ratios) (Galoski et al., 2019; Glendell et al., 2018; Liu et al., 2021a; Zhang et al., 2017) and compound-specific stable isotope (CSSI) signatures of long-chain (longer than C22) fatty acids (LCFAs) (Alewell et al., 2016; Hirave et al., 2020b), have been successfully applied to distinguish sediment sources originating from different land uses at a catchment scale. However, as tracers such as fatty acids and *n*-alkanes can persist in sediments for decades to centuries (Smeaton et al., 2021) the “fingerprint” for a specific land use can be considered to reflect both past and present biomarkers at a particular site and moment. Consequently, due to the agricultural rotation, arable land and temporary grassland may end up with similar signatures (Upadhayay et al., 2017). Tracing the fate of terrestrial-to-aquatic fluxes of sediment can be further complicated by the direct deposition of plant or woody material in the streams and rivers from which the sediment samples are taken, masking the signature from any eroded terrestrial soil. Combining soil biomarkers of plant, fungal and bacterial origin may allow greater discrimination between land uses and provide a fingerprint more characteristic of the soil rather than the current land cover vegetation.

Microbial communities have the potential to identify sediment originating from different land uses (Zhang et al., 2016b). Soil microbial communities directly affect soil functionality through cycling of soil nutrients and carbon storage and, as the spatial distributions of soil microbial communities have been shown to depend mainly on soil properties (Xue et al., 2018), it is likely that this will also represent the heterogeneity in soil type and land cover. To be recognized as a

suitable tracer, a biomarker needs to be unique with respect to the sources they need to discriminate, and not be altered over time in transport or within their depositional environment (conservative). Short chain (shorter than C22) neutral lipid fatty acids (SC-NLFA) can be of microbial or fungal rather than plant origin and have conventionally not been used as tracers in biogeochemical fingerprinting. These fatty acids (FA) are conserved and transformed into the neutral lipids of higher trophic consumers within the soil (Ruess et al., 2005). Neutral lipid biomarkers can persist in soils for decades and have proved to be effective in distinguishing past land use (Lavrieux et al., 2012). However, evidence that shorter chain FA may be preferentially degraded by soil microorganisms (Matsumoto et al., 2007) could suggest legacy effects of past crop cover or agricultural rotation may not be as pronounced in the signature of SC-NLFA (Blake et al., 2012). Previous studies have shown that C16 and C18 length fatty acids can distinguish crop-specific signatures (Blake et al., 2012), that fatty acids, considered common to prokaryotic and eukaryotic organisms, were particularly relevant for land use discrimination (Ferrari et al., 2015) and that lipid composition can show the effects of catchment land use on particulate OM in streams (Lu et al., 2014). The potential for SC-NLFA to distinguish between historical land uses by identifying specific microbial/fungal communities opens the potential for improved source attribution and commensurately, a need to verify any improvement.

Fingerprinting methods to distinguish land use sources are often carried out using only one type of biomarker such as CSSI of LCFAs (Alewell et al., 2016; Hirave et al., 2020b) or *n*-alkanes (Galoski et al., 2019) which may lead to difficulties in land use source differentiation (Alewell et al., 2016; Glendell et al., 2018). Even in OCF studies where more than one type of tracer is used (Glendell et al., 2018; Liu et al., 2021a; Zhang et al., 2017) there has not been an explicit investigation into which combination of tracers provided the best capacity for land use source discrimination by reproducing known source apportionments. To this end, this study; i) uses multiple types of biomarkers (*n*-alkane ratios and SC-NLFA) and their CSSIs to estimate the proportional contribution of land use sources to streambed sediment mixtures and ii) explores the use of virtual mixtures to

determine if addition or removal of tracers can improve relative error in source discrimination. Soil samples from four land uses from a Scottish catchment (Loch Davan) were used i) as sources to generate virtual sample mixtures and ii) to characterise the sources for OCF. The catchment has four major land uses (arable, pasture, forest and moorland) which are all potential sources of sediment within catchment streams. The aims of this study were to, i) use virtual mixtures and a Bayesian un-mixing model to determine which combination of tracers provided the best capacity for land use source discrimination by reproducing known source apportionments and ii) use the best set of tracers to estimate the proportional contribution of each land use to the catchment streambed sediments.

3.2 Material and methods

3.2.1 Study Site

The Dee is a major river in north-east Scotland whose catchment covers an area of about 2100km^2 on predominantly Precambrian metamorphic and igneous rocks. The Dee flows for over 130 km from its headwaters in the Cairngorms and reaches the North Sea on Scotland's east coast at Aberdeen. The Dee catchment is an important source of drinking water (Jenkins, D., 1985) and a designated Special Area of Conservation (SAC) due to the presence of species such as otter, Atlantic salmon and freshwater pearl mussel (https://sac.jncc.gov.uk/site/UK0030251). Loch Davan is a shallow (mean depth 1.2 m) throughflow lake located within the Muir of Dinnet National Nature Reserve (NNR) and drains through Davan Burn to the River Dee between Ballater and Aboyne (Jenkins, D., 1985). The main water input to Loch Davan is via Logie Burn and its feeder streams, and derives primarily from over-land surface flows (Smith, Tetzlaff and Soulsby, 2018). Loch Davan's catchment covers an area of *ca.* 34 km^2 in which Logie Burn and its feeder streams drain a variety of land uses including moorland (29%) and forest (22%) at higher elevation and arable (10%) and pasture (31%) at lower elevation (Figure 6b). The catchment reaches a maximum elevation in the west (750 m a.s.l.) gradually decreasing to the east and south to a minimum at Loch Davan (165 m a.s.l.). Areas of steepest slope

(13-37 degrees: Figure 6c) are found under moorland and forest land cover to the west and north-west of the catchment, with arable and pasture land cover dominating the relatively flat (typically < 3 degree slope) lowlands. The catchment mean annual precipitation is 780 mm with average annual minimum temperature of 3.5°C and average annual maximum temperature of 12.17°C (Met Office, 2021b). The major soil types observed in the catchment are mineral podzols (49%), brown soils (22%), and alluvial soils (11%) with around 5% of soils being peat or peaty gleys/podzols (“1:25,000 Hutton Soils Data” copyright and database right The James Hutton Institute (2018); Figure 6d). The lake area of Loch Davan has been significantly reduced over the last century, likely due to inputs of nutrient rich sediment due to land use intensification (Addy, Ghimire and Cooksley, 2012); between 2007 and 2018, the loch and its main feeder stream, Logie Burn, were classified as having poor to moderate ecological status (SEPA, 2021).

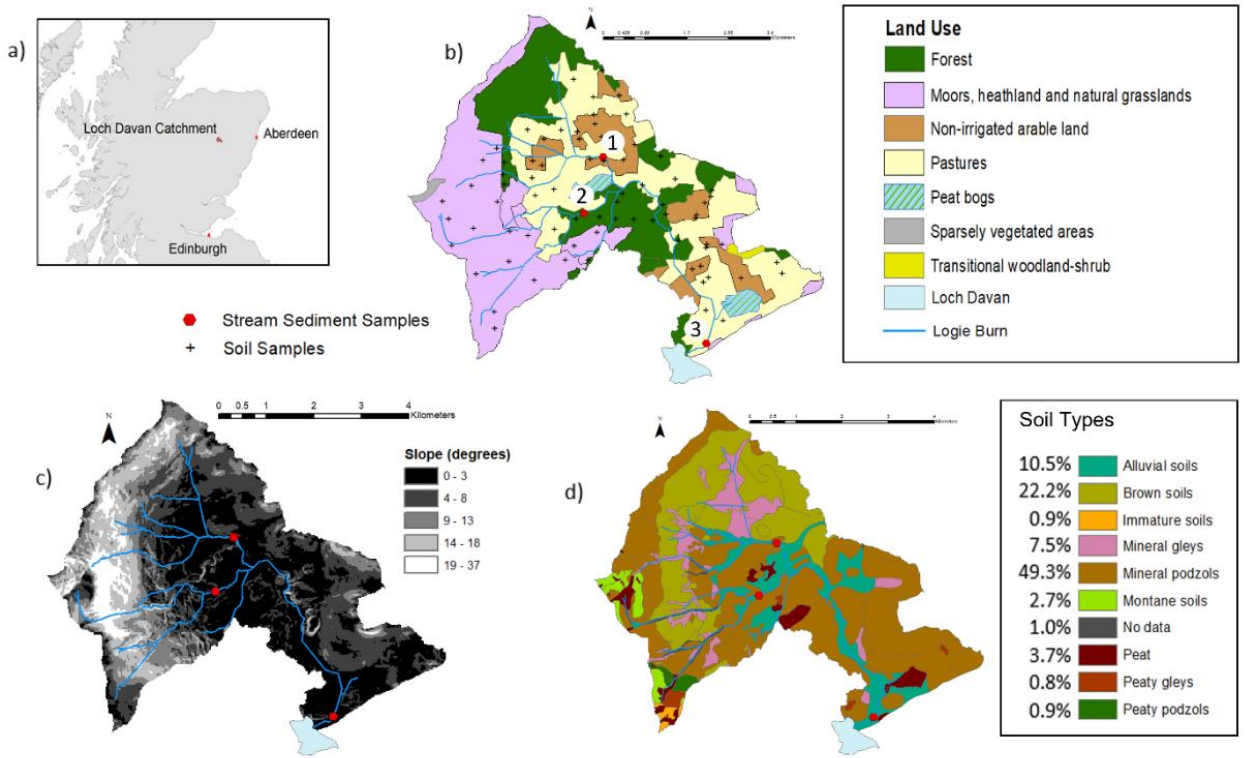

Figure 6: Loch Davan study catchment. a) Study catchment location, b) Land use of the Loch Davan catchment (34 km2), suspended and streambed sediment sampling locations (red dots: Sites 1, 2 and 3, referred to as BS1, BS2 and BS3) and terrestrial soil sampling locations (black crosses),based upon Corine land cover 2012 for the UK, Jersey and Guernsey (Cole et al., 2015), c) catchment slope (degrees) derived from OS Terrain 5 © Crown copyright and database rights 2021 Ordnance Survey (100025252)(Ordnance Survey, 2021), d) Catchment soils based on "1:25,000 Hutton Soils Data" copyright and database right The James Hutton Institute (2018). Used with the permission of The James Hutton Institute. All rights reserved.

3.2.2 Sample collection

In this study, a field campaign was carried out in June 2019 to collect soil and sediment samples within the Loch Davan catchment and Logie Burn stream network. Soil samples from four land uses (arable, pasture, forest and moorland) were collected to characterise potential sediment sources of OCF. Streambed samples were collected at three locations to estimate the proportional contribution of each of the land use source to the streambed sediments in two tributaries and a joint outlet (Figure 6b).

3.2.2.1 Source sampling

Replicate soil samples were taken to characterise each of the four land uses arable (n=16), forest (n=16), moorland (n=18) and pasture (n=19) at sites shown with a cross (+) in Figure 6b. Sampling sites were chosen on the basis of likely hydrological connectivity and were stratified by land use and soil type (Table 6). For each sampling point, litter was removed before taking a sample. Three replicate samples were taken at random within a 2 m radius of the sampling point using a steel cylinder (6cm depth and 6cm diameter). All samples were georeferenced by using a GPS device (horizontal accuracy sub-meter real-time), stored in plastic bags and freeze-dried on return to the laboratory. The samples were then passed through a 2 mm sieve to remove stones and larger organic material before being ground. A composite sample was formed for each site by adding an equal weight of each of the three finely ground samples. Samples were stored in sealed containers at room temperature until required for analysis.

Table 6 Number of soil samples taken for each land use and soil type combination

	Alluvial soils	Brown soils	Mineral gleys	Mineral podzols	Peaty gleys	Peaty podzols	No data	Montane soils	Total
arable	2	3	2	9	0	0	0	0	16
forest	2	2	2	10	0	0	0	0	16
moorland	3	4	4	3	1	1	1	1	18
pasture	4	3	4	7	1	0	0	0	19
Total	11	12	12	29	2	1	1	1	

3.2.2.2 Streambed sampling

Bed sediment samples were taken at 3 locations (Figure 6b), representing two tributaries and a joint outlet. The locations were carefully chosen above their confluence in the stream network so the contributions from each tributary could be assessed. Logie Burn originates in two main headwaters (Figure 6) with the northern most branch (BS1) supporting similar cover of pasture (30%), forest (29%) and moorland (28%) with around 10% arable land. The western branch (BS2) predominantly passes though moorland (78%) with around 14% of the land use being pasture, less than 5% forest and no arable land. A third site (BS3) was located close to the outlet of Logie Burn to Loch Davan integrating input from the whole catchment. At each site three samples of bed sediments were taken with a steel cylinder (6 cm depth and 6 cm diameter) along a transect across the streambed and composited. All samples were georeferenced using GPS, stored in plastic bags and freeze-dried on return to the laboratory. The samples were then passed through a 2 mm sieve to remove stones and larger organic material before being ground and stored at room temperature until further analysis.

3.2.3 Laboratory Analysis

3.2.3.1 Extraction of *n*-alkanes

To isolate the hydrocarbon fraction of the samples for analysis, total lipid extraction was followed by lipid fractionation (Dove and Mayes, 2006). For quality and quantification control purposes, the following solution was added by weight as the internal standard for alkanes: docosane (C_{22}) and tetratriacontane (C_{34}) in decane (0.03mg/g each alkane, 50µl solution to each sample) was added prior to extraction. First 3 ml of 1 M Ethanolic KOH solution was added to each sample in a tube before they were capped and heated for 16 hours at 90°C in a dry-block heater. The following steps were then repeated twice: 3 ml *N*-heptane was added to each tube which were capped and swirled before 1 ml of deionised water was added and the tubes re-capped and shaken vigorously; after separation into two liquid layers, the top (non-aqueous) layer was transferred to a new glass tube. The resulting solution was evaporated to dryness on a dry-block heater fitted with a sample concentrator blowing nitrogen (N_2) into the tube. The resultant was re-

dissolved in 0.3 ml heptane with warming before transferring the sample to SPE-Si cartridge, adding 2 ml heptane and collecting the elution in a 1.5 ml autosampler vial. Solution in the vial was then evaporated to dryness.

3.2.3.2 Extraction of NLFAs

The samples (5 – 10 g) were analysed by lipid extraction with a single phase chloroform mixture before fractionation on a SPE Si column and mild methanolysis. The solvents chloroform and methanol (1:2) were used in lipid extraction and, in addition, 0.15 M of citrate buffer (0.8:1:2 of citrate buffer: chloroform: methanol (Bligh and Dyer (B&D) solvent ratio)). 15 - 20 ml B&D solvent was added to the sample in a glass media bottle (closed using PTFE lined cap) which was then sonicated for 30 minutes (in ultrasonic bath). This was followed by centrifuge at 700 RCF for 10 minutes before the upper layer was poured into a clean glass media bottle. Chloroform (4 ml) and citrate buffer (4 ml) were added before centrifuging at 700 RCF for 10 minutes. Successful separation was indicated by both layers appearing clear and, using a vacuum pump, the upper (aqueous) layer was removed and discarded leaving the bottom organic layer. The glass bottle was then placed in an evaporator at 37°C and dried under N_2.

The neutral lipids were then separated from the lipid extract by fractionation (Solid Phase Extraction). Commercially prepared SPE columns were loaded onto vacuum manifold and prepared with ~0.5 g sodium sulphate (Na_2SO_4) and chloroform before the lipid extracts were added along with 1 ml chloroform. Five ml chloroform was used to elute the neutral lipids (sterols). These were collected in a clean glass bottle placed in an evaporator at 37°C and dried under N_2 for 4-5 hours. To quantify the FAMES against an internal standard, 60 µL of C19:0 methyl ester (Methyl nonadecanoate in methanol: 25 mg L^{-1}) was added to the dried phospholipid fraction after SPE and evaporated to dryness under N_2**.**

The samples were then methylated by adding 1 ml of toluene:methanol (1:1) (stored on Na_2SO_4) and 1 ml of 0.56 g potassium hydroxide in 50 ml methanol to the neutral lipid fraction (NLF). This was swirled and incubated @37°C for 30 minutes. Subsequently, 0.25 ml of acetic acid 59 ml L^{-1}, 5 ml of hexane:chloroform

(4 : 1)(v/v) and 3 ml deionised water were added and the NLF glass bottle was centrifuged at 700 RCF for 10 minutes. The upper organic phase was collected in a Gilson pipettor and the lower aqueous phase discarded. The resultant liquid was dispensed through 10 ml pipette tip packed with glass-wool and Na_2SO_4 into clean glass bottle and rinsed with a few ml of hexane. The glass bottle was placed in an evaporator at 20-25°C and dried under N_2. The dried FAMEs were then stored in a freezer at -20°C.

3.2.3.3 Analysis of *n*-alkanes and FAMES by GC-C-IRMS

Individual *n*-alkane and FAMEs were quantified and their $\delta^{13}C$ values determined by GC-C-IRMS using a Trace GC Ultra gas chromatograph (Thermo Finnigan, Bremen, Germany) equipped with a GC PAL autosampler (CTC Analytics AG, Zwingen, Switzerland) following the method described in Thornton et al., (2011).

3.2.4 *N*-alkane and SC-NLFA tracers

3.2.4.1 *N*-alkanes

N-alkanes are widely used plant biomarkers (Bush and McInerney, 2013). These naturally occurring unbranched hydrocarbons are an important constituent of cuticular plant leaf-waxes, deposited in soil by leaf-fall, and are relatively resistant against degradation (Zech et al., 2011). *N*-alkanes are stable, long-lived molecules that can endure in the fossil record for millennia (Bush and McInerney, 2013). This has led to their use as biomarkers in tracing vegetation input to soil and sediments over decadal and centennial time scales (Chen et al., 2017, 2022; Glendell et al., 2018; Wang et al., 2015) and also in paleoecology and paleoclimatology (Glaser and Zech, 2005; Meyers, 2003; Zech et al., 2009). The longer the *n*-alkane chain length, the less soluble they are in water, reducing their metabolism by microorganisms (Cranwell, 1981; Ranjan et al., 2015). Consequently, alkanes of chain-length >C24 are generally resistant to biodegradation (Singh, Kumari and Mishra, 2012) making them suitable as conservative sediment tracers. Plants produce a range of *n*-alkanes with a strong odd-over-even predominance (OEP) and one or two dominant chain lengths: trees and shrubs are characterised by C27 or C29, grass is characterised by C31 or C33 (Bush and McInerney, 2013; Meyers, 2003; Zech et al., 2013) and lower

plants and mosses by C23 and C25. Short-chain length *n*-alkanes (<C23) are typically derived from aquatic algae (Ficken et al., 2000; Meyers, 2003). Variability in the carbon isotopic signatures ($\delta^{13}C$) of *n*-alkanes is driven both by plant physiology/biochemistry and environmental factors (e.g. temperature, humidity, isotopic composition of water/CO_2) and is therefore (theoretically) unique for each individual plant and able to differentiate between different land cover types (Cooper et al., 2015 and references therein).

N-alkane concentrations and $\delta^{13}C$ were obtained for carbon chain lengths C21 to C38 where $\delta^{13}C$ is defined as:

$$\delta^{13}C = R(^{13}C/^{12}C)_{sample}/R(^{13}C/^{12}C)_{ref} - 1 \quad \textbf{(3-1)}$$

where $R(^{13}C/^{12}C)_{sample}$ and $R(^{13}C/^{12}C)_{ref}$ are the absolute isotope ratios of a sample and the reference material (in this case - Vienna PeeDee Belemnite) respectively.

The data was sub-set (Figure 7a) to include only those biomarkers that were present in each soil sample and in all streambed sediment samples. This sub-set included carbon chain lengths C23-C31 from which ratios were then calculated for use as tracers: the relative percentage of *n*-alkanes C27, C29 and C31 (Torres et al., 2014); the C27 to C31 ratio (Puttock et al., 2014); P_{aq}, to understand aquatic versus terrestrial plant input (Ficken et al., 2000); the Odd-to-Even Predominance (OEP) (Zech et al., 2013; and the Average Chain length (ACL) (Fang et al., 2014) (Table 7).

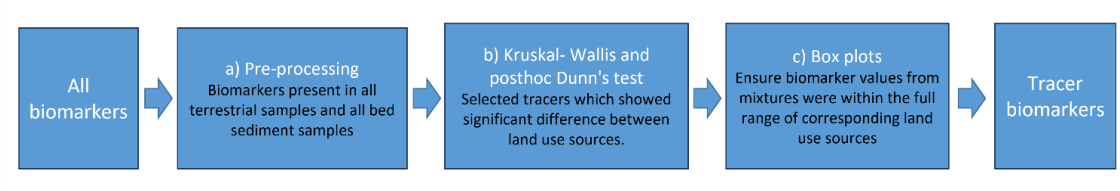

Figure 7 Summary of tracer selection methodology

Table 7 *N*-alkane ratios considered as tracers for land use discrimination

***n*-alkane ratios**	**Indicative of:**	**Reference**
C_{27} / C_{31}	C27 to C31 ratio estimating the proportion of wood to grass derived organic matter	(Puttock et al., 2014)
$\%\mathrm{Ci} = \frac{\mathrm{Ci}}{(\mathrm{C27} + \mathrm{C29} + \mathrm{C31})}$	% of alkane "i"	(Torres et al., 2014)
$PAQ = \frac{\mathrm{C23} + \mathrm{C25}}{\mathrm{C23} + \mathrm{C25} + \mathrm{C29} + \mathrm{C31}}$	Relative contribution of higher aquatic vs. terrestrial plants	(Ficken et al., 2000)
$OEP = \frac{\mathrm{C27} + \mathrm{C29} + \mathrm{C31}}{\mathrm{C26} + \mathrm{C28} + \mathrm{C30}}$	Organic matter degradation: odd-over-even predominance (OEP)	Adapted from (Zech et al., 2013)
$ACL = \frac{25 \times \mathrm{C25} + 27 \times \mathrm{C27} + 29 \times \mathrm{C29} + 31 \times \mathrm{C31}}{\mathrm{C25} + \mathrm{C27} + \mathrm{C29} + \mathrm{C31}}$	Average chain length (ACL) - weight-averaged number of carbon atoms of the higher plant C_{25}–C_{31} *n*-alkanes	Adapted from (Jeng, 2006)

3.2.4.2 SC-NLFA

Similar to *n*-alkanes, fatty acids are transferred from plant leaves and roots and bind strongly to mineral particles in the soil with a $\delta^{13}C$ signature reflecting plant cover C isotope (Blake et al., 2012). Different plant types produce the same fatty acids but with different CSSI signatures (Chikaraishi and Naraoka, 2003) which (once fresh plant material has degraded to humic substances within the soil) do not degrade over time (Blessing, Jochmann and Schmidt, 2008; Hirave et al., 2020b). Some Gram positive bacteria, particularly some actinobacteria, can accumulate large amounts of neutral lipids (Lanfranconi, Alvarez and Alvarez, 2015). These bacterial lipids are of increasing interest to the industrial market, in the production of components of cosmetics, lubricants, and coatings, or as a source for next generation biofuels (Lanfranconi, Alvarez and Alvarez, 2015;

Röttig and Steinbüchel, 2013). The NLFA 18:2ω6,9 is present in plant storage lipids and is also the dominant fatty acid in most fungi (Olsson et al., 2005). Ferrari et al. (2015) found that straight chain fatty acids, considered common to prokaryotic and eukaryotic organisms, were particularly relevant for land-use discrimination - especially 18:0. Neutral lipid molecular biomarkers such as iso- and anteiso-C15:0 fatty acid methyl esters (bacterial origin) can persist in soils for decades and have proved to be effective in distinguishing land use (Lavrieux et al., 2012). This suggests SC-NLFA could be suitable as conservative, land use specific sediment tracers. Seven of the 36 SC-NLFA biomarkers analysed in this study were found in both streambed sediments and all terrestrial soil samples: i15:0, a15:0, 16:0, 10-Methyl-16:0, 12-Me-16:0, 18:2ω6,9, and 18:0. The relative concentration of these seven SC-NLFA was then obtained by dividing the measured concentration by the sum of all concentrations.

3.2.4.3 Tracer Selection

Tracers should i) discriminate between all the potential sediment sources and, (ii) be conservative (remain stable during transport and deposition (Collins et al., 2020; Hirave et al., 2020a)). All tracer values were first checked for normal distribution using the Kolmogorov-Smirnov test. A Kruskal- Wallis (KW) and posthoc Dunn's test was then carried out to select tracers which showed significant differences between land use sources (Figure 7b). The tracers which passed the KW test were then assessed using box plots (Excel) to ensure biomarker values from all mixtures were within the full range of corresponding land use sources (Figure 7c). In addition, $\delta^{13}C$ biomarker tracers were only selected if their corresponding concentration values were within the range of stream sediment mixtures (Collins et al., 2020). The full range (excluding outliers) was used for the range test as, according to Bayesian inference, best practice suggests comparison of full distributions for hypothesis testing (Fenton and Neil, 2018). The streambed sediment mixtures are represented by a single measurement without any knowledge of the potential mean and distribution. This single measurement could represent a value close to the maximum or minimum of the possible tracer values rather than the mean and therefore selecting tracers

based solely on the means and inter-quartile range of the sources was considered too restrictive.

Unless otherwise stated, all MixSIAR runs, statistical and error analyses were carried out in R (version 3.6.3) (R Core Team, 2020) and RStudio (version 1.1.463) (RStudio Team, 2018).

3.2.5 Bayesian unmixing model (MixSIAR) implementation

The MixSIAR model was first developed for ecological studies but is increasingly being used in catchment sediment fingerprinting (Lachance et al., 2020; Smith, Karam and Lennard, 2018; Stenfert Kroese et al., 2020). Tracer properties can be characterised using the mean and standard deviation and the model is fitted using Markov chain Monte Carlo (MCMC). Source means and standard deviations used in the mixture likelihood are allowed to deviate from user specified values with the amount of deviation dependent on source sample sizes. A full description of this model can be found in Stock and Semmens (2016) and Stock et al. (2018). Sediment source proportions were estimated using 3000 MCMC simulations with MixSIAR formulated using a residual error term and an uninformative prior. The MCMC parameters were set to those for a “normal” run (Stock and Semmens, 2016) (chain length = 100,000, burn = 50,000, thin = 50, chains = 3) and the Gelman-Rubin diagnostic was used to evaluate convergence of all models.

3.2.6 Virtual Mixtures

Land use discrimination was assessed using “virtual” mixtures with 50/50 contributions from each of the four sources (arable, pasture, forest and moorland) by taking the mean of two sources to represent a 50% contribution from each (Collins et al., 2020). This resulted in six virtual 50/50 mixtures: Arable-Forest (AF50), Arable-Moorland (AM50), Arable-Pasture (AP50), Forest-Moorland (FM50), Forest-Pasture (FP50) and Moorland-Pasture (MP50). Errors were calculated as mean absolute differences between the modelled and virtual mixture composition.

3.3 Results and Discussion

3.3.1 *N*-alkane ratios

Plants produce a range of *n*-alkanes with a strong odd-over-even predominance (OEP) and one or two dominant chain lengths: trees and shrubs are characterised by C27 or C29, grass is characterised by C31 or C33 (Bush and McInerney, 2013; Meyers, 2003; Zech et al., 2013) and lower plants, macrophytes and mosses by C23 and C25. Within this catchment the relative proportions of *n*-alkanes in arable and forest soil samples were very similar (Figure 8). As expected, C27 and C29 chain lengths dominated the forest soil *n*-alkane signature (42%) with relatively smaller contributions from C31 which is indicative of grasslands (C31 32%) and homologues C23 and C25 (26%), indicative of lower plants, macrophytes and mosses. However, C27 and C29 were also dominant in arable soil samples (46%) and even more so in streambed sediment (BS) samples (53-56%). Moorland soil samples were dominated by C31 (46%) and had the smallest contribution from C23 and C25 (15%, cf. 26-46% for other land uses and 31-36% for BS). In contrast, pasture land soil samples were dominated by C23 and C25 (46%) and had the smallest contribution from C31 (17%) even though C31 is usually dominant in grasslands. It is possible that, in this catchment, pastures are located in wetter areas with more mosses contributing to higher C23 and C25 abundance.

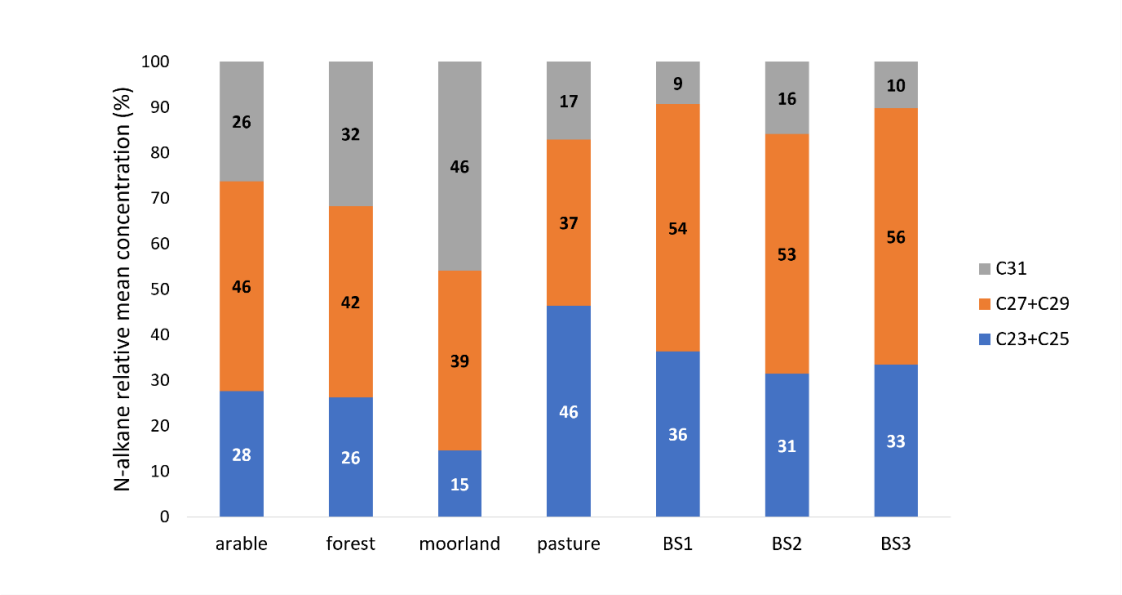

Figure 8: Relative mean concentration (%) for mid and long-chain *n*-alkane homologues for the soils of land uses, arable, forest, moorland and pasture streambed sediments BS1, BS2 and BS3.

The values of the *n*-alkane proxy for aquatic versus terrestrial plant input (PAQ) were similar in arable and forest soils (0.38±0.15 and 0.35±0.17 respectively), higher in pasture soils and streambed sediments (0.58±0.12 and 0.43 to 0.55, respectively) and lower in moorland soils (0.18±0.14) (Table 8; Figure 9). These values for PAQ are larger than those ascribed by Ankit et al., (2022) to terrestrial vegetation (<0.1) and actually lie predominantly in the range attributed to emergent macrophytes (0.1–0.4) (Ankit et al., (2022). Although, it seems unlikely that aquatic macrophytes would make a significant contribution to terrestrial soils across the catchment, their presence could account for the relatively higher PAQ and C23/C25 contribution in streambed sediments and possibly in pasture soils if these are located in wetter areas. Although the differences in PAQ between soil types were not significant (Kruskal-Wallis $p<0.05$), alluvial soils (recent riverine and lacustrine alluvial deposits) showed a relatively larger PAQ (Figure 10). The number of soils samples taken on alluvial soils for each land use (Table 6: arable 2 of 16 = 12.5%; forest 2 of 16 = 12.5%; moorland 3 of 18 = 17% and pasture 4 of 19 = 21%) is unlikely to account for the differences in PAQ seen for those land uses as moorland and pasture had similar percentages of alluvial soil samples but had the lowest and highest values of PAQ respectively.

OEP is often used as a measure of organic matter degradation with lower OEPs indicative of higher degradation (Zech et al., 2013). Stout, (2020) found the OEP was relatively lower for soil compared to the less degraded leaves/litter and in addition found preferential and progressive degradation of the more abundant C27/C29 relative to the less abundant C31/C33 from fresh leaves, through litter to the corresponding soil; the %C31 was relatively higher for soil compared to the less degraded leaves/litter. In this study, the OEP values of both streambed sediments and pasture soils were much smaller than those in arable, forest or moorland soils, which could suggest that they were more degraded. However, their corresponding %C31, which (particularly for the bed sediments) are relatively depleted would suggest the opposite. The *n*-alkane ratios for alluvial soils which showed significantly larger (Kruskal-Wallis $p<0.05$) %C27 and lower %C31 than the other soil types (Figure 10). The range of values for these ratios seen in the alluvial soil type was similar to that seen in streambed sediments which also showed relatively large %C27 and lower %C31. Light soil fractions can exhibit relatively higher amounts of mid-chain *n*-alkanes with low CPI values compared to bulk soil (Carbon preference index (CPI) is another *n*-alkane ratio proxy for the predominance of odd over even, similar to OEP) (Griepentrog et al., 2016). As finer sediments are more likely to be mobilised during water run-off than coarser sediments (Sirjani, Mahmoodabadi and Cerdà, 2022), streambed sediments could become relatively enriched in finer soil particles. This could account for the relatively large proportions of *n*-alkanes C25-C29 compared to C31 (Figure 8) as well as the low OEP values (Figure 9) seen in streambed sediments.

Although contribution from aquatic macrophytes/lower plants and mosses could account for the relatively higher C23/C25 (and PAQ) contribution in streambed sediments, equally elevated values were found in pasture soils. A larger input of pasture soil (relative to other land uses) to streambed sediments could account for their relatively higher C23/C25. When studying emergent aquatic plants He et al., (2020) found that long chain *n*-alkanes (e.g., C29) were predominantly derived from leaves (as opposed to roots) in wetland surface sediments/soils but that the contribution from mid-chain *n*-alkanes (e.g., C23) from roots was likely

equal to or greater than those from leaves. Griepentrog et al. (2016) also found the relative abundance of *n*-alkanes differed depending on the specific origin of the OM. For forest vegetation they found root biomass was characterized by a higher relative abundance of mid-chain *n*-alkanes (<C26) and low CPI whereas leaves had much higher CPI since they consisted almost exclusively of C27 and C29. Therefore, if a similar characterisation of the relative abundance of *n*-alkanes is found in pasture vegetation, a larger contribution of *n*-alkanes from roots rather than leaves could be contributing to relatively higher C23 abundance in pasture soils.

The ranges of *n*-alkane ratios in streambed sediments were outside the maximum and minimum values for the land use sources for C27/C31 and %C31 (Figure 9). The difference in range between the streambed sediment *n*-alkanes and those of the terrestrial land uses was primarily due to the relative depletion and enrichment of %C31 and %C27 respectively in the streambed sediments which commensurately reduced the average chain length (ACL) and increased the C27/C31 ratio (Table 8). On average, pasture soils also showed a depletion and enrichment of %C31 and %C27 respectively, relative to the other land uses (Table 8), however, the smallest %C31 and largest %C27 and ratios were found in forest soils (Figure 9). Within a forest environment both leaves and needles show increased C27/C31 ratio compared with soil, with C27 being particularly dominant in leaves. Hence, the higher C27/C31 ratio seen in forest soil samples could be due to a higher contribution of less degraded leaves/needles or litter (Griepentrog et al., 2016). An input of less degraded leaves/needles or litter to the streams could also account for the relatively high C27/C31 ratio found in streambed sediments. However, the relatively higher %C31 of less degraded leaves/litter would also be accompanied by a corresponding increase in OEP (Stout 2020), which was not observed in streambed sediments in this study. An alternative explanation could be related to bacterial sources of *n*-alkanes, with distributions from C11 to C35 often without an increase in OEP (Ladygina, Dedyukhina and Vainshtein, 2006). A microbial *n*-alkane pool could be responsible for mid and long-chain *n*-alkanes with low OEP in leaf litter samples (Zech et al., 2011). Grimalt et al., (1988) found that, when sediments from a

previously freeze-dried core were stored under water for a month, the *n*-alkane profiles previously ranging between C25 and C33 with high OEP were transformed into mixtures of C22-C29 *n*-alkanes with negligible OEP. They suggested this could be due to microbial transformations either due to *n*-alkane sources of bacterial origin, or to the re-working of organic matter by bacteria. Increased presence or activity of microbes due to the presence of water could account for the lower presence of long-chained *n*-alkanes (C31) and low OEP in the streambed sediment samples and possibly in the alluvial soils. The low OEP and relatively low %C31 seen in pasture soils cannot be directly linked with water sources and are interspersed with arable land throughout the catchment (Figure 6b). However, soil sampling sites were chosen on the basis of likely hydrological connectivity with the streams, that is, located on accumulated flow lines, so it these locations could be expected to support high soil moisture content. However, this explanation is confounded by the fact that similar reduction in OEP was not observed in samples taken in other land uses, which were also preferentially located in hydrologically well-connected locations.

In summary, the *n*-alkane values of the streambed sediments are similar to the forest soils in terms of their lower %C31 and higher %C27 values and similar to the pasture soils in their low OEP. Tracer conservativeness relies on these characteristics having the same source, that is, the high C27/C31 and low OEP are due to the presence of forest soil and pasture soil respectively in the streambed sediments and not significantly to the direct input of leaves/litter and/or microbial transformations as discussed above. As the streambed sediment mixtures are represented by a single measurement without any knowledge of the potential mean and distribution, the single measurement could represent a value close to the maximum or minimum of the possible tracer values rather than the mean. It is recommended in future fingerprinting studies to take a larger number of samples to represent the streambed sediments and so characterise a distribution which can be compared more easily with those of the terrestrial sources. More confidence that *n*-alkane ratios in the streambed sediments show the same range as the land use soils would lead to more confidence in rejecting alternative sources for streambed OC. The following tracer selection was carried

out on the assumption that any tracer for which all streambed sediment samples fell within the full range of corresponding land use sources could be classed as conservative.

Table 8 Mean (+/- 1SD) values of *n*-alkane ratios for forest, pasture, arable and moorland land uses and streambed sediment sources (BS1, BS2 and BS3)

	C27/C31	%C27	%C29	%C31	OEP	PAQ	ACL
arable (16)	1.10± 0.99	30.63± 9.65	34.10± 2.54	35.27± 9.69	4.26± 2.72	0.38± 0.15	28.38± 0.55
forest (16)	1.02± 1.01	29.90± 12.78	29.42± 3.56	40.68± 13.02	3.76± 2.09	0.35± 0.17	28.55± 0.74
moorland (18)	0.45± 0.56	17.60± 9.95	30.24± 5.53	52.17± 12.63	7.22± 3.40	0.18± 0.14	29.34± 0.66
pasture (19)	1.20± 0.55	35.07± 6.26	33.55± 1.62	31.38± 5.20	0.87± 0.93	0.58± 0.12	28.03± 0.36
BS 1	3.59	52.73	32.56	14.70	1.23	0.55	27.42
BS 2	1.72	39.83	37.02	23.15	1.71	0.43	27.93
BS 3	3.08	47.13	37.54	15.32	1.82	0.49	27.64

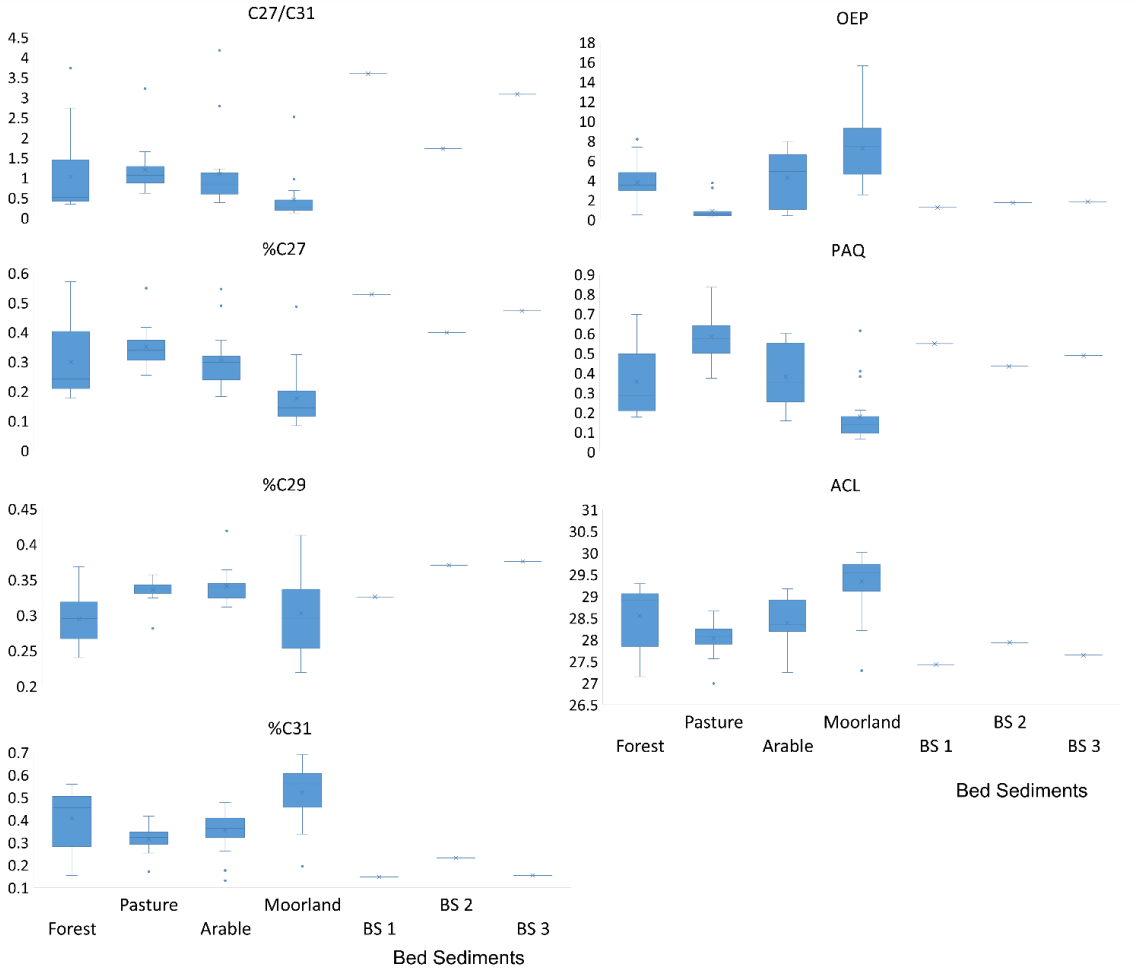

Figure 9: Range of *n*-alkanes ratios C27/C31, %C27, %C29, %C31, OEP, PAQ and ACL from forest, pasture, arable and moorland land uses and streambed sediment sources. The box is extended from the 25–75 percentiles, the line is plotted at the median and whiskers show the maximum to minimum range excluding outliers (dots).

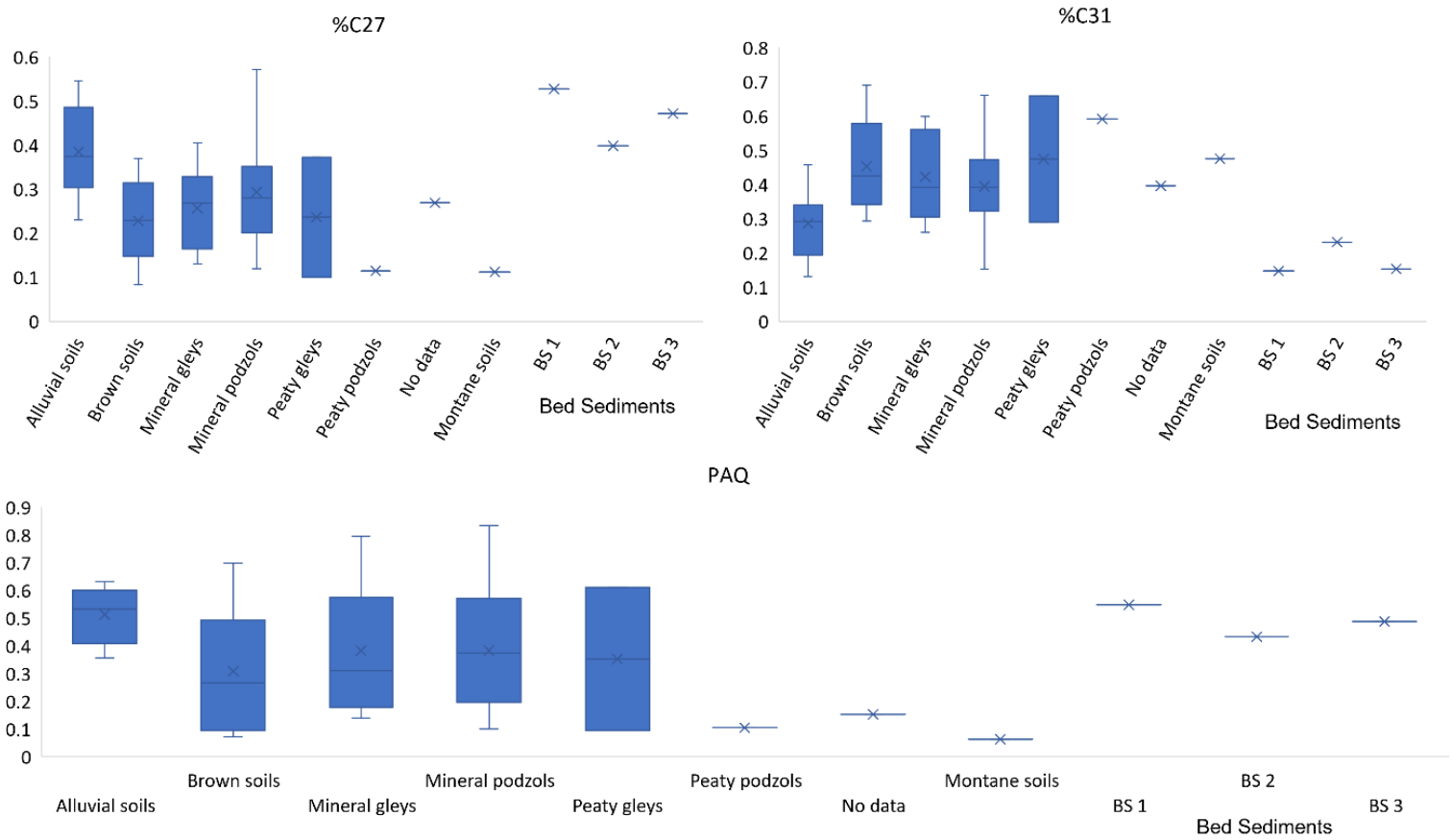

Figure 10 Range of *n*-alkanes ratios %C27 and %C31 from different soil types (Alluvial, Brown soils, Mineral Gleys, Mineral Podzols, Peaty Gleys, Peaty Podzols and Montane soils) and streambed sediment sources The box is extended from the 25–75 percentiles, the line is plotted at the median and whiskers show the maximum to minimum range excluding outliers.

3.3.1.1 Tracer selection

All *n*-alkane ratios showed significant differences between land use sources (Table 9). The ranges of C27/C31 and %C31 ratios in streambed sediments were outside the maximum and minimum values for the land use sources (Figure 9). Hence the remaining five *n*-alkane ratios (%C27, %C29, OEP, PAQ and ACL) were selected as tracers. Individually, only OEP and PAQ ratios could discriminate between most land uses, however together, these five biomarkers could discriminate between all land cover class combinations (Table 9). To distinguish four land use sources, a minimum of three tracers is required (Phillips and Gregg, 2003). The availability of five conservative *n*-alkane biomarkers confirms their suitability to be used without the need for additional types of biomarkers to distinguish between the four land use sources in this catchment.

Table 9: Kruskal-Wallis (KW) and posthoc Dunn's test: significant differences in *n*-alkane ratios ($p < 0.05$) distinguished between soil samples from different land use sources. Sources in bold indicate *n*-alkane ratios for streambed sediment within the range for terrestrial sediments

	Significant difference ($p<0.05$)						
	C27/C31	**%C27**	**%C29**	%C31	**OEP**	**PAQ**	**ACL**
Arable-Forest			✓				
Arable-Moorland	✓	✓	✓	✓		✓	✓
Arable-Pasture					✓	✓	
Forest-Moorland	✓	✓			✓	✓	✓
Forest-Pasture			✓	✓	✓	✓	
Moorland-Pasture	✓	✓	✓	✓	✓	✓	✓

3.3.2 *N*-alkane CSSI $\delta^{13}C$

Five of the 18 CSSI $\delta^{13}C$ biomarker signatures measured in this fingerprinting study were detected in both streambed sediments and all terrestrial soil samples (C23, C25, C27, C29 and C31). The range of *n*-alkane CSSI $\delta^{13}C$ values in the

soil samples and streambed sediment samples were all within those typical of *n*-alkanes in C3 land plants (ca. 39-30‰ (Chikaraishi and Naraoka, 2003)) except for C23 which showed less depleted values in both terrestrial samples (arable, forest and moorland) and streambed sediment samples BS1 and BS2 (Figure 11). However, some of the streambed sediment CSSI $\delta^{13}C$ signatures for C25, C27 and C29 chain lengths were less negative than, and outside the maximum and minimum values for, the land use sources (Figure 11). In their study of peat deposits Yan et al., (2021) revealed preferential degradation under aerobic conditions of mid-chain *n*-alkanes relative to their long-chain homologs (C29 and C31), resulting in an increase in both the relative proportions of long-chain *n*-alkanes and less depleted $\delta^{13}C$ values of mid-chain *n*-alkanes. However, it seems unlikely that this is the cause of the less depleted $\delta^{13}C$ values of C25-C29 *n*-alkanes in the streambed sediments in this study, as relative proportions of *n*-alkanes C25-C29, indicative of lower plants and woody material, are greater than the longer chain C31, indicative of grasslands (Figure 8). Alternatively, Wang et al., (2016) study of *n*-alkanes in fine and coarse particle fractions of surface peat revealed that $\delta^{13}C$ values of odd-numbered *n*-alkanes (C23– C33) were generally enriched in the finer fraction. They attributed this to greater heterotrophic reworking during degradation within the finer fractions compared to the coarser fraction. If finer sediments were preferentially mobilised during water run-off, streambed sediments may have become relatively enriched in finer soil particles (Nitzsche et al., 2022; Sirjani, Mahmoodabadi and Cerdà, 2022).

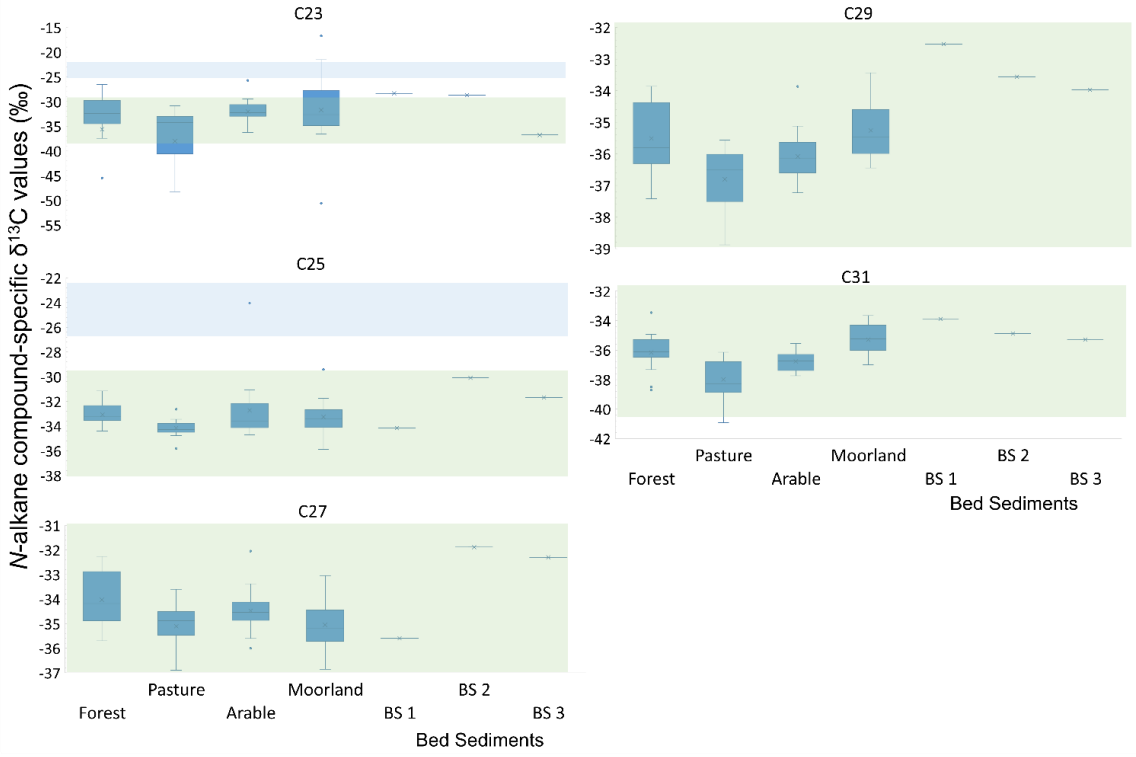

Figure 11: Range of $\delta^{13}C$ values (‰) of *n*-alkanes (C23-C31) from forest, pasture, arable and moorland land uses and streambed sediment sources The box is extended from the 25–75 percentiles, the line is plotted at the median and whiskers show the maximum to minimum range excluding outliers (dots). For comparison, typical *n*-alkane $\delta^{13}C$ values for C3 land plants (ca. 39-30‰) and freshwater plants (ca. 27-23‰) are shown as green and blue shaded areas respectively (Chikaraishi and Naraoka, 2003).

3.3.2.1 Tracer Selection

All the CSSI $\delta^{13}C$ in the soil samples were found to distinguish between land uses (Table 10). However, the CSSI $\delta^{13}C$ biomarker signatures for C25, C27 and C29 were outside the maximum and minimum values for the land use sources (Figure 11). Hence, only C23 and C31 CSSI signatures were selected as tracers and, together, these two biomarker signatures discriminated between all land cover class combinations except between arable and forest, and moorland and forest (Table 10). The availability of only two conservative *n*-alkane CSSI $\delta^{13}C$ biomarker signatures meant that they could not be used on their own to

distinguish between four land use sources in this catchment and would not be able to discriminate well between forest land cover and either arable or moorland.

Table 10: Kruskal- Wallis (KW) and posthoc Dunn's test: significant differences in *n*-alkane CSSI $\delta^{13}C$ ($p < 0.05$) distinguished between soil samples from different land use sources. Sources in bold indicate *n*-alkane CSSI $\delta^{13}C$ value for streambed sediment within the range for terrestrial sediments

	Significant difference ($p<0.05$)				
	C23	C25	C27	C29	**C31**
Arable-Forest					
Arable-Moorland					✓
Arable-Pasture	✓	✓			
Forest-Moorland			✓		
Forest-Pasture		✓	✓	✓	✓
Moorland-Pasture		✓		✓	✓

3.3.3 SC-NLFA concentrations

Seven of the 36 SC-NLFA biomarkers analysed in this study were detected in both streambed sediments and all terrestrial soil samples: i15:0, a15:0, 16:00, 10-Methyl-16:0, 12-Me-16:0, 18:2ω6,9, 18:00. Of these, all SC-NLFA relative concentrations (with the exception of 16:00) could distinguish between land uses (Table 11). Biomarkers a15:0 and 12-Me-16:0 were outside the maximum and minimum values for the land use sources and, therefore, only four SC-NLFA biomarkers (i15:0, 10-Methyl-16:0, 18:2ω6,9 and 18:00) were selected as tracers and, together, these biomarkers could discriminate between all land cover class combinations except arable and pasture (Table 11). The availability of four conservative SC-NLFA relative concentration biomarkers meant that they could, if required, be used without the need for additional biomarkers to distinguish between the four land use sources in this catchment.

Iso 15:0 (i15:0) is a biomarker for gram-positive bacteria and has been used to study trophic relationships in soil food webs (Haubert et al., 2006) and 10-Methyl-16:0 is characteristic of actinomycetes (Tekaya et al., 2021). Actinomycetes are especially abundant in soils, particularly soils which are alkaline or rich in organic matter, where they form an important part of the microbial population (Barka et al., 2016; Zaitlin et al., 2003). Large numbers of actinomycetes enter freshwater from land with soil runoff (Zaitlin et al., 2003). NLFA 18:2ω6,9 is present in plant storage lipids and is the dominant fatty acid in most fungi (Olsson et al., 2005). Within a forest environment Ferlian et al., (2014) found the fungal biomarker 18:2ω6,9 was more abundant in litter as compared to soil whereas the opposite was true of bacterial biomarkers such as i15:0 which were more abundant in the soil.

The relative mean concentrations of SC-NLFA i15, 10-Methyl-16, 18:2ω6, and 18:0 for forest soil samples were very different from samples from other land uses (Figure 12) with roughly equal contributions from all four biomarkers (i15:0 32%, 10-Methyl-16:0 22%, 18:2ω6,9 21% and 18:0 25%). Arable and moorland show a similar profile dominated by the fungal biomarker 18:2ω6,9 (50% and 59% respectively) with correspondingly smaller contributions from the bacterial biomarkers i15:0 and 10-Methyl-16:0 (combined contribution of 18% and 19% respectively) and biomarker 18:0 (32% and 22% respectively) ubiquitous in both bacteria and plants. The relative mean concentrations of SC-NLFA in pasture land soil samples had a larger contribution from the bacterial biomarkers i15:0 and 10-Methyl-16:0 (combined contribution of 29%) than those in arable/moorland soils and a correspondingly smaller contribution from the fungal biomarker 18:2ω6,9 (37% respectively). The study of Zaitlin et al., (2003) found actinomycetes were especially abundant in runoff from terrestrial sources with faecal contamination, suggesting an increased contribution of bacterial biomarkers in pasture land relative to arable or moorland could be due to the presence of grazing animals. It is not known why bacterial biomarkers dominate the signature in forest soils, however, bacterial and fungal communities can vary with nutrient availability and particle size fractions (Hemkemeyer et al., 2018, 2019; Zhang et al., 2016a) contributing to spatial heterogeneity and bacterial

diversity between land uses. There is a relatively larger contribution from bacterial biomarkers in the streambed sediments (BS1 29%, BS2 45%, and BS3 37%) relative to most of the land uses (arable 18%, moorland 19%, pasture 29% and forest 54%). This could be due to a larger contribution from forest soils to streambed sediments as the sample site for BS2 is within an area of forest. Alternatively, the range of $\delta^{13}C$ of *n*-alkanes suggested streambed sediments could have become relatively enriched in finer soil particles, and in the study of Hemkemeyer et al., (2018) actinobacteria were shown to exhibit preference for the fine silt particle fraction.

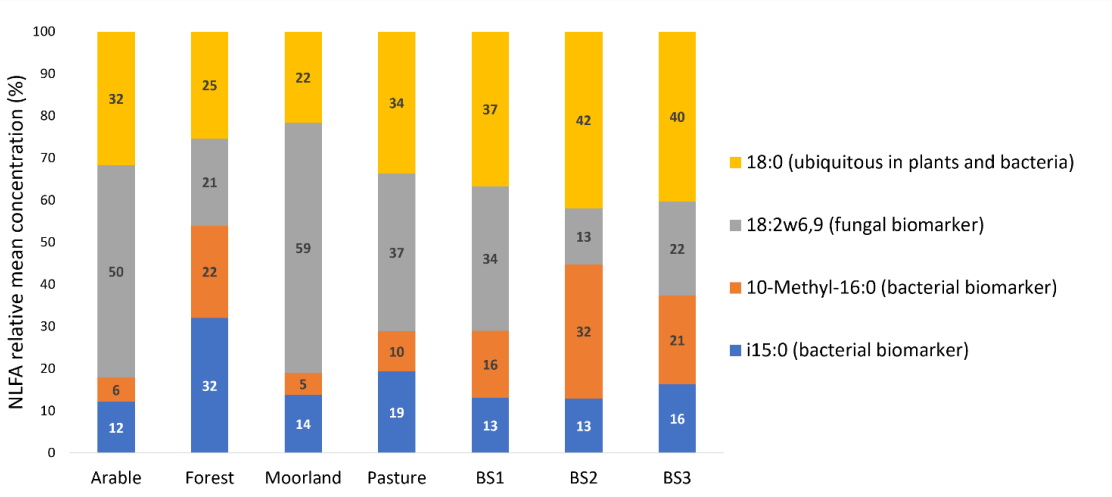

Figure 12: Relative mean concentration (%) for SC-NLFA for the soils of land uses, arable, forest, moorland and pasture streambed sediments BS1, BS2 and BS3

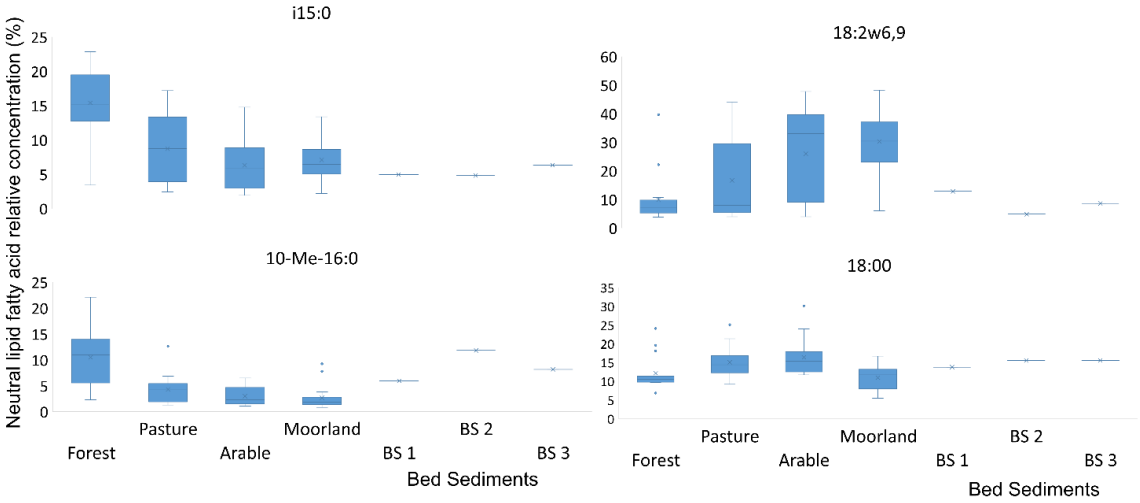

Figure 13 Range of SC-NLFA i15:0, 10-Methyl-16:0, 18:2ω6,9 and 18:00 from forest, pasture, arable and moorland land uses and streambed sediment sources The box is extended from the 25–75 percentiles, the line is plotted at the median and whiskers show the maximum to minimum range excluding outliers (dots).

Table 11: Kruskal- Wallis (KW) and posthoc Dunn's test: significant differences in Neutral lipid fatty acid (NLFA) relative concentration ($p < 0.05$) distinguished between soil samples from different land use sources. Sources in bold indicate NLFA concentrations for streambed sediment within the range for terrestrial sediments

	Significant difference ($p<0.05$)						
	i15:0	a15:0	**16:0**	**10-Methyl-16:0**	12-Methyl-16:0	**18:2ω6,9**	**18:0**
Arable-Forest	✓			✓		✓	✓
Arable-Moorland					✓		✓
Arable-Pasture							
Forest-Moorland	✓	✓		✓	✓	✓	
Forest-Pasture	✓			✓			✓
Moorland-Pasture		✓			✓	✓	✓

3.3.4 SC-NLFA CSSI $\delta^{13}C$

CSSI $\delta^{13}C$ signatures of conservative SC-NLFAs (selected above) (i.e., i15:0, 16:00, 10-Methyl-16:0, 18:2ω6,9 and 18:00) (Table 7) were considered as potential tracers. Of these, all SC-NLFA CSSI $\delta^{13}C$ (with the exception of 16:00) could distinguish between land uses (Table 12). The CSSI $\delta^{13}C$ values for i15:0 and 18:2ω6,9 were outside the maximum and minimum values for the land use sources and therefore only 10-Methyl-16:0 and 18:00 were selected as tracers (Figure 14). Together, these biomarkers could only discriminate between forest land and the other three land uses (Table 12). The availability of only two conservative SC-NLFA CSSI $\delta^{13}C$ biomarkers and their ability to distinguish a limited number of land use classes meant that they could not be used on their own to distinguish between the four land use sources in this catchment.

Table 12: Kruskal- Wallis (KW) and posthoc Dunn's test: significant differences in NLFA CSSI $\delta^{13}C$ ($p < 0.05$) distinguished between soil samples from different land use sources. Sources in bold indicate NLFA CSSI $\delta^{13}C$ for streambed sediment within the range for terrestrial sediments

	Significant difference ($p<0.05$)				
	i15:0	16:00	**10-Methyl-16:0**	18:2ω6,9	**18:00**
Arable-Forest			✓	✓	
Arable-Moorland					
Arable-Pasture					
Forest-Moorland			✓		
Forest-Pasture	✓		✓	✓	✓
Moorland-Pasture	✓				

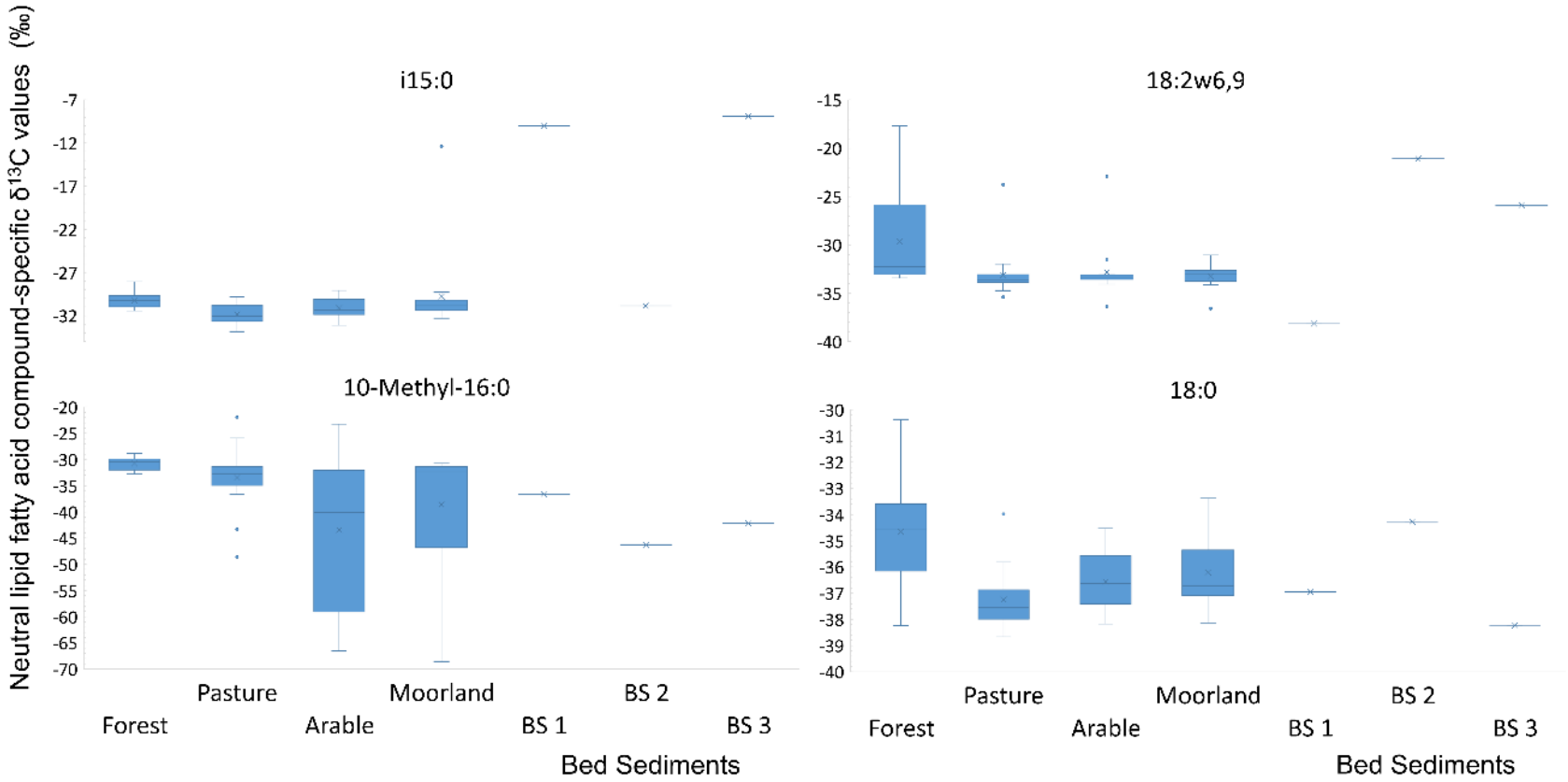

Figure 14: Range of δ^{13}C values (‰) of SC-NLFA from forest, pasture, arable and moorland land uses and streambed sediment sources The box is extended from the 25–75 percentiles, the line is plotted at the median and whiskers show the maximum to minimum range excluding outliers (dots).

3.3.5 Combination of tracers that provided the best land use source discrimination

Six “virtual” mixtures with 50/50 contributions from each of the four sources (arable, pasture, forest and moorland) were created to test the performance of MixSIAR in distinguishing between land uses when using the following tracer combinations; a) *n*-alkane ratios alone (baseline scenario), b) *n*-alkane ratios + CSSI signatures, c) *n*-alkane ratios + SC-NLFA concentrations, d) *n*-alkane ratios + SC-NLFA concentrations + SC-NLFA CSSI signatures and e) all tracers (Table 13). The use of additional biomarkers resulted in statistically significant differences in errors. Scenario b resulted in a significant increase in error when distinguishing arable land use from forest (21.2%) or moorland (7.2%) but a decrease in error when distinguishing all other land uses (Table 13). If the “best” tracer set is defined as minimising the error when distinguishing between land use sources, then using a tracer combination of *n*-alkane ratios + CSSI (Scenario b) was the most accurate (6.2% error) in distinguishing between arable and pasture land use sources. Scenario c resulted in a significant decrease in error when distinguishing all land use combinations (error reduction 1.6-8.2%). Using a tracer combination of *n*-alkane ratios + NLFA concentrations (Scenario b) was best when distinguishing between moorland and either arable or pasture land use sources. Scenario d also resulted in a significant decrease in error when distinguishing all land use combinations (error reduction 1.8-9%). Using a tracer combination of *n*-alkane ratios + NLFA concentrations + CSSI (Scenario d) was best when distinguishing between forest and either arable or moorland land use sources. Combining all the tracers (Scenario e) generally decreased the error compared to the baseline scenario (a) but showed larger errors compared to scenarios c and d. Distinguishing between arable and pasture land is known to be difficult due to agricultural rotation (Glendell et al., 2018; Upadhayay et al., 2017) and, for the baseline scenario (a) *n*-alkane ratios alone), relatively high errors were found when trying to distinguish between pasture and arable land (19.6% Table 13). However, even higher errors were found when distinguishing pasture from forest land cover (23% Table 13) and the addition of SC-NLFA biomarkers (Scenario d) reduced this error by 9%. Despite the individual SC-

NLFA tracers not being able to distinguish between arable and pasture land (Table 11 and Table 12), the addition of SC-NLFA biomarkers to n-alkanes did improve the discrimination between these two land uses. However, it was the addition of *n*-alkane CSSI $\delta^{13}C$ to the baseline that provided the greatest reduction in error when discriminating between these two land uses. These results suggest that if a catchment OCF study was required to distinguish only arable and pasture land use, the combined use of *n*-alkane ratios and CSSI should improve the discrimination. However, for this catchment, where discrimination between four different land uses is required, the combination of *n*-alkane ratios and SC-NLFA tracers (Scenario d) provided the best capacity for land use source discrimination based on the reproduction of known source apportionments.

This study has shown that the use of a combination of SOC biomarkers of plant, bacterial and fungal origin (*n*-alkane ratios and SC-NLFA) can reduce the error in distinguishing soil from different land uses. In addition, differences in soil fatty acid profiles (particularly NLFA) can be useful as markers to differentiate soils with different history of use (Ferrari et al., 2015). Soil fungal community structures under afforestation have been shown to be controlled by original land use practices (Xue et al., 2022) and soil biomarkers of bacterial origin (e.g. fatty acid methyl esters) have proved to be effective, not only in distinguishing current land uses, but also in distinguishing soil under land that had changed use decades before (e.g. grassland to forest (Lavrieux et al., 2012)). Combining SOC biomarkers from different soil communities may allow future studies to achieve even more accurate SOC source attribution using multiple source group classifications based not just on the current land use but on known conversions of land use (e.g., cropland to forest). If SC-NLFA could distinguish former grassland under afforestation from existing forest and grasslands these tracers could be used to see the effect of this land use change on the sources of sediments in nearby streams.

Table 13: Mean absolute differences between the modelled and virtual mixture composition (%) with biomarkers for Scenario a) *n*-alkane ratios alone (baseline scenario), b) *n*-alkane ratios + CSSI signatures, c) *n*-alkane ratios + SC-NLFA

concentrations, d) *n*-alkane ratios + SC-NLFA concentrations + SC-NLFA CSSI signatures and e) All tracers. Land use 50/50 combinations: Arable-Forest (AF50), Arable-Moorland (AM50), Arable-Pasture (AP50), Forest-Moorland (FM50), Forest-Pasture (FP50) and Moorland-Pasture (MP50). Asterisk (*) indicates significant difference from baseline (Scenario a); (p<0.05)).

	Mean absolute differences between the modelled and virtual mixture composition				
	a	**b**	**c**	**d**	**e**
AF50	8.6	29.8*	5.2*	2.6*	12.8*
AM50	10.2	17.4*	2.0*	2.2*	9.4
AP50	19.6	6.2*	13.6*	16.8*	8.2*
FM50	5.2	4.8*	3.6*	0.2*	4.4*
FP50	23.0	21.6	18.8*	14.0*	13.6*
MP50	9.4	7.2*	4.0*	7.6*	5.8*
Mean Error	12.7	14.5	7.9	7.2	9.0
Number of tracers	5	7	9	11	13

3.3.6 Contribution of land use sources to catchment streambed sediments

In this study catchment, where discrimination between four different land uses was required, the combination of *n*-alkane ratios and SC-NLFA tracers (Scenario d) provided the most accurate land use source discrimination based on their reproduction of known source apportionment. Modelling the relative land use contribution to the three streambed sediment samples using this tracer set and MixSIAR estimated that the main source of OC was pasture land cover type at all sites (68-80%: Figure 15).

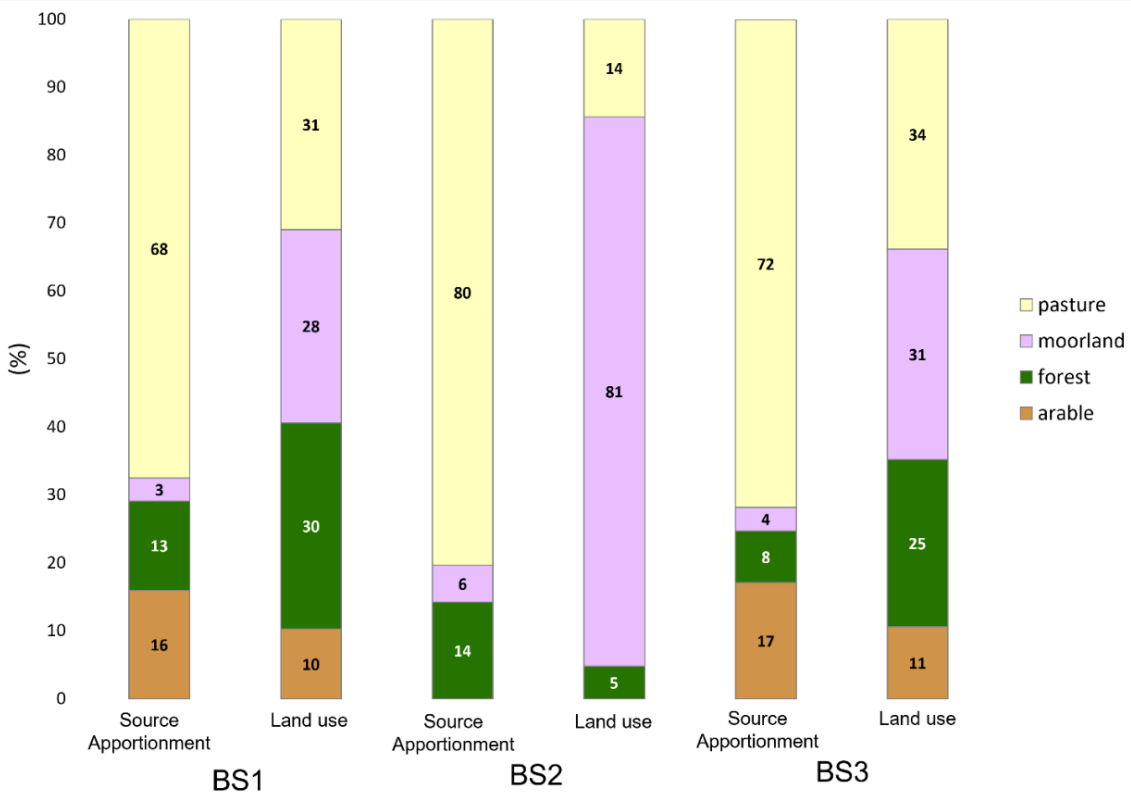

Figure 15: Percentage contribution of four land use sources (arable, forest, moorland and pasture) modelled using sediment fingerprinting (*n*-alkane ratios, and short chain (<C22) NLFA concentrations and CSSI signatures as tracers) and a Bayesian unmixing model (MixSIAR) for three streambed sediment samples (BS1, BS2 and BS3) – in each case this accompanied by the corresponding percentage land use cover for the sub-catchments of BS1, BS2 and BS3.

Arable land use covered approximately 10% of the BS3 catchment area and also of the sub-catchment relating to BS1. At both BS1 and BS3, arable land made a larger contribution to the streambed sediments (16% and 17% respectively: Figure 15) than would be expected given the amount of arable land within those sub-catchments. For *ca.* 400 m upstream of BS1 the stream is passing through arable land, some of which is located on steeper slopes (> 5°) which could have led to a locally higher level of erosion and input of arable soil to the stream (Wischmeier and Smith, 1978). Similarly, Pulley and Collins, (2018) found sediment sources in close proximity to their sediment sampling locations were of the greatest importance in their fingerprinting study in a UK agricultural catchment, and Lei et al., (2021) found that concentrations of nutrients in streams

were intensified by steeper slopes in agricultural and pasture fields in Germany. These results support other studies that have found arable land makes a larger contribution to river sediments than would be predicted from the proportion of land that it covers within a catchment (Wang et al., 2021).

At streambed sites BS1 and BS3 30% and 25% of the respective sub-catchment land is covered in forest, however forest land contributed only 13% and 8% respectively to the streambed sediments. These results are similar to a study carried out in another Aberdeenshire catchment (Tarland (Hirave et al., 2020a)) which found minimal inputs from forest land uses to the headwater stream suspended sediment flux (ca. 2%) due to high canopy cover and a dense organic layer on the soil surface resulting in low erosion rates. Wang et al., (2021) also found the contributions from forest and moorland to riverbed sediments were considerably smaller than those from arable land (forest 8% and moorland 6%: cf. arable 45%). However, forest accounts for less than 5% of the land cover in the sub-catchment at BS2 but contributed 14% of the streambed OC. The forest land in the BS2 sub-catchment is located on land at low risk of erosion (Lilly and Baggaley, 2018), however, all forest land is in close proximity to BS2, suggesting that these proximal areas had a large influence on the composition of streambed sediments, possibly through direct input of woody material to the stream (Lavrieux et al., 2019).

When considering BS3, located at the catchment outlet, nearly 30% percent of the catchment land cover is moorland, however, the MixSIAR model predicted a contribution of only 3% from moorland. Similarly, at BS2 and BS3, moorland encompasses nearly 80% and 30% of the land cover respectively but made the smallest contribution to the streambed sediments (20% and 3% respectively). Moorland covers large areas of the Loch Davan catchment and is located on the steepest slopes (Figure 6c) in areas at higher erosion risk (Lilly and Baggaley, 2018). The erosion risk map covering this catchment (Lilly and Baggaley, 2018) was constructed by estimating the erosion risk of bare soil under severe or protracted rainfall, with steeper slopes resulting in faster runoff. The minimal input of moorland soil to the streambed sediments suggests that despite their location

on steep slopes the vegetation cover found on these moorlands makes this land use relatively resistant to soil erosion. Hirave et al., (2020a) also found that moorland contributed marginally to suspended stream sediments (<2%), despite covering 16% of the catchment area, which they attributed to the thick organic layer covering the soil surface for this land use resulting in less erodibility of the soil.

At each streambed site there was a larger contribution from pasture land to the streambed sediments (BS1 68%, BS2 80% and BS3 72% respectively: Figure 15) than would be expected given the amount of pasture land within those sub-catchments (30%, 14% and 30% respectively). This study supports the high contribution (annual average 56-79%) of permanent grasslands to the suspended sediments and higher soil erosion rate estimates from improved grassland (as opposed to extensive arable land use), reported for other areas of in Scotland (Hirave et al., 2020a; Rickson et al., 2019).

3.4 Conclusion

Using a Bayesian un-mixing model, the performance of the combined *n*-alkane and SC-NLFA biomarkers in distinguishing land use was compared to OCF using *n*-alkane biomarkers alone. The addition of SC-NLFA biomarkers led to a significant decrease in error when distinguishing between all land uses (error reduction 1.8-9%). Distinguishing between arable and pasture land is known to be difficult due to agricultural rotation and, although the addition of SC-NLFA biomarkers did improve the discrimination between arable and pasture land, it was the addition of *n*-alkane CSSI $\delta^{13}C$ to the baseline that provided the greatest reduction in error when discriminating between these land uses. The results of this study suggest that if a catchment OCF study was required to distinguish only arable and pasture land use, the combined use of *n*-alkane ratios and CSSI should improve the discrimination. However, for this catchment, where discrimination between four different land uses was required, the combination of *n*-alkane ratios and SC-NLFA tracers provided the best capacity for land use source discrimination based on their reproduction of known source apportionments. The contribution of land use sources to streambed sediments

was estimated using a combination of *n*-alkane ratios and SC-NLFA biomarkers and results identified pasture to be the main contributor to streambed OC (68-80% of OC), followed by arable or forest land (8-17%) and moorland (3-6%). The use of virtual mixtures as presented in this study provides a simple method that could be carried out before a OCF study to determine if addition or removal of tracers can improve relative error in source discrimination. Further studies are required to determine whether these findings can be generalised to other catchment settings by testing whether different sets of biomarkers (*n*-alkane, SC-NLFA, concentrations, CSSI $\delta^{13}C$ signatures) are consistent in better distinguishing between certain land use combinations (e.g., arable-pasture) in varied geographical areas.

3.5 References

Addy, S., Ghimire, S. and Cooksley, S. (2012) 'Assessment of the multiple benefits of river restoration: the Logie Burn meander reconnection project', BHS Eleventh National Symposium, Hydrology for a changing world, Dundee 2012, , pp. 01–05.

Alewell, C., Birkholz, A., Meusburger, K., Schindler Wildhaber, Y. and Mabit, L. (2016) 'Quantitative sediment source attribution with compound-specific isotope analysis in a C3 plant-dominated catchment (central Switzerland)', Biogeosciences, 13(5), pp. 1587–1596.

Ankit, Y., Muneer, W., Gaye, B., Lahajnar, N., Bhattacharya, S., Bulbul, M., Jehangir, A., Anoop, A. and Mishra, P.K. (2022) 'Apportioning sedimentary organic matter sources and its degradation state- Inferences based on aliphatic hydrocarbons amino acids and δ15N', Environmental Research, 205

Barka, E.A., Vatsa, P., Sanchez, L., Nathalie Gaveau-Vaillant, C.J., Klenk, H.-P., Clément, C., Ouhdouch, Y. and P. van Wezeld, G. (2016) 'Taxonomy, Physiology, and Natural Products of Actinobacteria', American Society for Microbiology, 80(1), pp. 1–43.

Battin, T.J., Luyssaert, S., Kaplan, L.A., Aufdenkampe, A.K., Richter, A. and Tranvik, L.J. (2009) ‘The boundless carbon cycle’, Nature Geoscience, 2(9) Nature Publishing Group, pp. 598–600.

Blake, W.H., Ficken, K.J., Taylor, P., Russell, M.A. and Walling, D.E. (2012) ‘Tracing crop-specific sediment sources in agricultural catchments’, Geomorphology, 139–140 Elsevier B.V., pp. 322–329.

Blessing, M., Jochmann, M.A. and Schmidt, T.C. (2008) ‘Pitfalls in compound-specific isotope analysis of environmental samples’, Analytical and Bioanalytical Chemistry, 390(2), pp. 591–603.

Bush, R.T. and McInerney, F.A. (2013) ‘Leaf wax n-alkane distributions in and across modern plants: Implications for paleoecology and chemotaxonomy’, Geochimica et Cosmochimica Acta, 117 Elsevier Ltd, pp. 161–179.

Chen, F.X., Fang, N.F., Wang, Y.X., Tong, L.S. and Shi, Z.H. (2017) ‘Biomarkers in sedimentary sequences: Indicators to track sediment sources over decadal timescales’, Geomorphology, 278 Elsevier B.V., pp. 1–11.

Chen, Y., Wang, Y., Yu, K., Zhao, Z. and Lang, X. (2022) ‘Occurrence characteristics and source appointment of polycyclic aromatic hydrocarbons and n-alkanes over the past 100 years in southwest China’, Science of The Total Environment, 808 Elsevier B.V., p. 151905.

Chikaraishi, Y. and Naraoka, H. (2003) Compound-specific δD-δ13C analyses of n-alkanes extracted from terrestrial and aquatic plants Phytochemistry.

Cole, B., King, S., Ogutu, B., Palmer, D., Smith, G. and Balzter, H. (2015) Corine land cover 2012 for the UK, Jersey and Guernsey., NERC Environmental Information Data Centre Available at: https://doi.org/10.5285/32533dd6-7c1b-43e1-b892-e80d61a5ea1d (Accessed: 18 January 2021).

Collins, A.L., Blackwell, M., Boeckx, P., Chivers, C.A., Emelko, M., Evrard, O., Foster, I., Gellis, A., Gholami, H., Granger, S., Harris, P., Horowitz, A.J., Laceby, J.P., Martinez-Carreras, N., Minella, J., Mol, L., Nosrati, K., Pulley, S., Silins, U., da Silva, Y.J., Stone, M., Tiecher, T., Upadhayay, H.R. and Zhang, Y. (2020)

Sediment source fingerprinting: benchmarking recent outputs, remaining challenges and emerging themes. Journal of Soils and Sediments.

Cooper, R.J., Pedentchouk, N., Hiscock, K.M., Disdle, P., Krueger, T. and Rawlins, B.G. (2015) 'Apportioning sources of organic matter in streambed sediments: An integrated molecular and compound-specific stable isotope approach', Science of the Total Environment, 520 Elsevier B.V., pp. 187–197.

Cranwell, P.A. (1981) 'Diagenesis of free and bound lipids in terrestrial detritus deposited in a lacustrine sediment', Organic Geochemistry, 3(3), pp. 79–89.

Dominati, E., Patterson, M. and Mackay, A. (2010) 'A framework for classifying and quantifying the natural capital and ecosystem services of soils', Ecological Economics, 69(9) Elsevier B.V., pp. 1858–1868.

Dove, H. and Mayes, R.W. (2006) 'Protocol for the analysis of n-alkanes and other plant-wax compounds and for their use as markers for quantifying the nutrient supply of large mammalian herbivores', Nature Protocols, 1(4), pp. 1680–1697.

Fang, J., Wu, F., Xiong, Y., Li, F., Du, X., An, D. and Wang, L. (2014) 'Source characterization of sedimentary organic matter using molecular and stable carbon isotopic composition of n-alkanes and fatty acids in sediment core from Lake Dianchi, China', Science of the Total Environment, 473–474, pp. 410–421.

Fenton, N. and Neil, M. (2018) Risk Assessment and Decision Analysis with Bayesian Networks. Boca Raton, Florida USA: CRC Press Taylor & Francis.

Ferlian, O., Cesarz, S., Marhan, S. and Scheu, S. (2014) 'Carbon food resources of earthworms of different ecological groups as indicated by 13C compound-specific stable isotope analysis', Soil Biology and Biochemistry, 77 Elsevier Ltd, pp. 22–30.

Ferrari, A.E., Ravnskov, S., Larsen, J., Tønnersen, T., Maronna, R.A. and Wall, L.G. (2015) 'Crop rotation and seasonal effects on fatty acid profiles of neutral and phospholipids extracted from no-till agricultural soils', Soil Use and Management, 31(1), pp. 165–175.

Ficken, K.J., Li, B., Swain, D.L. and Eglinton, G. (2000) ‘An n-alkane proxy for the sedimentary input of submerged/floating freshwater aquatic macrophytes’, Organic Geochemistry, 31(7–8), pp. 745–749.

Galoski, C.E., Jiménez Martínez, A.E., Schultz, G.B., dos Santos, I. and Froehner, S. (2019) ‘Use of n-alkanes to trace erosion and main sources of sediments in a watershed in southern Brazil’, Science of the Total Environment, 682 Elsevier B.V., pp. 447–456.

Glaser, B. and Zech, W. (2005) ‘Reconstruction of climate and landscape changes in a high mountain lake catchment in the Gorkha Himal, Nepal during the Late Glacial and Holocene as deduced from radiocarbon and compound-specific stable isotope analysis of terrestrial, aquatic and microbi’, Organic Geochemistry, 36(7), pp. 1086–1098.

Glendell, M., Jones, R., Dungait, J.A.J., Meusburger, K., Schwendel, A.C., Barclay, R., Barker, S., Haley, S., Quine, T.A. and Meersmans, J. (2018) ‘Tracing of particulate organic C sources across the terrestrial-aquatic continuum, a case study at the catchment scale (Carminowe Creek, southwest England)’, Science of the Total Environment, 616, pp. 1077–1088. Available at: 10.1016/j.scitotenv.2017.10.211 (Accessed: 5 September 2018).

Gobin, A., Jones, R., Kirkby, M., Campling, P., Govers, G., Kosmas, C. and Gentile, A.R. (2004) ‘Indicators for pan-European assessment and monitoring of soil erosion by water’, Environmental Science and Policy, 7(1), pp. 25–38.

Griepentrog, M., Bodé, S., Boeckx, P. and Wiesenberg, G.L.B. (2016) ‘The fate of plant wax lipids in a model forest ecosystem under elevated CO2 concentration and increased nitrogen deposition’, Organic Geochemistry, 98 Elsevier Ltd, pp. 131–140.

Grimalt, J.O., Torras, E. and Albaigés, J. (1988) ‘Bacterial reworking of sedimentary lipids during sample storage’, Organic Geochemistry, 13(4–6), pp. 741–746.

Hancock, G.J. and Revill, A.T. (2013) ‘Erosion source discrimination in a rural Australian catchment using compound-specific isotope analysis (CSIA)’, Hydrological Processes, 27(6), pp. 923–932.

Haubert, D., Häggblom, M.M., Langel, R., Scheu, S. and Ruess, L. (2006) ‘Trophic shift of stable isotopes and fatty acids in Collembola on bacterial diets’, Soil Biology and Biochemistry, 38(7), pp. 2004–2007.

He, D., Ladd, S.N., Saunders, C.J., Mead, R.N. and Jaff, R. (2020) ‘Distribution of n-alkanes and their δ2H and δ13C values in typical plants along a terrestrial-coastal-oceanic gradient’, Geochimica et Cosmochimica Acta, 281, pp. 31–52.

Hemkemeyer, M., Christensen, B.T., Tebbe, C.C. and Hartmann, M. (2019) ‘Taxon-specific fungal preference for distinct soil particle size fractions’, European Journal of Soil Biology, 94(March) Elsevier, p. 103103.

Hemkemeyer, M., Dohrmann, A.B., Christensen, B.T. and Tebbe, C.C. (2018) ‘Bacterial preferences for specific soil particle size fractions revealed by community analyses’, Frontiers in Microbiology, 9(FEB), pp. 1–13.

Hirave, P., Glendell, M., Birkholz, A. and Alewell, C. (2020a) ‘Compound-specific isotope analysis with nested sampling approach detects spatial and temporal variability in the sources of suspended sediments in a Scottish mesoscale catchment’, Science of The Total Environment, (xxxx) The Authors, p. 142916.

Hirave, P., Wiesenberg, G.L.B., Birkholz, A. and Alewell, C. (2020b) ‘Understanding the effects of early degradation on isotopic tracers: implications for sediment source attribution using compound-specific isotope analysis (CSIA)’, Biogeosciences Discussions, (June), pp. 1–18.

Jeng, W.L. (2006) ‘Higher plant n-alkane average chain length as an indicator of petrogenic hydrocarbon contamination in marine sediments’, Marine Chemistry, 102(3–4), pp. 242–251.

Jenkins, D. (ed.) (1985) The biology and management of the River Dee. Institute of Terrestrial Ecology.

Koch, A., McBratney, A., Adams, M., Field, D., Hill, R., Crawford, J., Minasny, B., Lal, R., Abbott, L., O'Donnell, A., Angers, D., Baldock, J., Barbier, E., Binkley, D., Parton, W., Wall, D.H., Bird, M., Bouma, J., Chenu, C., Flora, C.B., Goulding, K., Grunwald, S., Hempel, J., Jastrow, J., Lehmann, J., Lorenz, K., Morgan, C.L., Rice, C.W., Whitehead, D., Young, I. and Zimmermann, M. (2013) 'Soil Security: Solving the Global Soil Crisis', Global Policy, 4(4), pp. 434–441.

Lachance, C., Lobb, D.A., Pelletier, G., Thériault, G. and Chrétien, F. (2020) 'Determination of sediment sources in a mixed watershed within the Appalachian-St. Lawrence Lowland Regions of southern Quebec using sediment fingerprinting', Environmental Monitoring and Assessment, 192(9) Environmental Monitoring and Assessment

Ladygina, N., Dedyukhina, E.G. and Vainshtein, M.B. (2006) 'A review on microbial synthesis of hydrocarbons', Process Biochemistry, 41(5), pp. 1001–1014.

Lanfranconi, M.P., Alvarez, A.F. and Alvarez, H.M. (2015) 'Identification of genes coding for putative wax ester synthase/diacylglycerol acyltransferase enzymes in terrestrial and marine environments', AMB Express, 5(1) Springer Berlin Heidelberg, pp. 1–13.

Lavrieux, M., Birkholz, A., Meusburger, K., Wiesenberg, G.L.B., Gilli, A., Stamm, C. and Alewell, C. (2019) 'Plants or bacteria? 130 years of mixed imprints in Lake Baldegg sediments (Switzerland), as revealed by compound-specific isotope analysis (CSIA) and biomarker analysis', Biogeosciences, 16(10), pp. 2131–2146.

Lavrieux, M., Bréheret, J.G., Disnar, J.R., Jacob, J., Le Milbeau, C. and Zocatelli, R. (2012) 'Preservation of an ancient grassland biomarker signature in a forest soil from the French Massif Central', Organic Geochemistry, 51, pp. 1–10.

Lei, C., Wagner, P.D. and Fohrer, N. (2021) 'Effects of land cover, topography, and soil on stream water quality at multiple spatial and seasonal scales in a German lowland catchment', Ecological Indicators, 120(June 2020) Elsevier, p. 106940.

Lilly, A. and Baggaley, N.J. (2018) Soil erosion risk map of Scotland James Hutton Institute, Aberdeen

Liu, C., Hu, B.X., Li, Z., Yu, L., Peng, H., Wang, D. and Huang, X. (2021a) 'Linking soils and streams: Chemical composition and sources of eroded organic matter during rainfall events in a Loess hilly-gully region of China', Journal of Hydrology, 600(May) Elsevier B.V., p. 126518.

Liu, C., Wu, Z., Hu, B.X. and Li, Z. (2021b) 'Linking recent changes in sediment yields and aggregate-associated organic matter sources from a typical catchment of the Loess Plateau, China', Agriculture, Ecosystems and Environment, 321(July) Elsevier B.V., p. 107606.

Lu, Y.H., Canuel, E.A., Bauer, J.E. and Chambers, R.M. (2014) 'Effects of watershed land use on sources and nutritional value of particulate organic matter in temperate headwater streams', Aquatic Sciences, 76(3), pp. 419–436.

McBratney, A., Field, D.J. and Koch, A. (2014) 'The dimensions of soil security', Geoderma, 213 Elsevier B.V., pp. 203–213.

Met Office (2021) UK Climate Average. Available at: https://www.metoffice.gov.uk/research/climate/maps-and-data/uk-climate-averages/gfjuxqwcs (Accessed: 18 January 2021).

Meyers, P.A. (2003) 'Application of organic geochemistry to paleolimnological reconstruction: a summary of examples from the Laurention Great Lakes', Organic Geochemistry, 34, pp. 261–289.

Nitzsche, K.N., Kleeberg, A., Hoffmann, C., Merz, C., Premke, K., Gessler, A., Sommer, M. and Kayler, Z.E. (2022) 'Kettle holes reflect the biogeochemical characteristics of their catchment area and the intensity of the element-specific input', Journal of Soils and Sediments, Springer Berlin Heidelberg, pp. 994–1009.

Olsson, P.A., Van Aarle, I.M., Gavito, M.E., Bengtson, P. and Bengtsson, G. (2005) '13C incorporation into signature fatty acids as an assay for carbon allocation in arbuscular mycorrhiza', Applied and Environmental Microbiology, 71(5), pp. 2592–2599.

Ordnance Survey (2021) OS Terrain 5 [ASC geospatial data], Scale 1:10000, Tiles: nj30ne,nj30nw,nj30se,nj30sw,nj31se,nj31sw,nj40ne,nj40nw,nj40se,nj40sw,nj41se,nj41sw,nj50ne,nj50nw,nj50se,nj50sw,nj51se,nj51sw,no39ne,no39nw,no49ne,no49nw,no59ne,no59nw,., EDINA Digimap Ordnance Survey Service Available at: https://digimap.edina.ac.uk (Accessed: 14 December 2018).

Owens, P.N., Batalla, R.J., Collins, A.J., Gomez, B., Hicks, D.M., Horowitz, A.J., Kondolf, G.M., Marden, M., Page, M.J., Peacock, D.H., Petticrew, E.L., Salomons, W. and Trustrum, N.A. (2005) 'Fine-grained sediment in river systems: Environmental significance and management issues', River Research and Applications, 21(7), pp. 693–717.

Owens, P.N., Blake, W.H., Gaspar, L., Gateuille, D., Koiter, A.J., Lobb, D.A., Petticrew, E.L., Reiffarth, D.G., Smith, H.G. and Woodward, J.C. (2016) 'Fingerprinting and tracing the sources of soils and sediments: Earth and ocean science, geoarchaeological, forensic, and human health applications', Earth-Science Reviews, 162 Elsevier B.V., pp. 1–23.

Palazón, L., Latorre, B., Gaspar, L., Blake, W.H., Smith, H.G. and Navas, A. (2015) 'Comparing catchment sediment fingerprinting procedures using an auto-evaluation approach with virtual sample mixtures', Science of the Total Environment, 532 Elsevier B.V., pp. 456–466.

Phillips, D.L. and Gregg, J.W. (2003) 'Source partitioning using stable isotopes: Coping with too many sources', Oecologia, 136(2), pp. 261–269.

Pulley, S. and Collins, A.L. (2018) 'Tracing catchment fine sediment sources using the new SIFT (SedIment Fingerprinting Tool) open source software', Science of the Total Environment, 635 The Authors, pp. 838–858.

Puttock, A., Dungait, J.A.J., Macleod, C.J.A., Bol, R. and Brazier, R.E. (2014) 'Organic Carbon From Dryland Soils', Journal of Geophysical Research: Biogeosciences, 119, pp. 2345–2357.

R Core Team (2020) R: A language and environment for statistical computing 3.6.3. R Foundation for Statistical Computing, Vienna, Austria

Ranjan, R.K., Routh, J., Val Klump, J. and Ramanathan, A.L. (2015) 'Sediment biomarker profiles trace organic matter input in the Pichavaram mangrove complex, southeastern India', Marine Chemistry, 171 Elsevier B.V., pp. 44–57.

Rickson, R.J., Baggaley, N., Deeks, L.K., Graves, A., Hannam, J., Keay, C. and Lilly, A. (2019) Developing a method to estimate the costs of soil erosion in high-risk Scottish catchments. Report to the Scottish Government. Available online from https://www.gov.scot/ISBN/978-1-83960-754-7.

Röttig, A. and Steinbüchel, A. (2013) 'Acyltransferases in Bacteria', Microbiology and Molecular Biology Reviews, 77(2), pp. 277–321.

RStudio Team (2018) RStudio: Integrated Development for R 1.1.463. PBC, Boston, MA

Ruess, L., Schütz, K., Haubert, D., Häggblom, M.M., Kandeler, E. and Scheu, S. (2005) 'Application of lipid analysis to understand trophic interactions in soil', Ecology, 86(8), pp. 2075–2082.

Scheurer, K., Alewell, C., Bänninger, D. and Burkhardt-Holm, P. (2009) 'Climate and land-use changes affecting river sediment and brown trout in alpine countries-a review', Environmental Science and Pollution Research, 16(2), pp. 232–242.

SEPA (2021) Water Classification Hub., Scottish Environment Protection Agency

Singh, S.N., Kumari, B. and Mishra, S. (2012) 'Microbial Degradation of Alkanes', in Microbial Degradation of Xenobiotics. , pp. 439–469.

Sirjani, E., Mahmoodabadi, M. and Cerdà, A. (2022) 'Sediment transport mechanisms and selective removal of soil particles under unsteady-state conditions in a sheet erosion system', International Journal of Sediment Research, 37(2), pp. 151–161.

Smeaton, C., Cui, X., Bianchi, T.S., Cage, A.G., Howe, J.A. and Austin, W.E.N. (2021) ‘The evolution of a coastal carbon store over the last millennium’, Quaternary Science Reviews, 266 Elsevier Ltd, p. 107081.

Smith, A.A., Tetzlaff, D. and Soulsby, C. (2018) ‘On the Use of StorAge Selection Functions to Assess Time-Variant Travel Times in Lakes’, Water Resources Research, 54(7), pp. 5163–5185.

Smith, H.G., Karam, D.S. and Lennard, A.T. (2018) ‘Evaluating tracer selection for catchment sediment fingerprinting’, Journal of Soils and Sediments, 18(9) Journal of Soils and Sediments, pp. 3005–3019.

Stenfert Kroese, J., Batista, P.V.G., Jacobs, S.R., Breuer, L., Quinton, J.N. and Rufino, M.C. (2020) ‘Agricultural land is the main source of stream sediments after conversion of an African montane forest’, Scientific Reports, 10(1) Nature Publishing Group UK, p. 14827.

Stock, B.C., Jackson, A.L., Ward, E.J., Parnell, A.C., Phillips, D.L. and Semmens, B.X. (2018) MixSIAR model description

Stock, B.C. and Semmens, B.X. (2016) MixSIAR GUI User Manual. Version 3.1

Stout, S.A. (2020) ‘Leaf wax n-alkanes in leaves, litter, and surface soil in a low diversity, temperate deciduous angiosperm forest, Central Missouri, USA’, Chemistry and Ecology, Taylor & Francis, pp. 810–826.

Tekaya, M., Dahmen, S., Ben Mansour, M., Ferhout, H., Chehab, H., Hammami, M., Attia, F. and Mechri, B. (2021) ‘Foliar application of fertilizers and biostimulant has a strong impact on the olive (Olea europaea) rhizosphere microbial community profile and the abundance of arbuscular mycorrhizal fungi’, Rhizosphere, 19(June) Elsevier B.V., p. 100402.

Thornton, B., Zhang, Z., Mayes, R.W., Högberg, M.N. and Midwood, A.J. (2011) ‘Can gas chromatography combustion isotope ratio mass spectrometry be used to quantify organic compound abundance?’, Rapid communications in mass spectrometry : RCM, 25(17), pp. 2433–2438.

Torres, T., Ortiz, J.E., Martín-Sánchez, D., Arribas, I., Moreno, L., Ballesteros, B., Blázquez, A.N.A., Domínguez, J.A. and Estrella, T.R. (2014) 'The long pleistocene record from the pego-oliva marshland (Alicante-Valencia, Spain)', Geological Society Special Publication, 388(1), pp. 429–452.

Upadhayay, H.R., Bodé, S., Griepentrog, M., Huygens, D., Bajracharya, R.M., Blake, W.H., Dercon, G., Mabit, L., Gibbs, M., Semmens, B.X., Stock, B.C., Cornelis, W. and Boeckx, P. (2017) 'Methodological perspectives on the application of compound-specific stable isotope fingerprinting for sediment source apportionment', Journal of Soils and Sediments, 17(6) Journal of Soils and Sediments, pp. 1537–1553.

Walling, D.E., Owens, P.N. and Leeks, G.J.L. (1999) 'Fingerprinting suspended sediment sources in the catchment of the River Ouse, Yorkshire, UK', Hydrological Processes, 13(7), pp. 955–975.

Wang, X., Blake, W.H., Taylor, A., Kitch, J. and Millward, G. (2021) 'Evaluating the effectiveness of soil conservation at the basin scale using floodplain sedimentary archives', Science of the Total Environment, 792 Elsevier B.V., p. 148414.

Wang, X., Huang, X., Sachse, D., Hu, Y., Xue, J. and Meyers, P.A. (2016) 'Comparisons of lipid molecular and carbon isotopic compositions in two particle-size fractions from surface peat and their implications for lipid preservation', Environmental Earth Sciences, 75(15)

Wang, Y., Yang, H., Zhang, J., Xu, M. and Wu, C. (2015) 'Biomarker and stable carbon isotopic signatures for 100-200year sediment record in the Chaihe catchment in southwest China', Science of the Total Environment, 502 Elsevier B.V., pp. 266–275.

Wischmeier, W. and Smith, D. (1978) Predicting rainfall erosion losses: a guide to conservation planning. Agricultural Handbook No. 537. U. S. Department of Agriculture., Washington (DC)

Xue, P.P., Carrillo, Y., Pino, V., Minasny, B. and McBratney, A.B. (2018) 'Soil Properties Drive Microbial Community Structure in a Large Scale Transect in South Eastern Australia', Scientific Reports, 8(1) Springer US, pp. 1–11.

Xue, Y., Chen, L., Zhao, Y., Feng, Q., Li, C. and Wei, Y. (2022) 'Shift of soil fungal communities under afforestation in Nanliu River Basin, southwest China', Journal of Environmental Management, 302(PB) Elsevier Ltd, p. 114130.

Yan, C., Zhang, Y., Zheng, M., Zhang, Y., Liu, M., Yang, T., Meyers, P.A. and Huang, X. (2021) 'Effects of redox conditions and temperature on the degradation of Sphagnumn-alkanes', Chemical Geology, 561(September 2020) Elsevier B.V., p. 119927.

Zaitlin, B., Watson, S.B., Dixon, J. and Steel, D. (2003) 'Actinomycetes in the Elbow River Basin, Alberta, Canada', Water Quality Research Journal of Canada, 38(1), pp. 115–125.

Zech, M., Buggle, B., Leiber, K., Marković, S., Glaser, B., Hambach, U., Huwe, B., Stevens, T., Sümegi, P., Wiesenberg, G. and Zöller, L. (2009) 'Reconstructing Quaternary vegetation history in the Carpathian Basin, SE-Europe, using n-alkane biomarkers as molecular fossils: Problems and possible solutions, potential and limitations', Quaternary Science Journal, 58(2), pp. 148–155.

Zech, M., Krause, T., Meszner, S. and Faust, D. (2013) 'Incorrect when uncorrected: Reconstructing vegetation history using n-alkane biomarkers in loess-paleosol sequences - A case study from the Saxonian loess region, Germany', Quaternary International, 296 Elsevier Ltd and INQUA, pp. 108–116.

Zech, M., Pedentchouk, N., Buggle, B., Leiber, K., Kalbitz, K., Marković, S.B. and Glaser, B. (2011) 'Effect of leaf litter degradation and seasonality on D/H isotope ratios of n-alkane biomarkers', Geochimica et Cosmochimica Acta, 75(17), pp. 4917–4928.

Zhang, Q., Liang, G., Zhou, W., Sun, J., Wang, X. and He, P. (2016a) 'Fatty-Acid Profiles and Enzyme Activities in Soil Particle-Size Fractions under Long-Term Fertilization', Soil Science Society of America Journal, 80(1), pp. 97–111.

Zhang, X., Gu, Q., Long, X.E., Li, Z.L., Liu, D.X., Ye, D.H., He, C.Q., Liu, X.Y., Väänänen, K. and Chen, X.P. (2016b) ‘Anthropogenic activities drive the microbial community and its function in urban river sediment’, Journal of Soils and Sediments, 16(2), pp. 716–725.

Zhang, Y., Collins, A.L., McMillan, S., Dixon, E.R., Cancer-Berroya, E., Poiret, C. and Stringfellow, A. (2017) ‘Fingerprinting source contributions to bed sediment-associated organic matter in the headwater subcatchments of the River Itchen SAC, Hampshire, UK’, River Research and Applications, 33(10), pp. 1515–1526.

4 Seasonal OC dynamics: Investigating challenges in *n*-alkane fingerprinting using streambed and suspended sediments

Abstract

Agricultural practices can accelerate the rates of soil erosion and organic carbon (OC) loss, increasing input of nutrient rich sediment to surface waters. These processes are potentially amplified by climate change and future increases in the frequency of extreme climatic events. It is, therefore, of vital importance to identify sources and drivers of OC transfer from land to water to inform effective management strategies for mitigating the on-site and off-site impacts of accelerated soil erosion.

Organic C fingerprinting (OCF) using *n*-alkanes is a valuable tool to estimate the relative contribution of different land use sources to sediment OC. However, there remain challenges in the application OCF including i) effects on tracer signatures due to sorting effect of particles by size during mobilization, transport and deposition and ii) ensuring all sources are included. With the aim of identifying methods to address these challenges, and thereby reduce uncertainty in source apportionment, an OCF study was carried out in a mixed land use catchment in Scotland.

Suspended sediments (SS) were collected bi-monthly at three stream sites (two headwater sub-catchments and catchment outlet) over a period of eighteen months (June 2019 – Dec 2020). OC land use source apportionment was estimated, using *n*-alkane fingerprinting and a Bayesian unmixing model, to identify seasonal changes in land use OC sources. Potential rainfall, stream discharge and agronomic drivers of these seasonal changes were then identified with the following specific aims. Firstly, to estimate effects due to enrichment in finer particles by comparing *n*-alkane signatures for i) SS, ii) streambed sediment (existing data), and iii) terrestrial soils. Secondly, to determine if the same drivers were important at a headwater sub-catchment and catchment scale. And finally,

to estimate if a small amount of arable land in a headwater sub-catchment made a substantial enough input to SS OC to be included as a fingerprinting source.

The methods employed in this study i) revealed SS rather than streambed sediment most closely approximated biomarker signatures in terrestrial soils, suggesting that differences in *n*-alkane signatures between terrestrial soil sources and stream sediments were unlikely to be affected by the enrichment in finer particles, ii) identified drivers of variation in SS source proportions in a headwater catchment included land preparation/planting and moorland heather burning in spring, and heavier prolonged rainfall in late autumn and winter, leading to saturated soils and increased runoff. These drivers were not detected at the catchment scale, where livestock poaching of riparian pasture soils may be driving increased OC input to streams especially in late autumn/winter and iii) validated the land use sources selected for OCF by identifying the small amount of arable land in a headwater sub-catchment made a substantial enough input to stream OC to be included as a fingerprinting source. In addition, the *n*-alkane ratio “PAQ” (used to understand aquatic versus terrestrial OC input) for arable, forest and pasture soils was found to be in the range normally associated with emergent macrophytes and mosses. This finding has implications for research interpreting the origins of aquatic sediments using the expected ranges of PAQ in terrestrial and aquatic vegetation - especially in climates which provide ideal conditions for the growth of mosses in source soils.

By revealing that *n*-alkanes signatures were unlikely to be affected by the enrichment in finer particles, and validating the choice of land use sources, these methods addressed two of the key challenges in OCF, and thereby increased confidence in the source apportionment.

Keywords: *organic carbon dynamics, erosion, bed sediment, suspended sediment, n-alkane fingerprinting*

4.1 Introduction

Soils provide vital ecosystem services, including food and timber production and water filtering capacity and are of increasing importance for climate regulation

through storage of carbon (Vogel et al., 2018; Wiesmeier et al., 2019). Soil erosion and organic carbon (OC) loss are natural catchment processes that can be intensified by agricultural practices, leading to loss of soil resources and increasing input of nutrient rich sediment to waterways (Addy, Ghimire and Cooksley, 2012; Blake et al., 2021; Wiesmeier et al., 2015; Wohl et al., 2015). Erosion processes will be amplified by climate change and predicted increases in extreme climatic events (Jung, Lee and Park, 2014; Klimaszyk and Rzymski, 2013; Scheurer et al., 2009). Because of the inherent variability of waterways, good ecological status cannot be defined using absolute standards and the Water Framework Directive 2000/60/EC (WFD) instead defines it as “a slight departure from the biological community which would be expected in conditions of minimal anthropogenic impact”. It is, therefore, of vital importance to identify anthropogenic impacts on terrestrial-to-aquatic fluxes of OC, to inform effective management strategies and mitigate the impacts of soil OC loss on waterbody ecological status. In addition, the relative contribution from terrestrial sources to streams varies spatially as well as temporally (Huisman et al., 2013; Koiter et al., 2013a; Lamba, Karthikeyan and Thompson, 2015). It is, therefore, important to assess OC dynamics at both upstream sites, and at the catchment outlet, to reduce ambiguity in OC source identification (Hirave et al., 2020a; Lamba, Karthikeyan and Thompson, 2015).

The relative contribution of different terrestrial sources to organic matter load in waterways can be estimated using OC fingerprinting (OCF) techniques using plant-specific biomarkers such as *n*-alkanes and long-chain fatty acids (Alewell et al., 2016; Chen et al., 2017; Glendell et al., 2018; Hirave et al., 2020a; Zhang et al., 2017). The temporal variability of soil erosion rates, and hence terrestrial-to-aquatic transfer of soil OC, varies between different land uses. In arable land, connectivity, run-off and erosion rates vary seasonally according to crop type, inter-crop groundcover and harvest times, whereas permanent vegetation cover in forest and moorland is usually associated with reduced sediment fluxes through interception of runoff, increased water infiltration and organic matter accumulation (Sherriff et al., 2019). Fingerprinting of SS can reveal temporal variability in sediment sources during individual hydrological events (Alewell et

al., 2016; García-Comendador et al., 2021; Liu et al., 2017; Mukundan et al., 2010; Uber et al., 2019) as well as seasonal variability in sediment sources (Hirave et al., 2020a; Lamba, Karthikeyan and Thompson, 2015; Pulley et al., 2019). Organic sediment fingerprinting techniques using plant-specific biomarkers such as *n*-alkanes are, therefore, a valuable tool to estimate the relative contribution of different land use sources to organic matter load in waterways. However, although the utility and robustness of sediment fingerprinting approaches has been evaluated in numerous studies many challenges remain (Collins et al., 2020; Guzmán et al., 2013; Hirave et al., 2020b; Mukundan et al., 2012), including i) effects on tracer signatures due to sorting effect of particles by size during mobilization, transport and deposition and ii) ensuring all sources are included. Finding methods to assess the impact of particle size sorting and identify any “missing” sources would help to reduce uncertainty in source apportionment.

Biomarkers (Bush and McInerney, 2013) and the longer the *n*-alkane chain length, the less soluble they are in water. This lack of solubility reduces their metabolism by microorganisms (Cranwell, 1981; Ranjan et al., 2015), making *n*-alkanes of chain-length >C24 generally resistant to biodegradation (Singh, Kumari and Mishra, 2012) and suitable as conservative tracers in OCF. However, the sorting effect of particles by size during mobilization, transport and deposition processes is a key challenge to the assumption that biomarkers remain conservative (Laceby et al., 2017). In Chapters 2 and 3 it was shown that the signature of *n*-alkane biomarkers in streambed sediments differed from that of the terrestrial soils due to either i) input of less degraded organic matter (e.g. leaves/litter) to the streams directly from the riparian zone or ii) particle size effects due to finer, lighter particles being preferentially eroded and transported to the streams. If the latter, then the signature of *n*-alkane biomarkers of particles remaining in suspension and collected as suspended sediment (SS) would be expected to show even more deviation from terrestrial soils than the streambed sediments which would be expected to accumulate the coarser, heavier particles. It was hypothesised that differences in *n*-alkane signature were due to enrichment in finer particles and that this would be evidenced by the signature of *n*-alkane

biomarkers in streambed sediments, as opposed to SS, being most closely approximated to those in terrestrial soils.

Secondly, variation in source classification, and in particular the omission of an important source can alter the source apportionment (Vercruysse and Grabowski, 2018). In OCF studies, land use sources can be defined using large scale land cover maps such as Corine land cover 2012 for the UK, Jersey and Guernsey (Cole et al., 2015). However, as changes in agricultural management often happen at a faster rate than updates to large scale land cover maps, ground truthing may contradict the information in the maps, leading to uncertainty in the definition of land use sources.

In a mixed land use catchment in Scotland, SS were collected bi-monthly at three stream sites (two headwater sub-catchments and catchment outlet) over a period of eighteen months (June 2019 – Dec 2020). OC land use source apportionment was estimated, using *n*-alkane fingerprinting and a Bayesian unmixing model, to identify seasonal changes in land use OC sources. Potential rainfall, stream discharge and agronomic drivers of these seasonal changes were then identified with the following specific aims. Firstly, to estimate effects due to enrichment in finer particles by comparing *n*-alkane signatures for i) SS, ii) streambed sediment (existing data), and iii) terrestrial soils. Secondly, to determine if the same drivers were important at a headwater sub-catchment and catchment scale. And finally, to estimate if a small amount of arable land in a headwater sub-catchment made a substantial enough input to SS OC to be included as a fingerprinting source.

4.2 Material and methods

4.2.1 Study site

Loch Davan is a shallow (mean depth 1.2 m) lake located within the Muir of Dinnet National Nature Reserve (NNR) and derives inputs primarily from over-land surface flows (Smith, Tetzlaff and Soulsby, 2018). The lake area has been significantly reduced over the last century, likely due to inputs of nutrient rich sediment resulting from land use intensification (Addy, Ghimire and Cooksley, 2012). Between 2007 and 2018, the loch and its main feeder stream, Logie Burn,

were classified as having poor to moderate ecological status (SEPA, 2021). The catchment (*ca.* 34 km^2) includes a mix of land uses (moorland 29%, forest 22%, arable 10% and pasture 31%) and soil types (mineral podzols 49%, brown soils 22%, alluvial soils 11% and peat or peaty gleys/podzols c.a. 5%) (Figure 24b and d). Areas of steepest slope (13-37 degrees: Figure 24c) are found under moorland and forest land cover to the west and north-west of the catchment with arable and pasture land cover dominating the relatively flat (typically < 3 degree slope) lowlands. The catchment mean annual precipitation is 780 mm with average annual minimum temperature of 3.5°C and average annual maximum temperature of 12.17°C (Met Office, 2021b).

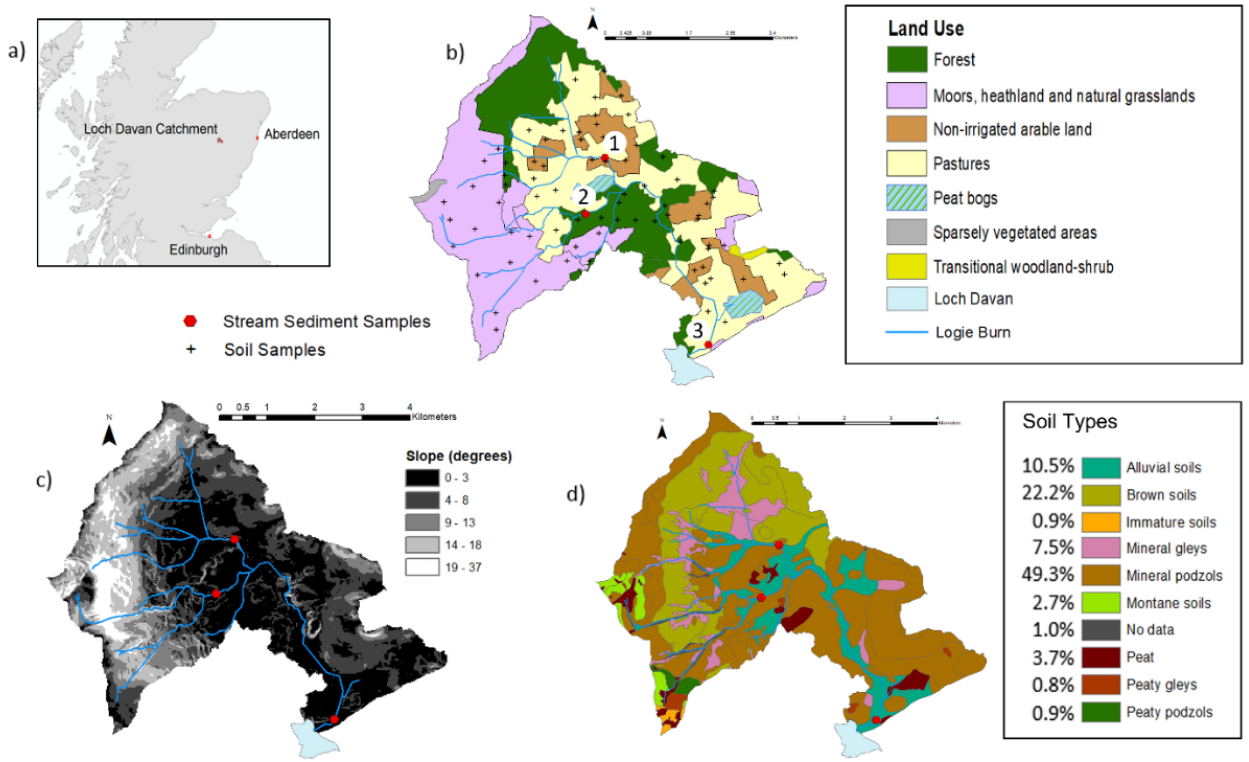

Figure 16: Loch Davan study catchment. a) Study catchment location, b) Land use in the Loch Davan catchment (34 km^2), suspended and streambed sediment sampling locations (red dots: Sites 1, 2 and 3) and terrestrial soil sampling locations (black crosses),based upon Corine land cover 2012 for the UK, Jersey and Guernsey (Cole et al., 2015), c) catchment slope (degrees) derived from OS Terrain 5 © Crown copyright and database rights 2021 Ordnance Survey (100025252)(Ordnance Survey, 2021), d) Catchment soils based on "1:25,000 Hutton Soils Data" copyright and database right The James Hutton Institute (2018). Used with the permission of The James Hutton Institute. All rights reserved.

Table 14: Characteristics of Loch Davan and catchment (CEH, 2021)

Loch Davan		Catchment	
Surface area (km^2)	0.42	Area (km^2)	33.83
Mean depth (m)	1.2	Catchment-to-lake ratio	80.2
Maximum depth (m)	2.7	Mean elevation (m)	278.25
Elevation (Above Ordnance Datum) (m)	167	Mean slope (°)	6.44
Perimeter length (km)	3		
Water body volume (m^3)	505,904		

4.2.2 Sample collection

A field campaign was carried out in June 2019 to collect soil and sediment samples within the Loch Davan catchment and Logie Burn stream network to characterise the four land use sources (arable (n=16), forest (n=16), moorland (n=18) and pasture (n=19)) and streambed sediments in terms of their *n*-alkane concentrations and $\delta^{13}C$ compound-specific stable isotope (CSSI) composition (sampling sites shown in Figure 6b). Suspended and bed sediment sample locations were chosen just above junctions in the stream network so the contributions from each sub-catchment could be quantified. The northern sub-catchment (Site 1) has almost equal extents of pasture (30%), forest (29%) and moorland (28%) with around 10% arable land. In the western sub-catchment (Site 2), moorland is the dominant land cover (78%) with around 14% of land use being pasture, less than 5% forest and no arable land. Site 3 was located close to the outlet of Logie Burn to Loch Davan to integrate the input from the whole catchment which has a land use composition of arable (10%), pasture (34%), forest (25%) and moorland (31%).

The methods for collection, processing and analysis of the terrestrial and bed sediment samples and detailed description of the *n*-alkane tracers can be found in Chapter 3.

Suspended sediments were collected bi-monthly at the three sites over a period of eighteen months (June 2019 – Dec 2020) to characterise the seasonal

changes in OC flux. Time integrated mass samplers (Phillips, Russell and Walling, 2000) were used to collect SS at all sampling locations. Unfortunately, due to high flows at Site 1, the sampler was lost twice, and therefore no suspended sediments were collected between August 2019 and January 2020. Suspended sediment from the traps was collected and placed in clean food grade plastic buckets, left to settle for 5 days before the supernatant was removed and the remaining water left to evaporate at room temperature for up to 6 weeks. The dried sediment was then decanted and freeze dried. Samples collected after March 2020 were not freeze dried due to Covid-19 lockdown restrictions and were only air dried. Samples were weighed and passed through a 2 mm sieve before being ground and stored at room temperature until required for analysis.

4.2.3 Sample analysis

The suspended sediment samples were analysed for *n*-alkanes and $\delta^{13}C$ CSSI as described in Chapter 3.

Validating a terrestrial source of SS OC can be accomplished by measuring OC content and nitrogen content (%N); with lower C/N ratios (4 to 10) associated with organic matter derived from aquatic organisms, and higher values (≥ 20) indicative of a terrestrial origin (Ankit et al., 2022; Meyers, 1997).

All suspended sediment and terrestrial soil samples were analysed for carbon and nitrogen concentrations (%, w/w) using a Flash EA 1112 Series Elemental Analyser connected via a Conflo III to a Delta^{Plus} XP isotope ratio mass spectrometer (all Thermo Finnigan, Bremen, Germany). USGS40 was used as reference material for C and N concentrations, measured using the mass spectrometer area output. Long term precisions for a quality control standard (dried milled topsoil) were: total C 3.80 ± 0.15 % and total N 0.28 ± 0.02 % (mean ± SD). Data processing was carried out using Isodat 2.0 (Thermo Fisher Scientific, Bremen, Germany).

4.2.4 OC fingerprinting

4.2.4.1 Tracer selection

The *n*-alkane tracers considered in the OCF of suspended sediments are described in detail in Chapter 3 Section 2.4.1, and consist of: the relative percentage of *n*-alkanes C27, C29 and C31 (Torres et al., 2014); the C27 to C31 ratio (Puttock et al., 2014); PAQ, to understand aquatic versus terrestrial OC input (Ficken et al., 2000); the Odd-to-Even Predominance (OEP) (Zech et al., 2013; and the Average Chain length (ACL) (Fang et al., 2014).

All tracer values were first checked for normal distribution using the Kolmogorov-Smirnov test. A Kruskal- Wallis (KW) and posthoc Dunn's test was then carried out to select tracers which showed significant differences between land use sources (Figure 7b). The tracers which passed the KW test were then assessed using box plots in Excel to ensure biomarker values from all mixtures were within the full range of corresponding land use sources (Figure 7c). In addition, $\delta^{13}C$ *n*-alkane CSSIs were only selected if their corresponding concentration values were also within the range of values of stream sediment mixtures (Collins et al., 2020).

4.2.4.2 Source Classification

With reference to the Corine land cover 2012 for the UK, Jersey and Guernsey (Cole et al., 2015), the northern sub-catchment (Site 1) supported arable, pasture, forest and moorland land cover, but in the western sub-catchment (Site 2) arable land cover was missing (Figure 24b). However, areas of the Site 2 sub-catchment designated as pasture and moorland on the land cover map were found to be regularly ploughed and/or used for game crops (Game & Wildlife Conservation Trust, 2022) (Figure 17). It was uncertain whether the presence of these cropped fields would constitute a substantial enough arable source to warrant using a four-source classification (arable, pasture, forest and moorland) rather than a three-source (pasture, forest and moorland) model. Organic C fingerprinting at sites 1 and 3 was carried out using a four-source classification (arable, pasture, forest and moorland). Organic C fingerprinting at Site 2 was carried out using both a three-source classification (pasture, forest and moorland) and a four-source

classification (arable, pasture, forest and moorland). The best source classification was selected based whether land use source proportions, and changes in those proportions, could be explained using known drivers of OC dynamics within the catchment.

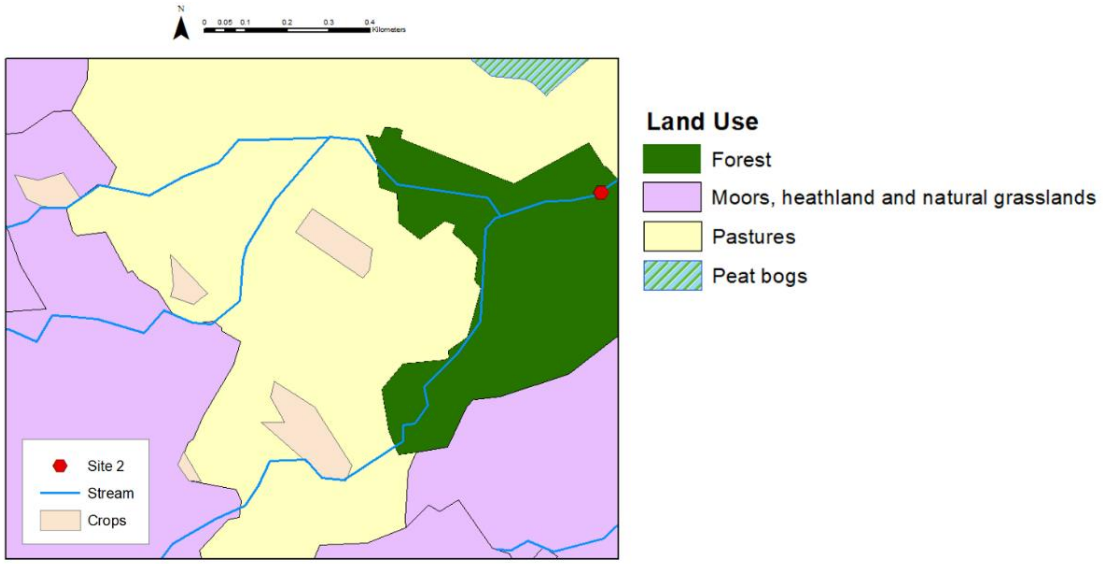

Figure 17 Location of Game Crops (Game & Wildlife Conservation Trust, 2022) in sub-catchment of Site 2

4.2.4.3 Bayesian unmixing model (MixSIAR) implementation

After selecting tracers, MixSIAR (Stock and Semmens, 2016) was used to model the land use source apportionment. The MixSIAR model was first developed for ecological studies but is increasingly applied in catchment sediment fingerprinting research (Lachance et al., 2020; Smith, Karam and Lennard, 2018; Stenfert Kroese et al., 2020). Tracer properties can be characterised using the mean and standard deviation and the model is fit using Markov Chain Monte Carlo (MCMC) methods. Sediment source proportions were estimated using 3000 MCMC simulations with MixSIAR formulated using a residual error term and an uninformative prior. The MCMC parameters were set to those for a “normal” run (Stock and Semmens, 2016) (chain length = 100,000, burn = 50,000, thin = 50, chains = 3) and the Gelman-Rubin diagnostic was used to evaluate convergence of all models.

Unless otherwise stated, all MixSIAR runs, statistical and error analyses were carried out in R (version 3.6.3) (R Core Team, 2020) and RStudio (version 1.1.463) (RStudio Team, 2018).

4.2.4.4 Virtual mixtures

Land use discrimination was assessed using “virtual” mixtures with 50/50 contributions from each of the four sources (arable, pasture, forest and moorland) by taking the mean of two sources to represent a 50% contribution from each (Batista, Laceby and Evrard, 2022; Collins et al., 2020). This resulted in six virtual 50/50 mixtures: Arable-Forest (AF50), Arable-Moorland (AM50), Arable-Pasture (AP50), Forest-Moorland (FM50), Forest-Pasture (FP50) and Moorland-Pasture (MP50). Errors were calculated as mean absolute differences between the modelled and virtual mixture composition.

4.2.5 Agricultural activities, rainfall and stream discharge data

Agricultural data was provided by the Game and Wildlife Conservancy Trust at Auchnerran Demonstration Farm, located within the Loch Davan catchment. Rainfall and stream discharge data was provided by the James Hutton Institute from a weather station located on Auchnerran Demonstration Farm.

Rainfall and Logie Burn discharge data were first aggregated by the time interval over which SS was collected (Table 15). Hourly rainfall data was first summed to calculate total rainfall per day. Mean rainfall per day, and mean stream discharge were then calculated for each SS period.

Table 15: Date and period of collection of suspended sediment samples

Sample name	Sample Date	Period of collection
August 2019	27/08/2019	19/06/2019 to 26/08/2019
October 2019	23/10/2019	27/08/2019 to 22/10/2019
December 2019	17/12/2019	23/10/2019 to 16/12/2019
February 2020	11/02/2020	17/12/2019 to 10/02/2020
April 2020	14/04/2020	11/02/2020 to 13/04/2020
June 2020	04/06/2020	14/04/2020 to 03/06/2020

July 2020	29/07/2020	04/06/2020 to 28/07/2020
September 2020	22/09/2020	29/07/2020 to 21/09/2020
November 2020	17/11/2020	22/09/2020 to 16/11/2020

The association between land use source proportions estimated using OCF and mean daily rainfall (mm), stream discharge (m^3 s^{-1}), and OC content and C/N of sediments, was assessed in Excel using the Pearson product-moment correlation coefficient (r).

4.3 Results and Discussion

Organic C fingerprinting using *n*-alkanes is a valuable tool to estimate the relative contribution of different land use sources to sediment OC. However, there remain challenges in the application OCF including i) effects on tracer signatures due to sorting effect of particles by size during mobilization, transport and deposition and ii) ensuring all sources are included. With the aim of identifying methods to address these challenges and thereby reduce uncertainty in source apportionment it was assessed i) whether the signature of *n*-alkane biomarkers of streambed sediments or SS most closely approximated those in terrestrial soils to evaluate whether differences in *n*-alkane signatures were due to enrichment in finer particles, ii) if the same drivers were important at a headwater sub-catchment and catchment scale (catchment outlet) and iii) if a small amount of arable land in a headwater sub-catchment made a substantial enough input to stream OC to be included as a fingerprinting source.

4.3.1 Composition of *n*-alkane biomarkers in streambed and suspended sediments

The OC content and %N values of SS (8-11% and 0.61-0.81% respectively) were higher than those in bed sediments (0.6-1.1% and 0.03-0.08% respectively). Organic carbon and nitrogen contents of muddy sediments were generally higher than those in sandy sediments and OC content and %N can decrease as sediments become sandier (Dai and Sun, 2007). Particle size fractions and sand/silt/clay variations have not been explicitly measured in this study and all

soils and sediments were sieved to <2 mm. However, a visual inspection revealed SS to be finer than either soils or bed sediments and the bed sediment samples were much sandier than SS. At sites 1 and 3 the average C/N ratio in streambed (13.39 and 15.66 respectively) and suspended (13.54±0.79 and 12.67±0.96 respectively) sediments was similar to those in arable and pasture soils. However, at Site 2, although suspended sediment C/N was again similar to that in arable and pasture soils (12.77±1.79) C/N in streambed sediment was comparable to moorland or forest soil (C/N=23). The sub-catchment of Site 2 is dominated by moorland and forest land cover (86%) which would be consistent with the higher C/N seen at this site, however, the streambed sediment OC at Site 2 has a combined contribution of only 20% from these two sources (Chapter 3), inconsistent with the high C/N ratio. It is not known why this streambed sample should show such a high C/N ratio.

At all sites, the %C31 (15 to 23) and %C27 (40 to 53) of streambed sediments were lower and higher than those observed in the terrestrial soils (%C31 ca. 31 to 52; mean %C27 ca.18 to 35), respectively (Table 16). Lower %C31 and higher %C27 are characteristic of less degraded leaves/litter relative to their associated soil (Stout, 2020) and could indicate input of this source to stream sediments (Chapter 2). However, this is usually commensurate with a relatively high OEP which was not observed in streambed sediments at any site (OEP 1.2-1.8 c.f. terrestrial soils mean OEP 0.9 to 7.2). Alternatively, finer sediments can show an increase in mid-chain length *n*-alkanes relative to longer-chain lengths when compared to coarser sediments (Griepentrog et al., 2016). Finer sediments are more likely to be mobilised during water run-off than coarser sediments (Sirjani, Mahmoodabadi and Cerdà, 2022), and therefore, aquatic sediments become relatively enriched in finer soil particles. In addition, particles remaining in suspension or resuspended from *in-situ* streambed sediments would be expected to be lighter/finer than the streambed sediments which would be expected to accumulate more of the coarser, heavier particles entering the streams. It was hypothesised that if relatively lower %C31 and higher %C27 in streambed sediments was due to an enrichment in finer particles, then %C31 and %C27 should be even lower and higher respectively in SS. In effect, the %C31 (mean

ca. 20 to 23) and %C27 (mean ca. 39-44) of SS were closer to those observed in terrestrial soils (mean %C31 31 to 52; %C27 18 to 35), than were the %C31 (15 to 23) and %C27 (40 to 53) of streambed sediments (Table 16). These results suggest relatively lower %C31 and higher %C27 in stream sediments were not due to an enrichment in finer particles.

Alternatively, the study of Grimalt et al. (1988) found that storing a previously dried soil sample under water at room temperature (~ 25°C) for a month changed the *n*-alkane signature, preferentially degrading long-chained *n*-alkanes in preference to mid-chain length *n*-alkanes due to microbial decomposition. This suggests relatively lower %C31 and higher %C27 could be caused by storage of samples under water at a room temperature of ca. 25°C. Following collection, soil samples are immediately dried (e.g., freeze drying), however, some aqueous samples may be left for excess water to evaporate before being further processed or stored. In this study, the SS samples were left in a laboratory for excess water to evaporate (a period of up to 6 weeks at an unspecified “room” temperature), in contrast to the streambed sediment samples which were freeze-dried immediately on return to the laboratory. Therefore, the effect reported by Grimalt et al., (1988) is unlikely to be responsible for the lower %C31 and higher %C27 ratios observed in streambed and SS in this study, as the %C31 and %C27 of SS were closer to those observed in terrestrial soils than were the %C31 and %C27 of streambed sediments.

Under field conditions, various mechanisms cause soil aggregates to break apart creating finer particle fractions; disintegration of aggregates is a complicated mixture of mechanical (raindrop impact, field traffic/tillage, roots, earthworms) and hydraulic stresses (Felde et al., 2021). The particle size selectivity of soil erosion is usually correlated to the energy of the erosive process (e.g., wind or water erosion) with greater erosive force resulting in less selectivity (Koiter et al., 2013b). In addition, Armstrong et al., (2011) found particle size distribution was notably finer for material eroded from lower slopes, which had broader slower flows. In this study the bulk soil fraction (<2000 µm) has been used to retain as much OC as possible within the soil and sediment samples. Bulk soil fraction

(<2000 µm) was also used in the fingerprinting studies of Glendell et al., (2018) and Hirave et al., (2020), whereas other studies restricted their particle sizes to <63 µm or <100 µm using various methods including; gently disaggregated and sieved (Blake et al., 2012), dry sample ground to fine powder (steel coffee grinder), sieved to <100 µm and reground (Gibbs, 2008) and dry sieved through a 63-µm sieve (Hancock and Revill, 2013). Felde et al., (2021) found different physical structure, bacterial diversity and organic matter composition when aggregates were dry crushed (broken down along more “natural planes of mechanical weakness”) compared to wet sieving. In addition, although it is generally accepted that OM (including *n*-alkanes) are preferentially associated with the finer particle size fractions (<63 µm) (Quenea et al., 2004; Quénéa et al., 2006), Geng et al. (2019) found the signature and preservation of *n*-alkanes differed between coarse (>250 µm) and fine (<250 µm) particulate organic matter; with the coarse fraction containing a greater abundance of *n*-alkanes (n > 20). Therefore, the process of isolating finer fractions could itself introduce uncertainty into source characterisation. The method presented here, of comparing streambed and suspended sediment to assess effects on tracer signatures due to sorting effect of particles by size, can be applied to any catchment for which there has been no restriction on particle size carried out during sample preparation. Therefore, avoiding potential effects on *n*-alkane signature introduced by the process of isolating finer particle fractions.

Table 16 Mean (+/- 1SD) values of OC content, %N, C/N, and *n*-alkane ratios in forest, pasture, arable and moorland sources and streambed and suspended sediments (adapted from Chapter 3 Table 3)

				***n*-alkanes**						
	OC content	**%N**	**C/N**	**C27/ C31**	**%C27**	**%C29**	**%C31**	**OEP**	**PAQ**	**ACL**
Soils										
arable (16)	3.79 ± 1.09	0.29 ± 0.08	13.72 ± 3.23	1.10 ± 0.99	30.63 ± 9.65	34.10 ± 2.54	35.27± 9.69	4.26 ± 2.72	0.38 ± 0.15	28.38 ± 0.55
forest (16)	12.31 ± 8.0	0.55 ± 0.34	22.59 ± 6.17	1.02 ± 1.01	29.90 ± 12.78	29.42 ± 3.56	40.68 ± 13.02	3.76 ± 2.09	0.35 ± 0.17	28.55 ± 0.74
moorland (18)	21.42 ± 13.88	0.99 ± 0.54	20.01 ± 6.21	0.45 ± 0.56	17.6 ± 9.95	30.24 ± 5.53	52.17 ± 12.63	7.22 ± 3.40	0.18 ± 0.14	29.34 ± 0.66
pasture (19)	3.67 ± 0.94	0.30 ± 0.07	12.54 ± 1.83	1.20 ± 0.55	35.07 ± 6.26	33.55 ± 1.62	31.38 ± 5.20	0.87 ± 0.93	0.58 ± 0.12	28.03 ± 0.36
Bed Sediment										
Site 1	1.08	0.08	13.39	3.59	52.73	32.56	14.70	1.23	0.55	27.42
Site 2	0.62	0.03	23.23	1.72	39.83	37.02	23.15	1.71	0.43	27.93
Site 3	0.99	0.06	15.66	3.08	47.13	37.54	15.32	1.82	0.49	27.64
Suspended Sediment										
Site 1 (7)	8.13 ± 2.70	0.61 ± 0.21	13.54 ± 0.79	1.73 ± 0.34	39±4	37±2	23 ± 2	4.18 ± 1.01	0.41 ± 0.10	27.94 ± 0.26
Site 2 (9)	10.65 ± 5.43	0.81 ± 0.32	12.77 ± 1.79	2.33 ± 0.54	44±3	36±3	20 ± 3	4.89 ± 1.39	0.48 ± 0.08	27.70 ± 0.15
Site 3 (9)	9.71 ± 2.64	0.76 ± 0.20	12.67 ± 0.96	1.88 ± 0.47	41±4	37±1	22 ± 3	4.74 ± 1.20	0.41 ± 0.07	27.91 ± 0.19

4.3.1.1 Tracer selection for OC fingerprinting

The ranges of *n*-alkane ratios in suspended sediments were outside the maximum and minimum values of land use sources for C27/C31 and %C31 *n*-alkane tracers (Figure 18). Hence the remaining five *n*-alkane ratios (%C27, %C29, OEP, PAQ and ACL) were selected as tracers. The ranges of all the CSSI $\delta^{13}C$ values (C23, C25, C27, C29 and C31) in suspended sediments (excluding outliers) were within the maximum and minimum values for the land use sources (excluding outliers) (Figure 19). However, the corresponding C27 *n*-alkane concentration was outside the maximum and minimum values for the land use sources and therefore, only CSSI signatures for C23, C25, C29 and C31 were selected as tracers.

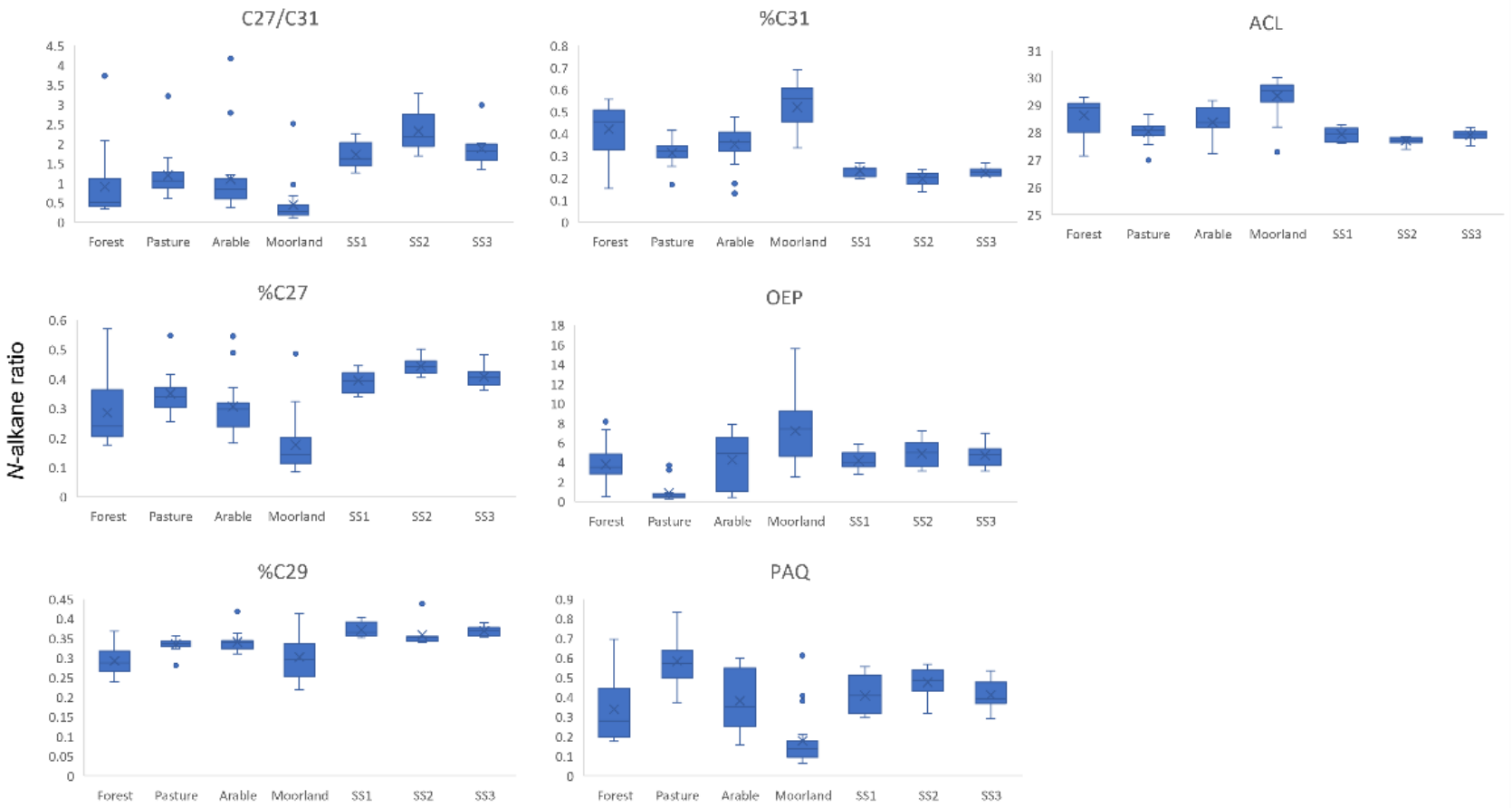

Figure 18: Range of *n*-alkane ratios from forest, pasture, arable and moorland land uses and suspended sediment sources The box is extended from the 25–75 percentiles, the line is plotted at the median, a cross marks the mean, and whiskers show the maximum to minimum range excluding outliers (dots).

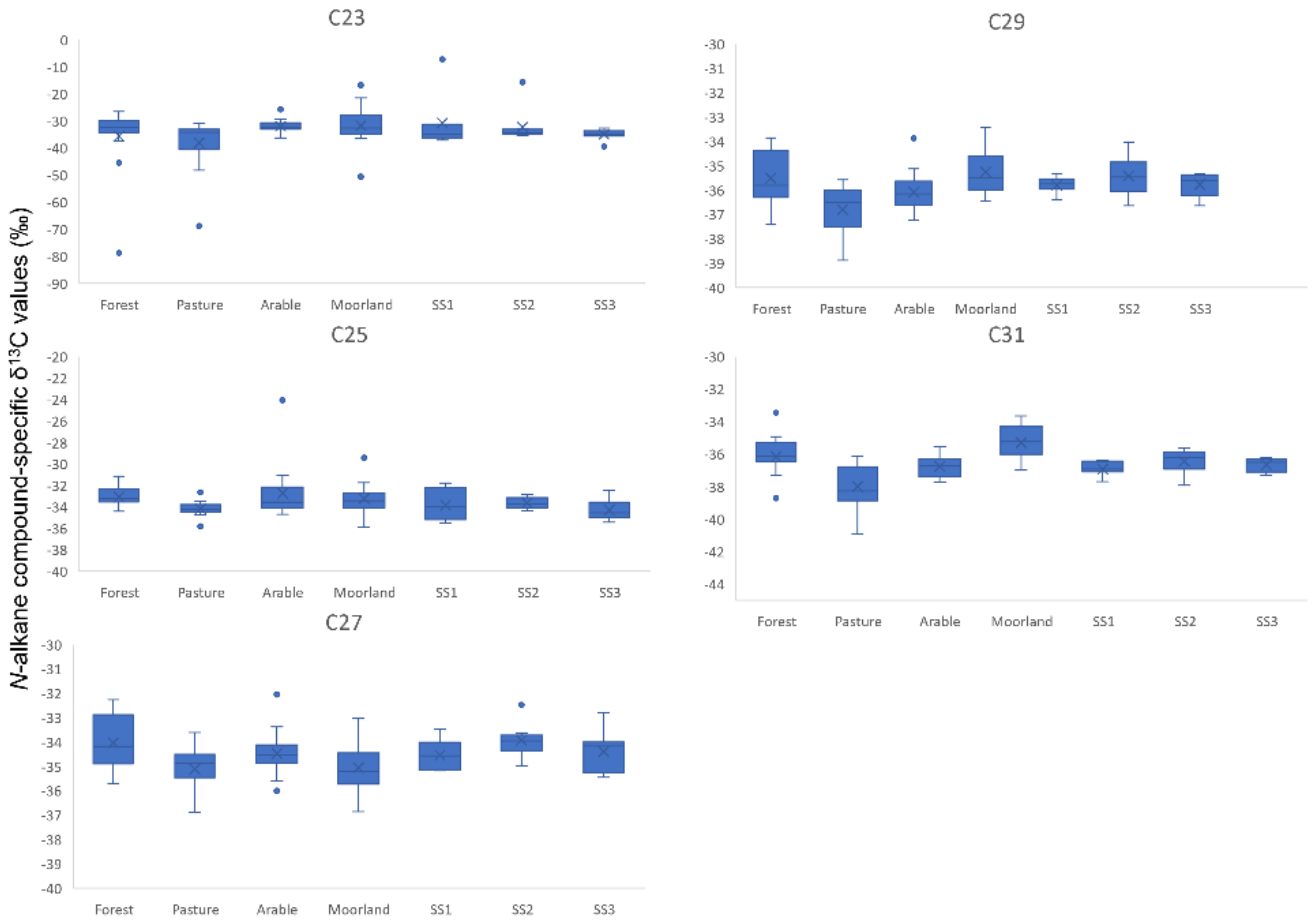

Figure 19: Range of $\delta^{13}C$ values (‰) of *n*-alkanes (C23-C31) from forest, pasture, arable and moorland land uses and suspended sediment sources. The box is extended from the 25–75 percentiles, the line is plotted at the median, a cross marks the mean, and whiskers show the maximum to minimum range excluding outliers (dots).

4.3.1.2 Land Use Discrimination

Six “virtual” mixtures with 50/50 contributions from each of the four sources (arable, pasture, forest and moorland) were created to test the performance of the following tracer combinations in MixSIAR model in distinguishing between land use sources: i) *n*-alkane ratios alone and ii) *n*-alkane ratios + CSSI signatures (Table 13). The use of the additional $\delta^{13}C$ biomarkers resulted in statistically significant differences in errors for all land use combinations except when distinguishing moorland and pasture (Table 13 MP50). Using both *n*-alkane ratios + CSSI signature resulted in a significant increase in error ($p < 0.05$) when distinguishing arable land use from forest (10.4%) and moorland (3%) but a decrease in error when distinguishing between all other land uses (except between moorland and pasture). Based on the mean error across all land uses, *n*-alkane ratios alone were chosen as tracers for OCF of SS.

Table 17: Mean absolute differences between the modelled and virtual mixture composition (%) with biomarkers for two scenarios i) *n*-alkane ratios alone, and ii) *n*-alkane ratios + CSSI signatures. Land use 50/50 combinations: Arable-Forest (AF50), Arable-Moorland (AM50), Arable-Pasture (AP50), Forest-Moorland (FM50), Forest-Pasture (FP50) and Moorland-Pasture (MP50). Asterisk (*) indicates significant difference in two scenarios ($p<0.05$)).

	Mean absolute differences between the modelled and virtual mixture composition in %	
	***n*-alkane ratios**	***n*-alkane ratios + CSSI signatures**
AF50	10	20.4*
AM50	10.4	13.4*
AP50	21	13*
FM50	3	1.2*
FP50	23.6	20.8*
MP50	9	9
Mean Error	12.8	13.0
Number of tracers	5	9

N-alkane signatures for the arable, temporary grassland (ley), grassland land in the Carminowe Creek catchment, Cornwall (Glendell et al., 2018) were very similar between arable and pasture land, likely due to agricultural rotation and, consequently, *n*-alkane signatures were only able to distinguish between woodland and “non-woodland” sources (Chapter 2). However, in this catchment, pastures were dominated by *n*-alkane chain lengths C23 and C25 characteristic of lower plants and mosses, creating a contrast with arable soils which were dominated by the longer chain lengths C27-C31, allowing *n*-alkanes to distinguish between cropland and permanent pasture.

4.3.2 Drivers of change in SS OC source attribution: Sites 1 and 3

The rainfall, stream discharge and agronomic drivers of seasonal changes in SS OC land use sources were identified at a headwater (Site 1) and catchment (Site 3) scale.

Arable land was the dominant land use source of SS OC at Site 1 throughout the monitoring period (June 2019 - November 2020), with contributions varying between a minimum of 37±26% in April 2020 and a maximum of 54±26% in June 2020 (Figure 20a). The mean contribution from arable soils over the monitoring period (June 2019 to December 2020) was 44±6%. On average, the contributions from forest and pasture soils were similar (21±2% and 23±4% respectively) and showed no substantial changes during the monitoring period. Moorland provided the least contribution to SS OC (13±7%) with the exceptions being in April and November 2020.

The mean SS OC content at Site 1 was 8.13±2.70% which is consistent with a mixture of input from the lower OC content arable and pasture soils (3.79±1.09% and 3.67±0.94% respectively) and the higher OC content moorland and forest soils (21.42±13.88% and 12.31±8.0% respectively). Organic matter from aquatic organisms (e.g. algae) usually have C/N values between 4 and 10, whereas protein-poor, cellulose-rich vascular land plants have higher C/N ratios >20 (Ankit et al., 2022; Meyers, 1997). However, the mean C/N ratios for the terrestrial land uses in this catchment were found to be 13.72±3.23 (arable) and 12.54±1.83 (pasture) with only moorland and forest showing C/N ratios greater than 20

(20.01±6.21 and 22.59±6.17 respectively). The C/N ratio of SS at Site 1 (13.54±0.79; Table 16, Figure 20b) was very similar to that in arable and pasture soils, indicating a terrestrial origin of SS OC dominated by either arable or pasture soils.

The relative contribution of terrestrial and aquatic OC to SS OC was evaluated using the PAQ index (Ficken et al., 2000) (Figure 20b). Ankit et al. (2022) ascribe PAQ values <0.1 to terrestrial vegetation, 0.1–0.4 to emergent macrophytes and values > 0.4–1 to sub-merged/floating aquatic plants. Alternatively, Li et al., (2022) found PAQ of terrestrial vegetation to be 0.2±0.2, macrophytes 0.9±0.1, and soil 0.2±0.1. In the Loch Davan catchment, the PAQ value in moorland soils (0.18±0.14) was similar to that found by Li et al., (2022) however the other terrestrial soils in this catchment showed greater mean values of 0.38±0.15 (arable), 0.35±0.17 (forest) and 0.58±0.12 (pasture) in the range usually attributed to macrophytes. Emergent macrophytes and mosses (Bush and McInerney, 2013; Ficken et al., 2000) show *n*-alkane signatures dominated by C23-C25 *n*-alkanes and commensurately high PAQ values. The relatively warm winters and cool, wet summers, in Scotland provide ideal conditions for mosses (https://www.nature.scot/plants-animals-and-fungi/mosses-and-liverworts) and therefore, the higher PAQ values in arable, forest and pasture soils in this catchment could be due to greater abundance of mosses. In addition, some of the lower lying pasture grazing areas in this catchment were located in a wet marsh habitat, which supported higher abundance of mosses and lower plants, likely contributing to the relatively higher PAQ seen in pasture soils (Game & Wildlife Conservation Trust, 2022). The relatively high mean PAQ values in the SS samples (Site 1 0.41±0.10, Site 2 0.48±0.08, and Site 3 0.41±0.07; Figure 20b, Table 16) were also in the range usually attributed to macrophytes (Ankit et al., 2022; Li et al., 2022). Although this could mean that SS OC was mainly derived from autochthonous (aquatic plant) sources, the allochthonous (terrestrial soil) sources in this catchment also show higher PAQ and the SS OC could therefore be derived from terrestrial sources. These results imply that care should be taken when interpreting terrestrial or aquatic origins of sediments using PAQ ranges typically attributed to terrestrial vegetation, emergent macrophytes and

sub-merged/floating aquatic plants, in climates providing ideal conditions for the growth of lower plants and mosses on source soils. The SS PAQ was lowest in April and November 2020 (Figure 20b, suggesting terrestrial input to SS OC may be highest at these times, likely due to agricultural operations in the spring and increased rainfall in the autumn.

April and November 2020 also corresponded with the highest predicted contributions to SS OC from moorland (Figure 20a). Runoff and erosion can take place when low intensity rain falls onto exposed saturated soils, most likely in winter and early spring (Evans and Brazier, 2005). In addition, higher winter rainfall may lead to increased erosion from steeper areas which might be less connected during drier periods (Hirave et al., 2020a). The relatively high rainfall in October/November 2020 (Figure 21b) most likely saturated the moorland soils and led to an increased runoff from the steeply sloping moorland. However, the largest contribution from moorland was in April 2020 (Figure 20a). Burning areas of moorland heather removes the older vegetation and allows plants to regenerate and is practiced widely across UK uplands as part of vegetation management for livestock and red grouse, as well as for conservation (Game & Wildlife Conservation Trust, 2022). Burning of sections of moorland took place in March 2020 (Figure 21a) and the process of burning and/or the resulting areas of sparser vegetation likely resulted in the increased contribution of moorland soil OC to SS OC in April 2020.

There was no significant correlation between SS source proportions and mean rainfall, however, this is not unexpected as runoff will depend on the saturation levels of soils with some soils only contributing sediments when they are saturated, leading to a delay between the onset of heavier rainfall and the increase in sediment contribution.

Percentage C and %N content of SS were highly correlated (r=0.96), suggesting a common source of both elements. The only notable difference between the two elements was in June 2020 when a relative increase in %N compared to OC content resulted in a relatively lower C/N ratio (Figure 20b). Fertiliser is applied to many arable/pasture fields near Site 1 in late March/April when the fields are

prepared, planted and fertilised (Figure 21a). Greater protection from erosion is afforded by the permanent vegetation found in woodland, permanent pasture or moorland compared to arable land which has more variable vegetation cover (Poesen, 2018). It is possible that the relatively bare fields present during the late spring/ early summer contributed to the relatively larger contribution from arable soil OC to SS OC in June 2020 and a consequently higher %N from the recent fertiliser application.

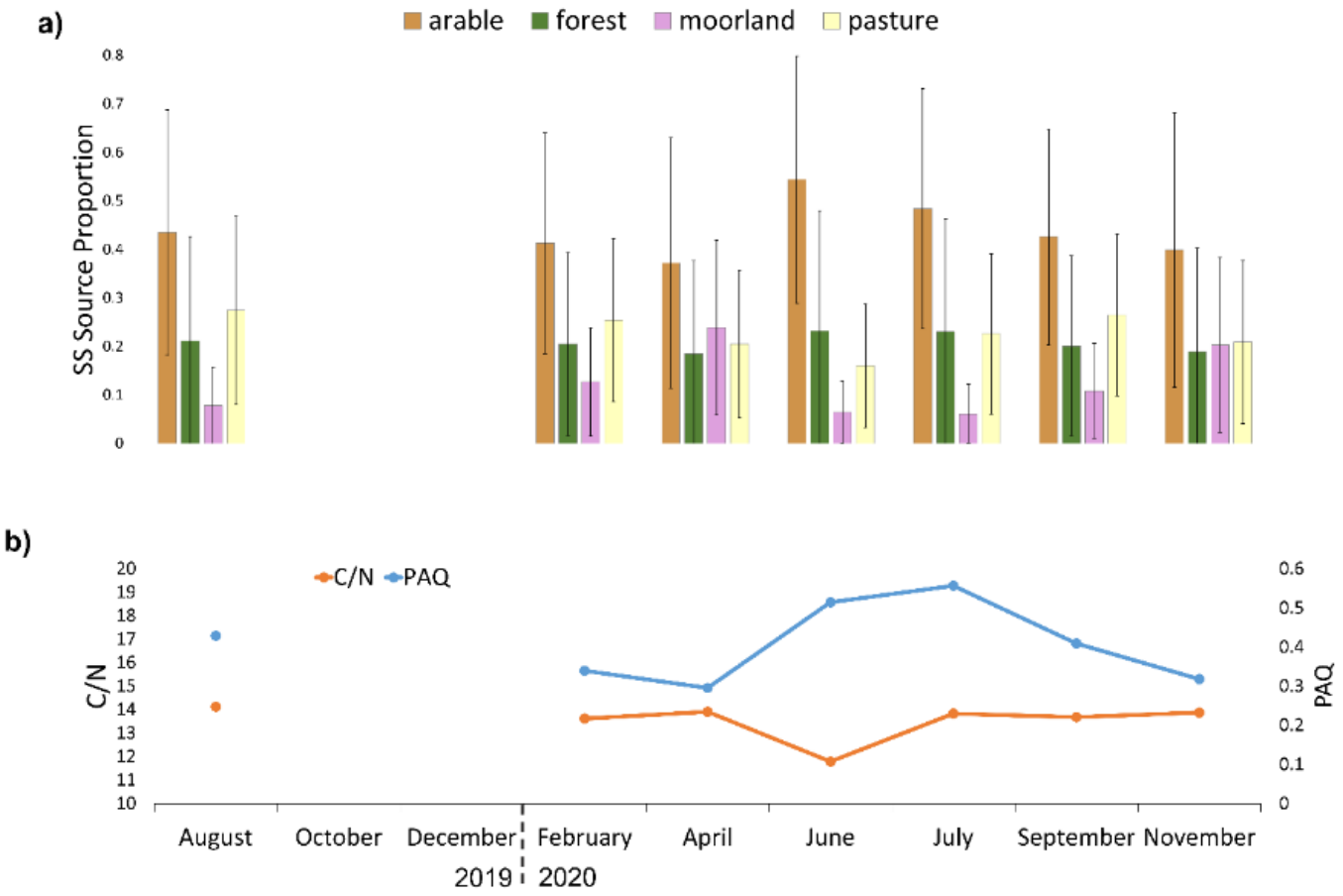

Figure 20 Site 1 a) Land use source proportions from arable, pasture, forest and moorland (error bars ±1 SD), c) Bulk C/N and n-alkane ratio PAQ, where PAQ = (C23+C25)/(C23+C25+C29+C31) (Ficken et al., 2000)

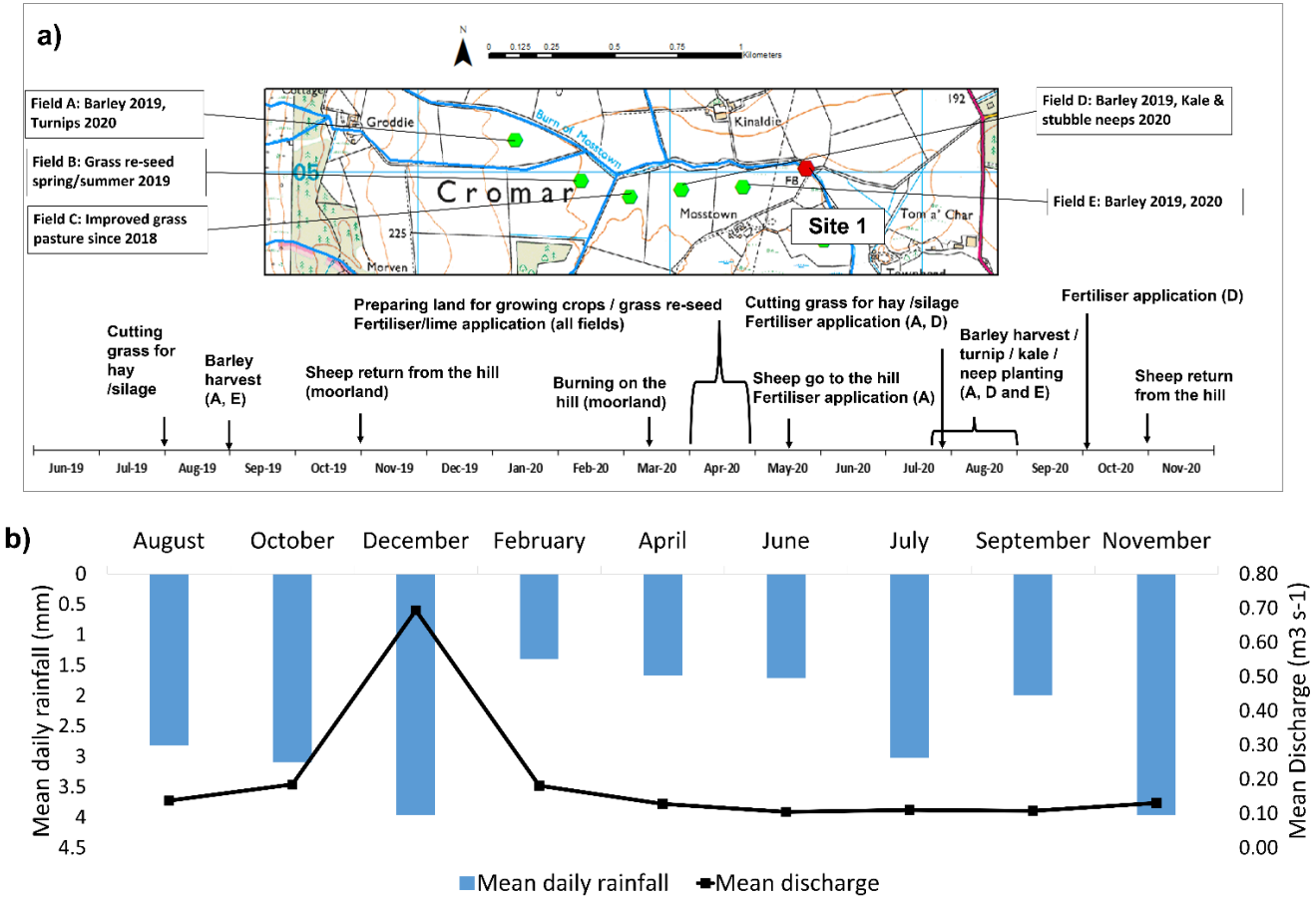

Figure 21 a) Agronomic practices and locations (personal communication from Auchnerran Demonstration Farm (Game & Wildlife Conservation Trust, 2022)) and b) Variation in mean daily rainfall (mm) and mean stream discharge (m^3 s^{-1}) over each sampling period in the Loch Davan catchment.

Near the catchment outlet (Site 3), arable land use was the dominant source of SS OC throughout the monitoring period, with contributions varying between 41±26% and 61±28%. The mean contribution of arable soils over the monitoring period (June 2019 to December 2020) was 46±7%. On average, the contributions from forest and pasture soils were similar (21±1% and 22±7% respectively) however, pasture showed relatively larger input of soil OC to SS OC in October 2019, February and November 2020. Moorland contributed the least soil OC to SS OC (11±0.06%) with the exception of December 2019, when it contributed more than either forest or pasture soil OC (23±18%, cf. 20±20% and 16±13%).

As at Site 1, the C/N ratio of SS at Site 3 (12.67±0.96; Table 16, Figure 22b) was very similar to that in arable and pasture soils, indicating a terrestrial origin of POC dominated by either arable or pasture soils. Percentage C and %N were highly correlated (r=0.90). A drop in the C/N ratio in June 2020 (Figure 22b) may be due to crop cultivation practices and nitrogen fertiliser applications known to take place in April/May in the north-west of the catchment (Figure 21a). However, no commensurate increase in arable soil contribution as at Site 1 was observed at this site. Alternatively, the relative increase in %N could be due to a slightly higher contribution of SOC from moorland soils (17% cf. mean 12%) in June 2020 as moorland soils show a higher %N (mean 0.99±0.54%) relative to the other land uses (0.29% to 0.55%) (Table 16). However, no corresponding increase in %N was seen in SS in December 2019 which had an even higher SOC contribution from moorland soils (24%).

The largest contribution at Site 3 from pasture soil to SS was observed in October 2019 and November 2020 (Figure 22a). Grazed grassland fields and stream channel banks with evidence of soil poaching can be important sediment sources (Blake et al., 2018; Mills and Bathurst, 2015; Pulley et al., 2019). Cattle were present, and had access to the Burn, in the autumn/winter of 2019 and 2020 when a degree of poaching occurred (personal communication from Auchnerran Demonstration Farm (Game & Wildlife Conservation Trust, 2022)). It is possible that this process contributed to the increased sediment input from pasture land during these months. Cattle access to streams for watering is a common practise

in this region, contributing to sediment mobilization and causing bank erosion and poaching of near-channel soils (Stutter, Langan and Demars, 2007). Alternatively, Huisman et al. (2013) found that streams contained and transported “newer” sediments in the spring season (based on ^{7}Be sediment dating), while relatively old sediments (165 to 318 days) were transported within the channel during autumn, suggesting that sediment resuspension could play a key role in stream channels during the latter part of the year. As streambed sediments in the Davan catchment were dominated by soil of pasture origin (Chapter 3), greater mobilisation of this sediment during autumn and winter months may have led to an increase in its contribution to SS at this time.

In this catchment, effective management strategies for mitigating the on-site and off-site impacts of soil erosion could include restricting livestock direct access to the streams, reducing the duration of the grazing season or grazing animals in areas less prone to erosion to avoid poaching issues in pasture soils. Arable soils were the dominant contributor to SS OC, especially during periods where the fields are relatively bare and/or when fields are well connected to the streams. Reduction in arable contribution to SS OC could therefore be achieved by reducing connectivity through the use of stream buffer strips and permanent riparian vegetation which would have the added benefit of reducing livestock direct access to streams.

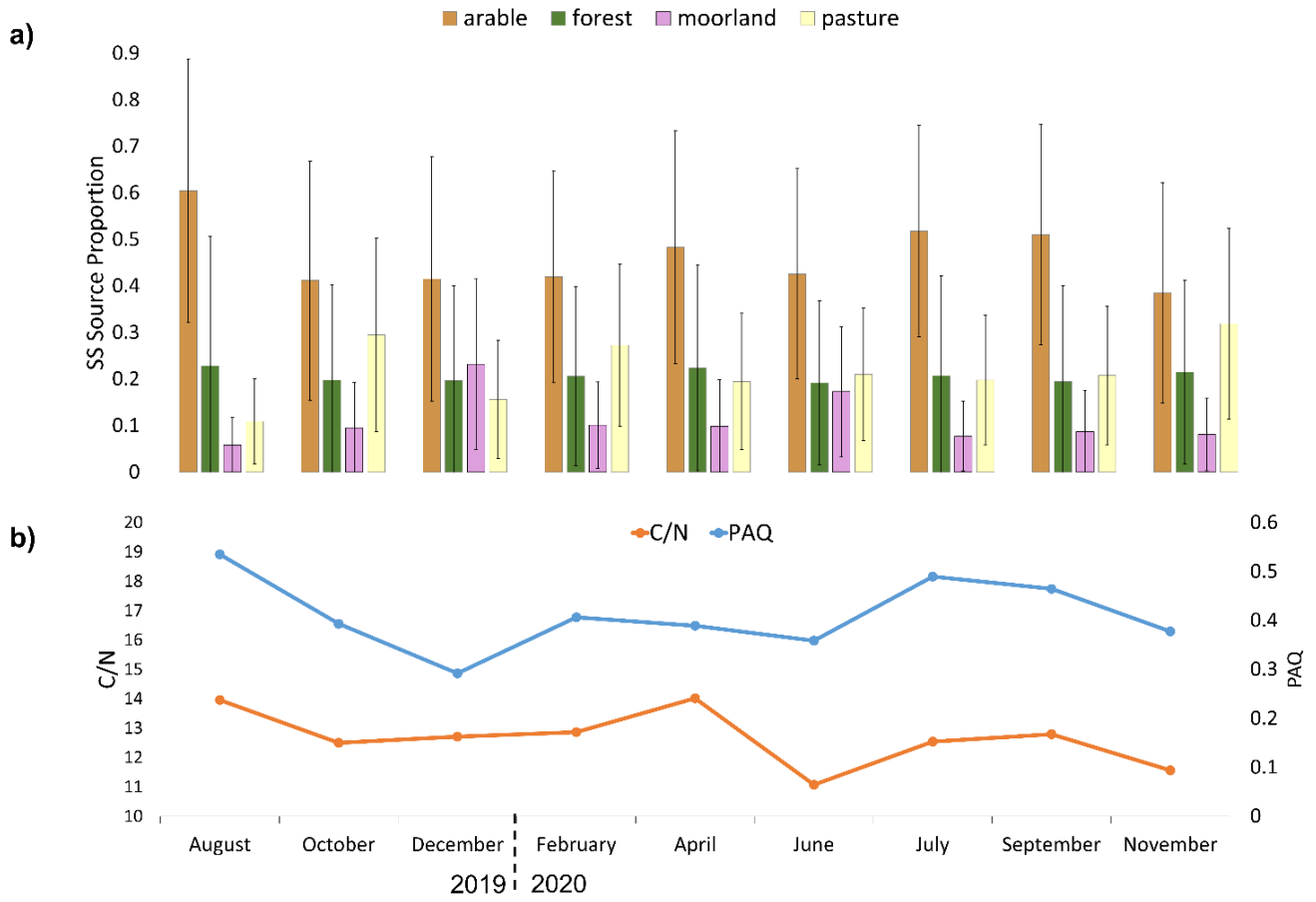

Figure 22 Site 3 a) Land use source proportions for arable, pasture, forest and moorland (error bars ±1 SD) and b) Bulk C/N and PAQ, where PAQ = (C23 + C25)/(C23+C25+C29+C31) (Ficken et al., 2000).

4.3.3 Defining source classifications for SS OCF: Site 2

At Site 1, arable soils were the dominant contributors to SS OC over the monitoring period. Contributions from forest and pasture soils were similar and showed no substantial changes during the monitoring period and moorland provided the smallest contribution, except for April and November 2020. Drivers of change in SS source proportion included land preparation/planting and moorland heather burning in spring, and heavier prolonged rainfall in late autumn and winter leading to saturated soils, increased runoff and stream discharge and remobilisation of streambed sediment. However, these drivers were not evident at the catchment outlet (Site 3) showing a lack of consistency between drivers detectable at headwater and catchment scale. At the catchment scale, SS OC source attribution revealed that livestock poaching of riparian pasture soils may be driving increased soil OC input to streams in late autumn/winter.

Table 18 Mean SS OC source contributions (%) for OCF carried out using a three source (forest, moorland and pasture) and four source (forest, moorland and pasture) classification.

	Mean contribution (%) (± 1 SD)	
	3 sources	4 sources
arable	N/A	44±9
forest	55±14	25±4
moorland	14±8	8±5
pasture	31±16	23±11

In contrast to Site 1, the dominant source of SS OC using a three-source classification at Site 2 was forest with a mean contribution of 55±14% (Table 18; Figure 23b). This forest contribution was much greater than seen at sites 1 or 3. Chapter 2 revealed that extensive riparian forest in the Carminowe Creek

catchment, Cornwall, disconnected upslope eroded SOC and direct input of litter and leaves dominated OC input to the streams. As Site 2 in the Davan catchment is located within forest land it is possible similar processes led to a greater contribution of forest-derived OC to SS OC. However, direct input of less degraded litter and leaves to the streams can be evidenced by higher OEP (odd-over-even predominance – a measure of organic matter degradation) and lower %C31 in SS relative to the terrestrial soils (Chapter 2). In this sub-catchment, although %C31 was lower than that in the terrestrial soils (20±3; terrestrial range 31 to 52), OEP was within the range of terrestrial soils (4.89±1.39; terrestrial range 0.89 to 7.22) (Table 16), suggesting that there was unlikely to be a substantial input of less degraded litter and leaves to the streams at Davan Site 2. Alternatively, there could be increased erosion of the riparian forest soil. If this was the case it would be expected that forest derived SOC input would increase following periods of high rainfall/stream discharge (October to December 2019, July 2020 and November 2020; Figure 21b). A relatively large contribution of forest derived SOC was observed in December 2019, however, no similar peak in forest SOC contribution was seen at the catchment outlet (Site 3). In addition, the largest forest SOC contribution was observed in June 2020 when the mean rainfall and stream discharge were both relatively low (Figure 21b).

Using a four-source classification, the contribution of forest to SS OC was slightly greater than that seen at Sites 1 and 3 (mean 25±4%; Site 1 and 3 both 21%), likely due to its forest location. However, the dominant SS OC source was from arable land, with a minimum contribution of 31±25% in August 2019 and a peak of 60±24% in December 2019 (Figure 23a). This result is surprising given the relatively small area of land used for growing crops in this sub-catchment. However, at least two of the arable fields were located next to the Burn and were highly connected (Figure 17). These results would support other studies that have found a larger contribution from arable land use to river sediments than would be expected from the proportion of land area within a catchment (Wang et al., 2021). Similar to the forest SOC contributions to SS OC in the three-source classification, the peaks in arable contribution in the four-source classification could be seen in December 2019 and June 2020. Although the peak forest SOC

contribution in the three-source model in June 2020 was difficult to explain, the increase in arable contribution in the four-source classification at this time could be due to runoff from the relatively bare fields present during the late spring/early summer (as seen at Site 1). The high contribution of SOC from arable soil to SS OC seen in November 2019 could be due to increased runoff due to higher rainfall and substantially higher stream discharge at this time of year (Figure 21b).

Since both peaks in arable contribution in the four-source classification can be explained by known OC drivers, and there were no satisfactory explanations for the corresponding peaks in forest contributions of the three-source model, it was concluded that the contribution of arable SOC to SS OC was substantial enough to make the four-source classification the best choice in this sub-catchment.

The SS PAQ was lowest in February 2020 (Figure 23b), suggesting terrestrial input to SS OC may reach a maximum at these times in this sub-catchment. The C/N ratio (and OC content, %N) peaked in February 2020 (Figure 23b) when the maximum contribution of moorland SOC to SS OC was evident in both the three-source and four-source classification models (Figure 23a and b). Unlike at Site 1, in the four-source classification model moorland contribution to SS OC in this sub-catchment was significantly positively correlated with OC content ($r=0.71$; $p<0.05$) and C/N ($r=0.85$; $p<0.05$). Similar to Site 1, if the relatively large rainfall seen in November 2019 saturated the moorland soils, there could have been an increased runoff from the steeply sloping moorlands in the winter period (Evans and Brazier, 2005). In this sub-catchment there was no evidence of increased contribution of SOC from moorland soils to SS OC due to burning of heather, as seen at Site 1 in April 2020.

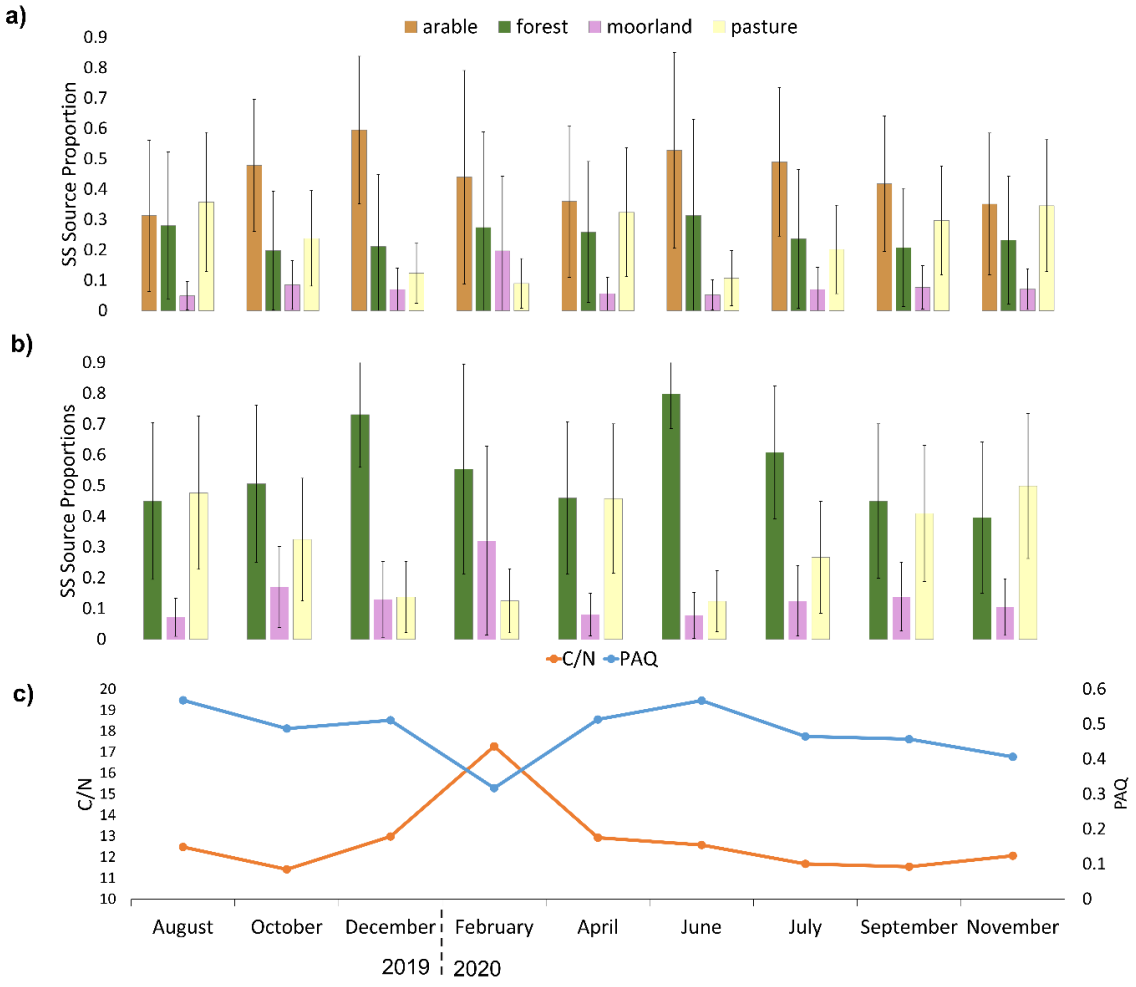

Figure 23 Site 2 a) Land use source proportions for four source OCF (arable, pasture, forest and moorland) (error bars ±1 SD, b) Land use source proportions for three source OCF (pasture, forest and moorland) (error bars ±1 SD), and c) Bulk C/N and PAQ, where PAQ = (C23 + C25)/(C23+C25+C29+C31)(Ficken et al., 2000)

4.4 Conclusions

Organic C fingerprinting using *n*-alkanes is a valuable tool to estimate the relative contribution of different land use sources to sediment OC. However, there remain challenges in the application OCF including i) effects on tracer signatures due to sorting effect of particles by size during mobilization, transport and deposition and ii) ensuring all sources are included. The methods employed in this study firstly revealed SS rather than streambed sediment most closely approximated biomarker signatures in terrestrial soils, suggesting that differences in *n*-alkane

signatures between terrestrial soil sources and stream sediments were unlikely to be affected by the enrichment in finer particles. Secondly, drivers of variation in SS source proportions in a headwater catchment included land preparation/planting and moorland heather burning in spring, and heavier prolonged rainfall in late autumn and winter, leading to saturated soils and increased runoff. These drivers were not detected at the catchment scale, where livestock poaching of riparian pasture soils may be driving increased OC input to streams especially in late autumn/winter. In addition, the unique finding of this study, that PAQ in arable, forest and pasture soils was in the range normally associated with emergent macrophytes and mosses, has implications for research interpreting the origins of aquatic sediments using the expected ranges of PAQ in terrestrial and aquatic vegetation (Ankit et al., 2022) - especially in climates, such as that in Scotland, providing the ideal conditions for the growth of mosses in source soils. Finally, the land use sources selected for OCF were validated by identifying the small amount of arable land in a headwater sub-catchment made a substantial enough input to stream OC to be included as a fingerprinting source.

By revealing that *n*-alkanes signatures were unlikely to be affected by the enrichment in finer particles, and validating the choice of land use sources, these methods addressed two of the key challenges in OCF, and thereby increased confidence in the source apportionment in this catchment.

4.5 References

Addy, S., Ghimire, S. and Cooksley, S. (2012) ‘Assessment of the multiple benefits of river restoration: the Logie Burn meander reconnection project’, BHS Eleventh National Symposium, Hydrology for a changing world, Dundee 2012, , pp. 01–05.

Alewell, C., Birkholz, A., Meusburger, K., Schindler Wildhaber, Y. and Mabit, L. (2016) ‘Quantitative sediment source attribution with compound-specific isotope analysis in a C3 plant-dominated catchment (central Switzerland)’, Biogeosciences, 13(5), pp. 1587–1596.

Ankit, Y., Muneer, W., Gaye, B., Lahajnar, N., Bhattacharya, S., Bulbul, M., Jehangir, A., Anoop, A. and Mishra, P.K. (2022) 'Apportioning sedimentary organic matter sources and its degradation state- Inferences based on aliphatic hydrocarbons amino acids and δ15N', Environmental Research, 205

Armstrong, A., Quinton, J.N., Heng, B.C.P. and Chandler, J.H. (2011) 'Variability of interrill erosion at low slopes', Earth Surface Processes and Landforms, 36(1), pp. 97–106.

Batista, P.V.G., Laceby, J.P. and Evrard, O. (2022) 'How to evaluate sediment fingerprinting source apportionments', Journal of Soils and Sediments, (0123456789) Springer Berlin Heidelberg

Blake, W.H., Boeckx, P., Stock, B.C., Smith, H.G., Bodé, S., Upadhayay, H.R., Gaspar, L., Goddard, R., Lennard, A.T., Lizaga, I., Lobb, D.A., Owens, P.N., Petticrew, E.L., Kuzyk, Z.Z.A., Gari, B.D., Munishi, L., Mtei, K., Nebiyu, A., Mabit, L., Navas, A. and Semmens, B.X. (2018) 'A deconvolutional Bayesian mixing model approach for river basin sediment source apportionment', Scientific Reports, 8(1), pp. 1–12.

Blake, W.H., Ficken, K.J., Taylor, P., Russell, M.A. and Walling, D.E. (2012) 'Tracing crop-specific sediment sources in agricultural catchments', Geomorphology, 139–140 Elsevier B.V., pp. 322–329.

Blake, W.H., Kelly, C., Wynants, M., Patrick, A., Lewin, S., Lawson, J., Nasolwa, E., Page, A., Nasseri, M., Marks, C., Gilvear, D., Mtei, K., Munishi, L. and Ndakidemi, P. (2021) 'Integrating land-water-people connectivity concepts across disciplines for co-design of soil erosion solutions', Land Degradation and Development, 32(12), pp. 3415–3430.

Bush, R.T. and McInerney, F.A. (2013) 'Leaf wax n-alkane distributions in and across modern plants: Implications for paleoecology and chemotaxonomy', Geochimica et Cosmochimica Acta, 117 Elsevier Ltd, pp. 161–179.

CEH (2021) Centre for Ecology and Hydrology UK Lakes Portal. Available at: https://eip.ceh.ac.uk/apps/lakes/detail.html#wbid=21123 (Accessed: 18 January 2021).

Chen, F.X., Fang, N.F., Wang, Y.X., Tong, L.S. and Shi, Z.H. (2017) 'Biomarkers in sedimentary sequences: Indicators to track sediment sources over decadal timescales', Geomorphology, 278 Elsevier B.V., pp. 1–11.

Cole, B., King, S., Ogutu, B., Palmer, D., Smith, G. and Balzter, H. (2015) Corine land cover 2012 for the UK, Jersey and Guernsey., NERC Environmental Information Data Centre Available at: https://doi.org/10.5285/32533dd6-7c1b-43e1-b892-e80d61a5ea1d (Accessed: 18 January 2021).

Collins, A.L., Blackwell, M., Boeckx, P., Chivers, C.A., Emelko, M., Evrard, O., Foster, I., Gellis, A., Gholami, H., Granger, S., Harris, P., Horowitz, A.J., Laceby, J.P., Martinez-Carreras, N., Minella, J., Mol, L., Nosrati, K., Pulley, S., Silins, U., da Silva, Y.J., Stone, M., Tiecher, T., Upadhayay, H.R. and Zhang, Y. (2020) Sediment source fingerprinting: benchmarking recent outputs, remaining challenges and emerging themes. Journal of Soils and Sediments.

Cranwell, P.A. (1981) 'Diagenesis of free and bound lipids in terrestrial detritus deposited in a lacustrine sediment', Organic Geochemistry, 3(3), pp. 79–89.

Dai, J. and Sun, M.Y. (2007) 'Organic matter sources and their use by bacteria in the sediments of the Altamaha estuary during high and low discharge periods', Organic Geochemistry, 38(1), pp. 1–15.

Evans, R. and Brazier, R. (2005) 'Evaluation of modelled spatially distributed predictions of soil erosion by water versus field-based assessments', Environmental Science and Policy, 8(5), pp. 493–501.

Fang, J., Wu, F., Xiong, Y., Li, F., Du, X., An, D. and Wang, L. (2014) 'Source characterization of sedimentary organic matter using molecular and stable carbon isotopic composition of n-alkanes and fatty acids in sediment core from Lake Dianchi, China', Science of the Total Environment, 473–474, pp. 410–421.

Felde, V.J.M.N.L., Schweizer, S.A., Biesgen, D., Ulbrich, A., Uteau, D., Knief, C., Graf-Rosenfellner, M., Kögel-Knabner, I. and Peth, S. (2021) 'Wet sieving versus dry crushing: Soil microaggregates reveal different physical structure, bacterial diversity and organic matter composition in a clay gradient', European Journal of Soil Science, 72(2), pp. 810–828.

Ficken, K.J., Li, B., Swain, D.L. and Eglinton, G. (2000) 'An n-alkane proxy for the sedimentary input of submerged/floating freshwater aquatic macrophytes', Organic Geochemistry, 31(7–8), pp. 745–749.

Game & Wildlife Conservation Trust (2022) Scottish Demonstration Farm Auchnerran.

García-Comendador, J., Martínez-Carreras, N., Fortesa, J., Company, J., Borràs, A. and Estrany, J. (2021) 'Combining sediment fingerprinting and hydro-sedimentary monitoring to assess suspended sediment provenance in a mid-mountainous Mediterranean catchment', Journal of Environmental Management, 299(August), p. 113593.

Geng, J., Cheng, S., Fang, H., Pei, J., Xu, M., Lu, M., Yang, Y., Cao, Z. and Li, Y. (2019) 'Different molecular characterization of soil particulate fractions under N deposition in a subtropical forest', Forests, 10(10), pp. 1–18.

Gibbs, M.M. (2008) 'Identifying source soils in contemporary estuarine sediments: A new compound-specific isotope method', Estuaries and Coasts, 31(2), pp. 344–359.

Glendell, M., Jones, R., Dungait, J.A.J., Meusburger, K., Schwendel, A.C., Barclay, R., Barker, S., Haley, S., Quine, T.A. and Meersmans, J. (2018) 'Tracing of particulate organic C sources across the terrestrial-aquatic continuum, a case study at the catchment scale (Carminowe Creek, southwest England)', Science of the Total Environment, 616, pp. 1077–1088. Available at: 10.1016/j.scitotenv.2017.10.211 (Accessed: 5 September 2018).

Griepentrog, M., Bodé, S., Boeckx, P. and Wiesenberg, G.L.B. (2016) 'The fate of plant wax lipids in a model forest ecosystem under elevated CO2 concentration

and increased nitrogen deposition', Organic Geochemistry, 98 Elsevier Ltd, pp. 131–140.

Grimalt, J.O., Torras, E. and Albaigés, J. (1988) 'Bacterial reworking of sedimentary lipids during sample storage', Organic Geochemistry, 13(4–6), pp. 741–746.

Guzmán, G., Quinton, J.N., Nearing, M.A., Mabit, L. and Gómez, J.A. (2013) 'Sediment tracers in water erosion studies: Current approaches and challenges', Journal of Soils and Sediments, 13(4), pp. 816–833.

Hancock, G.J. and Revill, A.T. (2013) 'Erosion source discrimination in a rural Australian catchment using compound-specific isotope analysis (CSIA)', Hydrological Processes, 27(6), pp. 923–932.

Hirave, P., Glendell, M., Birkholz, A. and Alewell, C. (2020a) 'Compound-specific isotope analysis with nested sampling approach detects spatial and temporal variability in the sources of suspended sediments in a Scottish mesoscale catchment', Science of The Total Environment, (xxxx) The Authors, p. 142916.

Hirave, P., Wiesenberg, G.L.B., Birkholz, A. and Alewell, C. (2020b) 'Understanding the effects of early degradation on isotopic tracers: implications for sediment source attribution using compound-specific isotope analysis (CSIA)', Biogeosciences Discussions, (June), pp. 1–18.

Huisman, N.L.H., Karthikeyan, K.G., Lamba, J., Thompson, A.M. and Peaslee, G. (2013) 'Quantification of seasonal sediment and phosphorus transport dynamics in an agricultural watershed using radiometric fingerprinting techniques', Journal of Soils and Sediments, 13(10), pp. 1724–1734.

Jung, B.-J., Lee, J.-K. and Park, J.-H. (2014) 'Storm pulses of particulate and dissolved organic carbon in a forested headwater stream and their environmental implications – importance of extreme rainfall events', Biogeosciences Discussions, 11(5), pp. 6877–6908.

Klimaszyk, P. and Rzymski, P. (2013) ‘Catchment vegetation can trigger lake dystrophy through changes in runoff water quality’, Annales de Limnologie, 49(3), pp. 191–197.

Koiter, A.J., Lobb, D.A., Owens, P.N., Petticrew, E.L., Tiessen, K.H.D. and Li, S. (2013a) ‘Investigating the role of connectivity and scale in assessing the sources of sediment in an agricultural watershed in the Canadian prairies using sediment source fingerprinting’, Journal of Soils and Sediments, 13(10), pp. 1676–1691.

Koiter, A.J., Owens, P.N., Petticrew, E.L. and Lobb, D.A. (2013b) ‘The behavioural characteristics of sediment properties and their implications for sediment fingerprinting as an approach for identifying sediment sources in river basins’, Earth-Science Reviews, 125 Elsevier B.V., pp. 24–42.

Laceby, J.P., Evrard, O., Smith, H.G., Blake, W.H., Olley, J.M., Minella, J.P.G. and Owens, P.N. (2017) ‘The challenges and opportunities of addressing particle size effects in sediment source fingerprinting: A review’, Earth-Science Reviews, 169(December 2016), pp. 85–103.

Lachance, C., Lobb, D.A., Pelletier, G., Thériault, G. and Chrétien, F. (2020) ‘Determination of sediment sources in a mixed watershed within the Appalachian-St. Lawrence Lowland Regions of southern Quebec using sediment fingerprinting’, Environmental Monitoring and Assessment, 192(9) Environmental Monitoring and Assessment

Lamba, J., Karthikeyan, K.G. and Thompson, A.M. (2015) ‘Apportionment of suspended sediment sources in an agricultural watershed using sediment fingerprinting’, Geoderma, 239 Elsevier B.V., pp. 25–33.

Li, J., Lv, L., Wang, R., Long, H. and Yang, X. (2022) ‘Spatial distribution of n-alkanes in the catchment and sediments of Lake Lugu, Southwest China: Implications for palaeoenvironment reconstruction’, Palaeogeography, Palaeoclimatology, Palaeoecology, 592(February) Elsevier B.V., p. 110895.

Liu, C., Li, Z., Dong, Y., Chang, X., Nie, X., Liu, L., Xiao, H., Wang, D. and Peng, H. (2017) ‘Response of sedimentary organic matter source to rainfall events using

stable carbon and nitrogen isotopes in a typical loess hilly-gully catchment of China', Journal of Hydrology, 552 Elsevier B.V., pp. 376–386.

Met Office (2021) UK Climate Average. Available at: https://www.metoffice.gov.uk/research/climate/maps-and-data/uk-climate-averages/gfjuxqwcs (Accessed: 18 January 2021).

Meyers, P.A. (1997) 'Organic geochemical proxies of paleoceanographic, paleolimnologic, and paleoclimatic processes', Organic Geochemistry, 27(5), pp. 213–250.

Mills, C.F. and Bathurst, J.C. (2015) 'Spatial variability of suspended sediment yield in a gravel-bed river across four orders of magnitude of catchment area', Catena, 133 Elsevier B.V., pp. 14–24.

Mukundan, R., Radcliffe, D.E., Ritchie, J.C., Risse, L.M. and McKinley, R.A. (2010) 'Sediment Fingerprinting to Determine the Source of Suspended Sediment in a Southern Piedmont Stream', Journal of Environmental Quality, 39(4), pp. 1328–1337.

Mukundan, R., Walling, D.E., Gellis, A.C., Slattery, M.C. and Radcliffe, D.E. (2012) 'Sediment Source Fingerprinting: Transforming From a Research Tool to a Management Tool', Journal of the American Water Resources Association, 48(6), pp. 1241–1257.

Ordnance Survey (2021) OS Terrain 5 [ASC geospatial data], Scale 1:10000, Tiles: nj30ne,nj30nw,nj30se,nj30sw,nj31se,nj31sw,nj40ne,nj40nw,nj40se,nj40sw,nj41se,nj41sw,nj50ne,nj50nw,nj50se,nj50sw,nj51se,nj51sw,no39ne,no39nw,no49ne,no49nw,no59ne,no59nw,., EDINA Digimap Ordnance Survey Service Available at: https://digimap.edina.ac.uk (Accessed: 14 December 2018).

Phillips, J.M., Russell, M.A. and Walling, D.E. (2000) 'Time-integrated sampling of fluvial suspended sediment: a simple methodology for small catchments', Hydrological Processes, 14(April), pp. 2589–2602.

Poesen, J. (2018) ‘Soil erosion in the Anthropocene: Research needs’, Earth Surface Processes and Landforms, 43(1), pp. 64–84.

Pulley, S., Goubet, A., Moser, I., Browning, S. and Collins, A.L. (2019) ‘The sources and dynamics of fine-grained sediment degrading the Freshwater Pearl Mussel (Margaritifera margaritifera) beds of the River Torridge, Devon, UK’, Science of the Total Environment, 657 The Authors, pp. 420–434.

Puttock, A., Dungait, J.A.J., Macleod, C.J.A., Bol, R. and Brazier, R.E. (2014) ‘Organic Carbon From Dryland Soils’, Journal of Geophysical Research: Biogeosciences, 119, pp. 2345–2357.

Quenea, K., Derenne, S., Largeau, C., Rumpel, C. and Mariotti, A. (2004) ‘Variation in lipid relative abundance and composition among different particle size fractions of a forest soil’, Organic Geochemistry, 35(11-12 SPEC. ISS.), pp. 1355–1370.

Quénéa, K., Largeau, C., Derenne, S., Spaccini, R., Bardoux, G. and Mariotti, A. (2006) ‘Molecular and isotopic study of lipids in particle size fractions of a sandy cultivated soil (Cestas cultivation sequence, southwest France): Sources, degradation, and comparison with Cestas forest soil’, Organic Geochemistry, 37(1), pp. 20–44.

R Core Team (2020) R: A language and environment for statistical computing 3.6.3. R Foundation for Statistical Computing, Vienna, Austria

Ranjan, R.K., Routh, J., Val Klump, J. and Ramanathan, A.L. (2015) ‘Sediment biomarker profiles trace organic matter input in the Pichavaram mangrove complex, southeastern India’, Marine Chemistry, 171 Elsevier B.V., pp. 44–57.

RStudio Team (2018) RStudio: Integrated Development for R 1.1.463. PBC, Boston, MA

Scheurer, K., Alewell, C., Bänninger, D. and Burkhardt-Holm, P. (2009) ‘Climate and land-use changes affecting river sediment and brown trout in alpine countries-a review’, Environmental Science and Pollution Research, 16(2), pp. 232–242.

SEPA (2021) Water Classification Hub., Scottish Environment Protection Agency

Sherriff, S.C., Rowan, J.S., Fenton, O., Jordan, P. and Ó hUallacháin, D. (2019) 'Influence of land management on soil erosion, connectivity, and sediment delivery in agricultural catchments: Closing the sediment budget', Land Degradation and Development, 30(18), pp. 2257–2271.

Singh, S.N., Kumari, B. and Mishra, S. (2012) 'Microbial Degradation of Alkanes', in Microbial Degradation of Xenobiotics. , pp. 439–469.

Sirjani, E., Mahmoodabadi, M. and Cerdà, A. (2022) 'Sediment transport mechanisms and selective removal of soil particles under unsteady-state conditions in a sheet erosion system', International Journal of Sediment Research, 37(2), pp. 151–161.

Smith, A.A., Tetzlaff, D. and Soulsby, C. (2018) 'On the Use of StorAge Selection Functions to Assess Time-Variant Travel Times in Lakes', Water Resources Research, 54(7), pp. 5163–5185.

Smith, H.G., Karam, D.S. and Lennard, A.T. (2018) 'Evaluating tracer selection for catchment sediment fingerprinting', Journal of Soils and Sediments, 18(9) Journal of Soils and Sediments, pp. 3005–3019.

Stenfert Kroese, J., Batista, P.V.G., Jacobs, S.R., Breuer, L., Quinton, J.N. and Rufino, M.C. (2020) 'Agricultural land is the main source of stream sediments after conversion of an African montane forest', Scientific Reports, 10(1) Nature Publishing Group UK, p. 14827.

Stock, B.C. and Semmens, B.X. (2016) MixSIAR GUI User Manual. Version 3.1

Stout, S.A. (2020) 'Leaf wax n-alkanes in leaves, litter, and surface soil in a low diversity, temperate deciduous angiosperm forest, Central Missouri, USA', Chemistry and Ecology, Taylor & Francis, pp. 810–826.

Stutter, M.I., Langan, S.J. and Demars, B.O.L. (2007) 'River sediments provide a link between catchment pressures and ecological status in a mixed land use Scottish River system', Water Research, 41(12), pp. 2803–2815.

Torres, T., Ortiz, J.E., Martín-Sánchez, D., Arribas, I., Moreno, L., Ballesteros, B., Blázquez, A.N.A., Domínguez, J.A. and Estrella, T.R. (2014) 'The long pleistocene record from the pego-oliva marshland (Alicante-Valencia, Spain)', Geological Society Special Publication, 388(1), pp. 429–452.

Uber, M., Legout, C., Nord, G., Crouzet, C., Demory, F. and Poulenard, J. (2019) 'Comparing alternative tracing measurements and mixing models to fingerprint suspended sediment sources in a mesoscale Mediterranean catchment', Journal of Soils and Sediments, 19(9) Journal of Soils and Sediments, pp. 3255–3273.

Vercruysse, K. and Grabowski, R.C. (2018) 'Using source-specific models to test the impact of sediment source classification on sediment fingerprinting', Hydrological Processes, 32(22), pp. 3402–3415.

Vogel, H.J., Bartke, S., Daedlow, K., Helming, K., Kögel-Knabner, I., Lang, B., Rabot, E., Russell, D., Stößel, B., Weller, U., Wiesmeier, M. and Wollschläger, U. (2018) 'A systemic approach for modeling soil functions', Soil, 4(1), pp. 83–92.

Wang, X., Blake, W.H., Taylor, A., Kitch, J. and Millward, G. (2021) 'Evaluating the effectiveness of soil conservation at the basin scale using floodplain sedimentary archives', Science of the Total Environment, 792 Elsevier B.V., p. 148414.

Wiesmeier, M., Lützow, M. von, Spörlein, P., Geuß, U., Hangen, E., Reischl, A., Schilling, B. and Kögel-Knabner, I. (2015) 'Land use effects on organic carbon storage in soils of Bavaria: The importance of soil types', Soil and Tillage Research, 146(PB) Elsevier B.V., pp. 296–302.

Wiesmeier, M., Urbanski, L., Hobley, E., Lang, B., von Lützow, M., Marin-Spiotta, E., van Wesemael, B., Rabot, E., Ließ, M., Garcia-Franco, N., Wollschläger, U., Vogel, H.J. and Kögel-Knabner, I. (2019) 'Soil organic carbon storage as a key function of soils - A review of drivers and indicators at various scales', Geoderma, 333(July 2018) Elsevier, pp. 149–162.

Wohl, E., Bledsoe, B.P., Jacobson, R.B., Poff, N.L., Rathburn, S.L., Walters, D.M. and Wilcox, A.C. (2015) ‘The natural sediment regime in rivers: Broadening the foundation for ecosystem management’, BioScience, 65(4), pp. 358–371.

Zhang, Y., Collins, A.L., McMillan, S., Dixon, E.R., Cancer-Berroya, E., Poiret, C. and Stringfellow, A. (2017) ‘Fingerprinting source contributions to bed sediment-associated organic matter in the headwater subcatchments of the River Itchen SAC, Hampshire, UK’, River Research and Applications, 33(10), pp. 1515–1526.

5 Using OC fingerprinting to evaluate the performance of erosion risk models in a Scottish catchment

Abstract

Tackling rural diffuse pollution, including surface runoff and soil erosion, is a key factor in river basin management to improve the status of waterbodies. Identification of hotspots, where a high risk of soil degradation could increase the risk of diffuse water pollution, are a key step in the implementation of Best Management Practices (BMP) so that land can be cultivated to maintain a healthy soil and environment and minimize the risk to watercourses. Hotspots can be identified by modelling catchment erosion using readily available empirical models such as the Revised Universal Soil Loss Equation (RUSLE) whose extensive application based on accessible data means that it can be easily applied in a wide variety of catchments. In addition, in Scotland, soil risk maps have been developed to help stakeholders plan agricultural activities to minimize the risk of erosion and manage their soils sustainably. The utility of these soil erosion and risk models in identifying hotspots, and guiding BMP, depends upon their accuracy and there is a need to assess model usefulness.

This study was carried out in the catchment of Loch Davan, Aberdeenshire, Scotland. Organic carbon loss models were constructed to compare land use specific OC yields based on RUSLE (which calculates long-term average annual soil loss in tons ha^{-1} yr^{-1}) and the Scottish erosion risk map (ERM) of Lilly and Baggaley, (2018) (which shows the risk of a bare soil being eroded by water). Existing OC fingerprinting (OCF) was used as a benchmark to determine which erosion model best identified the relative land use OC yields in streambed sediment.

Although, the ERM best identified the relative land use OC yields in streambed sediment, the results of RUSLE were very similar suggesting that, in this catchment, RUSLE erosion rate estimates could be used to quantify the amount of soil eroded from the high-risk areas defined by the ERM. In addition, the method identified that, in this catchment, the RUSLE C-factor for moorland should

be set similar to that for forest rather than the value quoted in the literature. In future studies, similarly adjusting all C-factors to get land use source proportions closer to those of the OC fingerprinting benchmark could ultimately result in more accurate RUSLE erosion rate estimates.

Keywords: terrestrial-aquatic fluxes, organic carbon loss modelling, sediment fingerprinting, erosion risk

5.1 Introduction

Soils provide many benefits for society including producing crops and timber, regulating water flow, and storing carbon. Although soil erosion is a natural process, modern land management techniques can lead to increased rates which impact crop yields, lead to a loss of soil carbon from the land, and pollute waterbodies (Lilly and Baggaley, 2014). Tackling rural diffuse pollution, including surface runoff and soil erosion, is a key factor in river basin management to improve the status of waterbodies. Pathways of pollution from agriculture to freshwater are complex and, often, poorly understood. Hotspots can contribute greater than average amounts of pollutants due to the combined effect soil properties and land management (Cloy et al., 2021). Identification of these hotspots, where a high risk of soil degradation could increase the risk of diffuse water pollution, are a key step in the implementation of Best Management Practices (BMP) so that land can be cultivated to maintain a healthy soil and environment and minimize the risk to watercourses (Baggaley et al., 2020). Hotspots can be identified by modelling catchment erosion. Erosion models include readily available empirical models such as the Revised Universal Soil Loss Equation (RUSLE) (Desmet and Govers, 1996; Renard et al., 1997; Wischmeier and Smith, 1978) whose extensive application based on accessible data means that it can be easily applied in a wide variety of catchments (Alewell et al., 2019; ESDAC, 2014, 2015a; Panagos et al., 2014, 2015a). In Scotland, new and improved tools have been developed to represent the specific soil conditions in this region and to predict how soils respond to land use and management pressures and soil risk maps have been made available to help stakeholders plan agricultural activities to minimize the risk of erosion and

manage their soils sustainably (Baggaley et al., 2020; Lilly and Baggaley, 2018). However, the utility of soil erosion and risk models in identifying hotspots and guiding BMP depends upon their accuracy (Batista et al., 2019) and needs to be evaluated.

The output of erosion models such as RUSLE have previously been assessed using sediment yield data (Borrelli et al., 2014; Sherriff et al., 2019). However, sediment yield at the outlet of a catchment reflects a complex suite of geomorphic processes. Individual models estimate erosion risk based on a specific process or processes (e.g., RUSLE-based models estimate soil loss due to inter-rill and rill erosion) whereas sediment yield will reflect all geomorphological processes active in the catchment (e.g., gullying, sediment deposition/remobilisation, tillage erosion, bank and channel erosion) (Borrelli et al., 2018a). Consequently, upslope soil erosion is not always associated with sediment yield if other processes (e.g. sediment storage) buffer the system (Boardman, 2001; Owens, 2020). Batista et al. (2019) refuted the notion that soil erosion models can be validated and instead emphasized the necessity of defining “fit-for-purpose tests” that allow for an assessment of model usefulness. There is, therefore a need to assess model usefulness using alternative approaches and one direct method of assessing sediment sources in a catchment is sediment source fingerprinting (Mukundan et al., 2012).

Fingerprinting methods using taxonomic /plant-specific tracers (*n*-alkanes) have been successfully applied to distinguish sediment sources originating from different land uses (Galoski et al., 2019; Glendell et al., 2018; Liu et al., 2021a; Zhang et al., 2017) and are an essential tool to quantify the relative contribution of different land use sources to organic matter load in waterways (Alewell et al., 2016; Chen et al., 2017; Glendell et al., 2018; Hancock and Revill, 2013; Liu et al., 2021b; Walling, Owens and Leeks, 1999). In Chapter 3, a unique combination of *n*-alkanes and short-chain neutral lipid fatty acids was used to estimate the proportion of streambed OC originating from different land uses in the catchment of Loch Davan, Aberdeenshire, NE Scotland. These OC fingerprinting (OCF) proportions could be considered as a “land use -specific” relative OC yield (Blake

et al., 2012) which could then be compared with the estimates of erosion risk models. When used as a benchmark, these OCF estimates could be an invaluable tool to assess the suitability of one erosion model over another for a given catchment. The closer the estimates of the erosion model to those of the OCF, the more confidence stakeholders could have that the processes represented by the erosion model and the areas it identifies as high risk are those that should be targeted for the implementation of BMP.

The erosion risk map developed by Lilly and Baggaley, (2018) (ERM) covers a large proportion of the Scottish mainland and shows the inherent risk of bare soil being eroded under intense or prolonged rainfall. It was hypothesised that OC erosion estimates made using the ERM, specifically developed for the wide range of mineral and organic soils and varied topography in Scotland, should be more accurate than those based on the widely used RUSLE model which was developed for use in agricultural environments with primarily mineral soils and moderate slopes (Wischmeier and Smith, 1978). To this end, in this study in the catchment of Loch Davan, land use specific OC yields from RUSLE and ERM are compared using the existing OCF as a benchmark to determine which erosion model best identifies the relative land use OC yields in streambed sediment and, therefore, the soil OC degradation hotspots to be targeted for BMP.

5.2 Material and methods

5.2.1 Study Site and existing OC fingerprinting data

Loch Davan is a shallow (mean depth 1.2 m) lake located within the Muir of Dinnet National Nature Reserve (NNR) and its catchment (*ca.* 34 km^2) has a mean annual precipitation of 780 mm and average temperature varying between 3.5°C and 12.17°C (Met Office, 2021b). The lake area of Loch Davan has been significantly reduced over the last century, likely due to inputs of nutrient rich sediment resulting from land use intensification (Addy, Ghimire and Cooksley, 2012) and between 2007 and 2018, the loch and its main feeder stream, Logie Burn, were classified as having poor to moderate ecological status (SEPA, 2021). The catchment drains a variety of land uses (moorland (29%), forest (22%), arable (10%) and pasture (31%) (Figure 24b)) and soil types (mineral podzols

(49%), brown soils (22%), alluvial soils (11%), peat or peaty gleys/podzols (5%) (Figure 24d)). Areas of steepest slope (13-37 degrees: Figure 24c) are found under moorland and forest land cover to the west and north-west of the catchment with arable and pasture land cover dominating the relatively flat (typically < 3 degree slope) lowlands.

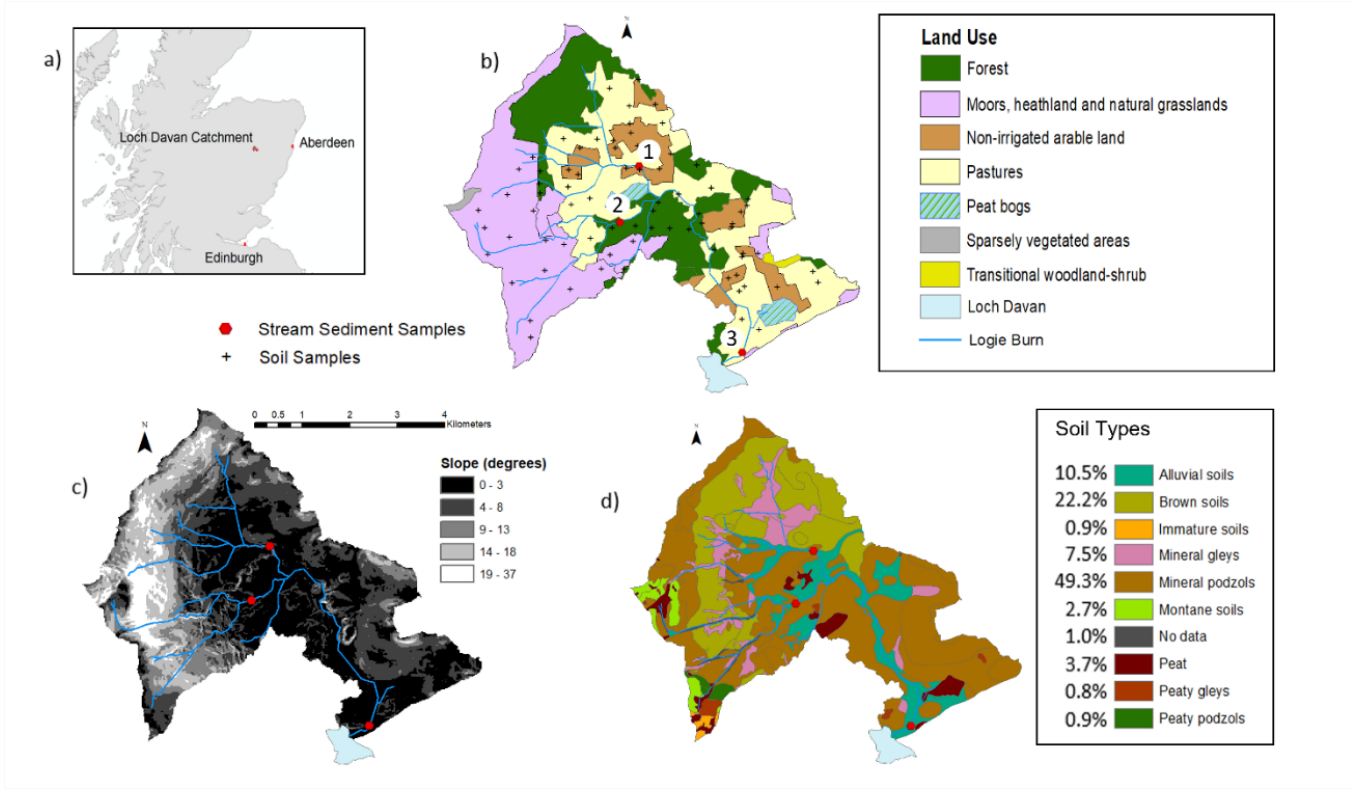

Figure 24: Loch Davan study catchment. a) Study catchment location, b) Land use of the Loch Davan catchment (34 km^2), suspended and streambed sediment sampling locations (red dots: Sites 1, 2 and 3) and terrestrial soil sampling locations (black crosses),based upon Corine land cover 2012 for the UK, Jersey and Guernsey (Cole et al., 2015), c) catchment slope (degrees) derived from OS Terrain 5 © Crown copyright and database rights 2021 Ordnance Survey (100025252)(Ordnance Survey, 2021), d) Catchment soils based on "1:25,000 Hutton Soils Data" copyright and database right The James Hutton Institute (2018). Used with the permission of The James Hutton Institute. All rights reserved.

5.2.2 Pre-existing data

The following existing data were used in this study (collection and analysis described in detail in Chapters 3 and 4 respectively):

1. Proportions of land use specific OC sources in streambed sediments at Sites 1, 2 and 3 (locations shown in Figure 24b) (to be used as OCF benchmark)
2. OC content (%OC) in soil samples (locations shown in Figure 24b)

5.2.3 Land use specific OC yield

The ERM (Lilly and Baggaley, 2018) (Figure 25) can be used to predict the relative contributions of sediment from each land use in terms of their risk of erosion, however the predictions are based on the inherent risk of bare soil and no account is taken of the different likelihood that soil will be bare due to differences in vegetation cover and land management. Therefore, for the purposes of this research the ERM was adapted to include the same "land use and management factor" as used within RUSLE to estimate the amount of bare soil coverage.

RUSLE utilises a dimensionless cover-management factor (C), defined by the land use and management, when calculating the long-term average annual soil loss according to the equation:

$$SL = R.K.L.S.C.P \quad \textbf{(5-1)}$$

where SL is the mean soil loss (t ha^{-1} yr^{-1}), R is the rainfall intensity factor (MJ mm ha^{-1} h^{-1} yr^{-1}), K is the soil erodibility factor (t ha h ha^{-1} MJ^{-1} mm^{-1}), S and L are the slope and slope-length factors, P is the dimensionless conservation support practice factor. A C factor map with a single C factor for each land use was created from the Corine land cover 2012 for the UK, Jersey and Guernsey (Cole et al., 2015) and the C-factor data of Europe described by (ESDAC, 2015a; Panagos et al., 2015b) in ESRI ArcMap (V10.6) (ESRI, 2017). This was done by assigning the values given in the table of C-factor per land-cover type and country (Table 19) to the respective land use areas in the Corine land cover map. The

likely variation in these land use values (Table 19: “Range”) were based on the most cited studies covering different countries in Europe reported by Panagos et al. (2015b). The remaining RUSLE factors were calculated as follows: The RUSLE R and K factors were derived respectively from maps generated and described by (ESDAC, 2015b; Panagos et al., 2015a) and (ESDAC, 2014; Panagos et al., 2014). The R and K factor maps were generated in ESRI ArcMap (V10.6) (ESRI, 2017) by interpolating a raster surface using kriging from points defined by the centroid of each cell of the original 500x500m resolution R and K maps. The conservation support practice factor (P) was not considered in this study and was set to 1. The RUSLE LS factors were generated from the DEM in R (version 3.6.3) (R Core Team, 2020) using packages “raster” (Hijmans, 2020) and “RSAGA” (Brenning, Becker and Bangs, 2018) using the method described by Desmet and Govers, (1996). The RUSLE factor maps were combined to produce RUSLE soil loss estimates within R.

Table 19: Range and mean of RUSLE C-factors used for calculation of average annual soil loss within the Loch Davan catchment (adapted from Panagos et al. (2015b: Table 2))

	C-factor	
Land Use	Range	Mean
Arable	0.07-0.35	0.21
Pasture	0.05-0.15	0.1
Forest	0.0001-0.003	0.0016
Moorland	0.01-0.1	0.055

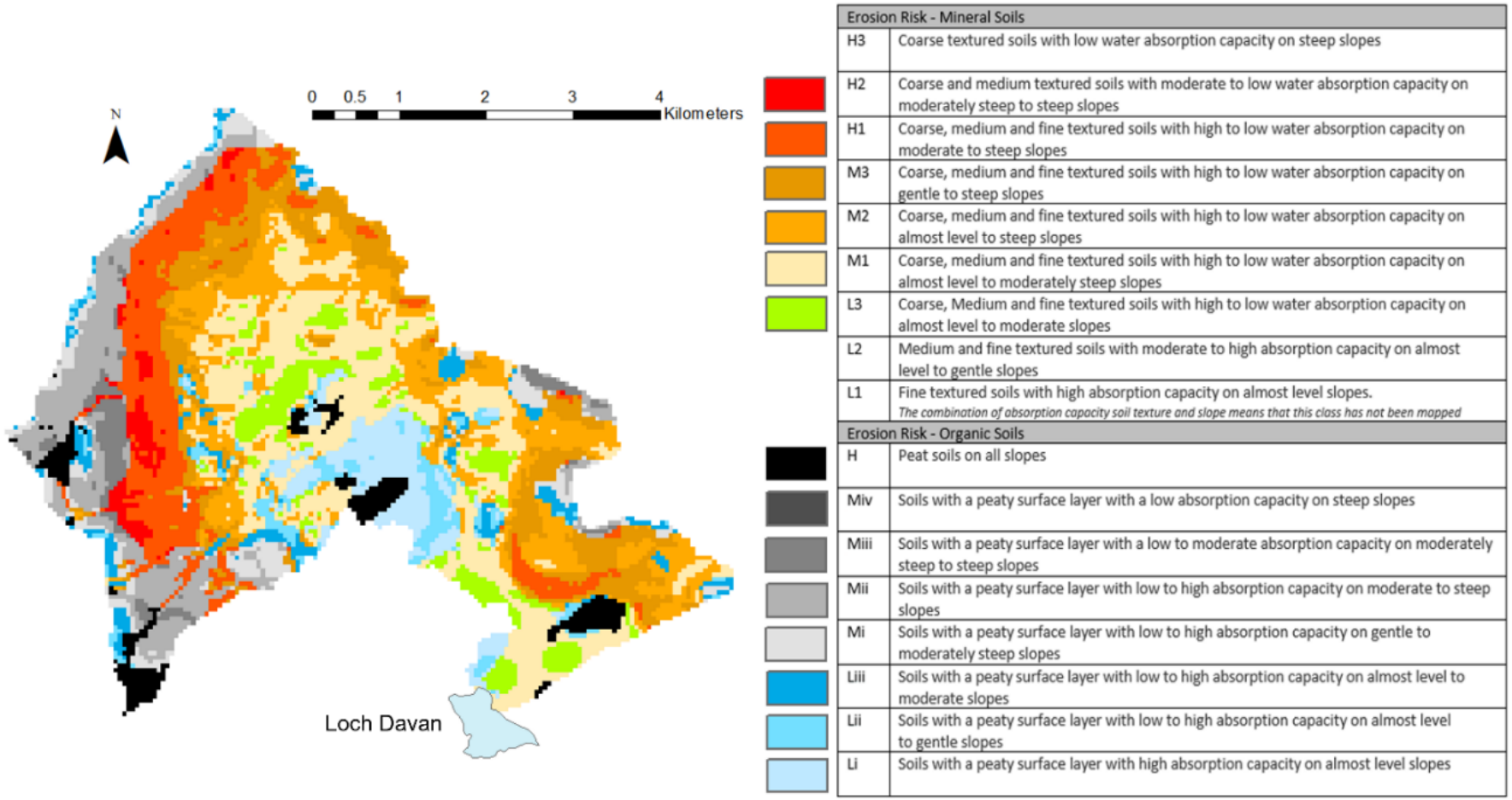

Erosion Risk - Mineral Soils	
H3	Coarse textured soils with low water absorption capacity on steep slopes
H2	Coarse and medium textured soils with moderate to low water absorption capacity on moderately steep to steep slopes
H1	Coarse, medium and fine textured soils with high to low water absorption capacity on moderate to steep slopes
M3	Coarse, medium and fine textured soils with high to low water absorption capacity on gentle to steep slopes
M2	Coarse, medium and fine textured soils with high to low water absorption capacity on almost level to steep slopes
M1	Coarse, medium and fine textured soils with high to low water absorption capacity on almost level to moderately steep slopes
L3	Coarse, Medium and fine textured soils with high to low water absorption capacity on almost level to moderate slopes
L2	Medium and fine textured soils with moderate to high absorption capacity on almost level to gentle slopes
L1	Fine textured soils with high absorption capacity on almost level slopes. *The combination of absorption capacity soil texture and slope means that this class has not been mapped*
Erosion Risk - Organic Soils	
H	Peat soils on all slopes
Miv	Soils with a peaty surface layer with a low absorption capacity on steep slopes
Miii	Soils with a peaty surface layer with a low to moderate absorption capacity on moderately steep to steep slopes
Mii	Soils with a peaty surface layer with low to high absorption capacity on moderate to steep slopes
Mi	Soils with a peaty surface layer with low to high absorption capacity on gentle to moderately steep slopes
Liii	Soils with a peaty surface layer with low to high absorption capacity on almost level to moderate slopes
Lii	Soils with a peaty surface layer with low to high absorption capacity on almost level to gentle slopes
Li	Soils with a peaty surface layer with high absorption capacity on almost level slopes

Figure 25: Erosion Risk Map of Loch Davan catchment adapted from Lilly, A. and Baggaley N.J. 2018. Soil erosion risk map of Scotland (partial cover). James Hutton Institute, Aberdeen.

Both RUSLE and ERM model on site soil erosion risk, not OC sediment yield (Alewell et al., 2019; Lilly and Baggaley, 2018; Wischmeier and Smith, 1978). Therefore, for comparison with the estimates of OCF these models were combined with i) an estimate of potential connectivity between areas of upslope erosion and streams and ii) the percentage of OC in soils.

5.2.3.1 Estimating connectivity between areas of upslope erosion and streams

To define the connectivity between upslope sediment sources and streams CI was calculated using ESRI ArcMap (V10.6) (ESRI, 2017) using the method of Cavalli et al. (2013) and the catchment DEM. This approach was selected as it requires a small number of parameters, uses widely available data, and is spatially explicit. For use as a weighting with RUSLE, CI was re-scaled from 0 to 1. The CI was classified into “high”, “medium” and “low” connectivity (Hooke, Souza and Marchamalo, 2021) using a quantile classification in ESRI ArcMap (V10.6).

5.2.3.2 Soil OC content (%)

The OC% of each soil sample was interpolated using universal kriging (sometimes called external drift kriging) implemented in R (version 3.6.3) (R Core Team, 2020) using packages “raster” (Hijmans, 2020), “sp” (Pebesma and Bivand, 2005) and “gstat” (Pebesma, 2004). Seven land-use and topographic environmental predictors were considered as covariates: land-use (pasture, woodland, arable and moorland), slope, curvature, accumulated flow, aspect, topographic wetness index (TWI) (Mayer et al., 2019) and soil type. Climate data were not considered as predictors as they were not expected to vary significantly across the catchment. The OC (%) values and covariates were first checked for normality using the Kolmogorov–Smirnov (K–S) test. OC (%) was then log-transformed to improve normal distribution for regression modelling. A back-transformation of OC (%) was carried out following prediction. The best model was assessed on the basis of the smallest Akaike Information Criterion (AIC) and highest adjusted R^2 (Meersmans et al., 2012). Covariates that were significantly ($p < 0.05$) associated with OC (%) were retained and the best model was selected

in a forward stepwise regression. A leave-one-out cross-validation routine was implemented, and the root mean square error (RMSE) and R^2 of the model performance calculated using the differences between the N “observed” values and model predictions.

5.2.3.3 Carbon Loss Models (CLM)

Four CLM were constructed in this study which will be referred to as RUSLE, RUSLE_ADJ, ERM_A, ERM_B and ERM_C and are described below (Figure 26).

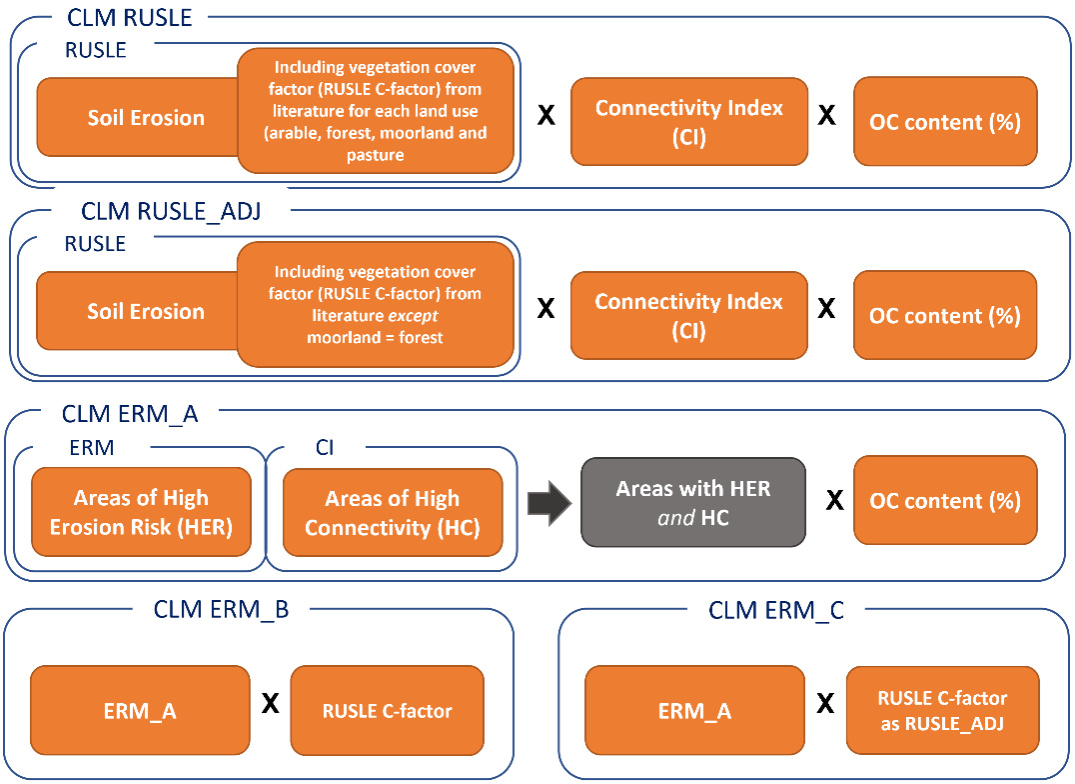

Figure 26: Structure of Carbon Loss Models (CLM) "RUSLE", RUSLE_ADJ”, "ERM_A", "ERM_B" and "ERM_C"

5.2.3.3.1 RUSLE

A CLM was constructed as follows:

$$CLM\ RUSLE = SOC\% \times SL \times CI \quad \textbf{(5-2)}$$

where SOC% is a map of the soil organic carbon content (%), SL is a soil loss map constructed using RUSLE and CI (re-scaled from 0 to 1) is a map of connectivity index as defined by Borselli et al., (2008) and Cavalli et al., (2013).

The value of C-factor within RUSLE model can be used to account for the differences in erosion potential between land uses and it was important to evaluate the magnitude of the errors associated with this factor as well as that introduced by the modelling of SOC content (%SOC) using a Monte Carlo analysis with 3,000 iterations. The RUSLE C factor was sampled from a uniform distribution defined by the minimum and maximum values found in the literature (Table 19) and %SOC content was sampled from a uniform distribution defined by +/-1 RMSE from the leave-one-out cross-validation of the %SOC content map. At each iteration the proportions of SOC loss from arable, forest, moorland and pasture land uses were calculated, generating a probability distribution from which the mean land use proportions were derived.

5.2.3.3.2 RUSLE_ADJ

The RUSLE C-factor (Table 19) used to account for vegetative cover and land management/grazing was around 35 times greater for moorland land use than it was for forest; implying less soil cover and/or greater erosional impact from land management/grazing for the moorland compared to forest land. In another mixed land use sub-catchment Hirave et al., (2020a) found that both forest and moorland contributed marginally to suspended stream sediments (<2%) which they attributed to well vegetated ground cover resulting in reduced soil erodibility. In addition, in their study to identify soil erosion rates in Scotland, Rickson et al., (2019) defined erosion rates for forest/woodland to be equal to those of wildscape (semi-natural landscape). It was hypothesised that the level of soil cover and impact of land management/grazing in moorland could be like that in forest land, and therefore, for this CLM (RUSLE_ADJ), the C-factor for moorland was set equal to that for forest.

5.2.3.3.3 ERM_A

Areas with both high erosion risk (HER) and high connectivity (HC) to the streams were identified in ESRI ArcMap (V10.6) (ESRI, 2017) by the overlap of areas designated “high” risk in the ERM (Lilly and Baggaley, 2018) and areas classified as “high” connectivity in the CI map. The proportion of these areas within each of the four land uses (arable, forest, moorland and pasture) was then calculated. In

a Monte Carlo analysis with 3,000 iterations the land use proportions were multiplied by soil %OC content sampled from a uniform distribution defined by the mean soil %OC for each land use +/-1 SD generating a probability distribution from which the mean land use proportions were derived.

5.2.3.3.4 ERM_B

The ERM predictions are based on the inherent soil erosion risk from bare soil and the land use proportions of soil OC input to the stream estimated by ERM_A do not take into account the vegetation cover and the likelihood that soil will be left bare. Hence, in ERM_B the proportions of soil OC input to the stream estimated by ERM_A were multiplied by the RUSLE C-factor (Figure 26, Table 19) to account for the likelihood that soil will be left bare due to differences in vegetation cover and land management practices.

5.2.3.3.5 ERM_C

Similar to CLM RUSLE_ADJ, for this CLM (ERM_C), the land use proportions of soil OC input to the stream found using ERM_A were multiplied by the RUSLE C-factor with the factor for moorland set equal to that for forest.

5.2.3.3.6 Comparing medium and high erosion risk levels

The three CLM, ERM_A, ERM_B and ERM_C, described above were applied to areas with high erosion risk and high connectivity to the streams. In addition, to assess if the SOC land use proportion defined by the OCF benchmark would be more closely matched by erosion rates from areas defined as “high” or “medium”, a second set of CLM was constructed. In the second set of CLM, areas were identified in ESRI ArcMap (V10.6) (ESRI, 2017) by the overlap of areas designated “high” and “medium” risk in the ERM, and areas classified as “high” connectivity in the CI map. The proportion of these areas within each of the four land uses (arable, forest, moorland and pasture) were then calculated and the three CLM, ERM_A, ERM_B and ERM_C, were constructed as described above.

5.2.4 Comparison CLM and OC fingerprinting land use specific OC yield

The land use specific OC yields of each CLM were compared using the existing OCF as a benchmark to determine which model best identified the relative OC yield in streambed sediments.

For each CLM the proportions of soil OC yield (loss) from arable, forest, moorland and pasture land uses were calculated. The absolute difference between these land use proportions and those estimated using OCF were then calculated.

The model that best identified the relative OC yield in streambed sediments was determined by finding the CLM that showed the lowest mean absolute difference for all land uses.

5.3 Results

5.3.1 Soil OC distribution

Interpolation of OC% using regression kriging found land use to be the best predictor of the quantity and spatial variability of soil OC% (R^2=0.46, RMSE=7.86: Table 20). The relationships between soil OC% and other covariates were much weaker (slope (R^2=0.19), aspect (R^2=0.1) and TWI (R^2=0.09)) and these covariates were not significant when modelled together with land use. No significant relationships with soil OC% were found for the other covariates (soil type, curvature and accumulated flow). These results support the assertion of Wiesmeier et al., (2019) that terrain attributes such as slope, aspect and curvature, although influential for soil OC content at small spatial scales (<100 m), are less relevant across larger landscapes, where soil OC is averaged across soil properties so that other factors (such as land use) become dominant.

Soils under moorland supported the largest soil OC% (21.4±13.9% (± 1 SD)) and %OC of forest soil was also relatively high (12.3±8.0). The similarity of the OC% of pasture (3.7±0.9) and arable soils (3.8±1.1) suggests that these land uses have similar levels of OC inputs and outputs and that pastures in this catchment may be temporary (in agricultural rotation) rather than permanent pastures (Martin et al., 2011; Meersmans et al., 2008).

Table 20: In the context of the linear regression relationship, the variables "forest", "moorland" and "pasture" are dummy variables which are equal to one when that land use is present and zero otherwise.

Regression relationship	RMSE	R^2	Mean total OC (%)
OC% = exp(1.3010 + 1.0513 (forest) + 1.5317 (moorland) – 0.0451 (pasture))	7.86	0.46	10.04

5.3.2 Comparison of land use specific OC yield using CLM and OCF

Land use specific OC yields from the eight CLM (RUSLE, RUSLE_ADJ and three ERM (ERM_A, ERM_B and ERM_C at two different erosion risk levels; Section 5.2.3.3) were compared using OCF as a benchmark to determine which model most closely approximated the relative OC yield in streambed sediments.

In this study catchment both RUSLE and the ERM identified areas at highest risk of erosion on steeply sloping (>8 degrees: Figure 24c) land in the north and west of the catchment (ERM_A Figure 27d; Figure 28d; Figure 29d) dominated by moorland. It was therefore unsurprising that most of CLM constructed using these models attributed the majority of eroded soil OC reaching the streams to moorland (48-96% Figure 27c-e; 68-100% Figure 28c-e; 34-93% Figure 29c-e), which contrasts with the OCF benchmark that estimated pasture as the dominant source of OC (68-80%) and a contribution of only 3-6% from moorland soils to streambed OC at all sites (Figure 27a; Figure 28a; Figure 29a).

5.3.2.1 CLM RUSLE and RUSLE_ADJ

At all sites CLM RUSLE attributed the majority of stream OC to moorland (85-98%) with correspondingly small amounts from other land uses (arable (4-5%), pasture (2-8%) and forest (1-8%)) (Figure 27b; Figure 28b; Figure 29b). At Site 2 CLM RUSLE_ADJ attributed the majority of stream OC to moorland (76%) with the remaining 24% attributed to pasture. At Sites 1 and 3 CLM RUSLE_ADJ attributed stream OC much more equally between moorland (36%), arable (24-26%) and pasture (33-34%) with only small amounts from forest land (4-8%).

CLM RUSLE_ADJ provided a closer match to the OCF benchmark than CLM RUSLE (mean absolute difference to OCF benchmark Site 1=20 cf. 42, Site 2=35cf. 46 and Site 3=20 cf. 41; Figure 30).

5.3.2.2 CLM ERM_A

For CLM ERM_A no account was taken of the likelihood that soil would be bare (exposed to erosion) due to differences in vegetation cover and land management (i.e. no C-factor; Section 5.2.3.3). Using only areas at “high” erosion risk (Figure 27d; Figure 28d; Figure 29d) CLM ERM_A attributed the majority of stream OC to moorland (Site 1=56%, Site 2=100%, Site 3=73%) with the remainder attributed to forest. Using areas at “high and medium” erosion risk (Figure 27e; Figure 28e; Figure 29e) CLM ERM_A again attributed the majority of stream OC to moorland (Site 1=61%, Site 2=99%, Site 3=72%) with very small amounts attributed to arable (1-2%) and pasture (1-6%) and the remainder attributed to forest. Neither of these CLM provided a close approximation to the OCF benchmark, with mean absolute differences to OCF benchmark of Site 1=42, Site 2=47 and Site 3=44 for “high risk” and Site 1=40, Site 2=47 and Site 3=36 for “high and medium risk”.

5.3.2.3 CLM ERM_B

For CLM ERM_B the likelihood that soil would be bare (exposed to erosion) due to differences in vegetation cover and land management was characterised using the RUSLE C-factor (Section 5.2.3.3). Using only areas at “high” erosion risk (Figure 27d; Figure 28d; Figure 29d) CLM ERM_B attributed the majority of stream OC to moorland (Site 1=96%, Site 2=100%, Site 3=93%) with very small amounts attributed to arable (3%), pasture (1-3%) and forest (1-3%). Using areas at “high and medium” erosion risk (Figure 27e; Figure 28e; Figure 29e) CLM ERM_B again attributed the majority of stream OC to moorland (Site 1=83%, Site 2=99%, Site 3=77%) with very small amounts attributed to arable (5-9%) and pasture (1-6%) and forest (1-2%). Neither of these CLM provided a close approximation to the OCF benchmark with mean absolute differences to OCF benchmark of Site 1=46, Site 2=47 and Site 3=45 for “high risk” and Site 1=40, Site 2=47 and Site 3=36 for “high and medium risk”.

5.3.2.4 CLM ERM_C

For CLM ERM_C the likelihood that soil would be bare (exposed to erosion) due to differences in vegetation cover and land management was characterised using the RUSLE_ADJ C-factor (moorland = forest; Section 5.2.3.3). Using only areas at “high” erosion risk (Figure 27d; Figure 28d; Figure 29d) CLM ERM_C still attributed the majority of stream OC to moorland (Site 1=48%, Site 2=100%, Site 3=34%) but with larger amounts attributed to arable (2-25%), pasture (12-29%) and forest (13-39%) at Sites 1 and 3. Using areas at “high and medium” erosion risk (Figure 27e; Figure 28e; Figure 29e) CLM ERM_C attributed the majority of stream OC to moorland only at Site 2 (68%). At Site 1 and Site 3 pasture was the dominant source (52% at each site) with lesser amounts attributed to arable (24% and 34% respectively), moorland (16% and 11% respectively) and forest (9% and 3% respectively). These CLM provided a closer approximation to the OCF benchmark than either ERM_A or ERM_B, with mean absolute differences to OCF benchmark at Site 1=35, Site 2=27 and Site 3=21 for “high risk” and Site 1=10, Site 2=31 and Site 3=12 for “high and medium risk”.

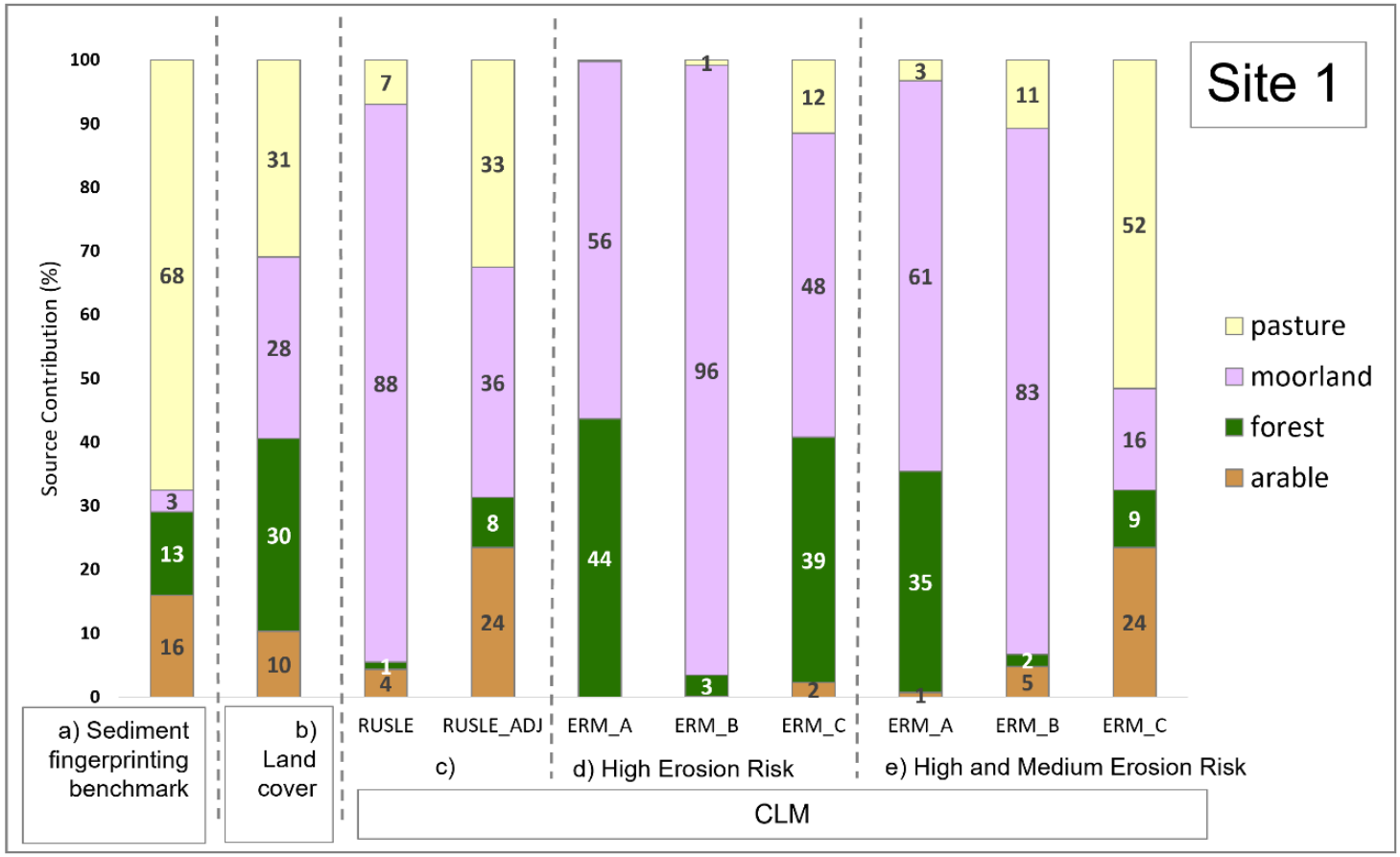

Figure 27: Source Contribution (%) at Site 1 streambed sediments estimated by a) Sediment fingerprinting, b) Land Cover and c) CLM RUSLE and CLM_RUSLE_ADJ, d) CLM ERM_A, ERM_B and ERM_C erosion risk level "High" and e) CLM ERM_A, ERM_B and ERM_C erosion risk level "High or Medium"

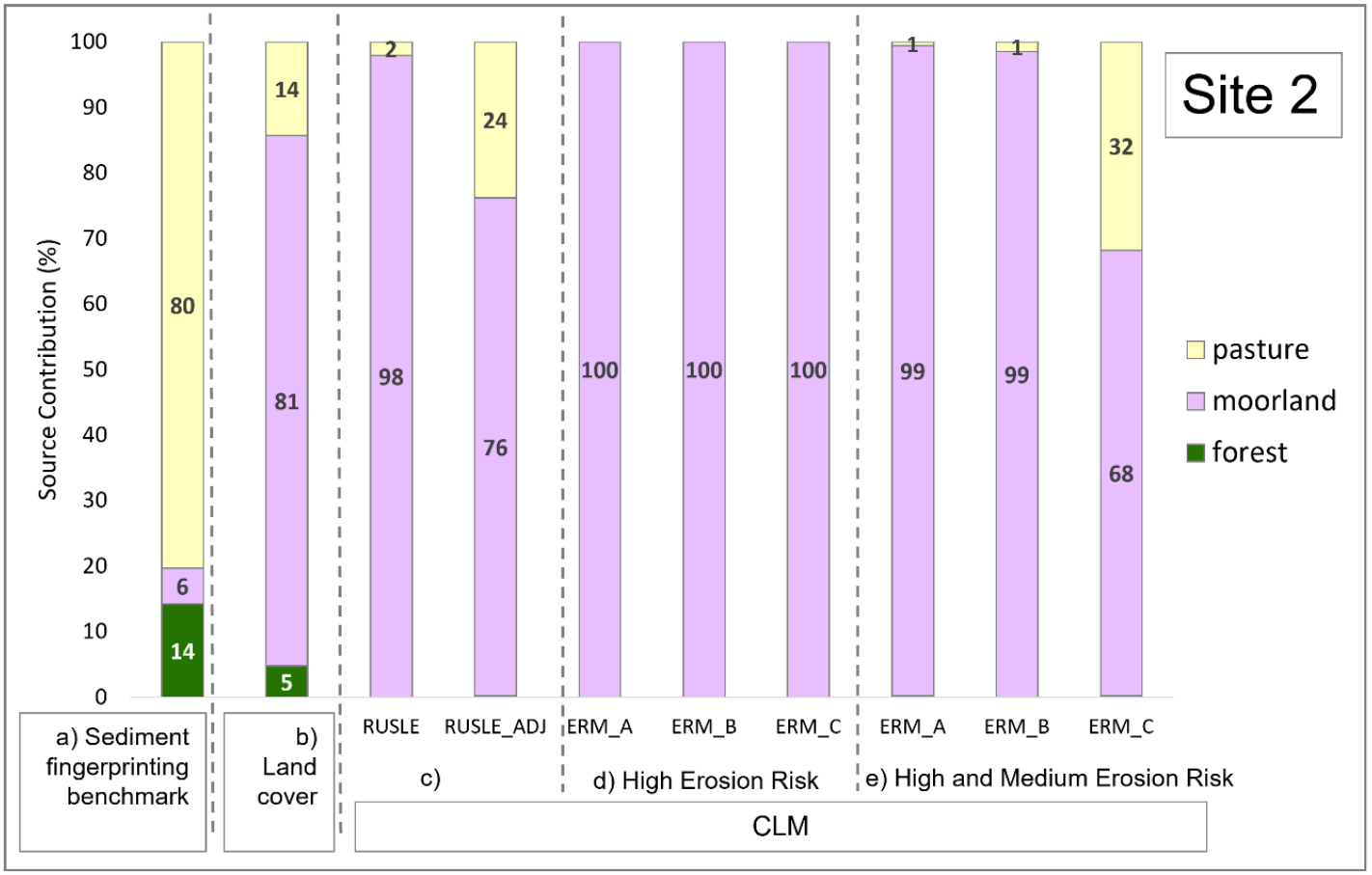

Figure 28: Source Contribution (%) at Site 2 streambed sediments estimated by a) Sediment fingerprinting, b) Land Cover and c) CLM RUSLE and CLM_RUSLE_ADJ, d) CLM ERM_A, ERM_B and ERM_C erosion risk level "High" and e) CLM ERM_A, ERM_B and ERM_C erosion risk level "High or Medium"

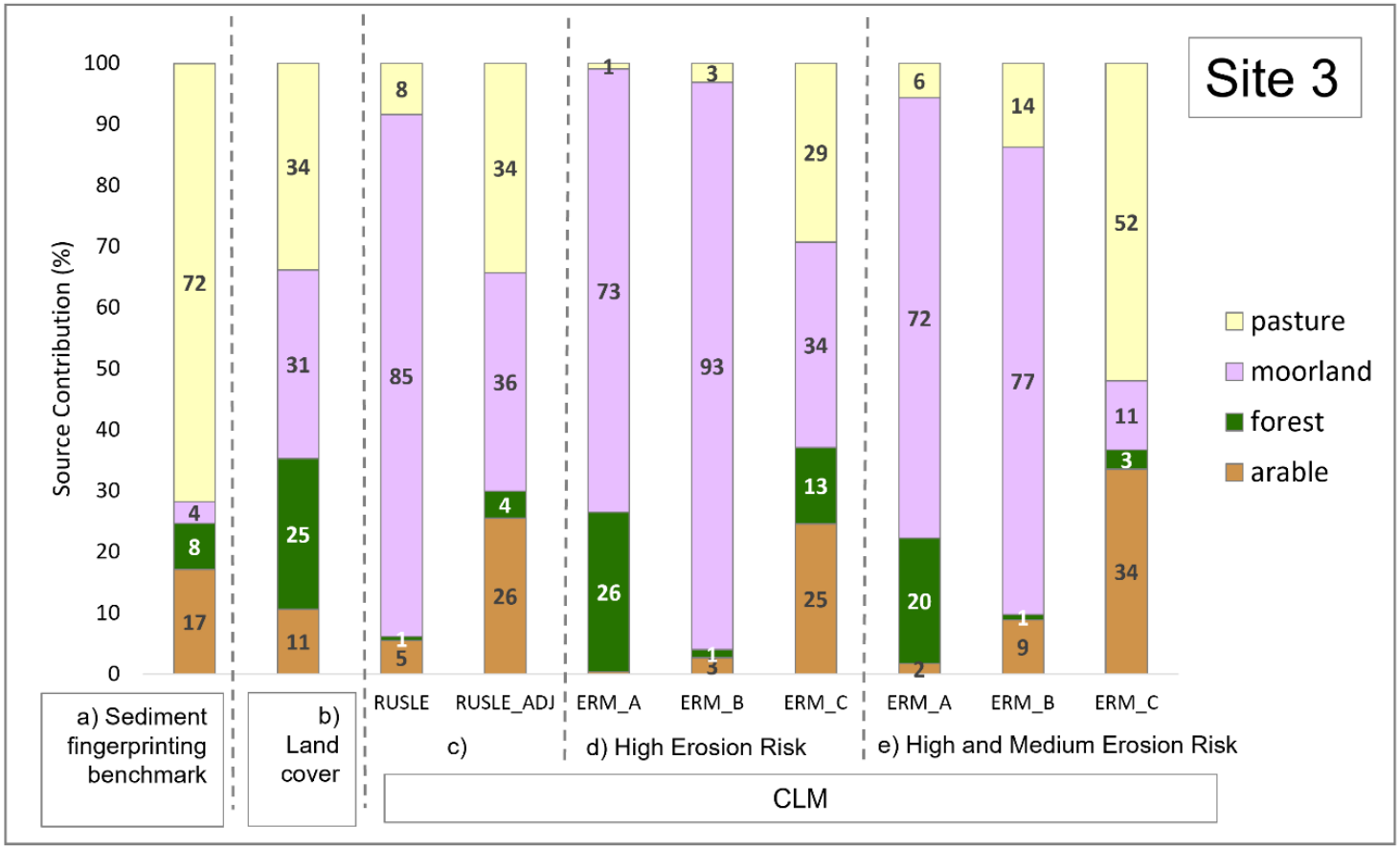

Figure 29: Source Contribution (%) at Site 3 streambed sediments estimated by a) Sediment fingerprinting, b) Land Cover and c) CLM RUSLE and CLM_RUSLE_ADJ, d) CLM ERM_A, ERM_B and ERM_C erosion risk level "High" and e) CLM ERM_A, ERM_B and ERM_C erosion risk level "High or Medium"

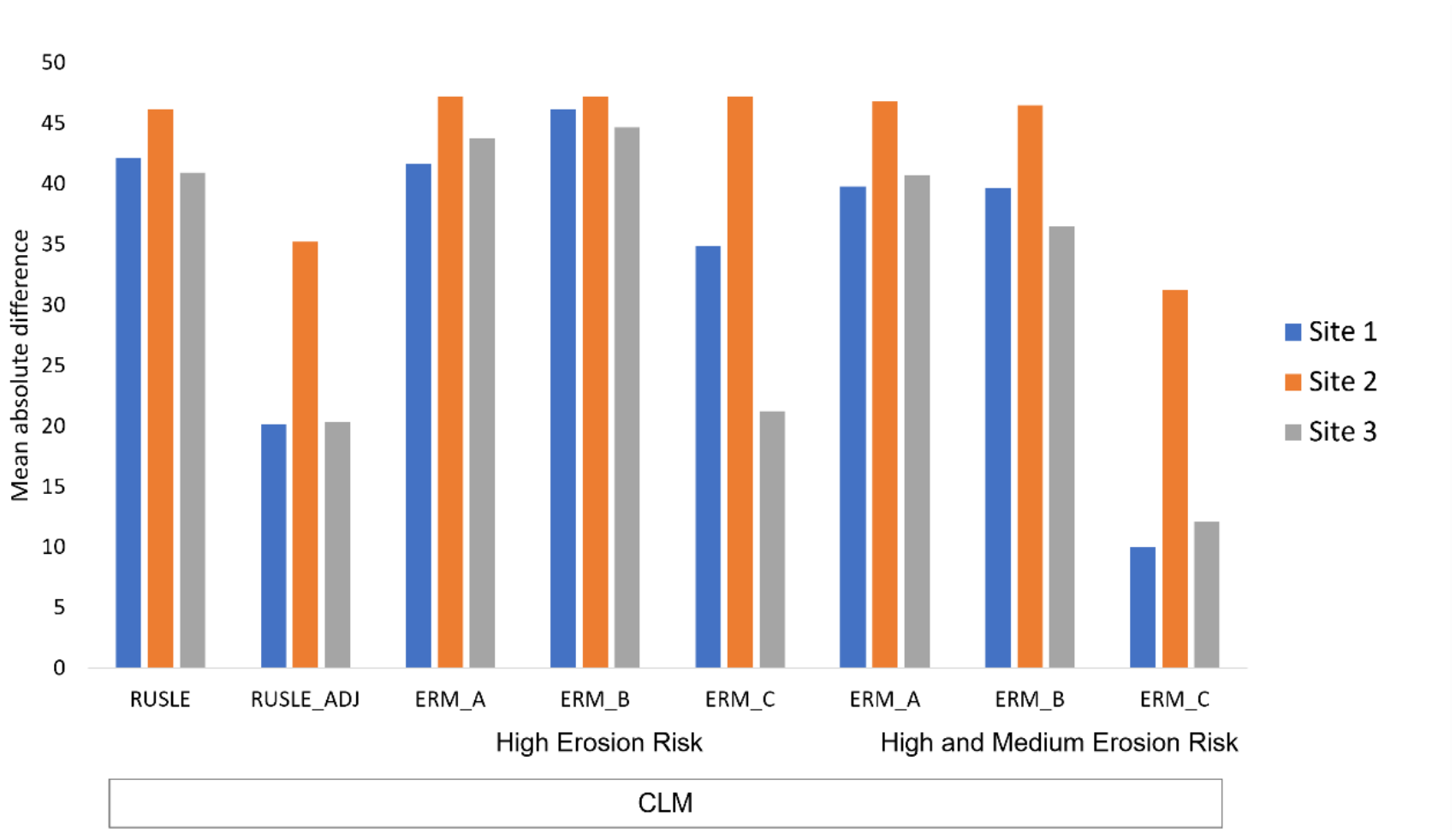

Figure 30: Mean absolute difference between OC land use source proportions estimated by CLM and OCF for streambed sediment sites 1, 2 and 3

5.3.2.5 Comparison between CLM RUSLE and CLM ERM

CLM ERM_C (high and medium risk) showed the lowest mean absolute difference to OCF benchmark for all land uses. This CLM was therefore selected to characterise the areas of Loch Davan catchment most likely to contribute OC to the feeder streams (Figure 31).

Using CLM with the RUSLE C-factor for moorland equal to that for forest (CLM RUSLE_ADJ and CLM_ERM_C) lowered the mean absolute difference between CLM and the OCF benchmark (e.g. Site 1 RUSLE=42, RUSLE_ADJ=20 and ERM_B=40, ERM_C=10 (high and medium erosion risk)). These results suggest that, as hypothesised, erosion from forest and moorland were more similar than the order of magnitude difference in C-factor reported by Panagos et al., (2015b) would suggest. This is likely due to the mostly mature heather, moorland vegetation providing cover similar to a woodland under-storey. CLM ERM_B land use source proportions were similar to those of CLM RUSLE (mean absolute difference <5 for all sites; Figure 32) and CLM ERM_C land use source proportions were similar to those of CLM RUSLE_ADJ (mean absolute difference 10, 4 and 13 for Sites 1, 2 and 3 respectively; Figure 32). Therefore, although it was not originally formulated for use on steep slopes and more organic soils such as those found in this Scottish catchment CLM RUSLE performed almost as well as the CLM ERM in this study once the C-factor had been calibrated using the OCF benchmark. Using RUSLE_ADJ mean soil erosion was estimated to be 0.83 t ha^{-1} yr^{-1} for arable land, 0.63 t ha^{-1} yr^{-1} for pasture land, 0.02 t ha^{-1} yr^{-1} for forest land and 0.04 t ha^{-1} yr^{-1} moorland. Areas identified as “high” risk and “medium” risk by the ERM had mean soil erosion estimates of 1.51 and 0.88 t ha^{-1} yr^{-1} respectively for arable land, 1.26 and 0.64 t ha^{-1} yr^{-1} respectively for pasture land, 0.04 and 0.03 t ha^{-1} yr^{-1} respectively for forest land and 0.04 and 0.04 t ha^{-1} yr^{-1} respectively for moorland (Table 21).The areas defined as high risk by the ERM showed a higher mean erosion rate than those defined as medium risk, except moorland which had the same erosion rate in both areas.

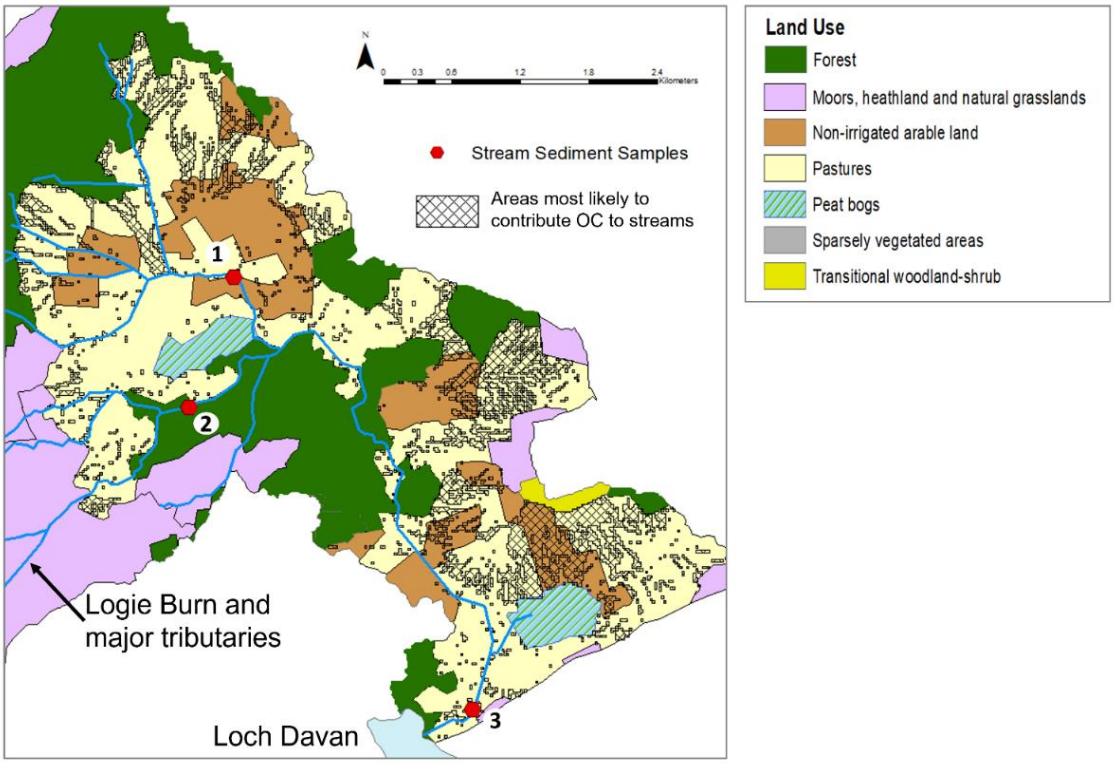

Figure 31: Areas most likely to provide OC to the Logie Burn and its major tributaries. These are areas with "High or Medium" erosion risk (Lilly and Baggaley, 2018) and high connectivity to the streams within arable or pasture land.

Table 21 Estimated rates of soil erosion (t ha^{-1} yr^{-1}) using RUSLE_ADJ for the whole Loch Davan catchment, and areas defined as "High" and "Medium" risk by ERM

	Mean soil erosion in t ha^{-1} yr^{-1}		
	Whole catchment	Areas defined as "High" risk by ERM	Areas defined as "Medium" risk by ERM
Arable	0.83	1.51	0.88
Pasture	0.63	1.26	0.64
Forest	0.02	0.04	0.03
Moorland	0.04	0.04	0.04

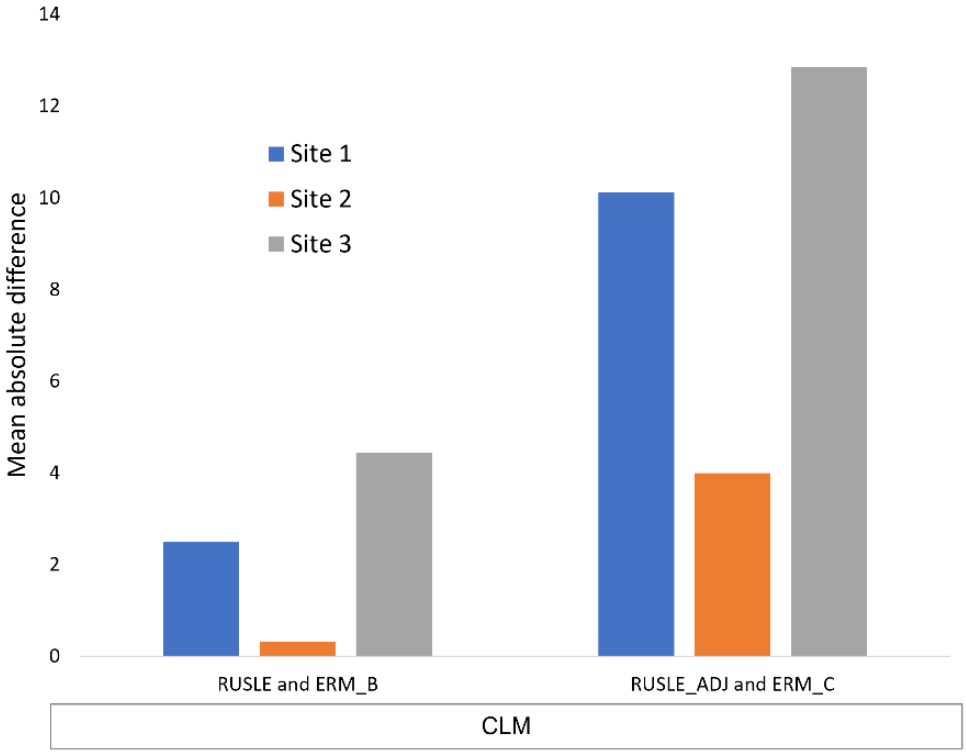

Figure 32 Mean absolute difference between OC land use source proportions estimated by CLM RUSLE and CLM ERM_B, and CLM RUSLE_ADJ and CLM ERM_C for streambed sediment sites 1, 2 and 3

5.4 Discussion

The addition of the land use and management factor (RUSLE C-factor) substantially increased the estimated contribution from moorland from 56% to 96% (Figure 27e ERM_A compared to ERM_B) and 61% to 85% (Figure 27f ERM_A compared to ERM_B) at Site 1, and 73% to 93% (Figure 28e ERM_A compared to ERM_B) and 61% to 85% (Figure 28f ERM_A compared to ERM_B) at Site 3 due to the following reasons. Firstly, although the C-factor for arable land is much higher than those for either moorland or forest due to the increased likelihood that arable land will have bare soil during tillage, crop planting and crop establishment, the amount of arable land at high soil erosion risk was so small that the C-factor made little difference to the estimated OC source proportions from arable land. Secondly, the C-factor for moorland sourced from the literature (mean 0.055: Table 19) was an order of magnitude larger than that for forest

(mean 0.0016: Table 19), greatly reducing the estimated contribution from forest land and commensurately increasing that from moorland. This large difference in C-factor between forest and moorland is also evident in the negligible amount of erosion predicted from forest land (1%) and the 88% contribution from moorland estimated by CLM RUSLE (Figure 27d). Panagos et al., (2015b), from whose European scale study the C-factors were sourced, describe moorland as "vegetation with low and closed cover, dominated by bushes, shrubs and herbaceous plants". Although a similar low and closed cover was found on the moorland for this catchment, it was hypothesised that the level of soil cover and impact of land management/grazing for the moorland should be similar to that for forest land and not have *ca.*35 times greater likelihood of erosion as is suggested by the relative sizes of the C-factors presented by Panagos et al., (2015b).

The results of this study showed that RUSLE performed almost as well as the ERM in comparison to the OCF benchmark. When tracing pathways of diffuse pollution from agriculture to the waterways there remains uncertainty in erosion rates for soil and land use combinations (Cloy et al., 2021). Erosion risk maps such as the ERM can identify areas where a high risk of soil degradation could increase the risk of diffuse water pollution (Baggaley et al., 2020), however they do not provide quantitative estimates of soil or OC erosion rates. The results of this study suggest that, for this catchment, RUSLE erosion rate estimates (t ha^{-1} yr^{-1}) could be used to quantify the amount of soil eroded from the high and medium risk areas defined by the ERM. The estimates of RUSLE_ADJ soil erosion for this catchment are less than the soil erosion rates per land use defined by Rickson et al., (2019) in their study to identify soil erosion rates in Scotland (mineral soils: arable 2.4 to 4.3 t ha^{-1} yr^{-1}, grasslands 2.4 to 4.3 t ha^{-1} yr^{-1}, forest 0.6 t ha^{-1} yr^{-1} and wildscape (semi-natural landscape) 0.6 t ha^{-1} yr^{-1}; organic soils: arable 5 to 10 t ha^{-1} yr^{-1}, grasslands 0.39 to 1 t ha^{-1} yr^{-1}, forest 0.13 t ha^{-1} yr^{-1} and wildscape 0.13 t ha^{-1} yr^{-1}). As the estimates of Rickson et al., (2019) were based on empirical observations and a literature review it is possible that those estimates came from more dramatic erosion events than those occurring in this catchment.

CLM ERM_C (high and medium erosion risk) showed the lowest mean absolute difference with the OCF benchmark for all land uses and was selected to characterise the areas of Loch Davan catchment most likely to contribute OC to the feeder streams. However, at Site 2 there was still a large discrepancy between the contribution from pasture and moorland estimated by the OCF (80% and 6% respectively) and that attributed by the CLM ERM_C (32% and 68% respectively). This is due in part to the negligible contribution predicted from forest from all CLMs in this sub-catchment, compared to the 14% attributed to forest by OCF. Unlike, Sites 1 and 3, Site 2 is located in an area of forest. Considering the low likelihood of soil erosion predicted by all the erosion risk models in this study it is possible that more direct input of forest leaves and litter contributed the majority of the forest OC to the stream at Site 2 rather than upslope eroded forest soil OC (Chapter 2). In addition, in chapter 4 it was found that poaching by cattle of the near-stream channel areas (especially during the winter months) could have contributed to sediment mobilization from pasture lands in this catchment. This more direct soil erosion source would not be present in the estimates of any of the CLM and may account for the larger proportion of pasture OC predicted by the OCF in contrast to the CLM at all sites.

The amount of eroded soil OC cannot be reliably equated with stream OC unless sites of intermediate storage or “buffers” are also considered and estimates of other OC sources e.g., more direct input of organic matter (litter/leaves/near-channel poaching by livestock) can be made (Chapter 2). Although it is virtually impossible to imagine a river catchment where upslope eroded soil OC is the only contributor to stream sediment OC, the better the OC sources can be defined when carrying out OCF the more valuable it becomes as a tool to validate the output of erosion risk models. In this study, the method identified that the RUSLE C-factor for moorland should be set similar to that for forest rather than the value quoted in the literature (Panagos et al., 2015b). In future studies, estimates of the C-factor for all land uses could also be adjusted within the Monte Carlo analysis to calibrate the model and obtain land use source proportions more closely approximating to those found by the OCF benchmark, ultimately resulting in more accurate erosion rate estimates. It is possible that a carbon loss model calibrated

in this way could then be applied with better confidence in similar catchments in the same geographical area where OCF has not been done, aiding catchment managers to map areas of high erosion risk and quantify OC losses.

5.5 Conclusions

In this study, it was hypothesised that OC erosion estimates made using the ERM, specifically developed for the wide range of mineral and organic soils and varied topography in Scotland, should be more accurate than those based on the RUSLE model which was developed for use in agricultural environments with primarily mineral soils and moderate slopes. To this end, land use specific OC yields from CLM constructed using RUSLE and ERM were compared using the existing OCF as a benchmark to determine which erosion model most closely approximated the relative land use OC yields in streambed sediment and, therefore, the soil OC degradation hotspots to be targeted for BMP. Although, the ERM most closely approximated the relative land use OC yields in streambed sediment based on mean absolute differences to the OCF benchmark, the results of RUSLE were very similar, suggesting that, in this catchment, RUSLE erosion rate estimates could be used to quantify the amount of soil eroded from the high-risk areas identified by the ERM. In addition, the method identified that the RUSLE C-factor for moorland should be set similar to that for forest rather than the value quoted in the literature (Panagos et al., 2015b) suggesting that in future studies, all land use C-factors could be adjusted similarly to get land use source proportions closer to those of the OCF benchmark and ultimately result in more accurate RUSLE erosion rate estimates.

5.6 References

Addy, S., Ghimire, S. and Cooksley, S. (2012) ‘Assessment of the multiple benefits of river restoration: the Logie Burn meander reconnection project’, BHS Eleventh National Symposium, Hydrology for a changing world, Dundee 2012, , pp. 01–05.

Alewell, C., Birkholz, A., Meusburger, K., Schindler Wildhaber, Y. and Mabit, L. (2016) ‘Quantitative sediment source attribution with compound-specific isotope

analysis in a C3 plant-dominated catchment (central Switzerland)', Biogeosciences, 13(5), pp. 1587–1596.

Alewell, C., Borrelli, P., Meusburger, K. and Panagos, P. (2019) 'Using the USLE: Chances, challenges and limitations of soil erosion modelling', International Soil and Water Conservation Research, 7(3) Elsevier Ltd, pp. 203–225.

Baggaley, N., Lilly, A., Blackstock, K., Dobbie, K., Carson, A. and Leith, F. (2020) 'Soil risk maps – Interpreting soils data for policy makers, agencies and industry', Soil Use and Management, 36(1), pp. 19–26.

Batista, P.V.G., Davies, J., Silva, M.L.N. and Quinton, J.N. (2019) 'On the evaluation of soil erosion models: Are we doing enough?', Earth-Science Reviews, 197(July) Elsevier, p. 102898.

Blake, W.H., Ficken, K.J., Taylor, P., Russell, M.A. and Walling, D.E. (2012) 'Tracing crop-specific sediment sources in agricultural catchments', Geomorphology, 139–140 Elsevier B.V., pp. 322–329.

Boardman, J. (2001) 'Classics in physical geography revisited', Progress in Physical Geography, 25(2), pp. 261–266.

Borrelli, P., Märker, M., Panagos, P. and Schütt, B. (2014) 'Modeling soil erosion and river sediment yield for an intermountain drainage basin of the Central Apennines, Italy', Catena, 114 Elsevier B.V., pp. 45–58.

Borrelli, P., Van Oost, K., Meusburger, K., Alewell, C., Lugato, E. and Panagos, P. (2018) 'A step towards a holistic assessment of soil degradation in Europe: Coupling on-site erosion with sediment transfer and carbon fluxes', Environmental Research, 161(May 2017) Elsevier Inc., pp. 291–298.

Borselli, L., Cassi, P. and Torri, D. (2008) 'Prolegomena to sediment and flow connectivity in the landscape: A GIS and field numerical assessment', Catena, 75(3), pp. 268–277.

Brenning, A., Becker, M. and Bangs, D. (2018) RSAGA: SAGA Geoprocessing and Terrain Analysis. R package 1.3.0.

Cavalli, M., Trevisani, S., Comiti, F. and Marchi, L. (2013) ‘Geomorphometric assessment of spatial sediment connectivity in small Alpine catchments’, Geomorphology, 188 Elsevier B.V., pp. 31–41.

Chen, F.X., Fang, N.F., Wang, Y.X., Tong, L.S. and Shi, Z.H. (2017) ‘Biomarkers in sedimentary sequences: Indicators to track sediment sources over decadal timescales’, Geomorphology, 278 Elsevier B.V., pp. 1–11.

Cloy, J.M., Lilly, A., Hargreaves, P.R., Gagkas, Z., Dolan, S., Baggaley, N.J., Stutter, M., Crooks, B., Elrick, G. and McKenzie, B.. (2021) A state of knowledge overview of identified pathways of diffuse pollutants to the water environment. CRW2018_18.

Cole, B., King, S., Ogutu, B., Palmer, D., Smith, G. and Balzter, H. (2015) Corine land cover 2012 for the UK, Jersey and Guernsey., NERC Environmental Information Data Centre Available at: https://doi.org/10.5285/32533dd6-7c1b-43e1-b892-e80d61a5ea1d (Accessed: 18 January 2021).

Desmet, P.J.J. and Govers, G. (1996) ‘A GIS procedure for automatically calculating the USLE LS factor on topographically complex landscape units’, Journal of Soil and Water Conservation, 51(5), pp. 427–433.

ESDAC (2014) Soil Erodibility (K- Factor) High Resolution dataset for Europe., Joint Research Centre of the European Commission Available at: https://esdac.jrc.ec.europa.eu/content/soil-erodibility-k-factor-high-resolution-dataset-europe (Accessed: 7 June 2019).

ESDAC (2015a) Estimating the soil erosion cover-management factor at European scale., Joint Research Centre of the European Commission Available at: https://esdac.jrc.ec.europa.eu/content/cover-management-factor-c-factor-eu (Accessed: 19 March 2012).

ESDAC (2015b) Rainfall Erosivity in the EU and Switzerland (R-factor)., European Commission, Joint Research Centre Available at: https://esdac.jrc.ec.europa.eu/content/rainfall-erosivity-european-union-and-switzerland (Accessed: 7 June 2019).

ESRI (2017) ArcGIS Desktop 10.6. Environmental Systems Research Institute, Redlands, CA

Galoski, C.E., Jiménez Martínez, A.E., Schultz, G.B., dos Santos, I. and Froehner, S. (2019) 'Use of n-alkanes to trace erosion and main sources of sediments in a watershed in southern Brazil', Science of the Total Environment, 682 Elsevier B.V., pp. 447–456.

Glendell, M., Jones, R., Dungait, J.A.J., Meusburger, K., Schwendel, A.C., Barclay, R., Barker, S., Haley, S., Quine, T.A. and Meersmans, J. (2018) 'Tracing of particulate organic C sources across the terrestrial-aquatic continuum, a case study at the catchment scale (Carminowe Creek, southwest England)', Science of the Total Environment, 616, pp. 1077–1088. Available at: 10.1016/j.scitotenv.2017.10.211 (Accessed: 5 September 2018).

Hancock, G.J. and Revill, A.T. (2013) 'Erosion source discrimination in a rural Australian catchment using compound-specific isotope analysis (CSIA)', Hydrological Processes, 27(6), pp. 923–932.

Hijmans, R.J. (2020) Raster: Geographic Data Analysis and Modeling. R package 3.0-12.

Hirave, P., Glendell, M., Birkholz, A. and Alewell, C. (2020) 'Compound-specific isotope analysis with nested sampling approach detects spatial and temporal variability in the sources of suspended sediments in a Scottish mesoscale catchment', Science of The Total Environment, (xxxx) The Authors, p. 142916.

Hooke, J., Souza, J. and Marchamalo, M. (2021) 'Evaluation of connectivity indices applied to a Mediterranean agricultural catchment', Catena, 207(August) Elsevier B.V., p. 105713.

Lilly, A. and Baggaley, N. (2014) Developing simple indicators to assess the role of soils in determining risks to water quality, CREW project number CD2012_42.

Lilly, A. and Baggaley, N.J. (2018) Soil erosion risk map of Scotland James Hutton Institute, Aberdeen

Liu, C., Hu, B.X., Li, Z., Yu, L., Peng, H., Wang, D. and Huang, X. (2021a) 'Linking soils and streams: Chemical composition and sources of eroded organic matter during rainfall events in a Loess hilly-gully region of China', Journal of Hydrology, 600(May) Elsevier B.V., p. 126518.

Liu, C., Wu, Z., Hu, B.X. and Li, Z. (2021b) 'Linking recent changes in sediment yields and aggregate-associated organic matter sources from a typical catchment of the Loess Plateau, China', Agriculture, Ecosystems and Environment, 321(July) Elsevier B.V., p. 107606.

Martin, M.P., Wattenbach, M., Smith, P., Meersmans, J., Jolivet, C., Boulonne, L. and Arrouays, D. (2011) 'Spatial distribution of soil organic carbon stocks in France', Biogeosciences, 8(5), pp. 1053–1065.

Mayer, S., Kühnel, A., Burmeister, J., Kögel-Knabner, I. and Wiesmeier, M. (2019) 'Controlling factors of organic carbon stocks in agricultural topsoils and subsoils of Bavaria', Soil and Tillage Research, 192(January) Elsevier, pp. 22–32.

Meersmans, J., Martin, M.P., De Ridder, F., Lacarce, E., Wetterlind, J., De Baets, S., Bas, C. Le, Louis, B.P., Orton, T.G., Bispo, A. and Arrouays, D. (2012) 'A novel soil organic C model using climate, soil type and management data at the national scale in France', Agronomy for Sustainable Development, 32(4), pp. 873–888.

Meersmans, J., De Ridder, F., Canters, F., De Baets, S. and Van Molle, M. (2008) 'A multiple regression approach to assess the spatial distribution of Soil Organic Carbon (SOC) at the regional scale (Flanders, Belgium)', Geoderma, 143(1–2), pp. 1–13.

Met Office (2021) UK Climate Average. Available at: https://www.metoffice.gov.uk/research/climate/maps-and-data/uk-climate-averages/gfjuxqwcs (Accessed: 18 January 2021).

Mukundan, R., Walling, D.E., Gellis, A.C., Slattery, M.C. and Radcliffe, D.E. (2012) 'Sediment Source Fingerprinting: Transforming From a Research Tool to

a Management Tool', Journal of the American Water Resources Association, 48(6), pp. 1241–1257.

Ordnance Survey (2021) OS Terrain 5 [ASC geospatial data], Scale 1:10000, Tiles: nj30ne,nj30nw,nj30se,nj30sw,nj31se,nj31sw,nj40ne,nj40nw,nj40se,nj40sw,nj41se,nj41sw,nj50ne,nj50nw,nj50se,nj50sw,nj51se,nj51sw,no39ne,no39nw,no49ne,no49nw,no59ne,no59nw,., EDINA Digimap Ordnance Survey Service Available at: https://digimap.edina.ac.uk (Accessed: 14 December 2018).

Owens, P.N. (2020) 'Soil erosion and sediment dynamics in the Anthropocene: a review of human impacts during a period of rapid global environmental change', Journal of Soils and Sediments, 20 Journal of Soils and Sediments, pp. 4115–4143.

Panagos, P., Ballabio, C., Borrelli, P., Meusburger, K., Klik, A., Rousseva, S., Tadić, M.P., Michaelides, S., Hrabalíková, M., Olsen, P., Aalto, J., Lakatos, M., Rymszewicz, A., Dumitrescu, A., Beguería, S. and Alewell, C. (2015a) 'Rainfall erosivity in Europe', Science of the Total Environment, 511, pp. 801–814.

Panagos, P., Borrelli, P., Meusburger, K., Alewell, C., Lugato, E. and Montanarella, L. (2015b) 'Estimating the soil erosion cover-management factor at the European scale', Land Use Policy, 48 Elsevier Ltd, pp. 38–50.

Panagos, P., Meusburger, K., Ballabio, C., Borrelli, P. and Alewell, C. (2014) 'Soil erodibility in Europe: A high-resolution dataset based on LUCAS', Science of the Total Environment, 479–480(1) Elsevier B.V., pp. 189–200.

Pebesma, E.J. (2004) 'Multivariable geostatistics in S: the gstat package', Computers and Geosciences, 30, pp. 683–691.

Pebesma, E.J. and Bivand, R.S. (2005) Classes and methods for spatial data in R: The sp package. R News 5 (2)

R Core Team (2020) R: A language and environment for statistical computing 3.6.3. R Foundation for Statistical Computing, Vienna, Austria

Renard, K.G., Foster, G.R., Weesies, G.A., Mc Cool, D.K. and Yoder, D.C. (1997) Predicting soil erosion by water: A guide to conservation planning with the revised universal soil loss equation (RUSLE).Agricultur. Washington, D.C.: U.S. Dept. of Agriculture, Agricultural Research Service.

Rickson, R.J., Baggaley, N., Deeks, L.K., Graves, A., Hannam, J., Keay, C. and Lilly, A. (2019) Developing a method to estimate the costs of soil erosion in high-risk Scottish catchments. Report to the Scottish Government. Available online from https://www.gov.scot/ISBN/978-1-83960-754-7.

SEPA (2021) Water Classification Hub., Scottish Environment Protection Agency

Sherriff, S.C., Rowan, J.S., Fenton, O., Jordan, P. and Ó hUallacháin, D. (2019) 'Influence of land management on soil erosion, connectivity, and sediment delivery in agricultural catchments: Closing the sediment budget', Land Degradation and Development, 30(18), pp. 2257–2271.

Walling, D.E., Owens, P.N. and Leeks, G.J.L. (1999) 'Fingerprinting suspended sediment sources in the catchment of the River Ouse, Yorkshire, UK', Hydrological Processes, 13(7), pp. 955–975.

Wiesmeier, M., Urbanski, L., Hobley, E., Lang, B., von Lützow, M., Marin-Spiotta, E., van Wesemael, B., Rabot, E., Ließ, M., Garcia-Franco, N., Wollschläger, U., Vogel, H.J. and Kögel-Knabner, I. (2019) 'Soil organic carbon storage as a key function of soils - A review of drivers and indicators at various scales', Geoderma, 333(July 2018) Elsevier, pp. 149–162.

Wischmeier, W. and Smith, D. (1978) Predicting rainfall erosion losses: a guide to conservation planning. Agricultural Handbook No. 537. U. S. Department of Agriculture., Washington (DC)

Zhang, Y., Collins, A.L., McMillan, S., Dixon, E.R., Cancer-Berroya, E., Poiret, C. and Stringfellow, A. (2017) 'Fingerprinting source contributions to bed sediment-associated organic matter in the headwater subcatchments of the River Itchen SAC, Hampshire, UK', River Research and Applications, 33(10), pp. 1515–1526.

6 Discussion

> *"…erosion models must be tested: if we fail to understand how far erosion models deviate from reality, then how useful can these models be – for scientists or decision-makers?*" (Batista et al., 2019)

Soil erosion and concomitant freshwater sedimentation are identified as major causes of terrestrial and aquatic degradation and, given the ecological and social costs resulting from these issues, they are becoming ever more prominent in the international environmental agenda (Upadhayay et al., 2017). The main objectives of the Water Framework Directive 2000/60/EC (WFD) are non-deterioration of water status and the achievement of good status for all EU waters (European Commission, 2010, 2022c; Voulvoulis, Arpon and Giakoumis, 2017). Because of inherent variability of waterways, good ecological status cannot be defined using absolute standards and WFD alternatively defines it as "a slight departure from the biological community which would be expected in conditions of minimal anthropogenic impact) (European Commission, 2022c). Therefore, although we do not want to remove the natural sediment resource from our waterways, it is of vital importance to identify sources of terrestrial-to-aquatic fluxes of soil OC at a river catchment scale so that anthropogenic impact can be estimated.

The aim of this research was to improve determination of the dominant terrestrial land-use sources of OC in freshwater sediment at a catchment scale and to assess the likely catchment processes driving spatial and temporal changes in these sources. This aim was achieved by, firstly, combining multiple modelling approaches to investigate catchment carbon dynamics allowing for an increased understanding of sediment and organic carbon transport processes at a catchment scale (Objective 1). The combined modelling approaches revealed extensive riparian woodland disconnected upslope eroded soil OC and, concomitantly, provided an input of woodland-derived OC to the streams. It was found that woodland contribution to streambed OC was derived from litter and leaves rather than soil erosion. In addition, ambiguity in OC origin was reduced by identifying not only the dominant land use source of stream OC (OC

fingerprinting (OCF)) but areas of high carbon loss and connectivity within the broad land use classifications (carbon loss modelling).

Secondly, combining OC biomarkers from different soil communities (plant, fungal, bacterial) reduced error when discriminating land use sources using OCF (Objective 2).

Thirdly, the longer-term accumulation of sediment on the streambed was required for comparison with the longer-term estimates of a carbon loss model. However, the shorter-term suspended sediment samples provided evidence of intra-annual variation in OC sources for comparison with agricultural and climate changes throughout the year (Objective 3). In addition, comparing suspended and streambed sediment was used to assess if particle size sorting due to mobilization, transportation and deposition processes affected biomarker tracers.

Finally, the land use specific OC yields (carbon loss models) using RUSLE and the Scottish erosion risk map (ERM) of Lilly and Baggaley, (2018) were compared using OCF as a benchmark to determine which erosion model best identified the relative land use OC yields in streambed sediment (Objective 4).

6.1 Combining multiple modelling approaches to investigate catchment carbon dynamics

Erosion models are employed to make quantitative estimates of how soil is redistributed in complex landscapes (Borrelli et al., 2018a; Panagos et al., 2015c; Schmidt, Alewell and Meusburger, 2019). This knowledge is vital to maintaining healthy soil ecosystems which are a key part of climate, biodiversity and economic objectives within the EU (e.g., Green Deal for Europe (European Commission, 2022a), EU Soil Observatory (European Commission, 2022b) and the Scottish Soil Framework (Scottish Government, 2009)). However, any model of real-world phenomena must undergo a “fit-for-purpose” test to give confidence that the model predictions do not deviate too far from “reality” (Batista et al., 2019). However, how can “reality” be defined? The output of erosion models such as RUSLE have previously been assessed using sediment yield data (Borrelli et al., 2014; Sherriff et al., 2019). However, individual models estimate

erosion risk based on a specific process or processes (e.g., RUSLE-based models estimate soil loss due to inter-rill and rill erosion) whereas sediment yield reflects all geomorphological processes active in the catchment (Borrelli et al., 2018a). OCF proportions could be considered as a “land use -specific” relative OC yield (Blake et al., 2012) which can then be compared with the estimates of carbon loss models. When used as a benchmark, OCF estimates can be an invaluable tool to assess if carbon loss models are “fit-for-purpose” or assess the suitability of one erosion model over another for a given catchment. However, similar to sediment yield, OCF of stream sediments reflects all OC input processes active in the catchment. Providing an equal comparison with estimates of OC loss made using carbon loss models requires confidence that the OC in the streams originates from the processes modelled by the carbon loss model (terrestrial soil erosion). Any discrepancy between carbon loss model estimates and those estimated by OCF methods can reveal the presence of a source not modelled by the erosion model to OC input to streams (Chapter 2). For example a mismatch between fingerprinting results and RUSLE estimates was attributed to stream bank erosion (Lamba, Karthikeyan and Thompson, 2015). However, although stream banks have long been considered as sources in OCF (Collins and Walling, 2007; Gateuille et al., 2019; Koiter et al., 2013a; Mukundan et al., 2010), Chapter 2 revealed an important source which, to the author’s knowledge, has never been incorporated as a source in OCF: direct input of woodland litter and leaves. If appropriate, characterising this direct woodland OC as a separate source within future fingerprinting studies should allow the contributions from any eroded woodland soil OC to be better estimated. Consequently, this will give more confidence in fingerprinting estimates of OC originating from eroded soil, facilitating their use as a “fit-for-purpose” test of carbon loss models.

In Chapter 5 estimates of relative contributions of OC from each land use source were used to assess the suitability of two different erosion models using OCF of streambed sediments as a benchmark. Estimates of the model closest to the benchmark should be more reliable (closer to “reality”). The areas of high erosion risk identified by the selected model, reduced ambiguity in OC origin by identifying specific areas within the broad OCF land use classifications. These areas provide

the potential to target individual stakeholder land or individual sections of hillside, rather than catchment wide land uses providing a more precise target or “hotspot” for best management practices (BMP).

6.1.1 Further research

RUSLE contains a “C-factor” to account for how land cover, crops and their management cause soil loss to vary between land uses. Comparative C-factor values quoted in the literature for arable, grassland and forest can often differ by an order of magnitude (e.g. arable ca.0.13, grassland ca.0.04 and forest ca.0.004 for the study by (Borrelli et al., 2014)) with the general assumption that erosion from arable land (with levels of vegetation cover potentially varying seasonally and yearly) will be greater than that from grassland which will be greater than that from forest. When estimating proportions of soil OC losses from each land use a limitation of RUSLE is that literature C-factor values for the same “land use” can also differ by orders of magnitude between studies (e.g. grasslands in Europe 0.005 (Van Rompaey and Govers, 2002), ca.0.04 (Borrelli et al., 2014)), often dominating the uncertainty in RUSLE results (Estrada-Carmona et al., 2017). In addition, recent studies have shown that the assumption that erosion from arable land was significantly greater than from non-arable land was increasingly uncertain (Hirave et al., 2020a; Rickson et al., 2019). In Chapter 5, it was identified that the RUSLE C-factor for moorland should be set similar to that for forest rather than the value quoted in the literature (Panagos et al., 2015b). In future studies, estimates of the C-factor for all land uses could also be adjusted within the Monte Carlo analysis to calibrate the model and obtain land use source proportions more closely approximating to those found by the OCF benchmark, ultimately resulting in more accurate erosion rate estimates. A carbon loss model calibrated in this way could then be applied with better confidence in similar catchments where OCF has not been done, aiding catchment managers to map areas of high erosion risk and quantify OC losses.

As noted in Chapter 2, the advantage of using RUSLE in a carbon loss model is that the extensive literature and data accessibility for RUSLE mean it can be easily applied in a wide variety of catchments using available data. However, the

disadvantage is that RUSLE models gross (rather than net) erosion rates. In this research it was used with a connectivity index which provided an estimate of connection between upslope areas of erosion and streams. Net catchment erosion can be modelled using sediment delivery models (e.g., WaTEM/SEDEM (Van Oost, Govers and Desmet, 2000; Van Rompaey et al., 2001; Verstraeten et al., 2002)). However, accurate predictions for these models require calibration, commonly carried out using outlet sediment yield data (Krasa et al., 2019; Luo et al., 2021). As sediment yield data are not available for many catchments, and are usually only available at the catchment outlet, incorporating these net catchment erosion models into a carbon loss model would facilitate calibration using the OCF land use -specific relative yields. In future studies, this could provide more accurate net rates of terrestrial-to-aquatic fluxes key to estimating anthropogenic impacts for assessment of water quality under directives such as WFD.

6.1.2 Research Impact

Organic carbon fingerprinting generates land use -specific relative OC yield which can then be compared with the estimates of a carbon loss model (constructed using any “net” erosion model). This combination of multiple modelling approaches can be employed in other catchments to:

i. increase understanding of sediment and organic carbon transport processes by estimating the relative land use contributions from soil OC erosion and also identifying the likelihood of other sources of OC input to streams
ii. assess the relative suitability of different erosion models using OCF of streambed sediments as a benchmark
iii. calibrate erosion models - including refinement of model parameters such as the RUSLE C-factor

6.2 OC fingerprinting tracers

N-alkane biomarkers in sediments provide a record of the kinds of plants that populate a catchment (i.e. where grasses are abundant, C31 is the dominant *n*-alkane, whereas C27 and C29 are more abundant where trees dominate (Puttock

et al., 2014)). Ideally, OC biomarkers will not change (i.e., show conservative behaviour) between sediment source (up slope point of erosion) and sink (stream) so that a direct comparison can be made. Yet, particle size and transport selectivity can result in downstream fining and an enrichment of organic matter content (Koiter et al., 2015). The particle size selectivity is usually correlated to the energy of the erosive process (e.g., water erosion) with greater erosive force resulting in less selectivity (Armstrong et al., 2011; Haddadchi, Olley and Pietsch, 2015; Koiter et al., 2013b). It was thought this particle size selectivity may have resulted in streambed sediment *n*-alkane ratios %C31 and %C27 that were lower and higher respectively than those observed in the associated terrestrial soils in the Loch Davan catchment (Chapter 3). It was hypothesised that any differences terrestrial and stream sediment *n*-alkane tracers would be more pronounced in suspended sediment (SS) than streambed sediments (which would be expected to accumulate the coarser, heavier particles entering the streams). However, the contrary was found (with SS *n*-alkane ratio values generally between those of the streambed sediments and terrestrial soils) and it was concluded that lower %C31 and higher %C27 were unlikely to be due to particle size fining.

In Chapter 3, it was reported that alluvial soils (recent riverine and lacustrine alluvial deposits) showed a similarly lower and higher %C31 and %C27 suggesting a link between lower and higher %C31 and %C27 values and current and previously aquatic environments. Lower and higher %C31 and %C27 values may be characteristic of *n*-alkanes in sediments that have spent (an unspecified) time in an aquatic environment. If SS is representative of “newer” sediment within the streams and bed sediment as “older” this would also explain why the %C31 and %C27 values of SS were closer to those of the terrestrial sources. If the lower and higher %C31 and %C27 signatures found in these two catchments (Carminowe Creek and Loch Davan) are replicated in other catchments this would have implications for the use of *n*-alkane ratios as conservative tracers in OCF as the *n*-alkane signatures would not be preserved between source and sink (stream).

In addition, alluvial soils the signatures of *n*-alkanes for arable, forest, moorland and pasture land uses are very similar and it is unlikely that *n*-alkanes could be used to distinguish between land uses in these soils The relative signatures of *n*-alkanes in pasture soils shows little difference between those in alluvial soils and those in all soil types (Figure 33). There is progressively more difference in the relative signatures of *n*-alkanes alluvial soils and those in all soil types for arable soils and forest soils with the greatest differences shown in moorland soils (Figure 33). It was discussed in Chapter 4 that pasture soils were likely to have a higher contribution from mosses and be relatively wetter than the other land uses. Therefore, it is hypothesised that the wetter the soils are within each land use, the less difference there will be between *n*-alkane signatures in alluvial soils and the other soil types. These results suggest that taking samples of land use sources in close proximity to stream channels (and likely on alluvial soils) may not be representative of soil from that land use in the wider catchment. More accurate OCF results may be obtained by characterising separate sources for “alluvial” and “wider catchment” sources.

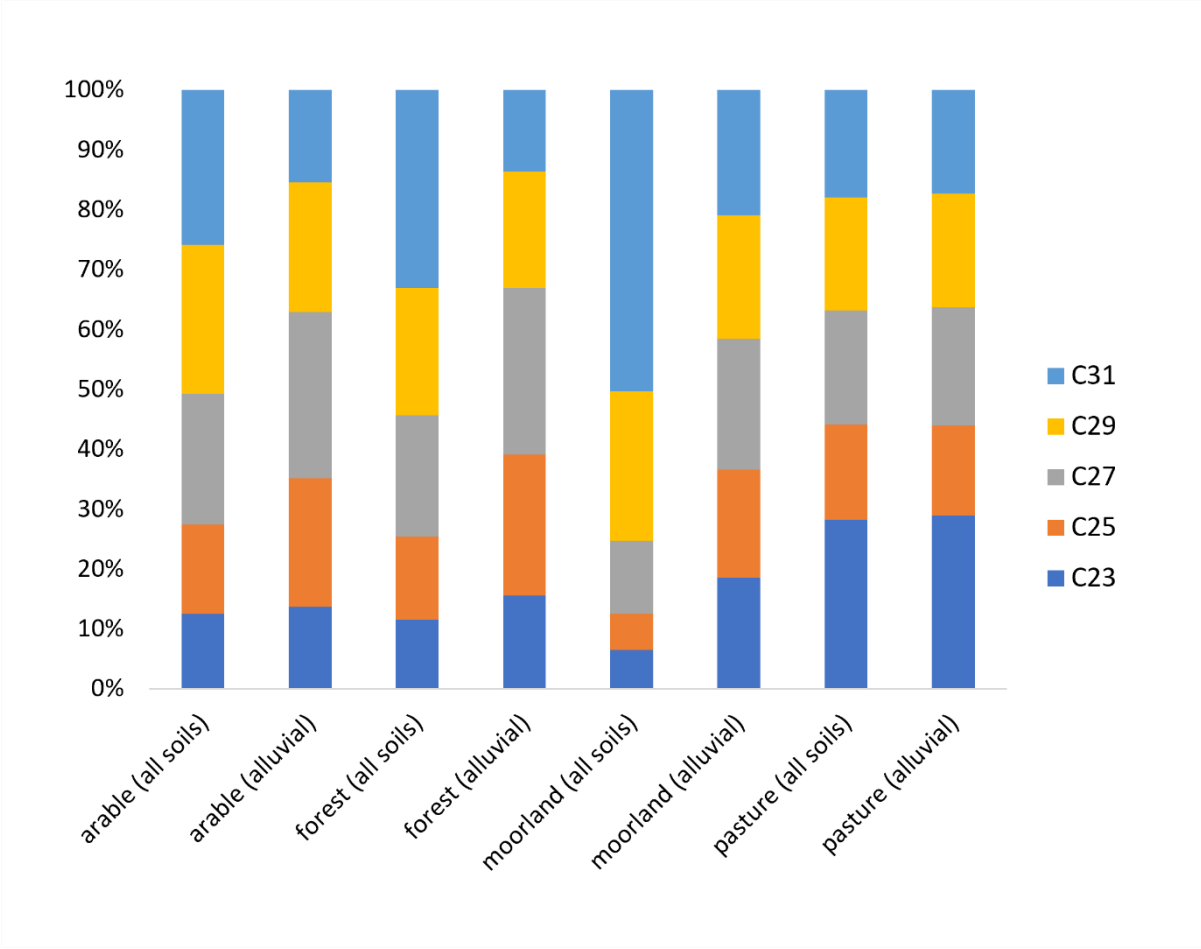

Figure 33: Signature of *n*-alkanes C23-C31 in alluvial soils and all soils in the Loch Davan catchment

The PAQ ratio (ratio of shorter-chain *n*-alkanes (C23+C25) contributed by macrophytes (higher aquatic plants) and mosses, to *n*-alkanes indicative of both aquatic and terrestrial vegetation (C23 +C25 +C29 +C31)) is often used to interpret the relative contribution of higher aquatic vs. terrestrial plants to sediments in rivers and lakes. The finding of this research, that PAQ in arable, forest and pasture soils was in the range normally associated with emergent macrophytes and mosses (Chapter 4), has implications for research interpreting the origins of aquatic sediments using the expected ranges of PAQ in terrestrial and aquatic vegetation - especially in climates, such as that in Scotland, providing the ideal conditions for the growth of mosses in source soils. Measuring PAQ in potential terrestrial and aquatic sources can lead to reliable estimates of terrestrial-to-aquatic contributions in surface sediments (Li et al., 2022). However,

this is not possible for palaeoenvironment reconstruction studies and the relative terrestrial and aquatic plant contributions are often evaluated using the PAQ ranges of (Ficken et al., 2000) with a PAQ value of < 0.1 used as a terrestrial plant indicator (Ankit et al., 2022; Tian et al., 2022; Wang et al., 2019). Although this PAQ range may be a reliable indicator of the presence of emergent macrophytes and mosses, and accordingly a wetter environment, the results presented in Chapter 4 suggest it may not be a reliable estimator of the absence of terrestrial soil input to lakes and sedimentary basins. It would be instructive to investigate PAQ in other areas that have similarly warm winters and cool, wet summers to those in Scotland to see if the relatively high PAQ values in soils are replicated.

As discussed in Chapter 3, distinguishing between arable and pasture land is known to be difficult due to agronomic rotation. In the Carminowe Creek catchment, Cornwall there was very little difference in the *n*-alkane signatures of arable, temporary grassland and permanent grassland and consequently the *n*-alkane biomarkers were only able to distinguish between two land uses: “woodland” and “not woodland” (Chapter 2). However, in the Loch Davan catchment pastures were dominated by *n*-alkane chain lengths C23 and C25, characteristic of lower plants and mosses, creating a contrast with arable soils which were dominated by longer chain lengths (C27-C31) allowing *n*-alkane tracers to distinguish between all land uses in the catchment including arable and pasture. However, investigations were still carried out to determine if sediment-associated SC-NLFA concentrations and carbon isotope signatures in addition to those for longer-chain *n*-alkane tracers, improved the ability of sediment fingerprinting to distinguish between land-use specific sources. This was tested using virtual mixtures and established that the addition of SC-NLFA biomarkers led to a significant decrease in error when distinguishing between all land (Chapter 3).

6.2.1 Further research

The streambed sediment *n*-alkane ratios %C31 and %C27 were lower and higher respectively than those observed in the associated terrestrial soils in both the

Loch Davan catchment in Scotland (Chapter 3) and in the Carminowe Creek catchment in Southern England (Glendell et al., 2018). Comparing these *n*-alkane ratios in the finer SS and coarser streambed sediments in the Loch Davan catchment suggested these differences were unlikely to be due to either i) an enrichment in finer particles or ii) the storage of terrestrial sediments in water (at room temperature). The use of *n*-alkanes as tracers in OCF would benefit from further research into this issue.

Although this research and that of others (Blake et al., 2012; Ferrari et al., 2015; Lavrieux et al., 2012; Lu et al., 2014) have confirmed SC-NLFA biomarkers can successfully distinguish different land uses there is little or no evidence to explain why they do so. In order to become a more widely used OCF tracer more research will be needed to confirm i) why SC-NLFA can distinguish between land uses and ii) how conservative they are, and over what time scales.

In the Carminowe Creek catchment, the *n*-alkane biomarkers were only able to distinguish between two land uses: “woodland” and “not woodland”. In addition, it is likely the woodland contribution to streambed OC was derived from litter and leaves rather than woodland soil. If, as suggested in Chapter 3, the plant, fungal and bacterial origin of SC-NLFA provide a fingerprint more characteristic of the soil rather than just the land cover vegetation, applying them in the Carminowe Creek catchment could improve discrimination between i) the arable, temporary grassland and permanent grassland land uses, and ii) woodland soils and woodland litter and leaves.

6.2.2 Research Impact

In future OCF studies, combining soil biomarkers of plant, fungal and bacterial origin could provide:

i. greater discrimination between land use sources
ii. a fingerprint more characteristic of the soil rather than just the land cover vegetation.

6.3 Sediment management in the Loch Davan catchment

The lake area of Loch Davan has been significantly reduced over the last century, likely due to inputs of nutrient rich sediment resulting from land use intensification (Addy, Ghimire and Cooksley, 2012) and between 2007 and 2018, the loch and its main feeder stream, Logie Burn, were classified as having poor to moderate ecological status (SEPA, 2021). Loch Davan and Logie Burn fall under the remit of SEPA's River Basin Management Planning for the River Dee catchment. With the aim of these waterbodies reaching "Good" water status by 2027 the action plan aimed at reducing diffuse source inputs.

To this end this research was carried out with the aim of i) identifying the land use sources of OC input to the Logie Burn and its tributaries, ii) identifying erosion risk "hotspots" and iii) estimating intra-annual agronomic and climate drivers of stream OC inputs.

6.3.1 Land use sources

Sediment fingerprinting using a novel combination of *n*-alkane and SC-NLFA biomarkers identified that pasture was the dominant contributor to streambed OC. The dominant contributor to SS was arable land. The OC content of SS was considerably higher than that in streambed sediments (Chapter 4, Table 16) consistent with SS having a finer particle size distribution (Koiter et al., 2015) and/or streambed sediments having a higher sand content (Dai and Sun, 2007). If livestock poaching of near channel land was the primary input mechanism for pasture soil to the streams (Chapter 4) it would be expected that soils would be delivered to the channel in larger masses due to compaction of the soil, shorter transport distances and direct input. These larger masses would be more likely to remain on the streambed rather than be quickly transported away in suspension. Mills and Bathurst, (2015) found livestock poaching of channel banks in areas of unfenced pasture, resulting in bank erosion and increased availability of sediment to water flows. Riparian soils prone to occasional flooding are often used for grassland as opposed to arable uses (Stutter, Langan and Demars, 2007) and, therefore, if OC from arable sources had to travel further to the streams the fining of particles due to mobilization, transportation and deposition

processes may result in most of the arable soil OC remaining in suspension. Although it does not make a dominant contribution to the streambed sediments, arable soil OC may make a larger contribution to the OC within Loch Davan where sediments are more likely to fall from suspension in the less vigorous hydrological environment.

6.3.2 Seasonal OC dynamics

Although temporal drivers of terrestrial-to-aquatic OC fluxes were identified in the Loch Davan catchment, the restricted time scale (June 2019 to November 2020) did not allow for an assessment of repeated or long-term drivers in this catchment which would be of greater utility to SEPA's River Basin Management. Drivers of change in SS source proportion included land preparation/planting and moorland heather burning in spring, and heavier prolonged rainfall in late autumn and winter leading to saturated soils, increased runoff and stream discharge and remobilisation of streambed sediment. SS proportions at the catchment outlet revealed that livestock poaching of riparian pasture soils may be driving increased OC input to streams in late autumn/winter.

In Chapter 4 the importance of source classification to source apportionment was discussed and it was shown how the drivers of terrestrial-to-aquatic OC fluxes were used to confirm that the presence of a small number of cropped fields in a sub-catchment (not present on the catchment land cover map) constituted a substantial enough arable source to warrant using a four-source classification (arable, pasture, forest and moorland) rather than a three-source (pasture, forest and moorland). The dominant arable contribution to SS OC in the sub-catchment was likely due to the fact the arable fields are located next to the Burn and, consequently, highly connected. The contributions of land use sources to SS OC estimated using the three and four -source classifications were very different; with the three-source classification showing a dominant forest contribution and the four-source a dominant arable contribution. These different estimations would have led to very different recommendations for BMP and assessment of anthropogenic impacts. This method would therefore be valuable in mixed land use catchments where multiple stream sediment sources require the definition of

source classes in multiple sub-catchments – particularly if up-to-date land cover maps are not available.

6.3.3 OC loss and soil erosion

There remains uncertainty in erosion rates for soil and land use combinations when tracing pathways of diffuse pollution from agricultural land to waterways (Cloy et al., 2021). The ERM (described in Chapter 5) has been used by the Scottish Environment Protection Agency (SEPA), Scottish Water and Scottish Government to assess the risks posed to waters from soils from field to regional scale (Baggaley et al., 2020), however they do not provide quantitative estimates of soil or OC erosion rates. In a recent report to the Scottish Government, Rickson et al., (2019) assessed the annual cost of erosion in Scotland by adopting the approach that soil erosion rates should be driven by land use, but the likelihood of erosion occurring should be driven by erosion risk class (as defined by the ERM). The similarity of the land use specific carbon loss estimates of RUSLE and ERM in this research (Chapter 5) suggested RUSLE erosion rate estimates could be used to quantify the amount of soil eroded from the high and medium risk areas defined by the ERM in this catchment. Areas identified as “high” risk and “medium” risk by the ERM had mean soil erosion estimates of 1.51 and 0.88 t ha^{-1} yr^{-1} respectively for arable land, 1.26 and 0.64 t ha^{-1} yr^{-1} respectively for pasture land, 0.04 and 0.03 t ha^{-1} yr^{-1} respectively for forest land and 0.04 and 0.04 t ha^{-1} yr^{-1} respectively for moorland (Table 21). These estimates are less than the soil erosion rates per land use defined by Rickson et al., (2019) in their study to identify soil erosion rates in Scotland (mineral soils: arable 2.4 to 4.3 t ha^{-1} yr^{-1}, grasslands 2.4 to 4.3 t ha^{-1} yr^{-1}, forest 0.6 t ha^{-1} yr^{-1} and wildscape (semi-natural landscape) 0.6 t ha^{-1} yr^{-1}; organic soils: arable 5 to 10 t ha^{-1} yr^{-1}, grasslands 0.39 to 1 t ha^{-1} yr^{-1}, forest 0.13 t ha^{-1} yr^{-1} and wildscape 0.13 t ha^{-1} yr^{-1}) suggesting the erosion rates for the Loch Davan catchment are relatively low.

6.3.4 Further Research

The estimates of Rickson et al., (2019) are intended to inform soil resource policies in Scotland and it would be instructive to compare these land use

estimates with the OCF benchmark in the Loch Davan catchment to see how well they perform.

At the start of this research, it was intended to take a lake core within Loch Davan to assess the longer-term sources of aqueous OC and their inter-annual variation. Restricted access to Loch Davan for the purposes of taking samples (outside the bird breeding season – i.e. before the end of March or after the end of August) coupled with Covid-19 lockdowns unfortunately prevented this. Assessment of the land use source contributions of OC within a lake core could provide confirmation that arable contribution dominates the lake sediment OC and discover if the improvement of water status from “Poor/Moderate” to “High” was due to a reduction in the amount of sediment coming from arable land.

6.3.5 Research Impact

Soil erosion in the Loch Davan catchment is not high and the water status classification for the loch and Logie Burn has risen from “Poor/Moderate” to “High” in the last few years (SEPA, 2021). However, reducing anthropogenically driven SS in the catchment would be beneficial for soil conservation and ensure the water quality status for Logie Burn and Loch Davan remain “high”.

Pasture land was the dominant contributor to streambed sediments. Given the likely role of grazing livestock in soil erosion, possible solutions to reduce soil erosion in pasture land are to: reduce livestock access to the streams through the use of stream buffer strips, reduce the length of the grazing season and move grazing animals to areas less prone to erosion and/or well connected to the streams to avoid poaching issues.

Arable soils were the dominant contributor to SS OC, especially during periods where the fields are relatively bare (e.g. following field planting/sowing). Reduction in arable contribution to SS OC could therefore be achieved by reducing the connectivity through the use of stream buffer strips and permanent riparian vegetation.

6.4 References

Addy, S., Ghimire, S. and Cooksley, S. (2012) ‘Assessment of the multiple benefits of river restoration: the Logie Burn meander reconnection project’, BHS Eleventh National Symposium, Hydrology for a changing world, Dundee 2012, , pp. 01–05.

Ankit, Y., Muneer, W., Gaye, B., Lahajnar, N., Bhattacharya, S., Bulbul, M., Jehangir, A., Anoop, A. and Mishra, P.K. (2022) ‘Apportioning sedimentary organic matter sources and its degradation state- Inferences based on aliphatic hydrocarbons amino acids and δ15N’, Environmental Research, 205

Armstrong, A., Quinton, J.N., Heng, B.C.P. and Chandler, J.H. (2011) ‘Variability of interrill erosion at low slopes’, Earth Surface Processes and Landforms, 36(1), pp. 97–106.

Baggaley, N., Lilly, A., Blackstock, K., Dobbie, K., Carson, A. and Leith, F. (2020) ‘Soil risk maps – Interpreting soils data for policy makers, agencies and industry’, Soil Use and Management, 36(1), pp. 19–26.

Batista, P.V.G., Davies, J., Silva, M.L.N. and Quinton, J.N. (2019) ‘On the evaluation of soil erosion models: Are we doing enough?’, Earth-Science Reviews, 197(July) Elsevier, p. 102898.

Blake, W.H., Ficken, K.J., Taylor, P., Russell, M.A. and Walling, D.E. (2012) ‘Tracing crop-specific sediment sources in agricultural catchments’, Geomorphology, 139–140 Elsevier B.V., pp. 322–329.

Borrelli, P., Märker, M., Panagos, P. and Schütt, B. (2014) ‘Modeling soil erosion and river sediment yield for an intermountain drainage basin of the Central Apennines, Italy’, Catena, 114 Elsevier B.V., pp. 45–58.

Borrelli, P., Van Oost, K., Meusburger, K., Alewell, C., Lugato, E. and Panagos, P. (2018) ‘A step towards a holistic assessment of soil degradation in Europe: Coupling on-site erosion with sediment transfer and carbon fluxes’, Environmental Research, 161(May 2017) Elsevier Inc., pp. 291–298.

Cloy, J.M., Lilly, A., Hargreaves, P.R., Gagkas, Z., Dolan, S., Baggaley, N.J., Stutter, M., Crooks, B., Elrick, G. and McKenzie, B.. (2021) A state of knowledge overview of identified pathways of diffuse pollutants to the water environment. CRW2018_18.

Collins, A.L. and Walling, D.E. (2007) 'The storage and provenance of fine sediment on the channel bed of two contrasting lowland permeable catchments', River Research and Applications, 23, pp. 429–450.

Dai, J. and Sun, M.Y. (2007) 'Organic matter sources and their use by bacteria in the sediments of the Altamaha estuary during high and low discharge periods', Organic Geochemistry, 38(1), pp. 1–15.

Estrada-Carmona, N., Harper, E.B., DeClerck, F. and Fremier, A.K. (2017) 'Quantifying model uncertainty to improve watershed-level ecosystem service quantification: a global sensitivity analysis of the RUSLE', International Journal of Biodiversity Science, Ecosystem Services and Management, 13(1) Taylor & Francis, pp. 40–50.

European Commission (2010) The EU Water Framework Directive

European Commission (2022a) Introduction to the EU Water Framework Directive. Available at: https://ec.europa.eu/environment/water/water-framework/info/intro_en.htm (Accessed: 13 March 2022).

European Commission (2022b) A European Green Deal: Striving to be the first climate-neutral continent. Available at: https://ec.europa.eu/info/strategy/priorities-2019-2024/european-green-deal_en (Accessed: 13 March 2022).

European Commission (2022c) EU Soil Observatory (EUSO). Available at: https://joint-research-centre.ec.europa.eu/eu-soil-observatory-euso_en (Accessed: 13 March 2022).

Ferrari, A.E., Ravnskov, S., Larsen, J., Tønnersen, T., Maronna, R.A. and Wall, L.G. (2015) 'Crop rotation and seasonal effects on fatty acid profiles of neutral

and phospholipids extracted from no-till agricultural soils', Soil Use and Management, 31(1), pp. 165–175.

Gateuille, D., Owens, P.N., Petticrew, E.L., Booth, B.P., French, T.D. and Déry, S.J. (2019) 'Determining contemporary and historical sediment sources in a large drainage basin impacted by cumulative effects: the regulated Nechako River, British Columbia, Canada', Journal of Soils and Sediments, 19(9) Journal of Soils and Sediments, pp. 3357–3373.

Glendell, M., Jones, R., Dungait, J.A.J., Meusburger, K., Schwendel, A.C., Barclay, R., Barker, S., Haley, S., Quine, T.A. and Meersmans, J. (2018) 'Tracing of particulate organic C sources across the terrestrial-aquatic continuum, a case study at the catchment scale (Carminowe Creek, southwest England)', Science of the Total Environment, 616, pp. 1077–1088. Available at: 10.1016/j.scitotenv.2017.10.211 (Accessed: 5 September 2018).

Haddadchi, A., Olley, J. and Pietsch, T. (2015) 'Quantifying sources of suspended sediment in three size fractions', Journal of Soils and Sediments, 15(10), pp. 2086–2100.

Hirave, P., Glendell, M., Birkholz, A. and Alewell, C. (2020) 'Compound-specific isotope analysis with nested sampling approach detects spatial and temporal variability in the sources of suspended sediments in a Scottish mesoscale catchment', Science of The Total Environment, (xxxx) The Authors, p. 142916.

Koiter, A.J., Lobb, D.A., Owens, P.N., Petticrew, E.L., Tiessen, K.H.D. and Li, S. (2013a) 'Investigating the role of connectivity and scale in assessing the sources of sediment in an agricultural watershed in the Canadian prairies using sediment source fingerprinting', Journal of Soils and Sediments, 13(10), pp. 1676–1691.

Koiter, A.J., Owens, P.N., Petticrew, E.L. and Lobb, D.A. (2015) 'The role of gravel channel beds on the particle size and organic matter selectivity of transported fine-grained sediment: implications for sediment fingerprinting and biogeochemical flux research', Journal of Soils and Sediments, 15(10), pp. 2174–2188.

Koiter, A.J., Owens, P.N., Petticrew, E.L. and Lobb, D.A. (2013b) 'The behavioural characteristics of sediment properties and their implications for sediment fingerprinting as an approach for identifying sediment sources in river basins', Earth-Science Reviews, 125 Elsevier B.V., pp. 24–42.

Krasa, J., Dostal, T., Jachymova, B., Bauer, M. and Devaty, J. (2019) 'Soil erosion as a source of sediment and phosphorus in rivers and reservoirs – Watershed analyses using WaTEM/SEDEM', Environmental Research, 171(January) Elsevier Inc., pp. 470–483.

Lamba, J., Karthikeyan, K.G. and Thompson, A.M. (2015) 'Apportionment of suspended sediment sources in an agricultural watershed using sediment fingerprinting', Geoderma, 239 Elsevier B.V., pp. 25–33.

Lavrieux, M., Bréheret, J.G., Disnar, J.R., Jacob, J., Le Milbeau, C. and Zocatelli, R. (2012) 'Preservation of an ancient grassland biomarker signature in a forest soil from the French Massif Central', Organic Geochemistry, 51, pp. 1–10.

Li, J., Lv, L., Wang, R., Long, H. and Yang, X. (2022) 'Spatial distribution of n-alkanes in the catchment and sediments of Lake Lugu, Southwest China: Implications for palaeoenvironment reconstruction', Palaeogeography, Palaeoclimatology, Palaeoecology, 592(February) Elsevier B.V., p. 110895.

Lilly, A. and Baggaley, N.J. (2018) Soil erosion risk map of Scotland James Hutton Institute, Aberdeen

Lu, Y.H., Canuel, E.A., Bauer, J.E. and Chambers, R.M. (2014) 'Effects of watershed land use on sources and nutritional value of particulate organic matter in temperate headwater streams', Aquatic Sciences, 76(3), pp. 419–436.

Luo, Y., Wang, H., Meersmans, J., Green, S.M., Quine, T.A. and Feng, S. (2021) 'Modeling soil erosion between 1985 and 2014 in three watersheds on the carbonate-rock dominated Guizhou Plateau, SW China, using WaTEM/SEDEM', Progress in Physical Geography, 45(1), pp. 53–81.

Mills, C.F. and Bathurst, J.C. (2015) ‘Spatial variability of suspended sediment yield in a gravel-bed river across four orders of magnitude of catchment area’, Catena, 133 Elsevier B.V., pp. 14–24.

Mukundan, R., Radcliffe, D.E., Ritchie, J.C., Risse, L.M. and McKinley, R.A. (2010) ‘Sediment Fingerprinting to Determine the Source of Suspended Sediment in a Southern Piedmont Stream’, Journal of Environmental Quality, 39(4), pp. 1328–1337.

Van Oost, K., Govers, G. and Desmet, P. (2000) ‘Evaluating the effects of changes in landscape structure on soil erosion by water and tillage’, Landscape Ecology, 15(6), pp. 577–589.

Panagos, P., Borrelli, P., Meusburger, K., Alewell, C., Lugato, E. and Montanarella, L. (2015a) ‘Estimating the soil erosion cover-management factor at the European scale’, Land Use Policy, 48 Elsevier Ltd, pp. 38–50.

Panagos, P., Borrelli, P., Poesen, J., Ballabio, C., Lugato, E., Meusburger, K., Montanarella, L. and Alewell, C. (2015b) ‘The new assessment of soil loss by water erosion in Europe’, Environmental Science and Policy, 54 Elsevier Ltd, pp. 438–447.

Puttock, A., Dungait, J.A.J., Macleod, C.J.A., Bol, R. and Brazier, R.E. (2014) ‘Organic Carbon From Dryland Soils’, Journal of Geophysical Research: Biogeosciences, 119, pp. 2345–2357.

Rickson, R.J., Baggaley, N., Deeks, L.K., Graves, A., Hannam, J., Keay, C. and Lilly, A. (2019) Developing a method to estimate the costs of soil erosion in high-risk Scottish catchments. Report to the Scottish Government. Available online from https://www.gov.scot/ISBN/978-1-83960-754-7.

Van Rompaey, A.J.J. and Govers, G. (2002) ‘Data quality and model complexity for regional scale soil erosion prediction’, International Journal of Geographical Information Science, 16(7), pp. 663–680.

Van Rompaey, A.J.J., Verstraeten, G., van Oost, K., Govers, G. and Poesen, J. (2001) ‘Modelling mean annual sediment yield using a distributed approach’, Earth Surface Processes and Landforms, 1236, pp. 1221–1236.

Schmidt, S., Alewell, C. and Meusburger, K. (2019) ‘Monthly RUSLE soil erosion risk of Swiss grasslands’, Journal of Maps, 15(2), pp. 247–256.

Scottish Government (2009) The Scottish Soil Framework.

SEPA (2021) Water Classification Hub., Scottish Environment Protection Agency

Sherriff, S.C., Rowan, J.S., Fenton, O., Jordan, P. and Ó hUallacháin, D. (2019) ‘Influence of land management on soil erosion, connectivity, and sediment delivery in agricultural catchments: Closing the sediment budget’, Land Degradation and Development, 30(18), pp. 2257–2271.

Stutter, M.I., Langan, S.J. and Demars, B.O.L. (2007) ‘River sediments provide a link between catchment pressures and ecological status in a mixed land use Scottish River system’, Water Research, 41(12), pp. 2803–2815.

Tian, Q., Fang, X., Zhang, W., Yang, Y. and Zhang, T. (2022) ‘Paleoecological and paleohydrological changes during the Eocene/Oligocene transition in the Qaidam Basin, NE Tibetan Plateau’, Journal of Asian Earth Sciences, 228(August 2021) Elsevier Ltd, p. 105130.

Upadhayay, H.R., Bodé, S., Griepentrog, M., Huygens, D., Bajracharya, R.M., Blake, W.H., Dercon, G., Mabit, L., Gibbs, M., Semmens, B.X., Stock, B.C., Cornelis, W. and Boeckx, P. (2017) ‘Methodological perspectives on the application of compound-specific stable isotope fingerprinting for sediment source apportionment’, Journal of Soils and Sediments, 17(6) Journal of Soils and Sediments, pp. 1537–1553.

Verstraeten, G., Van Oost, K., Van Rompaey, A., Poesen, J. and Govers, G. (2002) ‘Evaluating an integrated approach to catchment management to reduce soil loss and sediment pollution through modelling’, Soil Use and Management, 18(4), pp. 386–394.

Voulvoulis, N., Arpon, K.D. and Giakoumis, T. (2017) ‘The EU Water Framework Directive: From great expectations to problems with implementation’, Science of the Total Environment, 575 The Authors, pp. 358–366.

Wang, G., Wang, Y., Wei, Z., He, W., Ma, X., Sun, Z., Xua, L., Gong, J., Wang, Z. and Pan, Y. (2019) ‘Paleoclimate changes of the past 30 cal ka BP inferred from lipid biomarkers and geochemical records from Qionghai Lake southwest China’, Journal of Asian Earth Sciences, 172, pp. 346–358.

7 Conclusions

Quantifying land use sources and understanding the dynamics of organic carbon (OC) in river catchments is essential to reduce both on-site and off-site impacts of soil OC erosion. OC fingerprinting (OCF) is a popular tool to estimate the relative contribution of different land use sources to sediment OC, but this novel research has shown how it can also be an invaluable tool to understand catchment OC dynamics.

OCF and carbon loss modelling (a combination of "net" soil erosion modelling and OC spatial distribution modelling) was carried out using existing OC and *n*-alkane biomarker data from Carminowe Creek, a mixed land use catchment in Cornwall, UK (Objective 1; Chapter 2). While previous analysis of the data (Glendell et al., 2018) had revealed only a likely dominance of woodland soil OC (SOC) over arable SOC input to the stream. This unique combination of two sediment origin techniques crucially identified that riparian woodland disconnected upslope eroded SOC and, concomitantly, provided an input of woodland-derived OC to the streams, giving an increased understanding of sediment and OC transport processes in the study catchment.

Soil data from Loch Davan catchment Scotland has provided an unique, land use -specific dataset for soil and sediments containing: C and N content, bulk stable isotope $\delta^{13}C$ and $\delta^{15}N$, *n*-alkane concentrations, *n*-alkane compound-specific stable isotopes (CSSI) and short-chain (C<20) neutral lipid fatty acid biomarkers (SC-NLFA). The *n*-alkane concentration data from Carminowe Creek was only able to distinguish between two land uses, woodland and "not woodland" due to the similarity of the *n*-alkane signature in arable, temporary pasture (ley) and grassland land uses in that catchment. The Loch Davan catchment *n*-alkane concentrations, *n*-alkane CSSI and SC-NLFA biomarkers were used to find the effects of novel combinations of these biomarkers on land use source discrimination using a Bayesian un-mixing model (Objective 2; Chapter 3). In comparison to using only *n*-alkane concentrations, the combination of *n*-alkane concentration and CSSI improved the discrimination between arable and pasture land uses and using a combination of *n*-alkane concentration and SC-NLFA

reduced error when discriminating all four land uses (arable, pasture, forest and moorland).

Organic C fingerprinting using the longer-term accumulation of sediment on the streambed was required for comparison with the longer-term estimates of carbon loss modelling and the shorter-term suspended sediment (SS) samples provided evidence of intra-annual variation in OC sources (Objective 3; Chapter 4). An innovative, holistic approach assessed SS OC source proportions, in both streambed and suspended sediment, at a headwater sub-catchment and catchment scale. Different drivers of OC dynamics were detectable at the two different scales (sub-catchment and catchment scale), and different dominant land use sources were found in streambed and suspended sediment OC leading to improved identification of processes driving spatial and temporal OC dynamics. In addition, although OCF using *n*-alkanes is a valuable tool to estimate the relative contribution of different land use sources to sediment OC, there remain challenges in its application including i) effects on *n*-alkane signatures due to the sorting effect of particles by size during mobilization, transport and deposition and ii) ensuring all sources are included. The approaches presented in Chapter 4 provide a new method to address these key challenges in OCF and increased the confidence in source apportionment.

Soil erosion “hotspots” (where there is high risk of soil degradation) can be identified by modelling catchment erosion using a variety of different models such as the Revised Universal Soil Loss Equation (RUSLE) and the Scottish erosion risk map (ERM) of Lilly and Baggaley, (2018). In Chapter 5, a new method was presented of using streambed sediment land use -specific yields estimated using OCF as a benchmark to determine which erosion model best identified the relative land use OC yields in streambed sediment (Objective 4; Chapter 5). This method could be an invaluable new tool to assess the utility of these soil erosion risk models in identifying hotspots and guiding Best Management Practices (BMP).

The research has provided novel methods and datasets to improve determination of the dominant terrestrial land-use sources of organic carbon in freshwater

sediment at a catchment scale and identified catchment processes driving spatial and temporal changes in these sources. These methods will support the development of targeted sediment management strategies to reduce impacts on land productivity and water quality due to changes in climate and human activity. Ultimately, it will help to maintain the “healthy soils” that are a key part of policies and strategies to further climate, biodiversity and economic objectives within the EU and trying to ensure that, “by 2050, all soil ecosystems are in a healthy condition” (European Commission, 2021).

7.1 References

European Commission (2021) *EU Soil Strategy for 2030: Reaping the benefits of healthy soils for people, food, nature and climate*.

Glendell, M., Jones, R., Dungait, J.A.J., Meusburger, K., Schwendel, A.C., Barclay, R., Barker, S., Haley, S., Quine, T.A. and Meersmans, J. (2018) ‘Tracing of particulate organic C sources across the terrestrial-aquatic continuum, a case study at the catchment scale (Carminowe Creek, southwest England)’, *Science of the Total Environment*, 616, pp. 1077–1088. Available at: 10.1016/j.scitotenv.2017.10.211 (Accessed: 5 September 2018).

Lilly, A. and Baggaley, N.J. (2018) *Soil erosion risk map of Scotland* James Hutton Institute, Aberdeen

APPENDICES

Appendix A Loch Davan Data

The following tables are available at: “10.17862/cranfield.rd.19397651” where information on how to access other data used in this Thesis can also be found.

A.1 Loch Davan catchment soil and sediment samples

- Soil and bed sediment samples collected 18th-19th June 2019.
- Bed sediment samples: BS1 - bed sediment sample at Site 1, BS2 - bed sediment sample at Site 2 etc.
- Suspended sediment collectors were installed in the streams on the following dates: Sites 1 and 2: 18th June 2019, and Site 3 19th June 2019.
- Suspended sediment collected at the site and on the date recorded in the Sample ID (e.g. sample 270819-1 was collected at Site 1 on 27-08-2019 [sediment accumulated in the sediment collector between 19th June 2019 and 27th August 2019])
- Code N/A: no data available

Table 22 *N*-alkane concentration data (nano moles per g soil) for the Loch Davan catchment (BS = bed sediment data, SS suspended sediment data)

Land use	Sample ID	C23	C24	C25	C26	C27	C28	C29	C30	C31
Forest	A3	0.55	0.89	1.06	0.45	1.19	0.22	0.76	0.07	0.44
Forest	A4	0.28	0.76	0.25	0.32	0.38	0.20	0.54	0.09	0.81
Forest	A5	0.29	0.68	0.29	0.31	0.47	0.19	0.64	0.09	0.86
Forest	A6	0.42	0.62	0.49	0.27	0.62	0.13	0.48	0.05	0.40
Forest	A7	0.40	0.74	0.46	0.37	0.81	0.28	1.10	0.20	2.42
Forest	A8	0.70	0.91	1.27	0.47	1.52	0.22	0.74	0.07	0.41
Forest	A9	0.33	0.78	0.41	0.38	0.74	0.33	1.07	0.21	1.97
Forest	A10	0.42	0.69	0.38	0.40	0.76	0.56	1.59	0.30	1.97
Forest	A11	1.00	0.96	1.45	0.63	1.74	0.28	1.48	0.15	1.57
Forest	A12	0.25	0.88	1.22	0.48	1.97	0.43	2.13	0.31	4.77
Forest	A13	0.89	0.43	1.02	0.34	1.61	0.27	1.60	0.19	3.32
Forest	A14	0.52	0.74	0.57	0.43	0.85	0.35	1.25	0.21	2.03
Pasture	A16	0.51	0.63	0.71	0.31	0.79	0.17	0.74	0.09	0.63
Arable	A17	0.53	0.50	0.70	0.32	1.10	0.32	1.45	0.12	0.90
Arable	A18	1.50	0.78	2.31	0.69	3.05	0.31	1.81	0.09	0.73

Arable	A19	0.28	0.69	0.45	0.39	0.57	0.27	0.65	0.18	0.67
Arable	A20	0.65	0.59	0.83	0.41	1.30	0.51	2.15	0.43	2.91
Arable	A23	0.32	0.60	0.65	0.40	1.18	0.46	2.21	0.42	3.07
Arable	A24	1.55	0.44	1.65	0.38	2.21	0.24	1.52	0.09	0.79
Arable	A26	0.65	0.30	0.79	0.25	1.29	0.24	1.40	0.15	1.38
Arable	A28	0.30	0.28	0.32	0.12	0.97	0.26	1.49	0.14	1.65
Arable	A30	0.59	0.22	0.71	0.18	0.97	0.17	1.12	0.13	1.35
Arable	A31	0.48	0.41	0.64	0.25	1.13	0.26	1.55	0.18	1.87
Arable	A32	0.60	0.30	0.64	0.22	0.94	0.20	1.38	0.19	2.12
Moorland	A33	3.61	0.35	0.86	0.32	2.81	0.90	5.77	0.52	11.00
Moorland	A34	0.07	0.69	0.17	0.27	0.46	0.31	0.97	0.21	1.47
Moorland	A35	1.27	1.24	1.15	0.45	2.64	0.82	4.59	0.51	9.13
Moorland	A36	0.73	0.63	1.15	0.38	1.45	0.30	1.53	0.17	1.51
Moorland	A37	2.94	1.36	4.52	1.24	4.44	0.52	2.93	0.21	1.77
Moorland	A38	1.16	0.58	0.95	0.46	2.19	0.68	3.22	0.40	7.30
Moorland	A40	0.62	0.81	0.63	0.54	1.27	0.65	3.45	0.67	10.53
Moorland	A41	0.47	0.64	0.58	0.46	1.48	0.53	2.60	0.42	6.20
Moorland	A42	1.09	0.98	1.31	0.78	3.08	1.00	10.18	1.15	21.02
Moorland	A44	0.25	0.83	0.61	0.46	1.33	0.55	2.50	0.34	3.14
Forest	A45	0.31	0.53	0.39	0.26	0.70	0.21	0.83	0.11	1.34
Moorland	A46	2.94	0.89	2.46	0.81	5.74	1.20	13.76	1.66	37.69
Moorland	A47	0.37	0.82	0.79	0.49	1.41	0.52	2.58	0.52	7.80
Moorland	A48	0.77	0.76	0.76	0.48	1.42	0.56	2.95	0.41	6.53
Moorland	A49	1.27	0.79	1.10	0.68	2.63	0.98	6.76	0.77	13.58
Moorland	A50	0.39	0.63	0.41	0.39	1.63	0.68	2.03	0.19	2.40
Arable	A51	0.29	0.70	0.44	0.38	0.51	0.25	0.62	0.15	0.59
Pasture	A52	0.42	0.59	0.60	0.37	0.79	0.23	0.83	0.12	0.71
Pasture	A53	0.41	1.02	0.19	0.59	0.20	0.50	0.22	0.26	0.24
Arable	A54	0.54	1.33	0.27	0.88	0.37	0.76	0.44	0.40	0.52
Arable	A55	0.36	1.30	0.27	0.70	0.31	0.55	0.33	0.35	0.37
Pasture	A56	0.61	1.04	0.37	0.65	0.41	0.55	0.33	0.29	0.25
Pasture	A57	0.22	0.24	0.07	0.20	0.11	0.16	0.13	0.09	0.12
Pasture	A58	0.63	1.03	0.36	0.75	0.42	0.61	0.49	0.32	0.50

Pasture	A59	0.74	1.51	0.29	0.60	0.25	0.29	0.13	0.08	0.08
Pasture	A60	0.50	1.33	0.27	0.73	0.29	0.52	0.26	0.27	0.24
Pasture	A61	0.48	0.81	0.15	0.48	0.16	0.40	0.15	0.19	0.13
Pasture	A62	0.48	0.80	0.11	0.44	0.10	0.32	0.09	0.13	0.07
Pasture	A63	0.44	1.22	0.16	0.56	0.17	0.42	0.17	0.20	0.18
Pasture	A64	0.14	0.18	0.03	0.13	0.04	0.10	0.04	0.05	0.04
Moorland	A65	0.92	0.49	0.23	0.34	0.50	0.35	0.68	0.16	0.99
Pasture	A66	0.45	1.10	0.23	0.62	0.27	0.49	0.30	0.28	0.31
Pasture	A67	0.54	0.91	0.28	0.75	0.41	0.66	0.37	0.34	0.32
Pasture	A68	0.32	0.72	0.11	0.54	0.14	0.48	0.16	0.28	0.16
Pasture	A69	0.53	1.44	0.37	1.02	0.51	0.99	0.67	0.69	0.84
Pasture	A70	0.62	1.09	0.28	0.87	0.34	0.86	0.31	0.49	0.26
Pasture	A71	0.70	1.34	0.48	0.80	0.63	0.76	0.60	0.45	0.63
Forest	A72	0.75	2.62	0.51	2.78	1.00	1.34	0.95	0.54	1.61
Moorland	A73	0.59	0.94	0.68	1.46	2.39	2.08	8.82	1.21	10.17
Moorland	A74	0.10	0.10	0.07	0.16	0.16	0.13	0.47	0.08	0.55
Arable	A77	0.35	1.46	0.24	0.53	0.23	0.37	0.19	0.18	0.20
Forest	A78	0.79	2.13	0.49	1.65	0.55	0.46	0.30	0.09	0.26
Pasture	A79	0.60	1.38	0.24	0.67	0.27	0.52	0.27	0.29	0.27
Arable	A80	0.34	0.86	0.15	0.53	0.16	0.44	0.18	0.25	0.18
Forest	A101	0.90	1.82	0.34	1.62	0.55	0.88	0.83	0.32	1.08
BS	BS1	0.14	0.36	0.16	0.17	0.28	0.11	0.23	0.06	0.09
BS	BS2	0.14	0.50	0.20	0.24	0.32	0.16	0.20	0.09	0.09
BS	BS3	0.12	0.33	0.14	0.17	0.22	0.11	0.21	0.05	0.13
SS	270819-1	0.36	0.63	0.55	0.29	0.88	0.19	0.78	0.09	0.43
SS	110220-1	0.40	0.99	0.73	0.41	1.42	0.33	1.32	0.18	0.88
SS	140420-1	0.31	0.75	0.57	0.39	1.08	0.32	1.25	0.19	0.86
SS	040620-1	1.64	0.99	2.02	0.62	2.78	0.30	2.23	0.14	1.23
SS	290720-1	1.39	0.90	1.57	0.48	1.72	0.23	1.44	0.11	0.93
SS	220920-1	0.46	0.60	0.69	0.28	1.09	0.22	1.00	0.12	0.67
SS	171120-1	0.18	0.72	0.34	0.28	0.60	0.21	0.69	0.12	0.42
SS	270819-2	0.51	0.53	0.41	0.26	0.62	0.11	0.45	N/A	0.26
SS	231019-2	0.51	0.28	0.51	0.18	0.74	0.12	0.65	0.05	0.44

SS	171219-2	1.13	0.54	1.67	0.36	2.13	0.23	1.66	0.09	1.03
SS	110220-2	0.57	0.91	2.22	0.76	4.43	0.93	4.57	0.20	1.42
SS	140420-2	0.57	0.71	0.73	0.31	1.03	0.22	0.79	0.09	0.45
SS	040620-2	0.99	0.61	1.41	0.35	1.85	0.21	1.26	N/A	0.56
SS	290720-2	0.96	0.67	1.49	0.50	2.23	0.36	1.78	0.15	1.03
SS	220920-2	0.68	0.82	1.07	0.40	1.47	0.31	1.26	0.14	0.82
SS	171120-2	0.23	0.64	0.45	0.25	0.77	0.22	0.62	0.10	0.36
SS	270819-3	1.21	0.63	1.56	0.42	2.25	0.25	1.65	N/A	0.75
SS	231019-3	0.37	0.90	0.59	0.37	0.98	0.25	0.93	0.14	0.54
SS	171219-3	0.43	0.77	1.02	0.46	2.01	0.44	2.17	0.25	1.37
SS	110220-3	0.62	0.99	0.92	0.41	1.50	0.30	1.37	0.20	0.89
SS	140420-3	0.62	0.90	1.08	0.46	1.88	0.36	1.71	0.19	0.96
SS	040620-3	0.46	0.55	0.70	0.27	1.17	0.23	1.20	0.13	0.87
SS	290720-3	1.86	1.11	2.12	0.70	2.99	0.37	2.53	0.19	1.62
SS	220920-3	1.22	0.90	1.46	0.54	2.11	0.30	1.92	0.16	1.17
SS	171120-3	0.18	0.54	0.32	0.21	0.62	0.16	0.52	0.09	0.31

Table 23 *N*-alkane compound-specific $\delta^{13}C$ (‰) data for the Loch Davan catchment (BS = bed sediment data, SS suspended sediment data)

Land use	Sample ID	C23	C24	C25	C26	C27	C28	C29	C30	C31
Forest	A3	-26.53	-31.79	-33.55	-32.40	-33.82	-35.12	-35.71	-33.81	-38.72
Forest	A4	-45.46	-30.41	-34.41	-31.12	-35.14	-34.01	-36.25	-35.73	-36.40
Forest	A5	-34.55	-30.37	-33.33	-30.39	-34.92	-33.28	-35.93	-37.53	-36.45
Forest	A6	-34.27	-31.42	-34.38	-31.96	-34.74	-35.30	-37.42	-35.39	-38.50
Forest	A7	-32.68	-29.87	-33.34	-31.82	-35.27	-35.31	-36.32	-35.41	-36.40
Forest	A8	-34.32	-31.79	-33.55	-32.31	-32.75	-33.98	-34.30	-35.33	-37.33
Forest	A9	-27.37	-29.82	-33.07	-30.76	-33.28	-33.63	-34.60	-33.93	-35.25
Forest	A10	-32.04	-29.78	-34.02	-32.31	-34.45	-34.86	-34.67	-37.63	-36.08
Forest	A11	-29.30	-30.52	-33.09	-31.28	-32.70	-33.32	-33.86	-33.55	-34.92
Forest	A12	-37.45	-30.50	-32.31	-30.89	-33.32	-34.92	-36.28	-34.88	-36.05
Forest	A13	-32.08	-33.50	-32.39	-33.55	-32.27	-34.95	-34.21	-36.51	-35.05

Forest	A14	-34.01	-32.41	-32.83	-32.36	-34.79	-33.70	-36.31	-34.17	-35.87
Pasture	A16	-33.01	-32.16	-34.26	-32.51	-35.29	-32.75	-37.43	-35.55	-38.87
Arable	A17	-32.90	-32.14	-34.70	-32.56	-36.00	-35.51	-37.23	-36.21	-37.74
Arable	A18	-32.96	-33.00	-32.80	-32.92	-32.05	-34.97	-33.87	-37.53	-37.43
Arable	A19	-36.28	-30.80	-33.91	-31.54	-34.55	-33.65	-36.74	-32.78	-37.50
Arable	A20	-30.93	-30.60	-33.58	-31.98	-34.43	-34.19	-36.11	-34.22	-35.82
Arable	A23	-32.25	-26.09	-33.57	-33.18	-34.95	-33.76	-36.29	-34.56	-37.24
Arable	A24	-34.25	-24.76	-33.90	-32.87	-34.64	-35.04	-35.45	-34.71	-36.86
Arable	A26	-31.50	-20.50	-24.04	-33.90	-34.62	-33.91	-36.09	-34.40	-36.69
Arable	A28	-30.50	-23.42	-31.08	-24.86	-35.37	-33.26	-36.07	-32.91	-36.71
Arable	A30	-29.45	-19.72	-32.78	-26.68	-33.38	-33.26	-35.48	-35.66	-35.73
Arable	A31	-32.91	-30.80	-32.05	-31.59	-34.49	-34.60	-36.14	-34.47	-36.75
Arable	A32	-30.22	-16.90	-32.02	-27.94	-33.97	-32.20	-35.12	-33.24	-35.56
Moorland	A33	-35.37	-15.19	-29.42	-30.95	-35.71	-35.35	-36.32	-35.88	-35.82
Moorland	A34	-50.58	-26.48	-31.75	-29.40	-34.96	-32.12	-35.90	-31.64	-35.89
Moorland	A35	-34.73	-30.47	-32.69	-30.70	-35.53	-35.25	-36.43	-35.19	-35.94
Moorland	A36	-16.72	-30.03	-33.43	-32.46	-34.49	-34.88	-35.83	-35.89	-36.62
Moorland	A37	-36.55	-33.45	-33.07	-32.79	-33.04	-35.24	-35.35	-35.68	-36.46
Moorland	A38	-34.70	-32.06	-33.53	-32.78	-35.76	-35.34	-35.78	-35.27	-35.13
Moorland	A40	-26.89	-31.70	-34.28	-32.40	-34.30	-33.23	-34.27	-34.61	-34.27
Moorland	A41	-21.51	-32.63	-34.15	-33.27	-35.17	-34.45	-35.47	-34.75	-35.32
Moorland	A42	-33.83	-30.55	-34.10	-32.57	-35.23	-34.46	-34.70	-36.20	-35.23
Moorland	A44	-22.42	-30.46	-34.78	-31.63	-36.14	-34.63	-36.45	-34.80	-36.99
Forest	A45	-27.65	-28.42	-32.32	-29.73	-34.72	-33.47	-35.74	-35.41	-36.49
Moorland	A46	-36.00	-32.55	-35.89	-33.21	-35.91	-34.90	-35.68	-36.22	-35.25
Moorland	A47	-32.04	-29.49	-31.91	-30.66	-33.46	-33.49	-35.14	-34.12	-34.32
Moorland	A48	-32.32	-30.04	-33.53	-32.11	-35.23	-34.78	-34.99	-34.87	-34.82
Moorland	A49	-32.86	-32.09	-33.21	-33.28	-34.02	-34.20	-33.43	-34.90	-33.65
Moorland	A50	-31.44	-29.50	-32.68	-32.13	-36.86	-36.16	-36.26	-35.20	-36.20
Arable	A51	-25.73	-28.94	-32.48	-30.75	-34.04	-31.89	-36.27	-32.02	-36.93
Pasture	A52	-33.64	-29.44	-33.45	-31.60	-34.51	-33.40	-35.94	-35.38	-36.66
Pasture	A53	-30.86	-34.24	-34.37	-35.48	-35.74	-36.66	-37.75	-37.51	-38.39
Arable	A54	-31.95	-34.11	-33.58	-35.04	-35.60	-35.67	-36.16	-36.34	-36.19

Arable	A55	-32.98	-34.62	-34.71	-34.15	-34.36	-35.33	-36.62	-35.94	-36.63
Pasture	A56	-40.60	-34.46	-34.39	-35.18	-34.46	-36.22	-36.21	-36.97	-38.48
Pasture	A57	-36.13	-35.02	-34.38	-35.51	-34.85	-35.80	-35.62	-36.37	-36.49
Pasture	A58	-35.59	-34.18	-34.49	-35.45	-35.14	-35.98	-36.01	-36.80	-36.78
Pasture	A59	-41.85	-34.24	-34.75	-35.20	-35.41	-36.42	-37.51	-37.71	-39.48
Pasture	A60	-33.46	-33.62	-34.65	-34.73	-35.47	-35.63	-37.33	-37.07	-38.05
Pasture	A61	-34.22	-34.85	-34.28	-35.54	-35.89	-36.31	-37.86	-37.43	-39.20
Pasture	A62	-68.82	-34.45	-33.92	-35.55	-36.90	-36.94	-38.88	-38.29	-40.92
Pasture	A63	-35.06	-33.71	-33.55	-34.25	-35.34	-35.87	-37.37	-37.05	-37.85
Pasture	A64	-46.04	-35.32	-35.81	-36.09	-36.88	-36.51	-37.53	-37.22	-38.32
Moorland	A65	-28.11	-33.73	-33.63	-34.36	-34.97	-35.37	-35.48	-36.46	-35.11
Pasture	A66	-31.99	-33.16	-33.77	-34.07	-34.84	-34.93	-36.26	-35.98	-36.95
Pasture	A67	-40.61	-34.99	-34.76	-35.37	-34.67	-36.19	-36.49	-36.79	-38.27
Pasture	A68	-32.47	-33.51	-33.61	-34.19	-34.64	-35.16	-36.86	-36.05	-38.88
Pasture	A69	-48.24	-33.34	-34.12	-34.33	-34.88	-35.15	-36.50	-36.17	-37.12
Pasture	A70	-32.65	-33.58	-32.64	-35.54	-33.60	-35.36	-36.44	-35.84	-38.48
Pasture	A71	-33.98	-34.22	-34.05	-34.37	-34.33	-35.32	-35.65	-36.18	-36.14
Forest	A72	-31.26	-30.19	-31.16	-29.93	-32.74	-31.47	-34.16	-23.02	-33.45
Moorland	A73	-32.44	-33.03	-32.86	-33.90	-34.89	-35.15	-33.58	-35.32	-34.02
Moorland	A74	-32.99	-32.58	-33.45	-34.11	-35.27	-34.87	-33.62	-35.52	-34.29
Arable	A77	-32.27	-33.73	-34.26	-34.51	-34.63	-35.15	-36.56	-35.78	-36.74
Forest	A78	-78.77	-31.15	-32.07	-31.48	-33.92	-33.31	-36.52	-34.74	-36.17
Pasture	A79	-33.58	-33.54	-33.85	-34.27	-34.25	-34.92	-35.57	-35.87	-36.58
Arable	A80	-35.39	-33.89	-34.20	-34.81	-34.52	-35.60	-37.11	-36.14	-37.74
Forest	A101	-31.77	-32.35	-33.45	-32.61	-35.70	-34.34	-35.88	-35.71	-35.41
BS	BS1	-28.35	-31.16	-34.16	-30.34	-35.59	-30.18	-32.53	-31.69	-33.88
BS	BS2	-28.72	-28.23	-30.09	-30.57	-31.89	-29.03	-33.56	-31.54	-34.89
BS	BS3	-36.77	-30.45	-31.68	-30.05	-32.30	-30.51	-33.98	-31.51	-35.28
SS	270819-1	-37.13	-31.60	-34.00	-33.22	-35.11	-32.08	-36.41	-32.30	-37.69
SS	110220-1	-7.22	-32.37	-35.51	-32.23	-35.17	-32.41	-35.97	-32.10	-37.08
SS	140420-1	-36.20	-32.36	-35.18	-31.71	-35.16	-31.89	-35.83	-33.74	-36.93
SS	040620-1	-33.04	-31.00	-32.21	-28.70	-34.01	-34.19	-35.33	-35.55	-36.44
SS	290720-1	-31.22	-29.81	-31.78	-30.29	-33.49	-32.07	-35.75	-28.61	-37.07

SS	220920-1	-35.50	-32.93	-35.16	-33.11	-34.57	-31.41	-35.75	-30.56	-36.86
SS	171120-1	-35.05	-31.86	-33.16	-28.99	-34.28	-32.40	-35.54	-30.16	-36.38
SS	270819-2	-33.12	-29.40	-32.88	-32.12	-33.96	-35.30	-36.64	N/A	-37.92
SS	231019-2	-32.83	-32.39	-34.28	-33.34	-33.98	-32.95	-35.57	-36.95	-36.19
SS	171219-2	-35.00	-31.71	-34.34	-32.52	-34.53	-35.80	-36.41	-36.48	-37.08
SS	110220-2	-34.89	-31.93	-33.04	-31.66	-34.97	-36.41	-35.47	-33.28	-36.71
SS	140420-2	-34.31	-31.77	-33.92	-29.26	-34.21	-33.41	-35.70	-33.98	-36.78
SS	040620-2	-34.47	-32.40	-33.92	-33.71	-33.80	-34.93	-34.80	N/A	-35.64
SS	290720-2	-34.97	-32.47	-33.27	-32.82	-33.63	-33.91	-34.90	-35.72	-35.96
SS	220920-2	-15.67	-31.02	-33.38	-31.75	-33.80	-32.68	-35.30	-33.22	-35.87
SS	171120-2	-35.28	-36.03	-33.71	-21.05	-32.47	-31.98	-34.03	-30.09	-35.91
SS	270819-3	-35.61	-35.05	-35.44	-35.07	-35.45	-36.63	-36.23	N/A	-37.28
SS	231019-3	-39.47	-32.04	-34.95	-31.53	-34.45	-33.64	-36.64	-32.59	-37.22
SS	171219-3	-34.80	-32.73	-34.56	-33.84	-35.26	-33.47	-35.65	-29.30	-36.63
SS	110220-3	-34.94	-31.87	-34.39	-30.12	-35.28	-32.70	-35.34	-30.56	-36.25
SS	140420-3	-35.41	-33.51	-34.61	-32.99	-33.97	-31.97	-35.38	-31.11	-36.34
SS	040620-3	-34.11	-33.30	-35.00	-33.41	-34.13	-30.12	-36.23	-30.54	-37.01
SS	290720-3	-33.50	-29.97	-32.49	-29.04	-34.03	-30.64	-35.52	-35.45	-36.21
SS	220920-3	-32.65	-30.93	-32.73	-28.40	-32.81	-30.56	-35.37	-32.30	-36.51
SS	171120-3	-33.61	-33.28	-34.41	-24.41	-34.16	-31.94	-35.60	-31.22	-36.45

Table 24 Neutral lipid fatty acid (NLFA) concentrations (nano moles ester per g soil) for the Loch Davan catchment (BS = bed sediment data).

Land use	Sample ID	i15:0	a15:0	16:00	10-Me-16:0	12-Me-16:0	18:2w6,9	18:00
Forest	L3	10.48	5.24	37.17	3.54	3.23	22.18	18.17
Forest	L4	16.40	6.81	42.75	10.25	3.11	9.22	11.45
Forest	L5	19.62	7.82	45.38	7.92	3.02	6.50	9.75
Forest	L6	19.78	8.54	37.17	14.35	4.70	5.69	9.77
Forest	L7	12.65	9.10	39.64	18.89	5.28	4.46	9.96
Forest	L8	18.75	7.55	39.15	3.21	3.90	7.79	19.65
Forest	L9	18.77	6.96	38.07	12.40	3.32	9.87	10.60

Forest	L10	20.99	6.91	36.38	15.55	3.56	9.71	6.90
Forest	L11	19.07	8.71	40.77	11.66	3.92	5.80	10.07
Forest	L12	10.38	5.59	44.15	7.06	2.47	6.22	24.14
Forest	L13	22.83	8.63	37.76	8.75	3.21	7.60	11.21
Forest	L14	13.03	7.58	50.09	5.04	3.84	10.72	9.71
Pasture	L16	17.18	8.28	39.73	12.63	4.76	6.08	11.33
Arable	L17	12.07	12.65	47.57	5.81	3.63	4.68	13.59
Arable	L18	7.56	11.10	36.18	6.49	8.22	10.54	19.91
Arable	L19	14.76	11.28	44.87	6.42	4.35	3.97	14.35
Arable	L20	6.91	4.80	59.27	3.24	3.07	10.95	11.77
Arable	L23	2.28	4.21	25.35	1.63	2.10	47.81	16.62
Arable	L24	9.29	5.00	24.66	1.48	4.76	38.08	16.73
Arable	L26	4.97	4.72	34.28	1.12	2.68	35.72	16.52
Arable	L28	1.90	3.39	45.69	1.85	1.69	32.99	12.49
Arable	L30	2.56	4.90	29.11	2.76	3.42	40.15	17.10
Arable	L31	2.04	3.62	45.34	1.10	2.08	33.04	12.79
Arable	L32	5.94	4.45	25.77	1.52	3.27	40.81	18.24
Moorland	L33	5.93	5.63	47.77	2.65	2.37	23.17	12.49
Moorland	L34	8.23	4.17	45.94	1.74	1.54	26.80	11.58
Moorland	L35	6.15	3.82	48.91	1.88	1.61	25.38	12.26
Moorland	L36	5.98	4.62	35.06	1.14	2.21	34.46	16.54
Moorland	L37	9.70	7.06	35.31	3.32	3.20	27.45	13.96
Moorland	L38	7.52	6.41	36.06	2.01	2.08	37.70	8.22
Moorland	L40	4.57	4.63	34.83	1.42	2.60	44.57	7.39
Moorland	L41	5.50	3.79	41.71	1.83	1.88	32.30	12.98
Moorland	L42	2.17	3.33	36.02	1.19	2.23	48.24	6.82
Moorland	L44	4.37	2.85	58.40	0.83	1.21	22.67	9.69
Forest	L45	3.41	4.72	36.76	2.32	2.77	39.69	10.33
Moorland	L46	7.01	3.52	34.86	1.74	1.50	36.94	14.44
Moorland	L47	6.74	3.92	44.05	2.55	1.86	28.57	12.31
Moorland	L48	6.94	3.54	40.65	1.49	1.90	32.49	12.98
Moorland	L49	2.91	2.47	45.39	1.18	1.34	38.00	8.72
Moorland	L50	5.17	4.71	34.03	1.99	1.56	35.78	16.76

Arable	L51	4.82	5.44	31.25	2.13	2.66	41.54	12.15
Pasture	L52	2.69	5.21	28.54	2.93	3.72	44.12	12.79
Pasture	L53	6.78	5.02	32.40	2.34	2.96	29.54	20.96
Arable	L54	5.68	3.79	52.53	1.47	1.92	22.67	11.93
Arable	L55	5.98	5.53	31.22	2.43	2.92	37.60	14.32
Pasture	L56	4.74	3.76	43.65	1.63	3.14	28.55	14.52
Pasture	L57	3.90	3.68	47.77	1.80	1.71	28.66	12.47
Pasture	L58	3.82	2.93	54.47	1.30	1.75	21.93	13.80
Pasture	L59	5.04	4.29	40.34	1.53	2.65	30.42	15.73
Pasture	L60	3.03	4.07	34.99	1.89	3.19	36.65	16.18
Pasture	L61	2.42	4.61	40.46	1.96	2.31	31.82	16.41
Pasture	L62	9.84	6.93	61.93	4.87	2.74	4.43	9.26
Pasture	L63	14.97	9.46	49.13	6.86	3.69	4.15	11.75
Pasture	L64	9.33	6.36	61.05	4.20	2.81	5.42	10.85
Moorland	L65	13.36	6.03	57.83	3.82	2.80	5.99	10.17
Pasture	L66	11.99	6.90	51.53	3.66	3.94	7.94	14.05
Pasture	L67	7.46	6.89	51.41	5.06	4.10	7.88	17.20
Pasture	L68	8.73	10.34	38.38	6.67	6.26	8.24	21.38
Pasture	L69	13.33	9.37	45.56	4.65	3.80	6.46	16.83
Pasture	L70	15.84	10.93	46.06	6.59	4.28	3.99	12.30
Pasture	L71	13.43	8.95	49.14	5.45	4.14	4.43	14.46
Forest	L72	13.16	7.45	49.35	11.93	3.59	3.88	10.65
Moorland	L73	12.96	4.68	44.23	9.23	1.94	20.86	6.09
Moorland	L74	11.97	5.50	44.07	7.81	2.08	23.06	5.51
Arable	L77	9.52	8.68	33.92	5.05	5.88	6.77	30.17
Forest	L78	12.92	4.74	41.54	22.11	3.48	3.96	11.25
Pasture	L79	10.41	7.63	38.26	5.26	5.78	7.53	25.14
Arable	L80	4.08	5.03	50.80	3.60	3.86	8.59	24.03
Forest	L101	13.83	6.70	47.34	12.76	3.02	5.21	11.15
BS	BS1	4.94	15.80	35.63	5.94	11.00	12.88	13.80
BS	BS2	4.79	19.51	30.85	11.83	12.55	4.90	15.58
BS	BS3	6.32	16.65	33.93	8.16	10.69	8.64	15.61

Table 25 Neutral lipid fatty acid (NLFA) compound-specific $\delta^{13}C$ (‰) data for the Loch Davan catchment (BS = bed sediment data)

Land use	Sample ID	i15:0	a15:0	16:00	10-Me-16:0	12-Me-16:0	18:2w6,9	18:00
Forest	L3	-31.23	-40.52	-34.35	-32.27	-31.75	-33.31	-36.72
Forest	L4	-28.07	-26.38	-32.86	-28.85	-30.27	-32.57	-33.57
Forest	L5	-30.17	-27.90	-36.84	-30.21	-28.65	-31.07	-32.26
Forest	L6	-30.60	-29.94	-33.80	-30.19	-30.69	-32.61	-34.54
Forest	L7	-30.23	-28.35	-32.90	-29.81	-29.52	-31.93	-33.13
Forest	L8	-31.35	-32.40	-34.30	-32.77	-31.50	-21.71	-34.60
Forest	L9	-29.53	-28.65	-33.32	-30.62	-32.06	-17.66	-34.54
Forest	L10	-29.46	-28.13	-32.38	-29.71	-29.52	-24.11	-30.38
Forest	L11	-31.46	-30.03	-32.56	-32.39	-30.44	-21.15	-36.23
Forest	L12	-30.01	-27.15	-32.73	-30.07	-28.24	-31.79	-35.90
Forest	L13	-29.58	-28.73	-33.04	-30.95	-30.48	-33.14	-38.23
Forest	L14	-30.64	-27.80	-32.87	-32.11	-29.31	-33.38	-33.68
Pasture	L16	-29.87	-29.21	-33.85	-30.42	-30.31	-31.98	-33.98
Arable	L17	-32.59	-31.40	-34.21	-34.42	-32.30	-33.35	-36.29
Arable	L18	-30.05	-27.82	-34.02	-47.27	-30.71	-33.53	-34.53
Arable	L19	-31.89	-30.00	-33.78	-34.86	-30.81	-33.65	-36.15
Arable	L20	-30.38	-28.94	-32.94	-45.39	-31.39	-31.55	-35.73
Arable	L23	-30.18	-28.96	-35.31	-61.23	-28.27	-33.32	-37.31
Arable	L24	-30.73	-28.40	-35.31	-53.15	-32.18	-33.22	-36.70
Arable	L26	-33.11	-29.64	-34.45	-61.04	-32.52	-34.07	-38.18
Arable	L28	-31.37	-27.85	-34.09	-31.05	-29.69	-33.06	-36.56
Arable	L30	-29.15	-28.23	-34.32	-32.01	-31.25	-33.35	-35.50
Arable	L31	-31.36	-28.72	-34.19	-66.56	-29.14	-33.21	-35.52
Arable	L32	-29.53	-27.42	-34.11	-61.20	-31.65	-33.32	-35.30
Moorland	L33	-31.38	-28.55	-33.98	-31.42	-31.64	-32.39	-36.24
Moorland	L34	-30.57	-29.64	-33.99	-30.73	-31.20	-32.64	-37.03
Moorland	L35	-31.40	-44.66	-33.98	-31.11	-31.28	-32.89	-36.85
Moorland	L36	-30.40	-28.57	-34.54	-68.57	-31.46	-33.86	-37.59
Moorland	L37	-32.30	-30.27	-35.35	-34.34	-33.12	-33.10	-36.26

Moorland	L38	-12.38	-42.68	-34.08	-44.74	-33.56	-33.00	-35.55
Moorland	L40	-30.75	-29.25	-33.94	-53.06	-38.46	-32.64	-33.37
Moorland	L41	-30.55	-28.50	-34.58	-32.65	-34.50	-32.86	-38.14
Moorland	L42	-31.67	-29.08	-35.43	-54.54	-33.26	-33.53	-37.10
Moorland	L44	-29.81	-27.77	-33.78	-57.10	-31.46	-33.65	-36.71
Forest	L45	-30.24	-29.06	-34.70	-29.99	-30.74	-33.44	-35.57
Moorland	L46	-31.43	-29.01	-35.62	-33.20	-31.85	-33.13	-36.74
Moorland	L47	-31.30	-45.67	-35.13	-32.10	-31.52	-33.74	-36.14
Moorland	L48	-30.97	-30.50	-33.07	-32.45	-32.82	-32.45	-37.42
Moorland	L49	-29.30	-29.05	-32.54	-32.33	-33.21	-34.10	-37.09
Moorland	L50	-31.21	-44.92	-34.87	-31.51	-30.01	-33.78	-36.86
Arable	L51	-31.77	-28.78	-34.99	-29.25	-45.46	-33.06	-36.98
Pasture	L52	-31.95	-29.05	-34.78	-32.79	-32.11	-33.28	-36.68
Pasture	L53	-31.02	-46.95	-36.21	-25.92	-32.87	-33.84	-38.67
Arable	L54	-31.66	-45.94	-34.47	-32.33	-34.66	-33.61	-37.68
Arable	L55	-32.87	-48.04	-35.51	-23.26	-32.50	-33.43	-37.41
Pasture	L56	-32.12	-28.59	-34.89	-31.35	-32.39	-33.64	-38.10
Pasture	L57	-30.45	-46.17	-34.25	-31.63	-33.24	-33.19	-36.88
Pasture	L58	-32.07	-45.91	-33.52	-33.38	-32.03	-33.66	-37.55
Pasture	L59	-32.83	-48.60	-34.78	-21.89	-33.26	-33.86	-37.94
Pasture	L60	-32.84	-45.94	-33.79	-30.06	-32.31	-32.34	-36.22
Pasture	L61	-32.11	-28.95	-34.26	-32.14	-32.51	-33.26	-37.71
Pasture	L62	-32.67	-30.72	-34.15	-34.24	-32.49	-34.46	-36.87
Pasture	L63	-33.86	-32.76	-34.28	-33.96	-31.34	-33.84	-35.82
Pasture	L64	-32.48	-29.76	-34.02	-34.97	-31.96	-34.75	-37.08
Moorland	L65	-29.68	-28.52	-31.90	-31.36	-29.79	-32.66	-34.77
Pasture	L66	-30.55	-29.47	-34.56	-43.30	-31.45	-34.30	-37.01
Pasture	L67	-30.80	-28.88	-33.80	-32.03	-31.28	-33.06	-37.77
Pasture	L68	-33.37	-29.41	-34.26	-32.70	-30.48	-32.68	-38.38
Pasture	L69	-32.45	-29.98	-35.31	-36.65	-32.41	-35.39	-37.83
Pasture	L70	-31.89	-30.11	-34.48	-33.18	-32.06	-33.82	-36.99
Pasture	L71	-31.55	-30.18	-34.11	-36.15	-32.02	-33.87	-38.05
Forest	L72	-30.61	-33.80	-34.44	-31.63	-30.44	-31.15	-34.19

Moorland	L73	-30.34	-27.92	-32.93	-31.27	-31.17	-31.05	-33.48
Moorland	L74	-31.11	-29.93	-33.76	-31.36	-30.78	-36.59	-34.40
Arable	L77	-31.85	-28.29	-34.73	-32.75	-31.39	-22.90	-37.41
Forest	L78	-30.26	-34.34	-34.31	-29.75	-31.73	-32.79	-33.99
Pasture	L79	-29.82	-27.50	-34.03	-48.56	-30.38	-23.78	-37.99
Arable	L80	-29.09	-26.81	-35.65	-49.56	-31.59	-36.38	-37.86
Forest	L101	-31.10	-29.07	-34.20	-31.25	-31.41	-32.83	-36.94
BS	BS1	-10.01	-29.08	-34.74	-36.59	-29.89	-38.17	-36.95
BS	BS2	-30.86	-29.82	-32.04	-46.30	-29.43	-21.08	-34.27
BS	BS3	-8.90	-30.35	-34.90	-42.22	-31.24	-25.89	-38.22

Table 26 C (%, w/w), N (%, w/w), $\delta^{13}C$ (‰) and $\delta^{15}N$ (‰) for the Loch Davan catchment (BS = bed sediment data, SS suspended sediment data)

Land Use	Sample ID	C (%, w/w)	$\delta^{13}C$ (‰)	N (%, w/w)	$\delta^{15}N$ (‰)
Forest	3	11.02	-29.18	0.81	4.47
Forest	4	8.92	-28.78	0.38	2.23
Forest	5	10.41	-28.36	0.53	3.31
Forest	6	6.35	-28.21	0.34	2.86
Forest	7	20.85	-28.35	0.70	3.32
Forest	8	5.70	-29.35	0.30	3.42
Forest	9	7.54	-28.42	0.22	3.35
Forest	10	27.55	-28.38	0.78	3.96
Forest	11	31.84	-28.81	1.59	2.05
Forest	12	7.95	-28.74	0.46	3.58
Forest	13	4.46	-28.80	0.19	1.15
Forest	14	8.95	-28.71	0.42	4.04
Pasture	16	3.42	-29.72	0.30	5.24
Arable	17	5.58	-29.76	0.41	2.58
Arable	18	3.94	-29.15	0.26	3.88
Arable	19	3.25	-29.76	0.24	3.91
Arable	20	4.65	-28.52	0.33	4.12
Arable	23	3.39	-28.63	0.29	6.24

Arable	24	5.83	-29.20	0.44	4.64
Arable	26	3.91	-28.63	0.33	5.77
Arable	28	4.41	-28.53	0.35	4.35
Arable	30	3.81	-28.47	0.26	5.30
Arable	31	5.09	-28.52	0.40	5.26
Arable	32	3.24	-28.61	0.24	6.81
Moorland	33	25.89	-28.55	1.46	2.01
Moorland	34	5.73	-28.32	0.44	0.22
Moorland	35	18.15	-29.05	1.00	0.31
Moorland	36	4.74	-29.12	0.38	4.88
Moorland	37	25.00	-29.59	1.59	3.19
Moorland	38	18.22	-28.84	1.03	1.26
Moorland	40	14.01	-28.06	0.56	1.15
Moorland	41	10.69	-28.79	0.62	1.63
Moorland	42	23.41	-28.49	0.89	0.58
Moorland	44	7.83	-28.94	0.30	2.34
Forest	45	11.37	-28.78	0.41	0.02
Moorland	46	39.78	-28.69	2.06	1.27
Moorland	47	7.81	-28.41	0.53	4.44
Moorland	48	9.70	-28.60	0.47	1.01
Moorland	49	37.95	-27.68	1.91	3.24
Moorland	50	23.66	-29.38	1.46	0.95
Arable	51	2.43	-29.03	0.23	6.89
Pasture	52	1.91	-28.88	0.15	5.04
Pasture	53	4.45	-29.41	0.29	7.09
Arable	54	4.51	-29.18	0.34	3.85
Arable	55	3.02	-29.11	0.22	6.55
Pasture	56	4.91	-29.70	0.34	4.60
Pasture	57	4.42	-29.36	0.38	4.88
Pasture	58	5.24	-29.20	0.43	5.35
Pasture	59	4.32	-30.03	0.27	4.52
Pasture	60	3.21	-29.05	0.30	5.81
Pasture	61	2.62	-29.91	0.22	4.63

Pasture	62	3.00	-29.78	0.28	3.76
Pasture	63	4.47	-29.40	0.36	4.71
Pasture	64	5.15	-29.36	0.45	4.48
Moorland	65	7.45	-27.90	0.52	2.30
Pasture	66	3.09	-28.87	0.29	6.64
Pasture	67	4.38	-29.53	0.29	5.44
Pasture	68	2.32	-29.59	0.19	5.30
Pasture	69	2.85	-29.18	0.29	6.06
Pasture	70	3.14	-29.85	0.20	4.87
Pasture	71	3.84	-28.85	0.30	6.36
Forest	72	8.28	-28.18	0.42	2.03
Moorland	73	47.69	-28.17	1.42	-0.67
Moorland	74	34.83	-28.91	1.09	-0.58
Arable	77	3.40	-29.11	0.28	7.45
Forest	78	17.62	-27.22	0.77	1.46
Pasture	79	2.97	-28.51	0.26	7.51
Arable	80	2.15	-29.61	0.19	6.81
Forest	101	8.24	-28.32	0.51	3.68
BS	BS1	1.08	-29.33	0.08	3.61
BS	BS2	0.62	-26.36	0.03	4.88
BS	BS3	0.99	-29.75	0.06	4.21
SS	270819-1	8.15	-30.00	0.58	3.68
SS	110220-1	12.53	-29.92	0.92	3.31
SS	140420-1	5.50	-29.63	0.40	3.19
SS	040620-1	9.05	-29.65	0.77	4.15
SS	290720-1	8.75	-29.81	0.63	4.17
SS	220920-1	8.77	-29.87	0.64	3.44
SS	171120-1	4.18	-29.54	0.30	3.09
SS	270819-2	7.91	-29.11	0.63	3.19
SS	231019-2	4.63	-29.06	0.41	2.34
SS	171219-2	8.64	-29.39	0.67	3.05
SS	110220-2	22.22	-30.10	1.29	1.40
SS	140420-2	14.11	-29.43	1.09	2.77

SS	040620-2	10.02	-29.26	0.80	3.64
SS	290720-2	12.52	-29.37	1.07	3.46
SS	220920-2	11.31	-28.85	0.98	4.71
SS	171120-2	4.51	-28.92	0.37	0.79
SS	270819-3	12.38	-30.08	0.89	4.66
SS	231019-3	9.90	-30.01	0.79	3.98
SS	171219-3	6.72	-29.75	0.53	3.74
SS	110220-3	9.62	-29.86	0.75	4.07
SS	140420-3	12.30	-29.88	0.88	4.50
SS	040620-3	11.88	-29.94	1.07	5.77
SS	290720-3	10.16	-29.96	0.81	5.39
SS	220920-3	9.97	-30.04	0.78	4.69
SS	171120-3	4.43	-29.65	0.38	4.60